Thimo te Molder

Cellulosic Glycols

Identification and Prevention of Catalyst Deactivation

Cellulosic Glycols

Identification and Prevention of Catalyst Deactivation

Thimo Daniel Jozef te Molder

Cellulosic Glycols

Identification and Prevention of Catalyst Deactivation

PROEFSCHRIFT

ter verkrijging van
de graad van doctor aan de Universiteit Twente,
op gezag de rector magnificus,
prof. dr. ir. A. Veldkamp,
volgens besluit van het College voor Promoties
in het openbaar te verdedigen
op vrijdag 3 juni 2022 om 14:45 uur

door

Thimo Daniel Jozef te Molder
geboren op 15 oktober 1992
in Winterswijk, Nederland

Dit proefschrift is goedgekeurd door:

de promotoren:
prof.dr. S.R.A. Kersten
prof.dr. J.P. Lange

en de copromotor:
dr. ir. M.P. Ruiz

This work was conducted in the Sustainable Process Technology (SPT) group of the Faculty of Science and Technology at the University of Twente, The Netherlands. This work was financially supported by Shell Global Solutions, Amsterdam, The Netherlands.

Cover design by Sam Benou
Printed by Gildeprint
Lay-out in LaTeX by T.D.J. te Molder
ISBN: 978-90-365-5364-3
DOI: 10.3990/1.9789036553643

PROMOTIECOMMISSIE:

Voorzitter :	prof. dr. J.L. Herek	Universiteit Twente
Promotoren:	prof. dr. S.R.A. Kersten	Universiteit Twente
	prof. dr. J.P. Lange	Universiteit Twente
copromotor:	dr. ir. M.P. Ruiz	Universiteit Twente
Leden:	prof. dr. P.J. Deuss	Rijksuniversiteit Groningen
	prof. dr. P.C.A. Bruijnincx	Universiteit Utrecht
	prof. dr.ir. L. Lefferts	Universiteit Twente
	prof. dr.ir. G. Brem	Universiteit Twente
Referenten:	dr. F. Neira D'Angelo	Universiteit Eindhoven
	dr. E. van der Heide	Shell Technology Centre Amsterdam

aan mijn vader, Emiel te Molder

Table of Contents

Introduction

"Some men see things as they are and say, why?
I dream things that never were and say, why not."

- George Bernard Shaw -

1.1 The carbon economy

Carbon-based molecules have been the primary energy source and carrier throughout the history of mankind, first in the form of biomass, but is now dominated by fossil carbon. The deployment of renewable energy sources, such as wind and solar, is on the rise and could substitute fossil fuels. However, these alternatives do not provide a basis for the production of carbon-based chemicals. Next to energy, around 14% of oil and 8% gas is used for the production of chemicals[1]. The majority is used for the production of ammonia (185 Mt/a), methanol (100 Mt/a), light olefins (255 Mt/a) and BTX (110 Mt/a)[1]. The latter two are typically produced from oil and generally end up in polymers for a wide variety of applications. It is important to realise that the use of these polymers more than offsets the emissions associated with their chemical manufacturing[2]. For example, the manufacturing of insulation material requires less energy than what is being saved by the achieved reduction in heat demand. More importantly, plastics typically outperform alternative materials, such as glass[3], on various performance indicators such as energy consumption (production and distribution) and water use. In an era where energy efficiency will play a key role, plastics can be, in the authors view, considered indisputable for alternative materials. Plastics have been demonized due to generation of incredible amounts of litter but this, in the authors view, is a result of 1) mankind's irresponsible handling of waste and 2) poor economic incentive to collect and recycle plastics. Collection and subsequent recycling of single use plastics is the preferred option to minimize the use of fossil carbon[4].However, recycling will inevitably be accompanied by carbon losses which requires the influx of new carbon. Moreover, mankind should tap into alternative carbon-sources to meet the growing demand[4].

1.2 Alternative carbon

Renewable carbon is derived from the atmosphere in the form of CO_2, which is captured by biomass and reduced to sugars by utilising solar energy in a process called photosynthesis ($\sim$1% solar efficiency[5],[6]). Alternatively, CO_2 can be directly captured by *"artificial trees"* but is available in the atmosphere at only $\sim$400 ppm. Even if captured, a large energy input is required to reduce CO_2 from its oxidation state of +4, to for example, -1 to produce ethylene glycol. Harvesting biomass seems a more attractive option as it is 1) a concentrated carbon source, and 2) has a more desirable oxidation state, e.g. 0 for

sugar, which theoretically requires less energy input for its conversion to fuels and chemicals.[4] Although biomass can be converted to a transportation fuel (e.g. conversion to ethanol), in the authors view, lignocellulosic biomass should predominately be used for the manufacturing of materials or chemicals and not as transportation fuel. For example, the combination of 1) photovoltaic electricity and battery electric vehicle for transportation outperforms 2) photosynthesis to grow biomass, followed by conversion to a fuel for an internal combustion engine by a factor 10-100 in terms of overall efficiency[7]–[9], and option 2 would therefore require vastly more arable land.

1.3 Bio-economy

Mankind has a long history of utilizing biomass as a raw material and energy source, besides food. Until the late 1800, biomass has been the primary energy fuel but it has also been utilized for the production of chemicals. Well known is the dry distillation of wood for the production of methanol and acetic acid, despite low yields or the saponification of animal fat to soap[10]. However, more sophisticated examples are known, e.g. Quaker Oats has produced $\sim$ 2.5 tons of furfural per day from oat husks since 1922[11]. The furfural was subsequently used as precursor for Nylon by DuPont until $\sim$1960. The rise of fossil fuels has undone a lot of the efforts to produce chemicals from wood. Currently, $\sim$9%[12] (2018) of the total energy mix is supplied by biomass, though mostly in primitive applications such as heating and cooking in the developing world. Pulp production according to the Kraft process invented by Carl F. Dahl in 1879 has resisted the dominance of fossil derivatives. Current pulp production (2017) is around $\sim$190 Mt/a, which means an influx of $\sim$480 Mt/a of pulpwood and, thus, within similar order of magnitude as the production of base chemicals[13]. Approximately the double, $\sim$800 Mt/a of wood, is used as sawlogs (e.g. for construction)[13]. The utilization of biomass and its conversion to products (bio-refining) on a large scale is thus common practise.

However, the substitution of fossil-derived chemicals by their biomass-derived equivalents requires the expansion of biomass harvesting. Biomass availability is conservatively estimated at 6-18 Gt/a[14] and, therefore, it should be more than enough to cover the production of base chemicals. In particular the use of lignocellulosic biomass as feedstock which is non-edible and widely available seems attractive. Moreover, cultivation of sugar rich plants is

often accompanied with the generation of lignocellulosic by-product, for example, for every share of sugar cane an equal amount of bagasse is produced amounting to 220 Mt/a of bagasse[15].

1.4 Target chemical

Economic incentive is the primary reason for process development. It is therefore potent to focus on products that show economic potential. For that two main strategies are postulated[4],[16],[17]: 1) existing products that match in functionality compared to the feed (oxygenates in case of biomass) or 2) novel materials that can be derived from biomass without extensive processing (e.g. nanocellulose). The latter requires the development of a new market, which history has shown to take $\sim$40 years to develop into a mature market[4], whereas the first can be used in existing infrastructure and therefore allows faster deployment.

Along the principles discussed, glycols are an attractive candidate to be produced from biomass, which has been recognized before[18]. The atomic ratio of sugar (C:2H:O) and ethylene glycol (C:3H:O) show a perfect match in carbon to oxygen ratio and only requires the introduction of hydrogen, which allows theoretical mass yields of 100 wt .%. Ethylene glycol finds its main use as polyester in textiles and PET bottles and to a lesser extent as coolant[19]. It is among the bulk chemicals with a market size of $\sim$30 million[20] tonnes per annum (4% expected growth) and trades for $\sim$€850 $\pm$ 100 per tonne[16] (2010-2014). Ethylene glycol is also constituent of the PEF (polyethylene furanoate) polymer which is a bio-derived alternative to PET with superior barrier properties[21]. Note that the production of propylene glycol (PG) from biomass is also attractive, but ethylene glycol (EG) is preferred as its market size is substantially bigger.

1.5 Lignocellulose composition

Only sugars can be converted to glycols via the route of interest in this work, namely by aldol cleavage and subsequent hydrogenation of the intermediate. However, other components present in the biomass could potentially spoil the yield, for example by poisoning of the catalyst. It is therefore worthwhile to provide some general understanding of lignocellulosic biomass composition.

Lignocellulosic biomass consists for $\sim$60-75 wt.% of polysaccharides, sub-

divided in ∼50 wt.% cellulose and ∼25 wt.% hemicellulose. Cellulose is a straight chain polymer composed of anhydroglucopyranose units coupled by $\beta(1\rightarrow4)$ glycosidic bonds, with a typical degree of polymerization of 2000-15000[22]. Cellulose consists of crystalline and amorphous regions. Hemicellulose is a branched amorphous hetero-polymer and therefore much more susceptible for acid, base or enzymatic attack than cellulose. It can be composed of hexoses (glucose, mannose and galactose) and pentoses (xylose and arabinose), depending on the plant species. The hemicellulose in softwood (Gymnosperm) mostly consists of glucomannans (hexose-based) whereas hardwoods and herbaceous species (both Angiosperms) predominantly contain pentose-based hemicelluloses, such as xylan[23]. In addition to saccharides, hemicellulose is composed of sugar acids (e.g. glucuronic acid), acetylgroups and ferulic and p-coumaric acids. Lignin is a crosslinked phenolic bio-polymer assembled from p-coumaryl, sinapyl and coniferyl alcohol units via radical polymerisation[24] and typically present in biomass in concentrations ranging 15 to 35 wt.%[25],[26]. These three bio-polymers make up the plant cell wall.

Woody biomass also contains a group of components, generally referred to as extractives, ranging from a few percent up to 10 wt.%[27]. These are low molecular weight components that can be extracted from the biomass with an organic solvent and/or hot water. The majority consists of hydrocarbon/oxygenates, such as terpenes, tannins, fatty acids, waxes, lignans, stilbenes and sterols.

Additionally, a minor share of lignocellulosic biomass is composed inorganic components. Its inorganic composition depends on soil characteristics and the biomass specie[28]. The majority of the inorganic material is silica which is absorbed by the plant in the form of silicic acid or its ionized form and assimilated into particles[29]. Typically, silica levels in lignocellulosic biomass are $\leq$ 1 wt.% for wood species but significantly higher for grass types 5-10 wt.%. Besides silica, major inorganic biomass constituents are Na, K, Mg, Ca (alkali and alkaline earth metals)[28],[30]. Also, other metals are present but typically at much lower levels, most prominently iron, aluminium, manganese and zinc[28]. These ions are present in the form of 1) salts (carbonates, oxalates, chlorides, etc.), or 2) ionically bound to carboxyl or hydroxylgroups of the hemicellulose and lignin.

The majority of plant species also take up sulphur and nitrogen via its roots in

the form of sulphate, nitrate and ammonium[30]. These are subsequently reduced and built into amino acids which are then mainly assembled in proteins. S levels in lignocellulosic biomass are typically lower than 0.2 wt.%, whereas the N content can be up to 1.5 wt.% (grasses), but is more generally between 0.1 and 0.5 wt.%[31]. Phosphorus is classified as a primary macronutrient and taken up in the form of phosphate, (hydrogen phosphate or dihydrogen phosphate, depending on the pH). It is key to cells energy management in the form of adenosine phosphates (ADP, ATP)[30].

1.6 Ethylene glycol (EG) production pathways

Fossil-based ethylene glycol is predominantly produced from ethylene via the partial oxidation to ethylene oxide (EO) followed by subsequent thermal hydrolysis to ethylene glycol[32], where both steps can be run at carbon efficiencies of $\sim$90%[33], resulting in an overall carbon efficiency of $\sim$81%, see *"ethylene route"* in Figure 1.1. The efficiency of the second step can be boosted to $\sim$100% by utilizing ethylene carbonate as intermediate[33]. This process is known as the OMEGA™ process which was initially developed by Mitsubishi Chemical Corporation but substantially refined by Shell after it acquired exclusive license in 2002[33]. EG can also be produced from syngas[32],[34], which is applied on industrial scale[35] via the oxidative carbonylation of methanol to dimethyl oxalate followed by hydrogenation over a copper catalyst. Both pathways primarily rely on fossil feeds, such as oil and coal.

However, biomass can be converted to syngas[36] or ethylene and thereby exploit the existing routes. The latter, which proceeds via the fermentation[37] of sugar to ethanol followed by dehydration[38] to ethylene, has been commercially applied[39], see glucose to ethanol in Figure 1.1. However, this pathway is limited by a theoretical efficiency of 66 C% due to the formation of CO_2 during the fermentation step (1 mole CO_2 per mole of ethanol)[37]. Furthermore, the multi-step process is circuitous as it starts with reductive steps followed by oxidative steps. This has incentivized the development of more direct pathways that make better use of the oxygen present in biomass, see *"direct biomass route"* in Figure 1.1. Preservation of oxygen present in sugar can be achieved by the aldol cleavage of glucose to glycolaldehyde and subsequent hydrogenation to EG. Selective production of glycolaldehyde (GA) can be achieved by 1) in the presence of a catalyst, e.g. a homogenous tungstate species, at mild temperatures of 220-260°C[40] or 2) non catalyti-

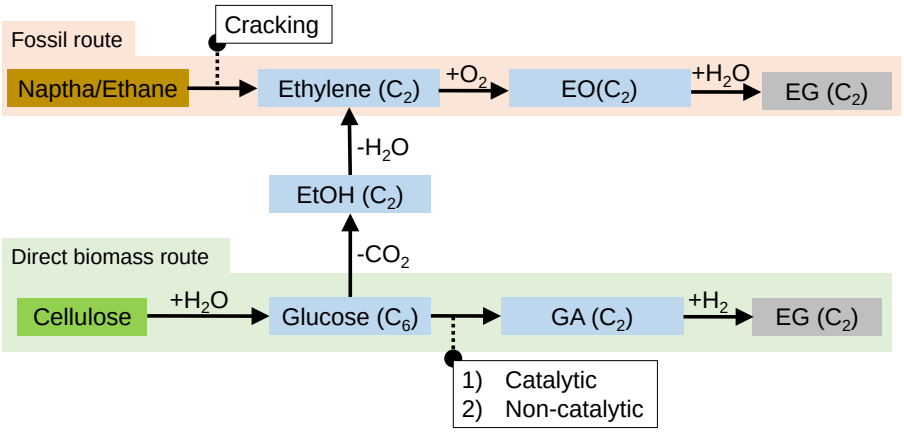

Figure 1.1: Current petrochemical route and proposed direct conversion of biomass (saccharide) to ethylene glycol (EG). EO = ethylene oxide, EtOH = ethanol, GA = glycolaldehyde.

cally (65-75 wt.%)[41],[42] via hydrous thermolysis at temperatures greater than 500°C[41] or in supercritical water (450°C, 35MPa, 0.25s)[42]. As glycolaldehyde is very reactive, all options require rapid quenching to avoid secondary decomposition of glycolaldehyde[43].

The second step, the conversion of glycolaldehyde to EG, can be achieved by catalytic hydrogenation with high selectivities (96 wt.%) at a mild temperatures (80°C)[44]. Both steps can also be combined in a single reactor which avoids the need for rapid quenching of the GA rich mixture, instead, GA is directly hydrogenated to EG which is rather stable at reaction conditions. EG yields of ∼70 wt.% for the conversion of glucose at 230°C in the presence of sodium metatungstate and Raney nickel are reported[45]. Further integration is possible by directly feeding polysaccharide to the reactor which is then in-situ depolymerised and converted to EG. Numerous studies[46] have successfully demonstrated this approach and yields up to ∼74 wt.%[47],[48] on cellulose basis are reported.

1.7 Commercial development

Several parties[45],[49]–[52] hold patents that target the conversion of sugar to glycol via tungstate catalysed hydrogenolysis pioneered by the group of Zhang et al[48]. We briefly discuss the initiatives that have gone public. Avan-

tium is developing their Ray Technology™ and are currently (2019) operating a demonstration plant with an annual capacity of 10 tonnes[53]. This technology is based on catalytic conversion which involves the cleavage of glucose to GA by a tungstate species and subsequent hydrogenation to EG in single step[54]. UPM hast started (2020) the construction of a biorefinery in Leuna (Germany) that has a total annual design output of 220,000 tonnes of EG, together with some propylene glycol (PG), industrial sugars and lignin-based functional fillers which involves an investment of €550 million[55]. The facility processes locally harvested beechwood. The wood is first disintegrated to sugars and lignin, which are independently processed after subsequent separation[56]–[58]. Valorisation of sugars to EG and PG proceeds through technology based on tungstate catalysed hydrogenolysis route[50],[59],[60] developed in collaboration[61] with Changchun Meihe and Coca-Cola. In parallel Haldor Topsoe has partnered with Braskem and are since 2019 demonstrating their proprietary MOSAIK™ technology in a 100 tonne per annum pilot plant[62]. Their technology is comprised of a hydrous thermolysis step which converts glucose to GA with yields of at least 66 wt.%[43],[63], but likely higher as combined GA and glyoxal yields of 75 wt.% are reported in the open literature[41]. GA (and glycoxal) is subsequently hydrogenated to EG with a selectivity exceeding 95%[44].

1.8 Chemistry: tungstate catalysed hydrogenolysis

This work focusses on the selective tungstate catalysed conversion of lignocellulosic biomass to EG. Although complex, the route has high potential as it allows the integration of multiple reaction steps in a single reactor. For example, birch wood was converted in a batch experiment to EG with a yield of 54 wt.% based on holocellulose content[64].

We consider a catalytic system depicted in Figure 1.2 in which (ligno)-cellulose is directly converted to ethylene and propylene glycol. As reviewed by Zheng et al.[65] selective EG production relies on balancing a series of reactions and selecting appropriate catalysts. In the following sections we will review the critical reactions required to produce EG and its most important by-products, namely PG, sugar alcohols (SA) and thermal decomposition products.

Briefly, cellulose is depolymerised to glucose and subsequently converted to glycolaldehyde in the presence of a homogenous tungstate species, which is

then hydrogenated to EG, see Figure 1.2. PG is formed via a similar route starting from fructose, which is formed via isomerization of glucose. Direct contacting of these saccharides with the hydrogenation catalyst yields sugar alcohols. These hydrogenation reactions compete with irreversible thermally induced side reactions of the aldoses.

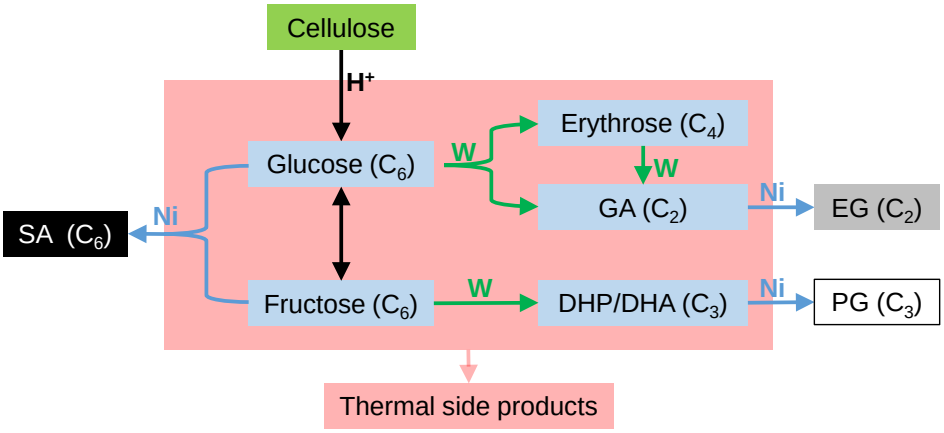

Figure 1.2: Simplified reaction system. EG = ethylene glycol, PG = propylene glycol, SA = sugar alcohols, DHP = dihydroxypropanal, DHA = dihydroxyacetone, GA = glycolaldehyde. Ni = Raney nickel catalyst, W = Homogenous tungstate catalyst. Adapted from ref[66]

The reaction is operated at mild acidic conditions for two reasons; 1) to facilitate cellulose depolymerisation and 2) to suppress the isomerisation of glucose to fructose which is base catalysed. The latter ultimately results in the formation of the less desired PG (see Figure 1.2), which will be discussed in detail later.

1.8.1 Aldol cleavage

The conversion of saccharides to C_2 and C_3 moieties proceeds via the aldol cleavage reaction, see Figure 1.3. As previously mentioned, this reaction can be achieved in the presence of water with selectivity's in the range of 65-75 wt.%[41],[42], but requires severe conditions in absence of catalysts, as found in hydrous pyrolysis[41] (>500°C) or supercritical water (450°C, 35 MPa)[42].

In 2008 Zhang et al. found in their pioneering work that this reaction is catalysed by tungsten[48], which allows lowering of operating temperature to the range of 220-260 °C[40] (see green arrows in Figure 1.2). Other metal-

based catalyst appeared to be active for aldol cleavage as well, as reviewed elsewhere[65]. Nevertheless, tungsten-based catalyst has remained the focus in the research field of the one-pot conversion of sugars to glycols and, to the best of our knowledge, delivers the highest selectivity to EG in such system. However, heterogeneous tungsten based catalysts suffered from W leaching to the reaction medium[64],[67]–[69], and instead were later applied in the form of homogenous catalysts[70],[71] such as tungstic acid, ammonium metatungstate (AMT) and phosphotungstic acid (HPW)[70],[72]. In this work we have selected a fully soluble sodium-polytungstate as aldol cleavage catalyst. This allows decoupling of the acidic and aldol cleavage functionalities of the hydrogenolysis system, which is not possible when an acidic tungstate species such as tungstic acid (H_2WO_4) is used.

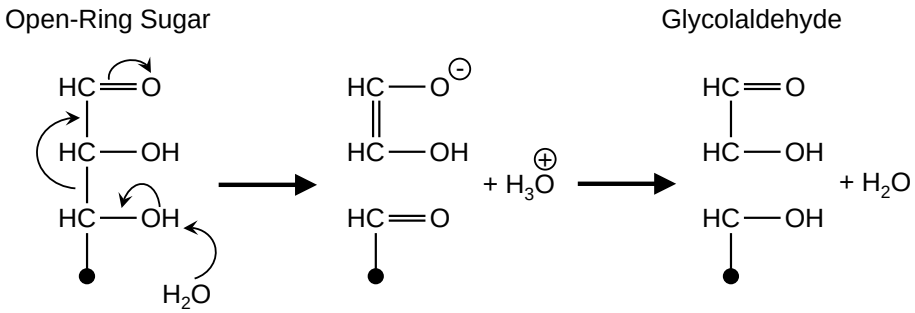

Figure 1.3: Proposed water-catalysed aldol cleavage of an aldose[43]

Key insights related to the mechanism were obtained in the work by Liu et al.[73] We have reproduced their experimental dataset here in Table 1.1 and will discuss their findings. Hexitol (77 C%) was the dominant product formed when glucose was hydrogenated in the presence of Ru/C (Table 1.1 entry 2). Under the addition of tungsten trioxide, however, the product slate shifted to glycols (73 C%) (Table 1.1 entry 4), revealing the critical role tungstates play in cracking sugar to C_2 and C_3 moieties. Erythrose, the C_4 intermediate that can emerge after cracking of glucose, can be further cracked to glycolaldehyde (C_2)[74]. Mannose, which is an epimer of glucose, gave very similar product yields (65 C% glycol) as glucose (Table 1.1 entry 6). When sorbitol was used as feed no conversion to polyols was observed (Table 1.1 entry 1), which shows that the carbonyl group is essential to induce the reaction. It is hypothesized that tungstate acts as a lewis-acid and complexes with the carbonyl group. Also the presence of a α-hydroxide (OH-group next to the

carbonyl group) is critical as 2-deoxy-glucose, for which the α-hydroxide is missing compared to glucose, did only give 2-deoxy-sorbitol and hence no glycol.

*Table 1.1: Product selectivity for the conversion of different sugars with and without WO_3 in the presence of Ru/C in the study by Liu et al.[73]. Conditions: 205° C, 10min, 6 Mpa H_2, 40mL H_2O, 0.1g sugar or sugar alcohol, 0.02g 3 wt.% Ru/C, 1.0 g WO_3. Sorbitol conversion was 1.4% and sugar conversions were all 100%.*The product was 2-deoxy-sorbitol. **The product was 2-deoxy-ribitol.*

			Selectivity (C%)							
Entry	Feed	WO_3 present	EG (C_2)	PG (C_3)	Glycerol (C_3)	Tetritols (C_4)	Pentitols (C_5)	Mannitol (C_6)	Sorbitol (C_6)	Sum
1	Sorbitol	Yes	0	0	0	0	0	0	100	100
2	Glucose	No	9	6	2	0	4	7	70	99
3	Fructose	No	8	7	3	0	2	36	44	99
4	Glucose	Yes	59	14	3	5	0	2	9	92
5	Fructose	Yes	16	48	18	1	0	9	11	103
6	Mannose	Yes	54	11	3	5	0	18	3	95
7	Xylose	Yes	32	36	10	5	16	-	-	98
8	Ribose	Yes	26	29	8	0	20	-	-	83
9	2-deoxy-glucose*	Yes	0	0	0	0	0	0	0	0
10	2-deoxy-ribose**	Yes	0	0	0	0	0	-	-	0

The hydrogenolysis of fructose in the presence of WO_3 predominantly delivers C_3 species (66 C% of PG and glycerol), (Table 1.1 entry 5) and suggests that aldose is preferred over ketose for EG production. A cleavage induced via the β-hydroxide would deliver two trioses (DHA+DHP), which result in glycerol and PG after hydrogenation. This hints at an important role in the mechanism for the β-hydroxide and suggests that the tungstate at least interacts with the carbonyl and β-hydroxide, similar as the water induced aldol cleavage, see Figure 1.3. A cleavage that proceeds via the α-hydroxide and the carbonyl group should after hydrogenation of the intermediates yield EG (C_2) and tetritol (C_4) or methanol (C_1) and pentitol (C_5). Despite a mass balance of $\sim$100% no C_1 species were reported and the C_5 yield was 0 C%, see Table 1.1 entry 5. Moreover, an insignificant amount of tetritols was reported (1 C%) and the EG yield (16 C%) was slightly increased compared to 8 C% in the absence of WO_3 (Table 1.1 entry 3). This shows that the tungstate catalysed aldol cleavage primarily proceeds via the carbonyl and β-hydroxide groups, but the presence of the α-hydroxide (OH-group next to the carbonyl group) is critical as well.

The cleavage of pentosan (C_5-sugar) would theoretically result in an equimolar amount of C_2 and C_3 species (or 40 C% EG and 60 C% PG). Indeed,

41 C% of the C_2+C_3 components was EG and 59 C% was C_3 (46 C% PG and 13 C% Glycerol) for both xylose and ribose feedstocks. Similar numbers (38 C% EG, 62 C% PG, no glycerol reported) were deducted from a different study which also ran hydrogenolysis with xylose as feed[75]. This reveals two important conclusions 1) C_3 intermediates (DHA/DHP) do not undergo additional cleavage to C_2 and C_1 species and 2) pentose sugars (C_5) are less desired than C_6 aldose when targeting the production of ethylene glycol. As mentioned in section 1.5, the hemicellulose fraction of hardwoods and herbaceous species is typically composed of pentosan and thus a less desirable feed when targeting EG. The hemicellulose could be removed upfront and used for the production of, for example, furfural. Alternatively, a softwood feedstock could be selected which is typically rich in glucomannan type (hexose-based) hemicellulose.

1.8.2 Hydrogenation

The C_2-C_3 aldose intermediates are subsequently hydrogenated to ethylene and propylene glycol in the same reactor vessel, which avoids the need to quench the aldose rich mixture to avert secondary decomposition reactions. This reaction is performed over a heterogenous metal catalyst in the presence of gaseous hydrogen. Various catalyst, typically Ru or Ni based, have been tested in batch experiments[76]. Catalytic systems composed of a homogenous tungstate catalyst and Raney nickel or Ru/C have shown good performance (i.e. >50% selectivity) in batch[70],[71]as well as continuous runs[45],[49].

But this can also proceed with higher aldose, e.g. glucose (C_6) to sorbitol or erythrose (C_4) to erythritol, which reduces the selectivity to glycols. The hydrogenation of glucose is more thoroughly studied than glycolaldehyde hydrogenation and typically considered to proceed via the Langmuir–Hinshelwood–Hougen–Watson (LHHW) mechanism[77]–[79]. However, these higher aldoses, such as glucose, are considered less reactive as their distribution towards the free aldehyde form, which is required for hydrogenation, is much lower than for glycolaldehyde[80]–[82]. It indeed appeared that glycolaldehyde is more reactive towards hydrogenation than glucose and was selectively ($\sim$100%) hydrogenated to EG whereas glucose showed little conversion (<10%) under sufficiently mild conditions (70°C) when starting with a 1:1 GA:Glucose mixture[83]. These results are in line with the study by Zhang et al.[84], who showed that GA is preferentially adsorbed on the hydrogenation

catalyst surface over glucose. This results in an intrinsic selectivity advantage when targeting EG.

Zhang et al.[84] also established that tungstate species deposit on the hydrogenation catalyst and thereby inhibit its activity, which is confirmed by patent literature[85],[86]. The deposited tungstate could be removed form the heterogenous metal catalyst by a washing step, which resulted in increased activity of the regenerated catalyst[85].

1.8.3 Thermally induced side reactions

Besides ethylene glycol and the by-products discussed above, other by-products are formed by irreversible thermal side reactions of the aldoses/ketoses, see *"thermal side products"* in Figure 1.2. These set of reactions are not specific to the tungstate catalyst hydrogenolysis targeting EG but are relevant to all sugar conversion processes. We therefore will not extensively review these types of reactions. Briefly, the sugar and its derivates undergo a variety of reactions such as dehydration and condensation that lead to the formation of heavy water insoluble material often referred to as *"humins"*[31],[87]. GA, which is typically not subject of such studies, is also prone to condensation reactions and subsequent formation of heavies[88]. These molecules tend to foul the hydrogenation catalyst surface which results in its deactivation.

1.9 Process development

High EG yields for the direct conversion of cellulose via the tungstate catalysed hydrogenolysis to EG have been reported. Moreover, substantial effort has been made to understand the reaction chemistry. But still, considerable hurdles must be taken to develop a cost-effective process based on lignocellulosic feedstock.

In this initial phase of process development, we will use performance criteria that were derived from existing fuel and chemical manufacturing processes[31],[89] to provide guidance, see Table 1.2. We will discuss whether reported performance meet these criteria and can, thereby, be considered as non-critical at this stage.

The academic literature typically focusses on achieving a high product selectivity and selectivities of $\sim$74wt.%[47],[48] have been reported for the direct

conversion of cellulose to EG which thereby meet the desired threshold (>70 wt.%), see Table 1.2. However, the high selectivity is generally achieved using low feed concentration and high catalyst to feed ratios. Consequently, this results in low reactor productivity and cannot prove low catalyst consumption; all important criteria according to Table 1.2.

Starting from glucose also high selectivities towards EG ($\sim$70 wt.%) were reported in the patent literature at more desired feed concentrations of $\sim$10wt.%[45]. The feedstock concentration criteria have also been met, despite a limited number of experiments, for the direct conversion of microcrystalline cellulose and pre-treated Miscanthus at 10 wt.% loading (EG yields $\geq$ 50 wt.%)[90],[91]. The minimum reactor productivity has been achieved in literature[74] and approached in a patent[45], see Table 1.2.

However, the catalyst consumption falls short and therefore requires attention as components present in biomass are known to impair the catalyst stability[31]. This criteria is therefore the primary focus of this thesis.

Table 1.2: Critical Performance of sugar-to-EG vs. operating window applied in fuel and chemical manufacturing processes[31],[89]

	Industrial window	Status
Catalyst consumption ($tonne_{product}$ / kg_{cat})	1-10	$\geq$0.14 (glucose)[45]
Productivity ($tonne_{product}$ / $m^3_{Reactor}$ h)	0.1-10	0.3[74], $\sim$0.06 (glucose)[45]
Selectivity (wt.%)	70-100	$\sim$74 wt.% (cellulose)[47],[48]; $\sim$70 wt.% (glucose)[45]
Feed concentration (wt.%)	3-100	$\sim$10 wt.% (glucose)[45],[54]

1.10 Thesis outline

The aim of this thesis is to develop a pretreatment concept that removes catalyst poisons from the feed prior to entering the hydrogenolysis reactor (prevention). This starts by identifying the catalyst poisons and tolerance of the catalyst towards these poisons. We thereby target the development of pretreatment processes that can be integrated with the hydrogenolysis process. We do not focus on the deactivating phenomena that are also observed when running with mono-saccharide as feedstock, but we pay specific attention to the fractions that are present in lignocellulosic biomass.

All relevant laboratory equipment, analytical equipment and procedures and definitions used in this thesis are presented in Chapter 2.

We have initially focussed on the impact of lignin on catalytic hydrogenolysis (Chapter 3), which is after holocellulose the major constituent of lignocellulose. We hypothesized that lignin fouling of the hydrogenation catalyst leads to its deactivation. This chapter has started with a thorough analysis of the literature data. Conflicting results reported in the literature have incentivized us to study the impact of lignin on catalytic hydrogenolysis ourselves. For that we have developed a flexible hydrogenolysis protocol that is sensitive to catalyst impurities and studied the impact of lignin in the presence an absence of the tungstate catalyst. Details on the development of this sensitive hydrogenolysis protocol are documented in Appendix A.

In Chapter 4 we have used our hydrogenolysis protocol to study the impact of inorganics that are present in the woody biomass on the catalytic hydrogenolysis. In addition to the hydrogenolysis protocol we have developed an analytical method to quantify the concentration of soluble, i.e. active, tungstate catalyst in the reactor effluent. We have applied acid-leaching which is a mild pretreatment that selectively removes the majority of inorganics from the biomass, in combination with model compound mixtures to gain understanding on the role of inorganics on catalyst deactivation.

The results obtained in Chapter 4 for woody biomass were not fully reproducible for hay (Chapter 5), an herbaceous specie which are typically rich in extractives, inorganics and proteins (sulphur/nitrogen). We have investigated the root cause for the observed deactivation phenomena seen for hay and thereby focused on the role of extractives and proteins (sulphur/nitrogen).

In Chapter 6 we studied the impact of particle size on the hydrogenolysis

outcome. Substantial particle size reduction (i.e. sub millimetre size) is associated with significant energy consumption. It is therefore desirable to understand the relationship between particle size and glycol yield.

The Chapters hereafter 7 & 8 focus on engineering aspects of the process. Chapter 7 gives an initial validation of pretreatment process that is integrated with the hydrogenolysis step. This solvent based pretreatment aims to remove catalyst poisons while relying on in-situ generated solvent. We avoided the use of inorganic additives such as hydrogen chloride or sulfuric acid, which is popular practice in biomass pretreatment, but are known catalyst poisons. In addition, we have performed initial estimations of the solvent recycle and energy requirements.

The ability of lignocellulosic biomass to trap a vast amount of liquid hampers the removal of contaminants from the biomass by solvent based pretreatments. In Chapter 8, we have investigated the implication of this phenomena for the removal of lignin. The liquid trapped by the solid residue contains dissolved lignin which cannot be removed. We propose to displace this spent solvent that contains dissolved lignin by fresh solvent utilizing countercurrent operation. Countercurrent pretreatment avoids the need for additional solvent, which would otherwise incur an economic penalty. We have used a batch reactor to mimic a three stage counter current pretreatment and compared this with single stage operation. Moreover, we have developed a mathematical model to describe the experimental results.

An overall conclusion and outlook is given in Chapter 9.

Materials and Methods

“Give me six hours to chop down a tree and I will spend the first four sharpening the axe."

- Abraham Lincoln -

2.1 Materials

The following chemicals were ordered from Sigma-Aldrich: Glacial acetic acid (≥99%), Ethanol (≥99%), Raney nickel (W.R. Grace and Co. Raney®2800) which was thoroughly washed with deionized water until neutral pH of the washing water was reached, sodium polytungstate (≥85% WO_3 basis), sodium hydroxide (≥99%), barium carbonate (≥99%) and microcrystalline cellulose (Avicel®PH-101, particle size ∼50 µm). Four biomass species were used in the study, namely poplar (hardwood), beech (hardwood), pine (softwood) and hay (herbaceous). Their composition is reported in Table 2.1. Poplar and beech wood were kindly provided by a local woodenshoe company, Pinewood (Lignocel 9) was acquired from Rettenmaier & Söhne GmbH and hay was purchased from a local garden and animal store. A variety of other particle size fractions were obtained by sieving and optionally combined with grinding (hammer mill). Pine and poplar of 1-2 mm and hay (53-355 µm) were used for pretreatment experiments. Biomass with particle size <53 µm and microcrystalline cellulose (Avicel®PH-101, ∼50µm) were used as benchmark feedstocks for hydrogenolysis experiments to represent untreated and deeply purified feedstock, respectively.

Table 2.1: Biomass composition on dry basis (Saccharide content, lignin, extractives, o-acetylgroups determined in duplicate, ash determination n=4) determined for 1-2 mm Poplar, Pine and Beech and 53-355 µm Hay.

	Cellulose	Poplar	Pine	Hay	Beech
H_2O extractive (wt.%)	-	7.2 ± 0.3	9.2 ± 0.4	23.1 ± 0.6	4.4 ± 0.4
EtOH extractive (wt.%)	-	1.8 ± 0.2	0.7 ± 0.5	2.0 ± 0.4	0
Lignin (wt.%)	-	21.4 ± 0.1	24.8 ± 0.2	18.5 ± 0.4	21.3 ± 0.7
o-Acetylgroups (wt.%)	-	3.1 ± 0.1	1.4 ± 0.1	2.0 ± 0.1	4.6
Saccharide composition					
Glucan (wt.%)	100	38.7 ± 0.1	36.6 ± 0.3	22.2 ± 0.5	35.1
Mannan (wt.%)	-	2.6 ± 0.6	10.5 ± 0.1	0	1
Galactan (wt.%)	-	0	1.4 ± 0.0	0	0
Xylan (wt.%)	-	10.9 ± 0.2	3.8 ± 0.0	10.6 ± 0.6	17.2
Arabinan (wt.%)	-	0.5 ± 0.2	1.4 ± 0.1	2.9 ± 0.1	0
Total ash (wt.%)	0.0 ± 0.0	0.8 ± 0.0	0.6 ± 0.1	4.5 ± 0.1	0.6 ± 0.05
Na (mmol kg^{-1})	0 ± 0	12 ± 1	3 ± 1	135.6 ± 2.4	1.4 ± 0.7
K (mmol kg^{-1})	0 ± 0	27 ± 3	7 ± 1	172.5 ± 0.9	18.8 ± 6.5
Mg (mmol kg^{-1})	0 ± 0	4 ± 1	6 ± 2	47.9 ± 0.5	3.9 ± 1.9
Ca (mmol kg^{-1})	0 ± 0	4 ± 1	15 ± 1	22.6 ± 1.9	7.8 ± 0.5
S (mmol kg^{-1})	<1.6	5	4.7	34.3	3
N (mmol kg^{-1})	16.4	35.7	31.4	929	57

2.2 Experimental procedures

2.2.1 Hydrogenolysis

A 45 mL batch autoclave equipped with a hollow shaft stirrer was used for catalytic hydrogenolysis experiments, which has been described in detail previously[92]. The reactor was mounted on a pneumatic arm, which allows rapid heating and quenching by submersion of the autoclave in a preheated fluidized sand bed or water bath respectively. The experiment was performed in a blast proof bunker, and pressure and temperature (thermocouple in the bottom of the autoclave) were monitored throughout the run.

In a typical experiment the autoclave was loaded with 14.25 g of an acetic acid/NaOH buffer (pH$\sim$3.3), 0.75 g of biomass, 0.021 g of retro-aldol catalyst (sodium polytungstate), 0.09 g of hydrogenation catalyst (Raney-Ni, dry basis) as a well-homogenized slurry and, optionally, an additive (e.g. a model compound) was added. Details about our hydrogenolysis protocol can be found in Appendix A. After loading the autoclave, it was sealed and

leak tested at 120 bar, followed by flushing with nitrogen (2x) and hydrogen (2x) and subsequently pressurized to ∼60 bar hydrogen. Under rapid stirring (∼1300 rpm) the autoclave was heated to the desired reaction temperature (245°C) by submersion in a preheated fluidized bed, which typically took less than 10 min. The start of the reaction time is defined as the moment that the reactor attained the desired temperature. Under catalyst lean conditions we observed that the EG yield (10 wt.%) and solid residue yield (23 wt.%) for a reaction time of 5 h was not significantly different than the ones obtained after 1 h of reaction time (Y_{EG} = 8 wt.%, 23 wt.% solid residue) and, therefore, we typically limited the reaction time to 1 h. The autoclave was rapidly cooled by submersion in the water bath after the desired reaction time was reached and depressurized once it attained room temperature. The reactor content was transferred to a glass bottle and subjected to pH measurement (Metrohm LL Unitrode Pt1000 probe) and a liquid sample was taken on which liquid chromatography (HPLC) was performed. The remaining solid material (catalyst and biomass residue) was separately collected by flushing of the reactor with deionized water.

The product yield was expressed on holocellulose basis as only sugar components can deliver glycols via the selected reaction chemistry, see equation 2.1. In this equation $m_{Product}$ is the mass of the product (e.g. EG), m_{Feed} is the mass of the biomass fed, and f_{Lignin}, $f_{H2O\text{-}extract}$, $f_{EtOH\text{-}extract}$, f_{Ash}, f_{Acetyl} are the lignin, water extractives, ethanol extractives, ash and acetyl weight fractions of the dry feedstock.

$$Y\ (\text{wt.\%}) = \frac{m_{Product}}{(1 - f_{Lignin} - f_{H_2O\text{-}extract} - f_{EtOH\text{-}extract} - f_{Ash} - f_{Acetyl})} \times 100 \quad (2.1)$$

2.2.2 Acid-leaching

Acetic acid leaching (10 wt.% acetic acid in water) was applied to selectively remove inorganic and water-soluble constituents from biomass. It was performed in a stirred vessel at room temperature for at least 24 h and a typical solids loading of 1 wt.%. Indeed, the total ash and AAEM content of the acid-leached (AL) feedstocks, see Table 2.2, was significantly decreased compared to the untreated feedstocks, see Table 2.1. We have not reassessed the content of the other biomass constituents as it is known that acetic acid

leaching at mild temperatures ($\leq$90°C) removes the extractives from biomass but conserves the cellulose, hemicellulose and lignin fractions[93]. We have therefore recalculated the biomass composition of the acid-leached feedstocks under the assumption that the water and ethanol extractives were removed during acid leaching, see Table 2.2.

*Table 2.2: Biomass composition of untreated and acid-leached (AL) feedstocks on dry basis. Quantification was performed at least in duplicate. *Recalculated from untreated feedstocks. WL+AL = First Water leached, followed by acid leaching.*

	AL Poplar	AL Pine	WL Hay	WL+AL Hay
H_2O extractive (wt.%)	-	-	0	0
EtOH extractive (wt.%)	-	-	2.6 $\pm$ 0.5	2.6 $\pm$ 0.5
Lignin (wt.%)	23.1	27.4	24.1 $\pm$ 0.5	24.1 $\pm$ 0.5
o-Acetylgroups (wt.%)	3.3	1.6	2.6 $\pm$ 0.1	2.6 $\pm$ 0.1
Saccharide composition				
Glucan (wt.%)	41.8	40.3	28.9 $\pm$ 0.7	28.9 $\pm$ 0.7
Mannan (wt.%)	2.8	11.6	0	0
Galactan (wt.%)	0	1.5	0	0
Xylan (wt.%)	11.8	4.2	13.7 $\pm$ 0.8	13.7 $\pm$ 0.8
Arabinan (wt.%)	0.5	1.5	3.8 $\pm$ 0.1	3.8 $\pm$ 0.1
Total ash (wt.%)	0.2 $\pm$ 0.1	0.1	1.9 $\pm$ 0.3	1.1 $\pm$ 0.0
Na (mmol kg^{-1})	0 $\pm$ 0	1 $\pm$ 1	2.9 $\pm$ 0.9	0.6 $\pm$ 0.3
K (mmol kg^{-1})	0 $\pm$ 0	1 $\pm$ 0	4.7 $\pm$ 1.1	0.4 $\pm$ 0.1
Mg (mmol kg^{-1})	0 $\pm$ 0	0 $\pm$ 0	4.9 $\pm$ 0.7	0.2 $\pm$ 0.0
Ca (mmol kg^{-1})	2 $\pm$ 0	1 $\pm$ 0	20.9 $\pm$ 2.5	1.1 $\pm$ 0.2
S (mmol kg^{-1})	-	-	23.7	22.8
N (mmol kg^{-1})	-	-	714	714

2.2.3 Pretreatment

Biomass pretreatment was carried out in a 200 mL stirred autoclave equipped with heating mantle and cooling jacket. Typical operating conditions were 10 wt.% biomass loading, 180-200°C and a reaction time of 1-5 h in a solvent mixture composed of water and/or ethanol and/or acetic acid. The experimental procedure of such experiment is schematically depicted in Figure 2.1. Prior to an experiment a leak test was performed, whereafter air was dissi-

pated from the reactor by flushing (3x) with nitrogen. After heating the autoclave was kept at the desired temperature for a set time. Hereafter the reactor was cooled to room temperature.

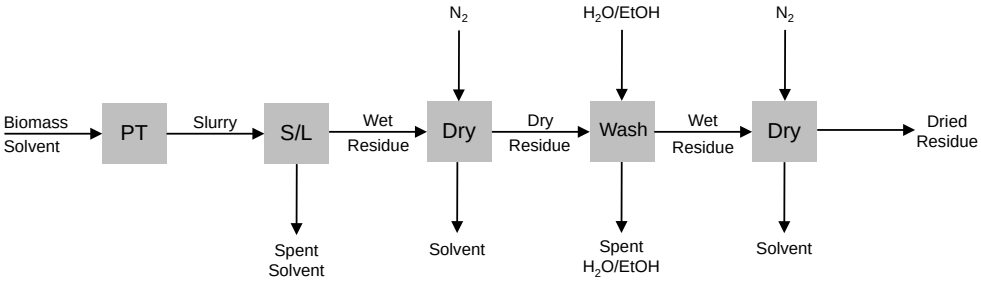

Figure 2.1: Schematic experimental pretreatment procedure.

The reactor content was filtered over a 5 µm wire mesh, see *"S/L"* in Figure 2.1. The wet cake was compressed in a pneumatic filter press under a pressure of $\sim$10 bar to squeeze out additional spent solvent. This solvent is defined as *"free liquid"*. Solvent that was not collected after filtration was removed by drying of the wet solid residue under a N_2 stream at room temperature until the weight of the solid residue remained constant, see *"Dry"* in Figure 2.1. This solvent is defined as *"trapped liquid"*.

The dried residue was washed with an ethanol water mixture (50/50 w/w) to remove deposited material such as lignin and sugars. Washing was performed in a stirred vessel at room temperature and the washing liquor was replenished after >24 h, until the liquor did not show significant colour change, see *"Wash"* in Figure 2.1. The washed residue was subsequently dried under a N_2 stream until no weight change was registered. The solid residue yield was calculated according to equation 2.2 in which $m_{\text{solid-residue}}$ is the mass of solid residue after washing and m_{Biomass} the mass of biomass fed.

$$Y_{SR}\ (\text{wt.\%}) = \frac{m_{\text{Solid residue}}}{m_{\text{Biomass}}} \times 100 \tag{2.2}$$

The composition of the feed and solid residue was determined following the procedures described in section 2.3.1. In combination with the solid residue yield, this allows us to calculate the retention, i.e. the fraction of a component that is present in the solid residue compared to the feed, see equation 2.3.

$$\text{Retention (wt.\%)} = \frac{f_{X,\text{Solid residue}} \times Y_{SR}/100}{f_{X,\text{Biomass}}} \times 100 \tag{2.3}$$

The lignin content of the spent solvent and washing liquors was determined by 1) precipitation of lignin by water addition (3:1 water to solvent ratio), 2) centrifugation of the emulsion and removal of the liquid fraction 3) washing of lignin by water and removal of this washing water 4) drying of lignin in the fumehood until no weight change was noted. The concentration of lignin in solvent follows from equation 2.4. The mass of solvent was corrected for the mass of the dissolved solids.

$$C_{\text{Lignin}} = \frac{m_{\text{Lignin}}}{m_{\text{Solvent}}} \tag{2.4}$$

2.3 Analytical procedures

2.3.1 Biomass characterisation

The composition of untreated and treated biomasses were determined based on well established protocols. The extractives content were quantified by soxhlet extraction with water (24 h) and thereafter ethanol (24 h) after intermittent drying following[94]. A two-step hydrolysis procedure performed in duplicate was used to determine the lignin, sugar and o-acetyl content[95]. In this procedure polysaccharides are hydrolysed to monosaccharides and o-acetyl groups to acetic acid whereas lignin remains as solid residue. Lignin was determined gravimetrically after drying of the solid residue. Sugars and o-acetyl groups were quantified via HPLC analysis of the liquid fraction. The ash content of biomasses was assessed via dry oxidation at 575°C for 24 h[96]. The AAEM content of this ash was quantified via ion chromatography (IC) after dissolution of the sample in 0.01 M nitric acid. Following the same procedure, a large batch of ash was prepared to be used as additive in hydrogenolysis experiments. The AAEM content of this batch was: 2.4 wt.% Na, 13.4 wt.% K, 0.6 wt.% Mg and 2.9 wt.% Ca.

2.3.2 High performance liquid chromatography (HPLC)

HPLC analysis was used to analyse the hydrogenolysis and acid hydrolysis liquids. Regular calibration of relevant components was performed to allow for quantification of the products of interest. The HPLC machine (Agilent

1200 series) was equipped with a refractive index detector (RID) and variable wavelength detector (VWD) operated at 285 nm and operated in two different configurations 1) with (Hi-Plex-H^+ column) operated at 65°C, running with 5 mM H_2SO_4 as eluent (0.6 mL min^{-1}) to fractionate the hydrogenolysis effluent and 2) Hi-Plex Pb column at 70°C and deionized water as eluent (0.6 mL min^{-1}) to separate monosaccharides. The samples were filtered (Whatman 0.2 µm filter) and diluted when necessary prior to HPLC analysis.

2.3.3 Ion chromatography (IC)

Sodium, potassium, calcium and magnesium content of the samples were quantified based on ion chromatography (IC) performed on a Metrohm 850 Professional IC equipped with a Metrosep C6 - 150/4.0 column at 20°C, running 0.1 M HNO_3 + 0.02 M dipicolinic acid as mobile phase. Samples were filtered (Whatman 0.2 µm filter) prior to analysis.

2.3.4 S and N quantification

The sulphur and nitrogen content of feedstocks were determined according to ASTM protocols, namely D1552 for sulphur and D5291 for nitrogen in case N > 1000 mg kg^{-1} else D5762 was applied.

Ethylene glycol from lignocellulosic biomass: the impact of lignin on catalytic hydrogenolysis

"Whenever you find yourself on the side of the majority,
it is time to pause and reflect."

- Mark Twain -

Abstract

Short polyols, such as ethylene glycol (EG), are a popular target of catalytic hydrogenolysis of saccharides. However, studies on the use of untreated or pretreated lignocellulosic biomass as feedstock for polyols production are scarce. In this work, we have studied the impact of lignin on the catalytic hydrogenolysis of different biomass samples, targeting ethylene glycol. We have first developed a hydrogenolysis protocol that is sensitive to lignin and feedstock impurities, such as ash and extractives. A matrix of biomass feedstocks with varying lignin content has been evaluated, by subjecting poplar, pine and hay, to solvent-based (water/ethanol/acetic acid) pretreatments and by preparing physical mixtures of pure microcrystalline cellulose with organosolv lignin. Lignin appeared to inhibit the activity of the hydrogenation catalyst, Raney nickel, by hindering the formation of sugar alcohols in the presence as well as in the absence of the tungstate catalyst. However, lignin is not the root cause for the low EG yield typically obtained with untreated lignocellulose, as treated lignocellulose delivered high EG yields (30-35 wt.%), irrespective of the lignin concentrations, which varied between 0 and 44 wt.%, under identical demanding experimental conditions.

This chapter is based on the following publication:

T.D.J. te Molder, S.R.A. Kersten, J. P. Lange and M. P. Ruiz, *Ethylene Glycol from Lignocellulosic Biomass: Impact of Lignin on Catalytic Hydrogenolysis*, **Industrial & Engineering Chemistry Research**, 2021, 60, 19, pp. 7043–7049, DOI: 10.1021/acs.iecr.1c01063

3.1 Introduction

The current benchmark for selective bio-ethylene glycol production is a multi-step process that proceeds via fermentation of sugar to ethanol followed by dehydration to ethylene[15], which is subsequently converted to ethylene glycol (EG) via the traditional petrochemical route[32]. A more direct route, but unfortunately unselective, is by hydrogenolysis of sugars, which leads to a mixture of EG, propylene glycol (PG) and glycerol[97],[98]. These polyols have been a popular target product from sugar because of their favourable match in atomic composition[97]. The seminal paper by Zhang et al.[99] demonstrated that the selectivity towards EG can be boosted by the use of a tungsten-based bifunctional catalyst. This new route has received significant attention from academia[46] and industry since then.

Cellulose is the most abundant saccharide available, at modest cost, and therefore an interesting feedstock for hydrogenolysis to EG. Various authors have reported the successful conversion of microcrystalline cellulose to EG with yields as high as $\sim$75 wt.%[68],[100],[101]. Typically, the conversion is performed in hot compressed water at 245°C[65], often supplemented with an acid[72], which facilitates in-situ depolymerisation of cellulose to glucose[76]. After hydrolysis, glucose undergoes aldol cleavage to glycolaldehyde, catalysed by a homogenous W-species, and is subsequently hydrogenated to EG over a metal catalyst[40],[76], see Figure 1.2 in Chapter 1. Propylene glycol (PG) is produced via a similar route, but it derives from fructose, which is formed by isomerisation of glucose. The production of these glycols (EG and PG) competes with thermal side reactions (e.g. HMF and humin formation) and the direct hydrogenation of (mono)-saccharides to sugar alcohols (SA). A proper balance between hydrogenation and aldol cleavage activity is required to yield EG[70]. This balance shifts to SA production in case the W-catalyst deactivates and to thermal side products when the hydrogenation catalyst deactivates.

However, native cellulose is usually present in a matrix made of lignin ($\sim$15-30 wt.% dry basis) and hemicellulose, in a form called lignocellulose. Understanding the impact of lignin on catalytic hydrogenolysis is key for the development of a suitable pretreatment technology that enables subsequent metal-based catalysed valorisation of the saccharide fraction. Lignin could impact the catalytic conversion to EG in several ways. For example, lignin may shield the cellulose, thus making it less accessible[102] for further conversion, or

lignin may impact the activity of the catalytic system (Figure 1.2 in chapter 1). Hence, several authors explored the potential of pretreatments to free the feedstock from potentially undesired lignin. We carefully analysed these past studies[64],[75],[91],[103],[104] (see Appendix A.3) and recognized that several studies underestimated their glycol yield at high lignin content because they reported it on biomass intake rather than saccharide intake[75],[91],[104]. After expression on holocellulose intake, some datasets still showed an inverse relationship between lignin content of the feed and EG yields[75],[91] (see open symbols in Figure 3.1). However, data from other studies, e.g. by Li et al.[64], show no clear relationship between the EG yield and the lignin content of different untreated feedstocks (see closed symbols in Figure 3.1).

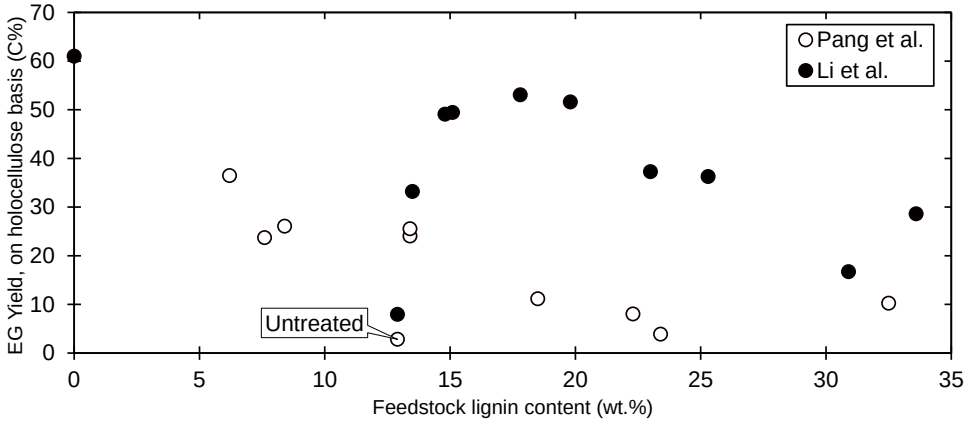

Figure 3.1: EG yield as function of the feedstock lignin content, based on hydrogenolysis data of untreated and pretreated corn stalk from Pang et al.[75] (open symbols) and of different untreated feedstocks from Li et al.[64] (closed symbols) Note: EG yields for the study by Pang et al.[75] were recalculated on holocellulose basis instead of biomass basis as reported in the original work, see Appendix A.3 for details.

Obviously, there is no clarity yet on the role of lignin in the catalytic hydrogenolysis to EG. In this context, the aim of this study is to elucidate the role of lignin on this reaction and investigate if lignin could be the cause of possible catalyst deactivation. To do that, the hydrogenolysis conditions were selected to maximize the sensitivity of the hydrogenolysis to lignin, rather than maximizing the EG yield. Three lignocellulosic biomass archetypes, namely hay (herbaceous), poplar (hardwood) and pine (softwood) were selected, to rule out feedstock as the key variable. Moreover, different solvent-based

(water/ethanol/acetic acid) pretreatments were applied to these feedstocks to create samples with a wide varying residual lignin content (0-44 wt.%). Additionally, physical mixtures of pure Avicel® cellulose and organosolv lignin have also been evaluated. Furthermore, we have studied the impact of lignin on the hydrogenation catalyst alone, by running tungstate-free experiments.

3.2 Results and discussion

3.2.1 Hydrogenolysis protocol

In this work, a sensitive hydrogenolysis protocol to maximize the deactivating role of feedstock components (e.g. lignin) has been designed. In our experiments, both a soluble tungsten species (sodium polytungstate, hereafter referred to as W-catalyst), and Raney nickel catalyst (referred to as Ni-catalyst) have been employed. Furthermore, a 2 wt.% buffered acetic acid solution has been used to control the pH around ∼3.3. Besides the main products (EG, PG, SA), numerous side products are formed in minor amounts, such as 1,2-butanediol, erythritol, glycerol, light alcohols and light organic acids. However, for the sake of clarity, we limit the discussion to the main products, EG, PG and SA.

We investigated the impact of W and Ni loading on product yield for biomass loading of 1 wt.% and found little yield differences when using pure cellulose or untreated poplar, see Appendix (A.1.2 and A.1.3). It is worth noting that changes in the structure of the biomass after pretreatment (e.g. improved cellulose accessibility) could also have an impact on the performance of the hydrogenolysis system (Figure 1.2 in Chapter 1). However, when operating in excess of catalyst at 1 wt.% biomass loading, it was observed that both untreated poplar (<53 µm) and micro crystalline cellulose (∼50 µm) resulted in similar EG yields (∼40 wt.%) (see Appendix A (Table A.1, entries 1 & 2)). This means that lignin is not hindering the micro-accessibility (i.e. at the cell wall level), at least for these feeds under the conditions studied.

A similar observation was made for poplar, basswood, ashtree and birch (∼50 wt.% EG yield), compared to microcrystalline cellulose (61 wt.% EG yield), in the work of Li et al.[64], see Figure 3.1. Also, from the studies by Pang et al.[91] and Zhou et al.[104] on Miscanthus and Jerusalem artichoke, respectively, it was concluded that pretreated and untreated samples gave the same EG yield (on holocellulose basis), when operating at 1 wt.% biomass loading,

see Appendix A.3 (Figure A.7 and Figure A.11). Thus, all these observations indicate that the biomass structure is not significantly limiting the EG yield. It also suggests that differences in the lignin structure in the various feedstocks may not critically impact the catalytic hydrogenolysis. This preliminary conclusion would require further studies for confirmation.

Nevertheless, operation at high biomass loading will be imperative for commercial operation, as discussed elsewhere[105]. We then raised the biomass loading to 5 wt.% and increased the catalysts loading proportionally, as proposed in the literature[91], and found again limited difference between pure cellulose and untreated lignocellulose, see Appendix A (Table A.1, entries 3 & 4). We then decided to increase the sensitivity of the protocol for catalyst poisoning by raising the biomass loading without raising the catalyst loading. With 5 wt.% biomass loading and 0.03 W-catalyst/biomass and 0.12 Ni/Biomass mass ratio, we eventually achieved good differentiation, with an EG yield of 32.2 ($\pm$0.5) wt.% (n=2) for microcrystalline cellulose, but only 8.3 ($\pm$0.4) wt.% (n=2) for untreated poplar, 8 wt.% for pine and 4 wt.% for hay. Details on the development of this hydrogenolysis protocol can be found in the Appendix A.1.1.

3.2.2 W-catalyst free experiments

We hypothesized that lignin may foul the hydrogenation catalyst, thereby blocking and inhibiting the hydrogenation of intermediates (e.g. glycolaldehyde, mono-saccharides), which would result in poor EG, PG and SA yields. Similar statements have been postulated previously[75],[91].

To systematically study the deactivation of the hydrogenation catalyst by lignin, W-catalyst free experiments with physical mixtures of cellulose and organosolv lignin in varying ratios were run. In the absence of W-catalyst, the dominant reaction product should be SA (see Figure 1.2 in Chapter 1). Indeed, SA was the main product for pure cellulose experiments, with 32 $\pm$ 0.8 wt.% yield (performed in duplicate), but the yield dropped to $\sim$13 wt.% when cellulose was mixed with 5 wt.% of lignin, and decreased further at higher lignin loading, e.g. to 9 wt.% at 25 wt.% lignin (see Figure 3.2, open circles). Note that the product yields are not limited by incomplete cellulose conversion as a catalyst free experiment gave a cellulose conversion > 90 wt.% after 1 h. Data for untreated poplar and pine appeared on the same line, as did a pretreated poplar sample with 39 wt.% lignin (see Figure 3.2, crosses and

closed triangle). A pretreated sample with 3.6 wt.% lignin showed a higher SA yield than expected. In contrast, untreated hay fell well below the line with only 2 wt.% of SA (see Figure 3.2, cross).

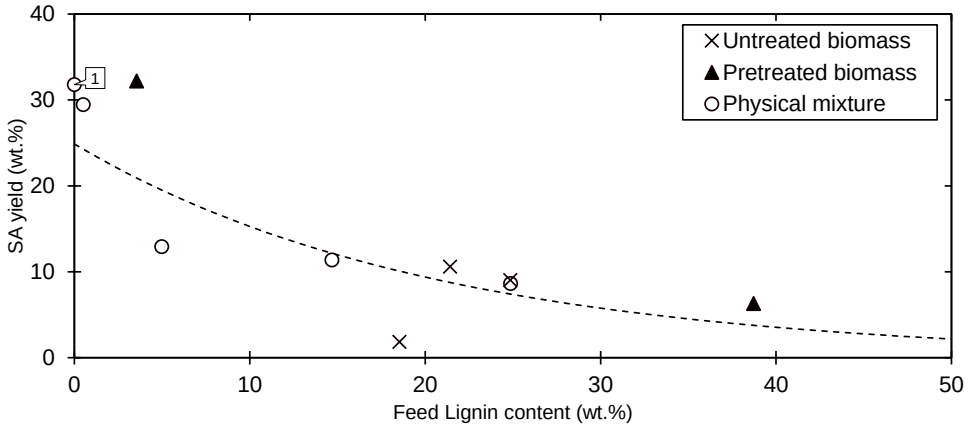

Figure 3.2: SA yield after hydrogenolysis over Raney nickel. Relevant conditions; 0.12 Ni-catalyst to biomass ratio biomass loading = 5 wt.%, T = 245°C, t = 1h, P_{H2} (initial) = 60 bar, $pH_{Initial}$ = ∼3.3, Ni-catalyst to biomass mass ratio 0.12. Experiment 1 was performed in duplicate, the error (±0.8 wt.%) bar is too small to be observed. Lines drawn for clarity.

This leads to the following conclusions. Firstly, lignin might deactivate the hydrogenation catalyst. This statement is further supported by a correlation coefficient of -0.85 between the SA yield and feed lignin content. Secondly, this deactivation appears similar for the native lignin found in untreated feedstock and the process lignin found in pretreated feed and used for cellulose/lignin mixtures, which suggests that the cellulose-lignin interaction does not significantly affect the hydrogenolysis outcome under the conditions studied. Thirdly, there seems to be other deactivating elements than lignin, as indicated by the hay experiments. This point warrants further studies.

Figure 3.2 is also conveying a worrisome message. The Ni-catalyst appears to lose ∼50% of its initial activity after having seen about half its weight of lignin. However, industrial processes are reported to normally operate with an overall catalyst consumption of 1 kg per ton of product[105]. Unless the Ni-catalyst activity stabilizes after initial poisoning with lignin, such consumption target would then limit the lignin content of the feed to the impractical level of some <0.1 wt.% or would require the Ni-catalyst to be regenerable. Both options clearly need further studies.

3.2.3 W-catalyst + Ni-catalyst

Then, pretreated biomass samples with varying lignin contents and physical mixtures of cellulose and lignin in the presence of W-catalyst and Ni-catalyst were tested, to study the overall deactivating role of lignin on EG yield according to our hydrogenolysis protocol (5 wt.% biomass loading, 0.12 Ni-catalyst to biomass ratio and 0.03 W-catalyst to biomass ratio).

Hydrogenolysis experiments are labour intensive, therefore, three key data points were selected and run in duplicate to validate the reproducibility of our protocol and labelled in Figure 3.3, as 1, 2 and 3. The error of these experiments is small, i.e. the error bars are typically too small to be observed and the difference in EG yield is less than ± 1 wt.%. This shows that our measurements are reproducible and, therefore, reliable.

When running experiments under our sensitive test conditions, it was confirmed that untreated biomass delivered much lower EG yield, namely 4 to 8 wt.% (see crosses in grey area in Figure 3.3), instead of 32 wt.% for cellulose. It was found that the EG yield for pretreated biomass was either very similar to the untreated biomass, namely $\leq$10 wt.%, or similar to pure cellulose at $\sim$32 wt.% (see filled triangles in Figure 3.3). Thus, no plausible relation with the feed lignin content was observed (correlation coefficient of -0.05, see Appendix A.3.6). In fact, very high EG yield, $\sim$35 wt.%, is obtained for a sample with an extremely high lignin content (39 wt.%). Moreover, the addition of organosolv lignin to cellulose as physical mixture also delivered similarly high EG yields, irrespective of lignin content. This also suggests that the precise location of lignin, i.e. bulk or surface, may not be critical, but this hypothesis requires further studies. These results suggest that the beneficial effect of most pretreatments on the EG yield is not so much due to the removal of lignin, but to other changes in the biomass. The topic is subject of further investigation in our laboratory.

We realised here that the effective catalyst to holocellulose ratio is increasing (by $\sim$30%) as lignin content of the feed is reduced from 25 to 0 wt.%, and this could affect the EG yield. But this possibility could be discarded by an additional test with constant holocellulose content, instead of constant biomass content, see Figure A.5 in Appendix A.2.1.

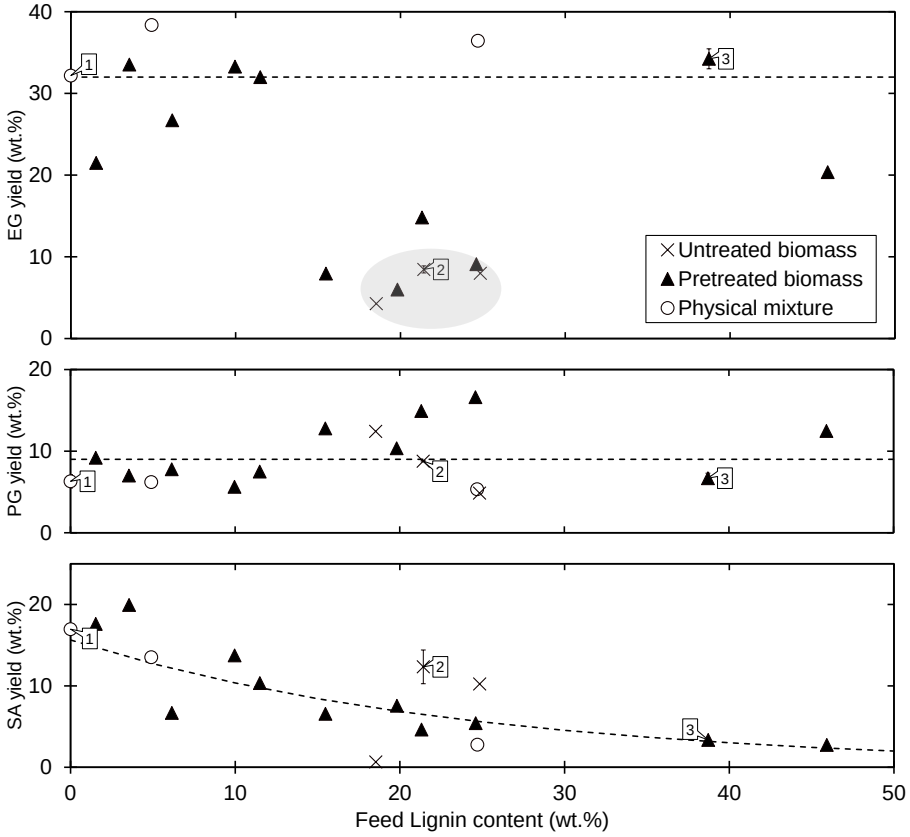

Figure 3.3: Product yields (EG, PG and SA) as a function of the feedstock lignin content in the catalytic hydrogenolysis. Reaction conditions: 5 wt.% biomass loading, T = 245°C, t = 1h, P_{H2} (initial) = 60 bar, $pH_{Initial}$ ∼3.3, Ni-catalyst to biomass mass ratio 0.12, W-catalyst to biomass mass ratio 0.03. Experiments 1, 2, 3 were performed in duplicate, the error bars are typically too small to be observed. Lines and grey area drawn for clarity. A more detailed figure is provided in Appendix A Figure A.6.

The lignin content of pretreated samples and physical mixture of cellulose and lignin did not seem to affect the PG yield (Figure 3.3). However, it depressed the competitive hydrogenation of sugar to SA (correlation coefficient of -0.65), as was also previously observed for W-catalyst free experiments (see Figure 3.2). Here untreated poplar and pine fell outside this general trend by delivering higher SA yield than treated samples or physical mixtures of similar lignin content (see Figure 3.3). The SA yield of ∼12 wt.% is fairly similar as for W-catalyst free experiments, namely ∼10 wt.% (see Figure 3.2), while the

EG yields was very poor (8 wt.%). This all suggests that the W-catalyst was readily deactivated.

Lignin inhibits the hydrogenation of saccharides over Raney nickel to SA, but retains sufficient activity to hydrogenate EG and PG intermediates which are notoriously more reactive[84]. Apparently, hydrogenation of GA to EG is not rate-limiting under the current concentrations and conditions, even at such low Ni-catalyst/biomass ratio of 0.12. Moreover, it has been observed that lignin does not significantly affect the aldol cleavage reaction. Most importantly, lignin is not the root cause for the low EG yield after hydrogenolysis of untreated lignocellulosic biomass. The true root cause should be sought elsewhere and is currently under further investigation.

3.2.4 Comparison with previous studies

These observations contradict earlier studies[75],[91] claiming that lignin is a key inhibitor in the catalytic hydrogenolysis to EG. An overview of relevant literature studies is presented in Table 3.1. Also, a statistical analysis of the literature data and results in this work was performed. Several studies reported their glycol yield on biomass intake[75],[91],[104], and were recalculated on holocellulose intake for the present discussion. Consequently, the reported depression of EG yield by lignin vanishes for pretreated Miscanthus (Pang et al.[91]) and for pretreated Jerusalem artichoke (Zhou et al.[104]), two herbaceous type biomass, when running at 1 wt.% biomass loading (see Appendix A.3 Figures A.7 and A.11).

A key dataset is provided by Li et al.[64] , who performed hydrogenolysis of 10 untreated lignocellulose species over Ni-W_2C catalysts at 1 wt.% biomass loading. The EG yields obtained in their work versus the respective lignin content of the feedstocks are plotted in Figure 3.1. Interestingly, hydrogenolysis of various untreated hardwood species (poplar, basswood, ashtree and birch) gave EG yields of 49 C% or higher, comparable to hydrogenolysis of microcrystalline cellulose (Y_{EG} = 61 C%). There is no apparent relation between the feedstock lignin content and the EG yield, which is supported by a poor correlation coefficient of -0.26 which we found for the dataset of Li et al.[64], see Appendix A.3.6. In fact, the poorest EG yield, 8 C%, was obtained for corn stalk, which had the lowest lignin content, 13 wt.%, of all untreated feedstocks. In a different study, Pang et al.[75] also observed a low EG yield of only 3 C% for untreated corn stalk. It is therefore unconvincing from Pang

et al.[75] to label lignin as key inhibitor for the hydrogenolysis of corn stalk. Furthermore, Pang et al.[75] found much higher EG (∼25 C%) and PG (∼15 C%) yields for pretreated samples of similar lignin content as the untreated feed (EG ∼3 C% & PG ≤3 C%).

*Table 3.1: Studies that investigated the catalytic hydrogenolysis of (pretreated) biomass targeting EG and PG. *A bifunctional catalyst was used.*

Study	Feedstock	Catalyst	Biomass loading (wt.%)	W-catalyst / biomass (w/w)	Hydrogenation-catalyst / biomass (w/w)
Pang et al.[75]	(Pretreated)-corn stalk	2% Ni-W_2C	1	0.3*	0.3*
Li et al.[64]	Various	4% Ni- 30% W_2C/AC	1	0.4*	0.4*
Zhou et al.[104]	(Pretreated)-Jerusalem artichoke	WO_3 + Raney Ni	1	0.3	0.3
Pang et al.[91]	(Pretreated)-Miscanthus	H_2WO_4 + Raney Ni	1, 6, 10	0.12	0.12
Fabičovicová et al.[103]	(Pretreated)-barley straw	Ru-W/AC	4.8	0.1	0.1*
This work	(Pretreated)-poplar, pine, hay	SPT + Raney Ni	5	0.03	0.12

The studies by Fabičovicová et al.[103] on barley straw and by Pang et al.[91] on Miscanthus were performed at substantially higher biomass loading (≥4.8 wt.%). In the work by Fabičovicová et al.[103] the EG yield was 2 C% for untreated barley straw, whereas an EG yield of 24 C% was obtained for a pretreated sample with similar lignin content (∼20 wt.%) as the untreated barley straw. Furthermore, the EG yield optimum was not found at the samples with the lowest lignin content. Again, these data hint that lignin is not the key inhibitor.

In the work by Pang et al.[91] for experiments at higher biomass loading (≥6 wt.%), the lignin content of the feed correlated very well with the EG yield (-0.96). However, pretreatment, considered as a binary parameter, resulted in a good correlation as well (0.8). It is therefore not possible to ascribe the increase in EG yield solely to the feedstock lignin content. Furthermore, the lignin content range of this dataset was limited, namely from 1.4 wt.% to 16 wt.%, and no samples with higher lignin content than the untreated feed were tested. Note that our hydrogenolysis protocol was very similar to the

hydrogenolysis protocol applied by Pang et al.[91] on the catalytic hydrogenolysis of Miscanthus. Both studies applied the same Raney nickel to biomass ratio (0.12). However, in our study 4 times less W-catalyst was used, namely a W-catalyst to biomass mass ratio of 0.03, compared to 0.12 in the work by Pang et al.[91] Beyond the study by Li et al.[64] , all other studies share the choice for a herbaceous type biomass (Miscanthus[91], barley straw[103], Jerusalem artichoke[104], corn stalk[75]). These are typically richer in extractives and ash and leaner in lignin, compared to woody biomass[27],[106]. In view of the literature results and this work, it can be concluded that lignin inhibits the hydrogenation function, but is not the key inhibitor on the EG yield.

3.3 Conclusion

In this work, we have focused on the conversion of three lignocellulosic biomass archetypes, hay (herbaceous), poplar (hardwood) and pine (softwood), which are inexpensive and abundant feeds. We investigated the impact of lignin on the hydrogenolysis performance.

A hydrogenolysis protocol that is sensitive to lignin and feedstock impurities, such as ash and extractives, has been developed. It also allows pH control and decoupling of the acidic, aldol cleavage and hydrogenation functionalities of the hydrogenolysis system (Figure 1.2 in Chapter 1). Key experiments were performed in duplicate and showed that the reproducibility of the hydrogenolysis test is very high, i.e. the EG yield difference between the duplicates was less than ± 1 wt.%). Under the same experimental conditions, untreated biomass gave a poor EG yield (4-8 wt.%), whereas microcrystalline cellulose gave an EG yield of 32 wt.%, at 5 wt.% biomass loading. However, a similar EG yield ($\sim$40 wt.%) for poplar (<53 µm) and cellulose at 1 wt.% biomass loading was obtained when operating in excess of catalyst. This shows that the EG yield was not limited by micro-accessibility of cellulose (at cell-wall level) in our tests, which evidences that our hydrogenolysis test is truly sensitive to feedstock impurities, e.g. potentially lignin.

W-catalyst free experiments showed that the hydrogenation catalyst is inhibited by lignin as the SA yielded decreased from 33 wt.% to 6 wt.% with increase in feed lignin content. This observation holds for physical mixtures of cellulose and lignin, as well as pretreated biomass samples. Native lignin (i.e. untreated biomass) did not deviate from processed lignin. The SA yield also decreased with increasing the feed lignin content for experiments with both W-catalyst and hydrogenation catalyst present. However, the EG yield did not show an apparent relation with the feed lignin content. Blends of cellulose and lignin powder systematically gave high EG yields, $\geq$ 32 wt.%. Pretreatment of biomass increased the EG yield in most cases to $\sim$32 wt.%, even for a sample with a lignin content of 39 wt.%. Hence, an important distinction should be made: lignin inhibits the hydrogenation of sugars over Raney nickel to SA, but Raney nickel appears to maintain sufficient activity to hydrogenate the more reactive glycolaldehyde and glyceraldehyde to EG and PG, respectively.

Thus, lignin may deactivate the hydrogenation function, but is not the

root cause for the low EG yield obtained after hydrogenolysis of untreated biomass. Furthermore, the results show that the homogenous tungstate catalyst is not deactivated by lignin.

From woody biomass to ethylene glycol: Inorganics removal boosts the yield

"What You See is All There Is (WYSIATI)"

- Daniel Kahneman -

Abstract

Tungstate-catalysed hydrogenolysis of sugars in untreated woody biomass to ethylene glycol (EG) has so far been unsuccessful. This work shows that production of EG is predominantly hampered by the presence of inorganic impurities in the biomass, which can be selectively removed by an acid leaching step at room temperature. Catalytic hydrogenolysis of untreated and acid-leached samples of woody biomass was run at 245°C, using sodium polytungstate and Raney nickel catalysts at low loadings that make them sensitive to deactivation by biomass impurities. Acid-leached pine and poplar samples gave a combined glycol yield (ethylene glycol + propylene glycol) of ∼44 wt.%, similar to micro crystalline cellulose, whereas their untreated counterpart only delivered a yield of 22 wt.%. Measurement of the dissolved fraction of the homogenous tungstate catalyst, i.e. active catalyst after the experiment, was found to be a key predictor of the EG yield: inorganic contaminants as calcium are indeed shown to precipitate the tungstate catalyst.

This chapter is based on the following publication:

Thimo D. J. te Molder, Sascha R. A. Kersten, Jean-Paul Lange and M. Pilar Ruiz, *From Woody Biomass to Ethylene Glycol: Inorganics Removal Boosts the Yield*, **Industrial & Engineering Chemistry Research**, 2021, 60, 37, pp. 13515–13522, DOI: 10.1021/acs.iecr.1c02353

4.1 Introduction

Ethylene glycol (EG) is among the bulk chemicals that are of great interest to be produced from sugars with very high atom efficiency. In 2008 Zhang et al.[99] discovered a selective route to convert saccharides to ethylene glycol via a bifunctional tungsten-Ni catalyst. Tungstate was found to be active for the cleavage reaction of monosaccharide to glycolaldehyde, which was subsequently hydrogenated over a metal catalyst, e.g. Raney nickel, to ethylene glycol, see Figure 1.2 in Chapter 1. Initially heterogeneous catalysts were developed[46],[67]–[69],[76], but they appeared to suffer from leaching of W to the reaction medium[64],[67]–[69]. On the contrary, a binary catalytic system of Raney nickel or Ru/C and tungstic acid could be recycled at least 20 times without significant loss of EG yield[70],[71]. We therefore selected similar catalysts, homogenous sodium polytungstate and heterogenous Raney nickel.

Cellulose is an attractive feedstock for hydrogenolysis as it is the most abundant polysaccharide available. Moreover, it is typically run in acidified hot compressed water ($\sim$245°C), which facilitates in-situ depolymerisation of cellulose. However, native cellulose is entangled by lignin and hemicellulose, which could inhibit the catalyst(s). When run in excess of catalyst, still similar yields for untreated biomass and microcrystalline cellulose were obtained, but when operating under catalyst lean conditions, untreated biomass delivered substantially lower EG yield than microcrystalline cellulose[66]. This means that one or multiple components present in biomass deactivate the catalyst(s). We have already shown in a previous study (Chapter 3) that lignin is not the key inhibitor[66].

Studies on catalyst deactivation for this specific chemistry and conditions are limited, but Pang et al.[90] previously showed that divalent ions (Mg, Ca, Fe) present in biomass, such as calcium, form insoluble tungstate precipitates (e.g. $CaWO_4$), which are not catalytically active. However, they performed hydrogenolysis of microcrystalline cellulose mixed with well soluble chloride-salts, which undermines the complexity of native biomass. Moreover, they applied a not representative and unrealistically high cation to WO_x molar ratio during their experiment (e.g. 1.4 for Calcium to WO_x)[90]. Thus, in their experiments, the presence of divalent ions in biomass does not readily explain low EG yields obtained after hydrogenolysis of untreated biomasses.

In our previous work (Chapter 3)[66], we developed a hydrogenolysis proto-

col that is highly sensitive to catalyst poisons. We demonstrated that lignin was not the main responsible for the low EG yield observed with untreated biomass and concluded that it did not significantly affected the hydrogenation of glycolaldehyde to EG[66]. Moreover, the previously discussed study by Pang et al.[90] provides a hint that inorganics present in biomass harm the WO_x-catalyst. Therefore, we hypothesized that the WO_x catalyst, which catalyses the cleavage of glucose to glycolaldehyde, was deactivated by inorganic components present in biomass. We have applied a novel low-severity pretreatment to selectively remove the majority of the inorganics from woody biomass, while leaving the cellulose, hemicellulose and lignin fractions untouched. These samples have been subjected to a poison-sensitive hydrogenolysis protocol[66] to study catalyst deactivation phenomena. Moreover, we have confirmed and quantified these effects by addition of corresponding model compounds to a cellulose reference experiment. To bolster the yield observations, we have developed a HPLC based analytical method to measure the quantity of dissolved tungstate, i.e. active tungstate catalyst, in the reactor effluent.

4.2 Results and discussion

4.2.1 Selective ash removal

In this work we have developed a method to measure the concentration of soluble sodium polytungstate after the experiment and reanalysed the effluent obtained after hydrogenolysis of (pretreated) biomass and physical mixtures of cellulose and lignin of our previous work (Chapter 3) with varying lignin content (0-44 wt.%)[66]. The pretreated samples were prepared by solvent-based (water/ethanol/acetic acid) pretreatments at 180-200°C for 0.5-5 h. The EG+PG yields appeared to drop with decreasing concentration of soluble W-species after the experiment, while all experiments started with the same catalyst and biomass loadings, see Figure 4.1. This means that components present in native biomass poison the tungstate catalyst, but can be removed by a pretreatment.

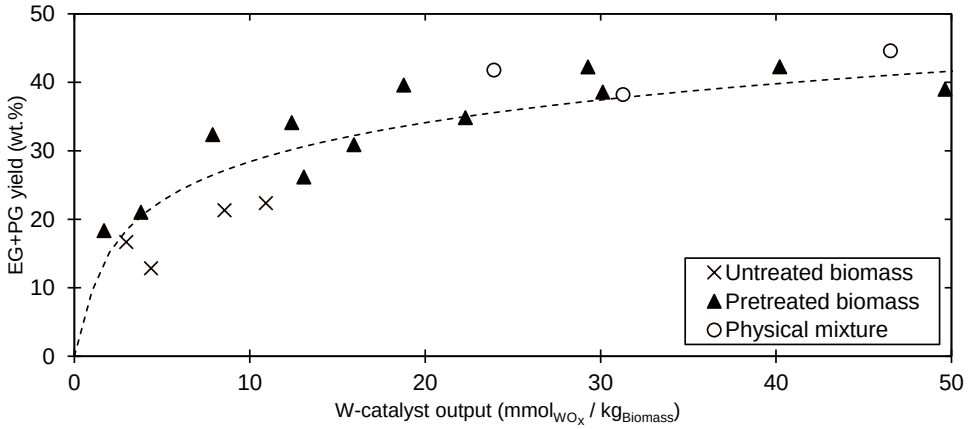

Figure 4.1: EG+PG yield expressed on holocellulose content for untreated biomass, pretreated biomass and physical mixtures of cellulose and lignin as function of W-catalyst output measured after the experiment per kg of biomass fed. EG+PG yield data from our previous work (Chapter 3)[66]. Reaction conditions: 5 wt.% biomass loading, T = 245°C, t = 1h, P_{H2} (Initial) = 60 bar, $pH_{Initial}$ ~3.3, Ni-catalyst to biomass mass ratio 0.12, W-catalyst to biomass mass ratio 0.03. Line drawn for clarity.

To test whether the removal of tungstate poisons from biomass by pretreatment is related to the inorganics content of the feed, poplar and pine wood were acid-leached with a solvent composed of 10 wt.% acetic acid in water for 24 h at room temperature, which selectively removes the majority of the ash and alkali and alkali earth metals (AAEM). Acid-leaching removed

some 80 wt.% of the total ash and >90 wt.% of the AAEM, see Table 2.1 in Chapter 2. We then subjected untreated and acid-leached feedstock to hydrogenolysis. The EG+PG yield of 45 wt.% observed for acid-leached poplar and acid-leached pine was identical to that of cellulose, our reference case, whereas untreated pine and poplar (n=2) gave a poor EG+PG yield of only ∼22 wt.% under our poison-sensitive conditions at a WO_4 input of 120 $mmol_{WOx}$ / $kg_{Biomass}$, see Figure 4.2. With increasing the tungstate loading, however, the combined glycol output of untreated poplar also started to approach that of cellulose.

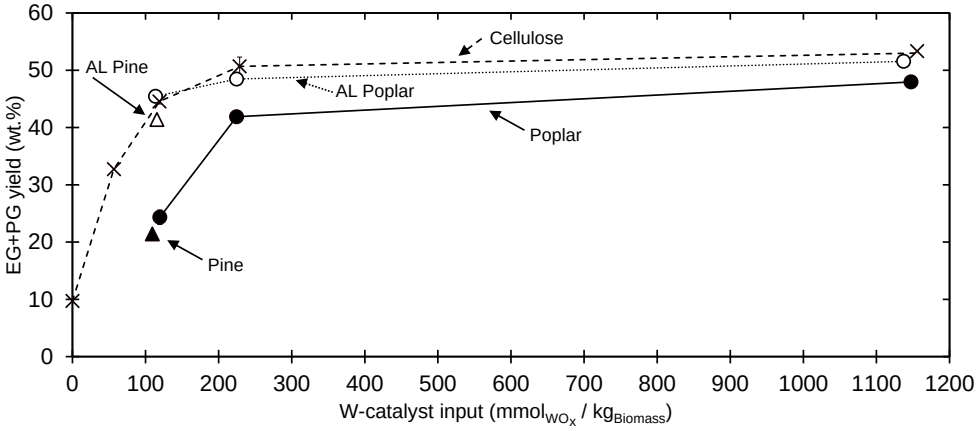

Figure 4.2: EG+PG yield expressed on holocellulose content for cellulose, poplar, pine, acid-leached poplar and acid-leached pine as function of W-catalyst input at the start of the experiment per kg of biomass fed. Reaction conditions: 5 wt.% biomass loading, T = 245 °C, t = 1 h, P_{H2} (Initial) = 60 bar, $pH_{Initial}$ ∼3.3, Ni-catalyst/Biomass mass ratio = 0.13. Experiments performed in duplicate: Poplar and cellulose at ∼120 and cellulose at ∼225 $mmol_{WOx}$ / $kg_{Biomass}$, error bars plotted but typically too small to be observed. Lines drawn for clarity

In fact, the EG+PG yields for (un)treated poplar, pine and cellulose are superimposed when plotted versus the output W concentration, see Figure B.6 in Appendix B, and was in line with the trend seen in Figure 4.1. Moreover, the EG+PG yield reported in Figure 4.1 and Figure 4.2 are superimposed when displayed against the output W concentration, see Figure B.3 in Appendix B. Thus, acid leaching clearly removes catalyst inhibitors that precipitate the tungstate catalyst.

Note that we report here EG+PG yield because the saccharide fraction of pine and poplar are partly composed of pentose (C_5), which delivers EG (C_2)

and PG (C_3), while cellulose is entirely composed of hexose (C_6), which theoretically could deliver solely EG (C_2). Due to the compositional difference, the woody biomasses delivered substantially higher PG yield of 9-12 wt.%, compared to ∼5 wt.% for cellulose, see Figure B.8 in Appendix B. On the other hand, cellulose gave some 5-9 wt.% more EG than acid-leached poplar and acid-leached pine, see Figure B.7 in Appendix B.

4.3 Addition of ash

To further investigate our hypothesis, we also added poplar ash to a cellulose reference experiment. The ash used as additive for these experiments was obtained by calcination of poplar at 575 °C for 24 h. Obviously, the ash is oxidized during combustion and therefore it is not fully representative of the ash present in native biomass. As can be observed in Figure 4.3, the EG yield plummeted from 45 wt.% to 28 wt.% after addition of just 1 wt.% ash to cellulose, which is comparable to the ash content of untreated poplar (0.8 ± 0.1 wt.%) and pine (0.6 ± 0.1 wt.%).

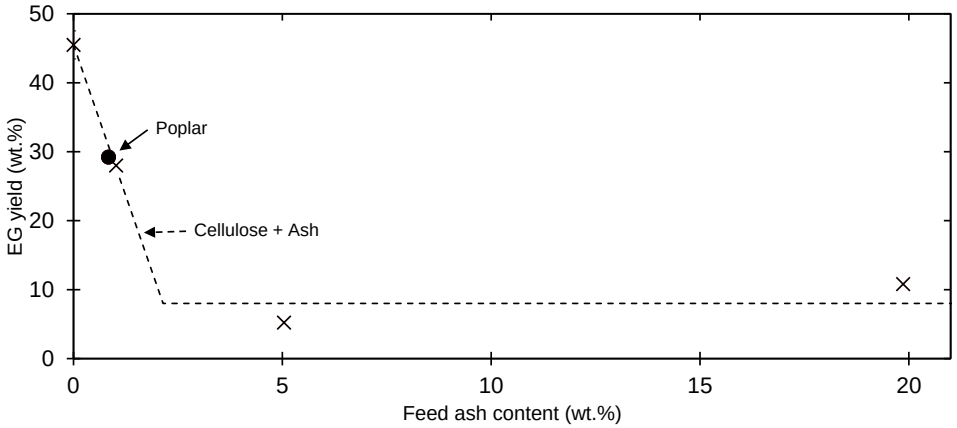

Figure 4.3: EG yield expressed on holocellulose content for mixtures of cellulose-ash and untreated poplar as function of the ash content of the feed (mixture). Reaction conditions: 5 wt.% biomass loading, T = 245°C, t = 1h,P_{H2} (Initial) = 60 bar, $pH_{Initial}$ ∼3.3, Ni-catalyst/Biomass mass ratio = 0.13 and W-catalyst/Biomass mass ratio = 0.06. The ash was obtained after combustion of poplar 575 °C for 24 h. Experiment with pure cellulose was performed in duplicate, error bars are plotted, but typically too small to be observed. Line drawn for clarity.

In fact, the EG yield obtained for untreated poplar was very similar, namely 29 wt.%. At the same time, the sugar alcohol (SA) yield increased slightly from

9 ± 2.5 wt.% to 14 wt.%, see Figure B.12 in Appendix B. This shows that the tungstate catalyst is deactivated by ash, but that the hydrogenation catalyst is still active. In addition, the W-catalyst concentration in the reactor effluent correlates with the EG yield, see Figure B.14 in Appendix B. When raising the share of ash in the feed mixture to 20 wt.%, however, the sugar alcohol yield drops to 3 wt.%, showing that large quantities of ash also inhibit the hydrogenation catalyst, see Figure B.12 in Appendix B. The increase in ash share in the feed mixture was accompanied by an increase in the pH of the reactor effluent. The pH was similar at 3.3-3.4 for the experiments performed with cellulose, untreated poplar and cellulose + 1 wt.% ash mixture, but rose substantially to 3.8 and 4.5 for mixtures with 5 and 20 wt.% ash, respectively, see Figure B.13 in Appendix B. pH measurement of the liquid effluent after the experiment is thus an easy tool to identify a probable impact of basic ash.

4.4 Addition of inorganic model compounds

It is now evident that inorganic components present in biomass (ash) precipitate the homogenous tungstate catalyst. To gain further understanding we subjected mixtures of cellulose and different salts to hydrogenolysis. Besides silica, alkali and alkaline earth metals are the most prominent inorganic constituents. Furthermore, trace amounts of iron, zinc and manganese are present in biomass. We evaluated their effect by adding the respective chloride salt, to the cellulose reference test at a 1:1 molar ratio of the cation to tungsten. We selected chloride salts for their relative high solubility in water. We are well aware that halogens, such as chloride, are poisonous to metal catalysts[107], such as Raney nickel, and we therefore performed a reference test with sodium chloride in a 20:1 molar ratio. Sodium was not expected to spoil the hydrogenolysis outcome as sodium tungstates are highly soluble[108]. Indeed, the addition of sodium chloride, even in a 20:1 molar ratio to the WO_x catalyst, did not reduce the ethylene-glycol yield, 51 wt.% compared to 46 ± 2 wt.% (n=2) for the reference test.

Once again the EG yield appeared to correlate well with the tungstate concentration measured in the reaction mixture after the experiment, see closed dots in Figure 4.4. At the same time, the product selectivity changed from EG to SA with decrease in W-catalyst output, as such that the sum of hydrogenated products (EG+PG+SA) remained 50-60 wt.%, see Figure B.15 in Appendix B. This test suggests that additives, which reduce the tungstate

concentration compared to the benchmark, form insoluble precipitates that are not catalytically active while the hydrogenation catalyst remained sufficiently active. Indeed, only 20% of the added calcium remained dissolved (Y_{EG} = 6 wt.%), whereas all the supplemented sodium (Y_{EG} = 51 wt.%) and potassium ($Y_{EG} \sim$ 48 wt.%) remained dissolved. These observations are in line with past reports on the solubility of various tungstates, i.e. poor solubility of calcium tungstate[109] and high solubility of sodium[108] and potassium tungstates. These results are also in agreement with the work by Pang et al.[90], who made the same observations after hydrogenolysis of microcrystalline cellulose and chloride salts. Moreover, Pang et al.[90] showed that $CaWO_4$ is inactive for aldol cleavage.

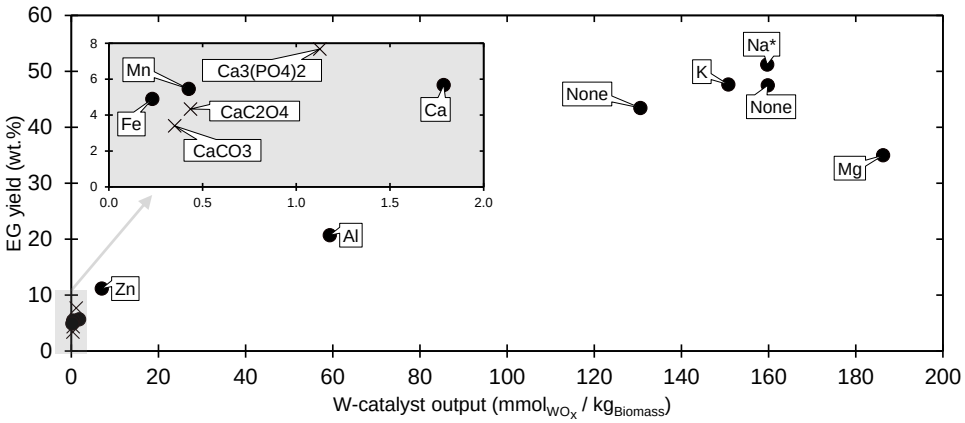

*Figure 4.4: EG yield after catalytic hydrogenolysis of cellulose in the presence of chloride salts (black dots) and various calcium salts (crosses) in a 1:1 cation to W molar ratio. *Sodium was added in a 20:1 molar ratio. **$CaSiO_3$ was added in a 1.5:1 cation to W molar ratio. Reaction conditions: 5 wt.% biomass loading, T = 245°C, t = 1h, P_{H2} (Initial) = 60 bar, $pH_{Initial} \sim$3.3, Ni-catalyst/Biomass mass ratio = 0.13 and W-cat/Bio ratio = 0.06. pH after the experiment is reported in Figure B.16 in Appendix B.*

Magnesium appears to deviate from the cluster seen around 160 mmol$_{WOx}$ / kg$_{Biomass}$, as it shows a low EG yield of 35 wt.% but a typical EG+PG+SA yield of ~60 wt.%. The change in selectivity towards SA suggests that magnesium is depressing the WO_x activity without precipitating it out of the solution, but requires further studies. A mildly negative effect of magnesium on the EG yield (46 C%) has been reported before (60 C% for the benchmark)[90].

We have noted a significantly lower pH (2.7) for the addition of aluminium

chloride compared to the benchmark experiments (3.2-3.3). The observed precipitation of tungstate by H^+ can, therefore, not be ruled out.

As the vast majority of cations in biomass are not present in the form of chlorides, we evaluated alternative and more representative calcium salts, namely, calcium carbonate, calcium oxalate, calcium phosphate and calcium silicate. These calcium salts are typically poorly soluble at neutral pH, but may show significant solubility at the acidic conditions under hydrogenolysis (pH $\sim$ 3.3). The EG yield was also low (< 8 wt.%) under the addition of these alternative calcium species. Again, the output tungstate concentration was low (< 2 $mmol_{WOx}$ / $kg_{Biomass}$), see crosses in Figure 4.4, and most of the calcium (> 70 wt.%) was consumed, indicating that tungstate was titrated by calcium. Thus a wide variety of calcium species deactivate the tungstate catalyst and are thereby detrimental for the EG yield. This suggests that their specific composition, i.e. cation-anion pair, can be ignored and that measurement of the feedstock divalent cation content would suffice to estimate the W-catalyst consumption

Albeit the poisoning effect of divalent ions, such as calcium, on tungstate species is evident, their presence in biomass does not readily explain the low EG output after hydrogenolysis of untreated biomass, compared to cellulose, as the tungstate to calcium+magnesium molar ratio in a typical WO_x-lean experiment with poplar is at least 3.6, and 1.5 for pine (See Appendix B.5.1). A potential explanation lies in the possible formation of tungstate salts (XWO_4) with non-equimolar distribution of tungstate and divalent ion, i.e. WO_x / X >1, which have previously been reported for calcium tungstates at acidic conditions[110], WO_x / Ca = 4 at pH = 5. We then ran several experiments with varied Ca^{2+} to WO_x molar ratio from 1 to 3 to find the stoichiometry, n, of the resulting $Ca(WO_x)_n$. An increase in added calcium resulted in a decrease in measured W-catalyst after the experiments, showing that calcium indeed precipitates the W-catalyst. Moreover, the EG yield versus the output W concentration roughly superimposed that of experiments with and without calcium, (Figure B.18 in Appendix B). The stoichiometry of the formed calcium tungstate $Ca(WO_x)_n$ appeared to be 1 as the amount of calcium that is consumed ($Ca_{Initial}$-Ca_{end}) was equal to the decrease in W-catalyst, see Figure 4.5. This observation is in line with the finding of Pang et al.[90], who observed $CaWO_4$ in the spent catalyst.

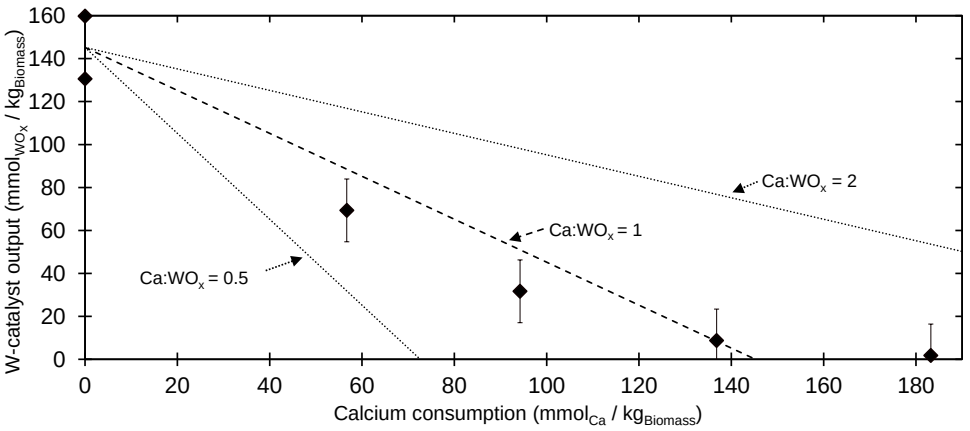

Figure 4.5: Measured quantity of W-catalyst in the reactor effluent after the experiment versus the amount of calcium consumed during the experiment ($Ca_{Initial}$-Ca_{End}). Reaction conditions: 5 wt.% biomass loading, T = 245° C, t = 1h, P_{H2} (Initial) = 60 bar, $pH_{Initial}$ ∼3.3, Ni-catalyst/Biomass mass ratio = 0.13. pH after the experiment was between 2.9-3.0 for measurements supplemented with $CaCl_2$ and 3.2-3.3 for measurements without additive, see Figure B.21 in Appendix B.

4.5 WO_x consumption - beyond Ca

It has become clear that the tungstate catalyst is deactivated by inorganic species present in biomass. With few exceptions it appears that the combined glycol yield data obtained in our previous work (Chapter 3)[66] and this work correlates well with the concentration of soluble tungstate species in the reactor effluent, see Figure B.4 in Appendix B. In particular, divalent cations appear to form insoluble tungstates. For industrial operation the catalyst consumption should be minimized and preferably stay below 1 $kg_{Catalyst}$ / $tonne_{product}$[89]. Under the assumption that one mole of cation precipitates one mole of WO_x, we derived that the maximum allowable divalent cation content of the biomass feedstock can be 4 mmol per kg biomass (Chapter 7)[111]. This assumption was validated in this chapter as we showed that calcium precipitates with tungstate in an equimolar ratio. Untreated poplar and pine do not meet this criterion as they contain 8.4 and 21.3 mmol Ca+Mg per kg biomass, respectively, but microcrystalline cellulose (Avicel®) does with 0 mmol Ca+Mg per kg biomass, see Table 2.1 in Chapter 2.

Acid leaching of biomass effectively removes the water-soluble fraction, the majority of the alkali and alkaline earth metals[112] and a major part of the overall ash, without deteriorating the cellulose, hemicellulose and lignin

fractions[93]. Moreover, acid leaching also extracts heavier metals, such as manganese[113] and iron[114] from the biomass. Our acid-leaching approach avoids the use of inorganic acids which can be poisonous to metal catalysts[31] and relies on organic acid which can be produced in-situ. This mild pretreatment avoids the hydrolysis of hemicellulose which typically accounts for $\sim$30% of the polysaccharide fraction in biomass and, as a result thereof, allows to achieve much higher glycol yields on overall biomass intake. Most importantly, acid-leached poplar and pine meet the specification of $\leq$4 mmol of Ca+Mg per kg biomass as they contain 2.1 and 1.1 mmol of calcium plus magnesium per kg biomass respectively, see Table 2.1 in Chapter 2. Note that water leaching is rather ineffective for the removal of divalent ions such as calcium[115]. Acid leaching was more effective in removing calcium and magnesium than the high severity pretreatments PT-A (Ethanol-water, 50/50, 200 °C, 3 h) and PT-B (70 wt.% Acetic acid in water, 180 °C, 1 h) reported in Chapter 7[111], whose solid residues had a combined calcium and magnesium content of 9 and 3.2 mmol per kg of biomass respectively. However, these high severity pretreatments also remove lignin. It appeared that lignin did not have a critical impact on the EG yield (Chapter 3), but lignin removal might be imperative for long term operation. Acid leaching does not remove lignin. It only only removes inorganics and water-soluble extractives. Acid leaching could be part of a multi-step pretreatment with the objective to remove inorganics from the biomass in case it turns out that lignin removal is critical.

Besides measurement of the calcium and magnesium content of the feedstock, the actual measured W-catalyst consumption could provide a much better picture on whether the targeted maximum of 4 mmol of divalent ions per kg biomass can be achieved. However, we observed that part of the tungstate is also consumed during the cellulose benchmark experiments, see entries 1 and 2 in Table 4.1. It turned out that this consumption was not related to the cellulose feedstock but to the presence of Raney nickel catalyst, see Appendix B.1. Nevertheless, untreated poplar and pine titrate all the soluble tungstate, see entries 3, 4 and 5 in Table 4.1, and thus contain tungstate poisons. In an additional experiment, Table 4.1 entry 8 which was run with excess of tungstate, we found that poplar (ash content of 0.8 $\pm$ 0.1 wt.%) consumed 118 $mmol_{WOx}$ per kg of biomass, which was somewhat less than the consumption found for a mixture of cellulose and 1 wt.% of poplar ash, namely 155 $mmol_{WOx}$ per kg of biomass. Correcting this number for the ac-

tual ash content of poplar wood, i.e. multiplying by 0.8/1, we find a tungstate consumption of 124 $mmol_{WOx}$ per kg of biomass, which is nearly equal to the previously mentioned consumption of 118 $mmol_{WOx}$ per kg of biomass for poplar wood (Table 4.1 entry 8). This suggests that the consumption of tungstate can be fully ascribed to the inorganics present in biomass.

Acid leaching successfully removes these components as the measured output concentration in the reactor effluent for acid leached poplar and pine (entries 8 and 9 in Table 4.1) is similar to the output concentration after hydrogenolysis of cellulose (entries 1 and 2 in Table 4.1).

Table 4.1: Tungstate input and output for various hydrogenolysis experiments. Reaction conditions: 5 wt.% biomass loading, T = 245°C, t = 1 h, P_{H2} (Initial) = 60 bar, $pH_{Initial}$ ~3.3, Ni-catalyst/Biomass mass ratio = 0.13.

N	Feedstock	Input ($mmol_{WOx}$ / $kg_{Biomass}$)	Output ($mmol_{WOx}$ / $kg_{Biomass}$)
1	Cellulose	119	36
2	Cellulose	120	60
3	Poplar	116	1
4	Poplar	120	0
5	Pine	109	1
6	Poplar	225	107
7	Cellulose + 1 wt.% Ash	226	71
8	Acid-Leached Poplar	114	39
9	Acid-Leached Pine	116	40

The tungstate consumption for untreated poplar and pine is at least 47±12 $mmol_{WOx}$ per kg of biomass more than found in the cellulose reference experiments. However, the Ca+Mg content of untreated poplar and pine are only 8 ± 2 and 21 ± 3 mmol / $kg_{Biomass}$ respectively, see Table 2.1 in Chapter 2. Although refinement of the experimental method to reduce error is desirable, the difference in the measured and expected W-catalyst consumption seems too large to be explained solely by the calcium and magnesium content of the feed. Moreover, the addition of poplar ash to cellulose was much more detrimental than what would be expected from its calcium plus magnesium content in comparison with the addition of $CaCl_2$, see Figure B.22 in Appendix B. Also the data on five (treated) substrates in the study by Pang et al.[90], which we carefully analysed, does not allow to explain poor gly-

col yields exclusively by divalent cation content of the respective feedstock, see Appendix B.2. It is therefore reasonable to expect that there are other tungstate catalyst inhibitors present in the ash beyond calcium and magnesium. The concentration of other divalent cations in biomass is typically much lower than that of calcium and magnesium[28] and therefore unlikely to provide an explanation. Silica typically accounts for the majority of inorganics in biomass but it was previously shown to be inert when added in the form of SiO_2 to a cellulose reference experiment[90]. Further studies are needed to explain the discrepancy.

We have experienced after running tungstate catalysed hydrogenolysis experiments for several years that this system is heavily intertwined. Our approach, comparing the experimental outcome with a benchmark, offsets, or at least dampens, errors that arise from the experimental procedure. For example, tungstate consumption by metals leached from the hydrogenation catalyst or experimental setup could be incorrectly attributed to the biomass feedstock, when not compared to a benchmark experiment. Leaching of metal, e.g. Ni, from the catalyst has been reported before[64] and poses, besides contaminants that are present in biomass, an additional deactivation risk for the tungstate catalyst. Furthermore, precipitation of tungstate with species present in biomass, e.g. calcium, on the surface of the hydrogenation catalyst poses another potential deactivation risk.

4.6 Conclusion

In this work we have shown that inorganics present in biomass, in particular divalent cations such as Ca^{2+}, are the primary inhibitor in the WO_x-catalysed hydrogenolysis of lignocellulosic biomass to ethylene glycol. The EG yield correlated well with the concentration of the soluble tungstate, i.e. active W-catalyst, in the reactor effluent. Divalent cations, such as Ca^{2+}, form insoluble precipitates with the homogenous tungstate catalyst. These inorganic components can be selectively removed by acid leaching, which is a very mild pretreatment performed at room temperature with a solution composed of 10 wt.% acetic acid in water. Such simple treatment boosts the EG+PG yield of poplar and pine from $\sim$22 to 44 wt.%, equal to the yield obtained with pure cellulose when operating under sensitive, WO_x-lean conditions. This poisoning effect is masked by operation with excessive WO_x loading, which also delivered a high glycol yield, 48 wt.%.

The claim that the inorganic fraction is the key inhibitor was further supported by the addition of ash to the cellulose reference experiment and seeing the EG yield dropping under 10 wt.% for the addition of 5 wt.% ash. Moreover, the hydrogenation catalyst appeared to suffer as well, since no sugar alcohol was produced for a mixture of cellulose and 20 wt.% ash. By mixing cellulose with an additive, we have shown that divalent ions deactivate the tungstate catalyst, by the formation of insoluble tungstate precipitates. The insoluble salt, at least for calcium, is composed of an equimolar amount of calcium and tungstate.

The calcium and magnesium content of the untreated feedstocks, however, could not explain the measured tungstate consumption, which requires further studies. Nevertheless, we experimentally showed that acid leaching effectively removed (nearly) all tungstate poisons from the biomass. Importantly, the content of divalent cations was reduced below 4 mmol per kg of biomass which is critical in the context of industrial operation.

Do not forget the classical catalyst poisons: The case of biomass to glycols via catalytic hydrogenolysis

"The dose makes the poison"

- Paracelsus -

Abstract

The conversion of herbaceous biomass to glycols via tungstate catalysed hydrogenolysis is challenging due to its high content of extractives, inorganics and S/N, compared to woody biomass. We tested the hydrogenolysis performance of hay in batch autoclave experiments in the presence of soluble sodium polytungstate and Raney nickel at 245°C, both in excess of catalyst as well as under catalyst-starving conditions. By this method we found that additional tungstate and Raney nickel poisons, or at least at much higher concentration, are present in the hay feedstock compared to woody biomass. It turned out that N and in particular S containing components present in Hay are the root cause for deactivation of the hydrogenation catalyst. From the experimental data we derived feedstock criteria for N and S that should be targeted in terms of catalyst consumption to operate in an industrially relevant window. These challenging criteria urge the development of effective pretreatments for S/N removal or the employment of S/N tolerant catalysts in the field of catalytic biomass conversion.

This chapter is based on the following publication:

T.D.J. te Molder, S.R.A. Kersten, J. P. Lange and M. P. Ruiz, *Do not forget the classical catalyst poisons: The case of biomass to glycols via catalytic hydrogenolysis*, **Biofuels, Bioproducts and Biorefining**, 2022, DOI: 10.1002/BBB.2372

5.1 Introduction

Ethylene glycol (EG) is a bulk chemical with a market size in the order of ∼30 million tonnes per annum[20], which is mainly used as one of the constituents in polyesters[19]. Ethylene glycol can be efficiently produced from sugar via aldol cleavage and subsequent hydrogenation of the glycolaldehyde intermediate[46],[76]. This reaction allows for a theoretical carbon and oxygen atom efficiency of 100%. The aldol cleavage of a mono-saccharide can be achieved by 1) hydrous pyrolysis[41],[42] or 2) catalytic cleavage in the presence of a tungstate catalyst[40]. The resulting glycolaldehyde is hydrogenated over an heterogenous catalyst such as Raney nickel[70] or Ru/C[71] to yield EG.

We have opted for the tungstate catalysed route as it allows the direct conversion of cellulose to EG via in-situ depolymerisation in acidic hot compressed water at ∼245 ℃[65]. The merger of all reaction steps in one-pot is an attractive feature of this process, and allows the direct conversion of microcrystalline cellulose to EG with yields as high as ∼75 wt.%[68],[100],[101]. However, cellulose is typically present in a matrix called lignocellulosic biomass, which delivers substantially lower glycol yields than pure cellulose[66],[75],[91],[116]. Additionally, it has been recently reported that components present in lignocellulosic biomass deactivate the catalyst(s) and thereby spoil the glycol yield[66],[116]. In the manufacturing of commodity chemicals typically 1 kg of catalyst requires to produce 1 tonne of product[89]. Therefore, the identification and quantification of catalyst poisons and subsequent development of pretreatment strategies to remove these poisons is key for commercial viability.

In our previous study (Chapter 3)[66] we have shown that lignin is not the key inhibitor when running under catalyst-sensitive conditions. In a follow-up study (Chapter 4)[116] we found that inorganics, in particular divalent cations, spoil the EG yield by precipitating the homogenous tungstate catalyst. Luckily, we showed that these contaminants can be selectively removed from the biomass by an acidic wash and, indeed, the treated wood species gave similar glycol yield as a cellulose reference test.

In this study, we focus on the effect of other components that may be present in biomass on the hydrogenolysis performance. Specifically, herbaceous biomasses are particularly rich in extractives, inorganics and S/N compo-

nents. We show here that the acid-leaching treatment that was effective for woody biomasses is not effective enough for hay, an herbaceous biomass species. We also delve into the observed catalyst deactivation phenomena caused by those other components present in hay.

5.2 Results and discussion

5.2.1 Experiments with hay

In this work we ran hydrogenolysis of hay under the same catalyst-sensitive conditions as in our previous work (Chapter 3[66] and 4)[116], see Table 5.1 entry 6, which resulted in a poor total glycol yield (EG+PG) of 15 wt.% compared to the cellulose reference test, 45 wt.% (Table 5.1 entry 1 and 2). Moreover, no dissolved tungstate was measured by HPLC in the reactor effluent, indicating that components present in hay, likely the divalent cations, consume the tungstate catalyst. Note that about half of the fed tungstate was also consumed in the cellulose reference test (Table 5.1 entry 1), which can be fully ascribed to the addition of Raney nickel catalyst in an acid buffer, as discussed in Appendix B.

*Table 5.1: Experiments conducted with cellulose and hay as feedstock for various ratios of Ni and W catalysts. Conditions: 5 wt.% biomass loading. Yields on holocellulose basis. *Data from our previous work (Chapter 4)[116]*

n	Feedstock	Biomass / Raney nickel ratio (w/w)	W-cat input ($mmol_{WOx}$ / $kg_{Biomass}$)	W-cat output ($mmol_{WOx}$ / $kg_{Biomass}$)	Yields (wt.%)			
					EG	PG	SA	Sum
1*	Cellulose	8.4	119	36	41	4	12	57
2*	Cellulose	9.6	120	60	39	5	12	56
3*	Poplar	8.7	120	0	11	15	20	45
4*	Poplar	7	116	1	10	13	12	36
5*	Poplar	7.1	1147	1045	38	10	2	50
6	Hay	8.1	117	1	8	7	1	16
7	Hay	9.3	1130	391	7	6	0	13
8	Hay	1.4	1134	444	35	24	6	65
9	WL Hay	8.4	1118	499	10	5	0	14
10	WL+AL Hay	8.7	1137	625	10	4	1	15

The same experiment performed with poplar as feed (Table 5.1 entries 3 and 4) also led to full consumption of dissolved tungstate and a low EG yield of 11 wt.%, similar to the 8 wt.% observed with hay (Table 5.1 entry 6). In both cases the EG yield was much lower than the 40 wt.% observed with cellulose (Table 5.1 entry 1 and 2). However, in contrast, the sum of hydrogenated products, including propylene glycol PG and sugar alcohol SA, was much

lower for hay, namely 15 wt.%, whereas poplar gave 40±5 wt.% and cellulose 56 wt.%. This result suggests that components present in hay deactivate both the homogenous tungstate catalyst as well as the heterogenous Raney nickel hydrogenation catalyst.

To further study these hypotheses, we raised the tungstate loading by ∼10 fold for both hay and poplar feeds, but it barely improved the glycol yield for hydrogenolysis of hay (13 wt.%, Table 5.1 entry 7) while strongly increased the EG yield for poplar (38 wt.%, Table 5.1 entry 5). Hay also consumed much more tungstate (740 $mmol_{WOx}$ per kg biomass) than poplar (∼100 $mmol_{WOx}$ per kg; Table 5.1 entry 5). However, the low EG yield was not limited by the availability of the tungstate catalyst as we measured more soluble tungstate (∼400 $mmol_{WOx}$ per kg hay) after the experiment than we did for the successful cellulose reference experiment (∼50 $mmol_{WOx}$ per kg, Table 5.1 entry 1). We then raised the Raney nickel load by 7-fold as well for hay, (Table 5.1 entry 8), and obtained a high EG yield of 35 wt.% and PG yield of 24 wt.%.

Thus, components present in hay (but not in poplar) seem to deactivate both homogenous tungstate catalyst and heterogenous Raney nickel catalyst. For woody biomass such as pine and poplar, we previously (Chapter 4)[116] found that only the homogenous catalyst was deactivated by (inorganic) impurities. Running poplar in excess of tungstate gave a high EG and PG yield (38 and 10 wt.%, see Table 5.1 entry 5). This does not mean that the Raney nickel poisons present in hay are not present in woody species, but at least they are at a much lower concentration.

Water leaching and acid leaching did not sufficiently remove these Raney nickel poisons as two tests with water-leached (WL) and acid-leached (AL) hay resulted in poor total glycol yield of ∼15 wt.%, see Table 5.1 entries 9 and 10. These treatments, in particular the acid leaching, appear to remove tungstate poisons as the residual W-catalyst concentration in the reactor effluent increased from ∼390 $mmol_{WOx}$ per kg for untreated hay to ∼500 $mmol_{WOx}$ per kg for WL hay, and ∼630 $mmol_{WOx}$ per kg for AL+WL hay.

However, the tungstate consumption for untreated, water leached and acid leached hay is in all cases much higher (>500 $mmol_{WOx}$ per kg) than what is expected from their respective Ca+Mg content (70.5 mmol per kg untreated hay, see Table 2.1 in Chapter 2) and cellulose benchmark experiments (83 and 60 $mmol_{WOx}$ per kg, Table 5.1 entries 1 and 2). We noticed this excessive WO_x consumption before in our previous work (Chapter 4)[116] for woody

biomasses. However, for woody biomasses we were able to remove the majority of these unknown poisons by acid leaching, which is apparently not possibly for hay. Unfortunately, we were unable to identify these unknown tungstate poisons as addition of waterglass (sodium-silicate), colloidal silica and monosodium-phosphate to the cellulose benchmark experiment did not lead to a noteworthy decrease in W-catalyst concentration in the reactor effluent, see Appendix C.1.2.

5.2.2 Analysis of literature

In our previous studies we have elucidated the role of lignin (Chapter 3)[66] and inorganics (Chapter 4)[116] on the catalytic hydrogenolysis that targets EG production. However, these fractions do not readily explain the deactivation observed when running experiments with hay as feed. Hay is particularly rich in extractives which could potentially explain the observed phenomena. We have therefore evaluated the extractives content of feedstocks reported in the literature versus the obtained EG+PG yield and found that the water-soluble extractives content of the feed correlates well with the EG yield for experiments ran at 1 wt.% biomass loading, see Figure 5.1. In particular the dataset by Li et al.[64] is relevant, as they tested 10 different untreated feedstocks and microcrystalline cellulose. The correlation coefficient for this dataset between extractives and the EG+PG yield was -0.9 (See Appendix C.3.1 for details on statistical data analysis of this dataset). Untreated Corn Stalk gave 8 wt.% of EG which was similar to the EG yield, 3 wt.%, reported by Pang et al.[75] for untreated Corn Stalk (see open and closed circle at 33 wt.% water extractives). Untreated Miscanthus[91] seems to fit the trend as well, although the high yield may also be due to the fact that this experiment was run in an excess of catalyst, which masks any sign of catalyst deactivation (see Appendix A)[66]. Also the experiment with Jerusalem artichoke stalk (JAS) in the study by Zhou et al.[104] was performed in excess of catalyst as we have shown previously (see Appendix A)[104], which explains that this datapoint deviates from the trend.

Other datasets from the literature, with experiments performed at higher biomass loading[91],[103], i.e. $\geq$4.8 wt.%, do not allow to properly study the extractives-glycol yield relationship as 1) the extractives content of the pre-treated substrates was not reported[103], and/or 2) the untreated feedstocks were lean in extractives ($\leq$5.3 wt.%)[91],[103].

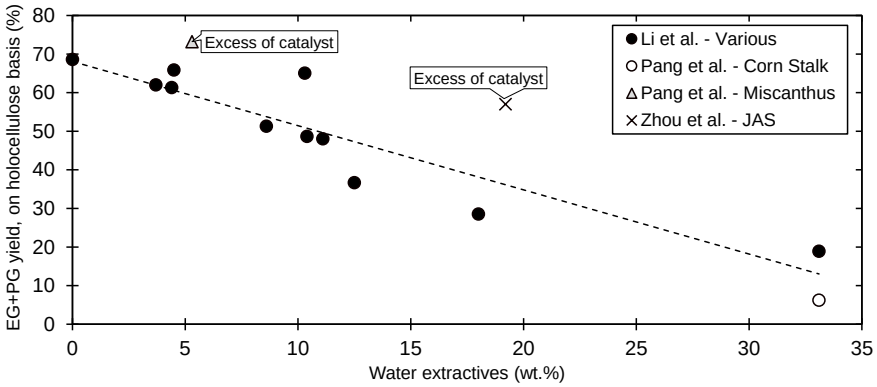

Figure 5.1: EG+PG yield expressed on holocellulose content for previous studies operated at 1 wt.% biomass loading. Various[64] and Corn Stalk[75] in C%, Miscanthus[91] and JAS[104] (Jerusalem Artichoke) in wt.%.

5.2.3 The addition of water-soluble extractives

From analysis of the literature data, in particular the study by Li et al.[64], it can be concluded that the water soluble extractives have a key impact on the glycol yield. To further study the impact of those catalyst poisons, we have added water-soluble extractives to the cellulose reference experiment. The water-soluble extractives were obtained by extraction of hay with water (at room temperature) followed by drying at room temperature. The dried water-solubles were insoluble in acetone and methanol. A feed mixture composed of cellulose and 25 wt.% of these water-soluble extractives resulted in a decline in the combined glycol yield from ∼50 wt.% to 16 wt.% after hydrogenolysis (Figure 5.2). A similar yield (13-16 wt.%) was obtained for untreated hay, which contains ∼23 wt.% extractives, see Table 5.1 entries 6 and 7. However, as discussed previously, water- (and acid-) leached hay still gave a poor total glycol yield of ∼15 wt.%. These results show that a part of the catalyst poisons present in hay can be removed by water leaching, but not all. We previously discussed (section 5.2.1) that the concentration of poisons in water and acid leached hay is still too high to result in an improvement of the glycol yield.

Water leaching of the biomass does extract organic as well as inorganic molecules. These inorganic molecules are known to deactivate the tungstate catalyst[90],[116]. We here found that the increase of extractives in the feed mixture correlated with a decline in the soluble tungstate present in the reac-

tor effluent, see Figure C.1 in Appendix C, which could explain the decline in total glycol yield.

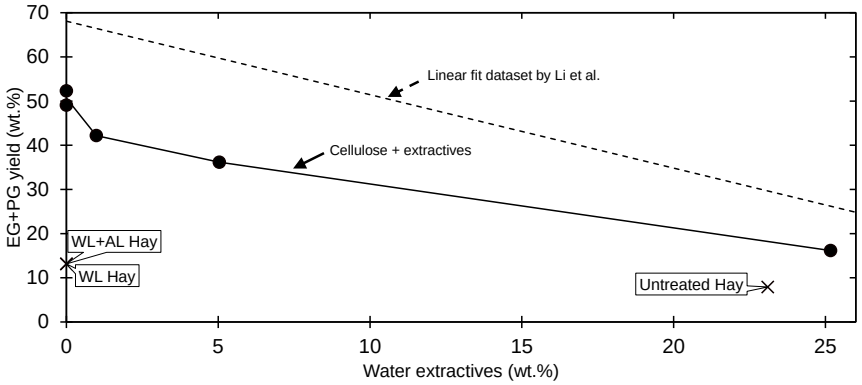

Figure 5.2: EG+PG yield expressed on holocellulose content for cellulose + water soluble extractives mixtures. Reaction conditions: 5 wt.% biomass loading, T = 245° C, t = 1 h, P_{H2} (Initial) = 60 bar, $pH_{Initial}$ ∼3.3, Ni-catalyst/Biomass mass ratio = 0.13. W-catalyst input ∼225 $mmol_{WOx}$ per $kg_{Biomass}$. Linear fit of dataset by Li et al.[64] corresponds to the fit determined in Figure 5.1 and is reported in C%. Lines drawn for clarity.

However, the sum of hydrogenated products (EG+PG+SA) also decreased with increasing of extractives in the feed mixture, which indicates that the hydrogenation catalyst deactivates as well, see Figure C.2 in Appendix C. The EG+PG+SA yield was systematically lower under the addition of extractives compared to cellulose reference experiments, despite similar tungstate levels in the reactor effluent. Ultimately, the yield drops to ∼18 wt.% for the addition of 25 wt.% extractives, whereas the cellulose reference test gives an EG+PG+SA yield of ∼45 wt.%. This shows that the water-soluble fraction contains components that can be removed by water washing but otherwise deactivates both tungstate and hydrogenation catalysts.

5.2.4 Sulphur and Nitrogen

Lignocellulosic biomass species that are rich in extractives are also typically rich in sulphur and nitrogen. Nitrogen[30] in plants is largely present in proteins while sulphur[117] is predominantly present in the form of proteins or as sulphate. These heteroatoms, in particular S, are notorious for deactivating metal hydrogenation catalysts. However, most studies[75],[91],[103],[104] in this field did not report both sulphur and nitrogen content of the (treated) feed-

stocks. Li et al.[64] tested 10 different untreated feedstocks and reported the sulphur and nitrogen content of these feedstocks in the supplementary information of their work. In addition to the glycol yield, they also reported the monomeric phenolics yield, which are obtained from lignin depolymerisation and subsequent hydrogenation of the reactive intermediates. The phenolics yield is therefore, in addition to the glycol yield, a potential marker for the activity of the hydrogenation catalyst. Indeed, only trace amounts of phenols are reported in the absence of hydrogenation catalyst. The EG+PG yield correlated well with the phenolics yield (correlation coefficient of 0.85), see Figure C.9 in Appendix C. We plotted the sulphur versus nitrogen content of the feedstocks in the study by Li et al.[64] and labelled the datapoints with their respective EG yield, see Figure C.10 in Appendix C. We found that a cluster of 7 different feedstocks with an average N and S content of 30$\pm$17 and 5.2$\pm$1.5 mmol kg^{-1} respectively gave an average EG+PG yield of 56 C%, whereas two outliers, Yate (9.4 $mmol_S$ kg^{-1} and 2285 $mmol_N$ kg^{-1}) and Corn stalk (46 $mmol_S$ kg^{-1} and 536 $mmol_N$ kg^{-1}) gave EG+PG yields of only 29 and 19 C%, respectively. The high sulphur content of Corn stalk was also mentioned by Li et al.[64] as a potential cause for the low EG yield. Also, the hay used in our study has a particular high S (34 mmol kg^{-1}) and N (930 mmol kg^{-1}) content, see Table 1. In comparison, the S and N content of poplar and pine used in our previous studies[66],[111],[116] are $\sim$5 mmol S kg^{-1} and 31-36 mmol N kg^{-1}.

We therefore hypothesized that the deactivation of the Raney nickel catalyst by components present in hay could be caused by these heteroatoms. To study our hypothesis, we ran tests with woody biomass, (treated) hay and physical mixtures of two amino acids, methionine (S+N) or glycine (N), and cellulose. We tried to selectively remove N and S from hay by applying mild extraction type pretreatments, but those attempts were rather unsuccessful, see Appendix C.1.3. We therefore opted to change the hay to Raney nickel catalyst loading in some experiments to adjust the S and N to catalyst ratio. We previously found that an increase in the Raney nickel to biomass ratio did not raise the glycol yield much, see Appendix A).

The glycol yield was $\geq$46 wt.% when the sulphur to metal catalyst ratio was lower than 67 $mmol_S$ per $kg_{Raney\ nickel}$, but dropped to 15-19 wt.% for $\sim$200 $mmol_S$ per $kg_{Raney\ nickel}$ for both (treated) hay, as well as a physical mixture of cellulose and methionine, see Figure 5.3 (A). The poisoning effect of N was

much less severe than that of S and appeared to result in a yield plateau. It decreased from 51 wt.% without addition of N, to 33 wt.% for a N to Raney nickel ratio of 5700 $mmol_N$ per kg of Raney nickel. This increase in glycine loading was accompanied by an increase in pH to 3.8, measured after the experiment, whereas the pH is typically 3.3. Decoupling the effect of N and pH would be problematic when further raising the glycine dosage and was, therefore, not attempted. Note that methionine contains S as well as N. However, S is much more poisonous than N, e.g. 200 $mmol_S$ per $kg_{Raney\ nickel}$ gave 19 wt.% glycol whereas 5700 $mmol_N$ per kg of Raney nickel still resulted in a glycol yield of 33 wt.%. The soluble tungstate concentration measured after the experiments for the model mixtures was comparable to the cellulose reference test, which suggests that these amino acids do not deactivate the tungstate catalyst. In general, the yield obtained after experiments with (treated) hay followed the trend seen with the model mixtures. Moreover, the SA yield displayed the same trend as observed for the glycol yield, see Figure C.4 in Appendix C. Besides the addition of S/N containing components, we also tested water-soluble acids (25 wt.% of tannic or glucuronic) but no negative effect on the glycol and SA yields was found, see Appendix C.1.5.

(A) Sulphur **(B) Nitrogen**

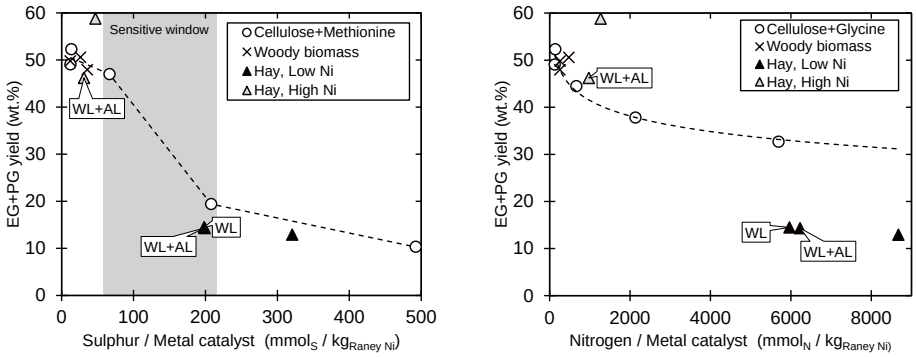

Figure 5.3: Combined glycol yield as function of sulphur and nitrogen of the feed to metal catalyst ratio for woody biomasses, hay, water-leached (WL) hay, water-leached and acid-leached (WL+AL) hay, and physical mixtures of cellulose and glycine (N) or Methionine (S+N). Reaction conditions: 5 wt.% biomass loading, T = 245°C, t = 1 h, P_{H2} (Initial) = 60 bar, $pH_{Initial}$ ∼3.3, Ni-catalyst/Biomass mass ratio; low Ni = 0.13, high Ni = 0.7. Sufficient W-catalyst present in the outlet stream to allow for high glycol yield. Lines to guide the eye.

We also prepared the same charts seen in Figure 5.3 adding the data derived

from the study by Li et al.[64], and found that their experimental results do match the trend observed in this work, despite the different catalyst (4%-Ni-30%W_2C/AC) and somewhat different operating conditions, see Figure C.11 and Figure C.12 in Appendix C. Corn stalk (high S, moderate N) falls in the *"sensitive window"* depicted in Figure 5.3 (A) and Yate (low S, high N) follows the general trend seen in Figure 5.3 (B). All other feedstocks except pine (n=5), deliver a high combined glycol yield of ∼50 % or more as these experiments had S and N to catalyst ratios smaller than 17 $mmol_S$ per $kg_{Catalyst}$ and 150 $mmol_N$ per $kg_{Catalyst}$ respectively.

Plants take up S in the form of sulphate via their roots, which is then reduced and converted to cysteine and later primarily used for the assembly of proteins[30]. Plants can therefore contain organic as well as inorganic sulphur. Besides the tests supplemented with methionine we also performed one run with sodium sulphate and found that its poisoning effect was much less severe than methionine. The experiment with ∼1700 $mmol_S$ per $kg_{Raney\ nickel}$ in the form of sodium sulphate delivered an EG+PG yield of ∼40 wt.%, whereas the EG+PG yield was already below 20 wt.% for ∼200 $mmol_S$ per $kg_{Raney\ nickel}$ when supplemented with methionine, see Figure C.6 in Appendix C. However, we detected H_2S in the outlet gas after the experiment, which indicates that sulphate was reduced over the Raney nickel catalyst under the experimental conditions. Still 91% of S was present in the form of sulphate in the reactor effluent. The 9% of sulphate that was converted amounts to ∼150 $mmol_S$ per $kg_{Raney\ nickel}$, which would fall in the *"sensitive window"* depicted in Figure 5.3 and is thus in line with the observations for mixtures of cellulose and methionine, see Figure C.6 in Appendix C. Thus, any form of sulphur containing components in the feed should be avoided.

Although it was not an initial objective of this study, we also estimated the maximum S-coverage of Raney to get an idea of the mode of deactivation, see Appendix C.1.7. The limit of ∼2700 $mmol_S$ per kg Raney nickel is much higher than the onset for deactivation seen between 67 and 200 $mmol_S$ per kg Raney nickel and cut off in activity at ∼400 $mmol_S$ per kg Raney nickel seen in the study by Philippov et al.[118], who studied the transfer hydrogenation of camphor by 2-propanol at 82°C. This advocates that the Raney nickel surface is composed of *"active sites"* over which the hydrogenation reactions occur. However, our experimental design is not optimal for this research objective as hydrogenation reactions compete with irreversible thermal side reactions.

As a consequence, a low glycol yield is not necessarily the result of a fully deactivated catalyst, but possibly the amount of active catalyst just dropped below the critical threshold that is required to sufficiently suppress thermal side reactions.

Catalysts employed in industrial processes for the production of fuels and commodity chemicals typically produced at least 1 ton of product per kg of catalyst prior to disposal of the catalyst[89]. With this criterion in mind, we can derive a preliminary sulphur and nitrogen target specification for the feedstock. Severe deactivation by sulphur was observed between 67-200 $mmol_S$ per $kg_{Raney\ nickel}$, which translates to the very challenging feedstock specification of < 67-200 µmole (2-6 mg) S per kg of biomass. The specification for N is milder at < 5.7 mmol (80 mg) N per kg of biomass, but this advantage is offset by the fact that biomass typically contains much more N than S.

Note that we did not observe a sudden drop in activity for the addition of N instead of S. In fact, it seems that a plateau is reached around a glycol yield of 33 wt.% compared to 51 wt.% for the reference test, for the maximum N to biomass ratio that we applied (5700 $mmol_N$ per kg of Raney nickel). This hints that an equilibrium is established and that the deactivation is possibly reversible. Further study is required to understand the deactivation phenomena by N and could potentially alleviate the proposed feedstock specification.

Overall, the results of this study suggest that N and in particular S are the root cause for deactivation of the hydrogenation catalyst and that these are accessible to the catalyst surface under the reaction conditions. This is remarkable as we found that several extraction-based pretreatments with water, acidified water (10 wt.% acetic acid) and ethanol at room temperature were rather ineffective for the removal of S and N from the biomass, see Appendix C.1.3 for details. Note that hydrogenolysis experiments are run in a similar solvent (acidified water, pH $\sim$3.3). This suggests that the biomass structure must be degraded to release the proteins/amino-acids in order to make them accessible to the Raney nickel catalyst surface, which apparently happens under typical hydrogenolysis conditions (245°C, pH $\sim$3.3).

5.3 Conclusion

In our previous work (Chapter 4)[116] we showed that critical tungstate poisons can be removed from biomass by an acidic wash, however, we failed to reproduce those results for hay, an herbaceous type of biomass. This biomass type is particularly rich in extractives, inorganics and proteins. It appeared that additional tungstate poisons, which we were unable to identify, are present in hay than in woody biomasses. More critically, we found that nitrogen and in particular sulphur containing components are the root cause for deactivation of the Raney nickel hydrogenation catalyst. This was shown by a series of experiments with physical mixtures of cellulose and methionine or glycine and experiments with (treated) biomass at various Raney nickel to biomass feed ratios.

The relatively good agreement between cellulose amino-acid mixtures and (mildly treated) biomasses suggests that sulphur/nitrogen in lignocellulosic biomass is accessible to the catalyst surface during the reaction conditions. But sulphur/nitrogen removal during non-destructive pretreatment was poor which suggests that the biomass structure needs to be degraded to release sulphur/nitrogen-containing molecules, which apparently materializes under hydrogenolysis conditions.

From the experimental data we derived the very challenging feedstock target specifications of 67-200 µmole sulphur and 5.7 mmol nitrogen per kg biomass or less to be attractive for industrial operation (i.e. 1 $\text{tonne}_{\text{Product}}$ per kg of spent catalyst[89]). Typical biomass feedstocks contain sulphur and nitrogen levels broadly exceeding these targets and we were unable to reduce them significantly by water, acidified water and ethanol extractions at mild temperatures. It should be noted that further study of these target criteria is desired as 1) the competition between hydrogenation and thermal side reactions might have resulted in a glycol yield drop prior to full deactivation of the catalyst and 2) catalyst deactivation under de addition of nitrogen-containing amino-acid resulted in a yield plateau. Both could result in less tight sulphur/nitrogen specifications for the feedstock.

Deactivation of heterogenous metal catalyst by nitrogen and in particular sulphur is well known in petrochemistry, but often ignored when studying the metal catalysed conversion of biomass. We here pinpoint its criticality and the need to develop pretreatment techniques that effectively remove these

nitrogen and sulphur containing components and/or the importance of sulphur/nitrogen resistant catalysts in biomass conversion.

Glycols from woody biomass: Size does not matter

“You should take the approach that you’re wrong.
Your goal is to be less wrong.”

- Elon Musk -

Abstract

This study presents the conversion of various particle size fractions of beech wood, from <53 µm to 5 mm and *"single particles"*, to ethylene and propylene glycol via tungstate-catalysed hydrogenolysis. The tests were performed in a batch autoclave in the presence of soluble sodium polytungstate and Raney nickel at 245°C. Surprisingly, the particle size did not impact the combined glycol yield (∼50 wt.%), which was very similar to a cellulose reference test. It turned out that the *"single particle"* was initially converted from the inside which was reflected by a decrease in density and mainly caused by hemicellulose conversion. After 5-15 minutes of reaction time the *"single particle"* fully disintegrated.

6.1 Introduction

Biomass and atmospheric CO_2 (very diluted) are the only alternative carbon sources to fossil fuels. Chemical intermediates such as glycols, which possess similar functionality and match in elemental composition with the biomass feedstock, are particular attractive candidates to be produced from biomass. Zhang et al.[99] pioneered a bi-catalytic route that allows selective formation of ethylene glycol from cellulose, with reported selectivities of up to $\sim$75 wt.%[68],[100],[101]. This pathway proceeds via the selective tungstate catalysed cleavage of sugar to glycolaldehyde, which is subsequently hydrogenated to ethylene glycol.

Cellulose, however, is not present in nature in its isolated form, but is packed together with lignin and hemicellulose in a matrix called lignocellulose. This matrix also contains minor fractions of inorganics, proteins and functional molecules, often referred to as extractives. Minimizing the catalyst consumption, i.e. avoiding catalyst deactivation, is critical for process feasibility. A typical ceiling for catalyst consumption is less than 1 kg per tonne of product[105], which means that extensive clean-up of the biomass feed is required to meet such criteria[111]. We have previously shown that the presence of inorganics (Chapter 4)[116], sulphur (proteins) (Chapter 5) and to a lesser extent lignin (Chapter 3)[66] obstruct one to meet the desired industrial window for catalyst consumption (1 kg_{cat} / $tonne_{product}$[105]). However, we typically worked with powdered biomass (sieve fraction <53µm), which requires extensive grinding and thus a substantial energy input[119],[120]. For example, Wang et al.[119] report a required electrical energy input of 2.4 MJ per kg of oven dried wood to obtain a median particle size of 100 µm, which is more than 10% of the energy content of wood. The energy requirement for mm size particles is more attractive, e.g. 0.05 MJ per kg of oven dried wood to obtain a fraction with a geometric mean diameter of 1.6 mm[119]. Particle size reduction can also be achieved by thermochemical treatment such as pulping, however, this approach also severely alters the product composition.

Knowledge on the relationship between glycol yield to biomass particle size is desirable to select an appropriate pretreatment. In this work, we have studied the impact of particle size of beech wood on the tungstate-catalysed hydrogenolysis that targets the production of ethylene and propylene glycol. We have evaluated powder (<53 µm), millimetre-sized particles (sieve fractions 1-2 mm and 4-5 mm) and specially manufactured slices (22 mm (ø) x

3 mm). These slices were manufactured as such that they exactly fitted in the bottom of the autoclave, see Figure 6.1. This simple approach allows to study a *"single particle"* while utilizing standard equipment (autoclave).

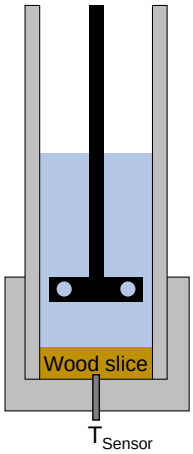

Figure 6.1: Schematic representation of wood slice (22 mm (ø) x 3 mm) fitted in the bottom of autoclave

6.2 Results and discussion

We initially hypothesised that a (poly)-saccharide released from the woody biomass would need to diffuse out of the pore before it can be stabilised by hydrogenation over the heterogenous Raney nickel catalyst. However, the aldose intermediates are very reactive and would irreversibly degrade when not hydrogenated rapidly to stable products[40]. For example the reported kinetic rate constant for glucose degradation (first order) is 0.35 mol L^{-1} s^{-1} at 245°C[40]. In contrast, intraparticle mass transport is slow as the typical time required for diffusion (1D) for a 1 mm distance would be in the order of 500s, see equation 6.1, in which x is the mean distance, D the diffusion coefficient and t is time. We thereby consider a diffusion coefficient of 10^{-9} (optimistic), which is typical for liquid phase diffusion, e.g. diffusion of a glucose molecule in water (1.6 x 10^{-10} at 20°C[121]). Note that these calculations are merely to demonstrate the disparity between the kinetic and mass transport rate. The relatively slow intraparticle mass transfer would thus obstruct the conversion of unstable saccharide to stable products. We therefore expect a lower glycol yield with an increase in particle size.

$$t = \frac{x^2}{2D} = \frac{(10^{-3})^2}{2 \times 10^{-9}} = 500\ s \tag{6.1}$$

We have run batch hydrogenolysis experiments of cellulose and various sieve fractions of beech wood to study the impact of particle size. To avoid running under poison-sensitive conditions, an excess of tungstate catalyst was applied (∼1130 $mmol_{WOx}$ per $kg_{Biomass}$), as we have previously found that inorganic contaminants in woody biomass deactivate the tungstate catalyst (Chapter 4)[116]. The combined glycol yield (EG+PG) for the various beech size fractions was very similar, ∼50 wt.%, and only slightly lower than the one found for cellulose, 54 wt.%, see Figure 6.2. The higher PG/EG ratio observed with beech wood, compared to cellulose, stems from the presence of xylan in the hemicellulose which tends to cleave to C_3+C_2 instead of only C_2 fragments. We have obtained very similar results for poplar wood, the sieve fractions smaller than 53 µm and between 4-5 mm both yielded 50 wt.% of EG+PG, see Figure D.1 in Appendix D. These observations oppose our initial hypothesis.

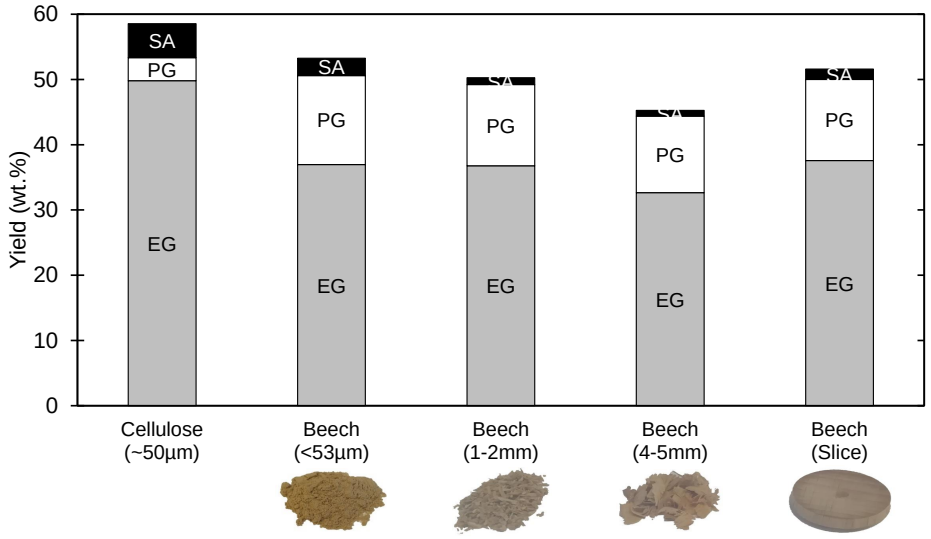

Figure 6.2: Hydrogenolysis of cellulose and various sieve fractions of Beech wood. Slice size = 22 mm (ø) x 3 mm (height). 5 wt.% biomass loading, T = 245° C, t = 1 h, P_{H2} (Initial) = 60 bar, $pH_{Initial}$ ∼3.3, Ni-catalyst/Biomass mass ratio = 0.13. W-catalyst input ∼1130 $mmol_{WOx}$ per $kg_{Biomass}$.

The results must be explained by a scenario in which no significant intraparticle mass transfer resistance exists. Rapid disintegration of large particles, thereby eliminating intraparticle mass transfer resistance, meets such scenario. To evaluate this new hypothesis, we performed hydrogenolysis of the smallest (<53µm) and largest (slice) particle fractions as function of the reaction time. Note that our set-up did not allow the withdrawal of liquid samples during the run and thus all data points are individual experiments. When the wood was only subjected to the heating trajectory to reach 245°C (i.e. 0 min of reaction time) a substantial glycol yield (20 wt.%) compared to the final glycol yield (50 wt.%) was formed for both the powder and the slice, see Figure 6.3. We did not observe any noteworthy products when the slice was only subjected to the heating trajectory up to 200°C and subsequently cooled down (data not displayed). The increase in glycol yield as function of time was slightly faster for wood powder than for the slices. Interestingly, in the experiments of short duration (i.e. 0 or 5 min of reaction time) we collected a solid residue that still had the shape of a slice and was dark-brown coloured. However, the slices were fully disintegrated for all experiments performed with a reaction time of 15 minutes or longer.

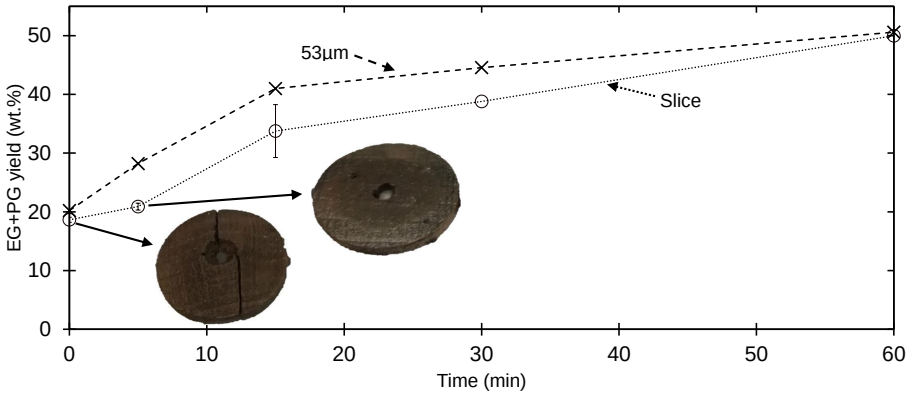

Figure 6.3: Hydrogenolysis of cellulose and various sieve fractions of Beech wood. Slice size = 22 mm (ø) x 3 mm (height). 5 wt.% biomass loading, T = 245° C, P_{H2} (Initial) = 60 bar, $pH_{Initial}$ ∼3.3, Ni-catalyst/Biomass mass ratio = 0.13. W-catalyst input ∼1130 $mmol_{WOx}$ per $kg_{Biomass}$.

For the slices that remained intact, the radius decreased by 10 or 30%, but we measured no significant change in the slice thickness. Interestingly, the particle density drastically decreased from ∼0.63 g cm^{-3} to 0.39 g cm^{-3}, which

was determined gravimetrically after it was dried by flushing with nitrogen until no weight change was registered, see Table 6.1. This information provides some useful insight in the mechanism; the reduction in particle density is not due to swelling, but due to the partial conversion of material within the biomass particle.

*Table 6.1: Experiments performed with a slice (22 mm (ø) x 3 mm (height)) that resulted in partial conversion. *Defined as the material that is no longer part of the slice.*

N	1	2	3
Reaction time (min)	0	5	5
Thickness Before (mm)	2.92	2.92	2.92
Thickness After (mm)	2.88	3	2.95
Diameter Before (mm)	22	22	22
Diameter After (mm)	19.94	19.72	15.5
Density before (g cm^{-3})	0.61	0.64	0.63
Density after (g cm^{-3})	0.37	0.38	0.38
Conversion* (wt.%)	50.3	52.2	70.4

Subjecting the beech slice to only the heating trajectory resulted in a considerable glycol yield ($\sim$20 wt.%), which means that a part of the saccharide fraction was converted during this initial phase. We speculate that the material that is digested during the initial part of the run is primarily hemicellulose, as it is much less recalcitrant than cellulose. The hemicellulose of beech wood is mainly composed of pentose (C_5), whereas cellulose is solely composed of hexose (C_6), which would upon hydrogenation result in the formation of pentitol (C_5) or hexitol (C_6) respectively. We therefore ran hydrogenolysis of the slice in absence of the tungstate catalyst and found that mainly pentitol (pentitol/hexitol = 7) was formed for a reaction time of 0 minutes, see Figure D.2 in Appendix D. Moreover, the pentitol yield was the same ($\sim$13 wt.%) for the experiments performed for 0 and 60 minutes. The pentitol to hexitol ratio dropped to 2 for the slice and 1 for beech powder when running the experiment for 1 hour, see Figure D.2 in Appendix D. We found similar outcomes for experiments run under W-catalyst sensitive conditions for a varied reaction time (0, 5, 15 and 60 minutes): 1) the pentitol yield was very similar for all experiments, and 2) the pentitol to hexitol ratio sharply dropped from 16 to

4 and 2, and ultimately 1.4 for reaction times of 0, 5, 15 and 60 minutes respectively, see Figures D.3 and D.4 in Appendix D. These observations show that the hemicellulose fraction is converted during the heating trajectory and suggest that hexose, i.e. cellulose, is released from the biomass matrix after the initial heating trajectory is passed.

More valuable information related to the fate of the hemicellulose and cellulose fractions can be derived from the EG to PG ratio, as the cleavage of 1 mol hexose theoretically yields 3 mol EG, whereas the cleavage of pentose results in 1 mol of EG and 1 mol of PG. In practise the EG to PG ratio for cellulose was between 12 and 18, see Figure D.5 in Appendix D. The EG to PG ratio for beech, both powder and slice, was around 3 independently of the run time, see Figure D.5 in Appendix D. An EG to PG ratio of 1 is expected when only hemicellulose (pentose) is released. This means that hemicellulose as well as cellulose are released during the heating trajectory, i.e. a reaction time of 0 minutes. The PG yield for beech powder and slice was 6 wt.%, while only 0.4 wt.% for cellulose. The difference, 5.6 wt.%, must therefore originate from hemicellulose. This PG formation is expected to be accompanied by the formation of 4.6 wt.% EG (1:1 mol/mol) but was significantly higher at 14 wt.% for both powder and slice. The discrepancy, 9 wt.% EG, likely stems from cellulose as a run for 0 minutes with microcrystalline cellulose gave an EG yield of 6 wt.%, see Figure D.6 in Appendix D.

Thus, during the initial trajectory (first 5 minutes) the majority of hemicellulose, a small part of cellulose and likely water-extractives, acetyl groups and some ash are released from the biomass matrix. The sum of these fractions is $\sim$30 wt.% and largely explains the 40% reduction in particle density observed for experiments performed with slices for 0 and 5 minutes, see Table 6.1.

To gain further understanding of the intraparticle mass transport we attempted to use the unwanted deactivation of tungstate by inorganic species (Chapter 4)[116] to our advantage. The tungstate poisons, such as Ca^{2+}, first need to be transported out of the particle before deactivation can occur. Or alternatively, the homogenous tungstate must be transported into the particle to interfere with the poisons. Deactivation of tungstate could therefore be postponed for particles of greater size. However, we found that hemicellulose is rapidly released from the slices, which could mean that tungstate poisons, such as divalent ions, are also readily transported out from them.

When run under tungstate lean conditions, we found that the EG yield increased with increasing particle size, from 19 to 29 wt.% for non-deashed wood, see Figure 6.4. The PG yield was rather similar ∼15 wt.% and the total glycol yield increased with increasing particle size, from 35 to 43 wt.%. At the same time, the SA yield appeared to decrease from 15 to 8 wt.%. This effect was not observed when the wood was deashed by an acid-leaching pretreatment and gave a similar glycol yield (47 wt.%) for all sieve fractions, see Figure D.7 in Appendix D.

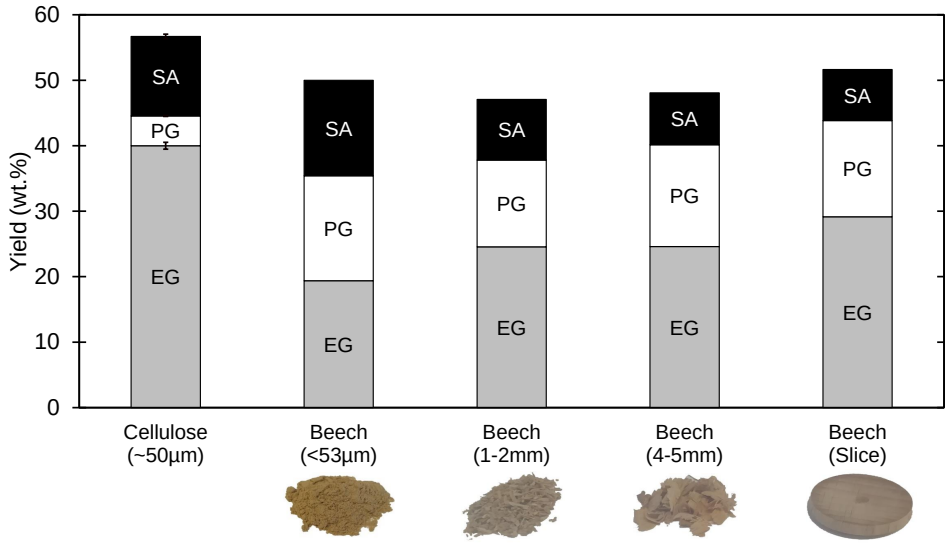

Figure 6.4: Hydrogenolysis of cellulose and various sieve fractions of Beech wood. Slice size = 22 mm (ø) x 3 mm (height). 5 wt.% biomass loading, T = 245° C, t = 1 h, P_{H2} (Initial) = 60 bar, $pH_{Initial}$ ∼3.3, Ni-catalyst/Biomass mass ratio = 0.13. W-catalyst input ∼120 $mmol_{WOx}$ per $kg_{Biomass}$.

This shift in selectivity from SA to EG for non-treated wood suggests that more active tungstate was available throughout the experiments run with bigger particles and thus that the release of tungstate poisons depends on the particle size, i.e. diffusion distance. However, the yield differences are not very dramatic. This is further confirmed by the observation of a higher concentration of soluble tungstate (measured by HPLC[116]) in the reactor effluent for the experiment with the slice than for smaller particles. This seems to explain its higher glycol yield, see Figure D.8 in Appendix D.

We have attempted to further stretch the intraparticle diffusion distance by

running experiments with a thicker block (22 mm (ø) x 10 mm (height)), which was roughly 3 times thicker than the slice. This increase in particle size was accompanied by an increase in biomass loading from 5 to 15 wt.% compared to the slice, as our setup did not allow to further raise the liquid loading. The combined glycol yield, 22 wt.% (entry 3 in Table 6.2), was reduced compared to the previously tested particle size fractions (∼50 wt.%), see Figure 6.2. However, it turned out that this yield reduction was the result of the increase in biomass loading from 5 wt.% to 15 wt.%, as the same combined glycol yield (21 wt.%) was obtained for 1-2 mm sieve fraction at comparably high biomass loading (15 wt.%), see entry 2 in Table 6.2.

*Table 6.2: Beech wood, Block dimensions = 22 mm (ø) x 10 mm (height). *Solvent composed of Water/Ethanol/Acetic-acid (50/48/2) was applied. Other relevant reaction conditions: T = 245° C, t = 1 h, P_{H2} (Initial) = 60 bar, $pH_{Initial}$ ∼3.3*

n	Feedstock size	Run time (min)	Loading (wt.%)	W-cat input ($mmol_{WOx}$ / $kg_{Biomass}$)	Biomass / Raney nickel ratio (w/w)	Yields (wt.%)			
						EG	PG	SA	Sum
1	1-2 mm	60	5	1117	8	37	12	1	50
2	1-2 mm	60	14	365	22	18	3	0	21
3	Block	60	15	351	22	18	4	0	23
4	Block	180	14	348	22	17	4	0	21
5*	Block	180	14	349	21	35	13	2	50

Interestingly, we observed a black ball of material that seemed glued to the stirrer at the end of the experiment (for the block only). The material was not soluble in the water, the hydrogenolysis solvent, but did dissolve in a 50/48/2 water/ethanol/acetic-acid mixture which suggests that the material was a lignin melt. Performing hydrogenolysis of the block (15 wt.% biomass loading) in this organic-solvent/water mixture resulted in the same combined glycol yield (50 wt.%) as we previously obtained for other particle size fractions at 5 wt.% biomass loading, see Figure 6.2. Despite delivering a representative glycol yield, the mechanism for biomass digestion is likely very different as this solvent facilitates the dissolution of lignin and thereby the rapid disintegration of the block. There can be several reasons for the yield increase when running in organic-solvent/water mixture. Possibly, the lower acidity of the solvent which retards the depolymerisation of hemicellulose thereby keeping the sugar to catalyst ratio relatively low. Alternatively, the organic solvent/water mixture allows the dissolution of lignin which might mitigate Raney nickel poisoning by lignin.

6.3 Conclusion

We have studied the influence of particle size on the catalytic conversion of biomass to glycols. Several particle size fractions of beech wood, ranging from powder (<53 µm), millimetre-sized (1-2 mm and 4-5 mm) and specially manufactured slices (*"single particle"*, dimensions = 22 mm (ø) x 3 mm) were subjected to hydrogenolysis. The particle size did not appear to impact the combined glycol yield which was ∼50 wt.% for all tested size fractions and similar to a cellulose reference test, when run under tungstate catalyst-rich conditions. The glycol yield was also identical for acid-leached wood independent of the particle size when run under tungstate sensitive conditions.

The majority of hemicellulose and a minor part of cellulose were already digested and converted to glycol (∼20 wt.% yield) during the heating trajectory (non-isothermal stage > 200°C) for both powder and slices. These fractions were converted from the *"inside"*, as slices with a ∼40% reduced density were collected after 0 and 5 minutes of run time. Between 5 and 15 minutes of reaction time the slices collapsed, and no residual particles were collected at the end of the experiment. After disintegration of the slice, similar glycol yields for wood powder and slice are indeed expected as in this scenario no significant intraparticle mass transfer resistance exists. However, the initial release of mainly hemicellulose and successful conversion to glycol cannot be explained by intraparticle diffusion which is in competition with thermal side reactions of the sugars. This hints at convective transport of hemicellulose (derivatives) from the particle, but requires further research.

Cellulosic glycols:
An integrated process concept for lignocellulose pretreatment and hydrogenolysis

"A problem well stated is a problem half solved"

- Charles F. Kettering -

Abstract

Lignocellulose is the most abundant source of saccharides and, therefore, a promising feedstock for glycols, such as ethylene-glycol, via catalytic hydrogenolysis of the contained polysaccharides. However, this catalytic hydrogenolysis step is hampered by the presence of lignin and other biomass contaminants, such as ash, which need to be removed in a pretreatment step. We propose an organosolv-like pre-treatment that can delignify and de-ash lignocellulose to a level that allows it to be upgraded to glycol with comparable yields as pure cellulose under demanding hydrogenolysis conditions. This work identifies the main design constraints of the integrated process and provides an initial experimental validation of it. Pretreatment of biomass in water/ethanol/acetic acid solutions at 180-200°C can reduce the lignin content of the solid residue down to $\leq$6 wt.%. The addition of an organic acid, such as acetic acid, appears important to improve the removal of the recalcitrant Ca^{2+}, which is a known inhibitor of the tungstate catalyst, typically used in this process. The pretreatment medium is designed to use the byproduct(s) of the process as organic solvent, to reduce the need for fresh solvent input. However, the process still requests a high solvent recovery (between 93.5 and 99.9 wt.%). This can be achieved by selecting a volatile organic solvent, as it allows recovery by evaporation from the dissolved lignin and ashes.

This chapter is based on the following publication:

Thimo D. J. te Molder, Sascha R. A. Kersten, Jean-Paul Lange and M. Pilar Ruiz, *Cellulosic glycols: an integrated process concept for lignocellulose pretreatment and hydrogenolysis*, **Biofuels, Bioproducts and Biorefining**, 2021, 15, 6, pp. 1725-1736, DOI: 10.1002/bbb.2269

7.1 Introduction

Ethylene glycol (EG) is a bulk chemical with an annual production of 20 million tons by 2010,[19] which is traditionally produced via the partial oxidation of ethylene to ethylene oxide followed by thermal hydrolysis to ethylene glycol[32]. In an alternative and more sustainable route, it can also be selectively produced from (poly)-saccharides, such as cellulose, with a high atom-economy via bi-catalytic hydrogenolysis[76]. The hydrogenolysis requires two catalysts, typically a homogenous tungstate for the aldol cleavage of glucose to glycolaldehyde, and a heterogeneous metal catalyst (e.g. Raney nickel) for hydrogenation of the glycolaldehyde to EG. The present case further requires the cellulose to be depolymerised to glucose in acidic conditions, e.g. hot compressed water (245°C)[46].

Most studies within this field used pure microcrystalline cellulose as model feedstock and demonstrated the viability of the process to produce EG under diluted feed concentrations (typically 1 wt.%). However, direct hydrogenolysis of untreated lignocellulose appeared problematic[66],[75],[91],[122], in particular when feed concentrations[91],[103], were raised from 1 wt.% to more practical though still modest levels of 5-10 wt.%. For example, Fabičovicová et al.[103] reported an EG yield of only 2 C% for untreated barley straw, while they achieved an EG yield of 36 % for pretreated barley straw.

The origin of these low yields is probably related to the presence of catalyst poisons within the biomass. In this context, we have previously reported that lignin deactivates the hydrogenation catalyst[66]. The hydrogenation catalyst is highly sensitive to components that interfere with its surface (viz. physisorption and chemisorption). Lignin, which is after holocellulose the major biomass constituent, is poorly soluble in water, i.e. the hydrogenolysis solvent, and, therefore, likely to foul the hydrogenation catalyst. Unfortunately, no quantitative relationship between these poisons and the catalyst stability is available. However, in our previous work[66] we did not observe a decrease in hydrogenation activity for feeds with a lignin content lower than 5 wt.%. Therefore, lignin content of the solid residue should be kept below 5 wt.%.

Besides lignin, inorganic compounds, i.e. ash, that are present in biomass[31] are preferably removed during pretreatment as well. The alkaline ash neutralizes the acids needed to run the catalytic hydrogenolysis at its optimal, mildly acidic condition (pH 3-5)[90]. More importantly, it is also known that the ho-

mogenous tungstate catalyst is prone to deactivation by divalent cations, e.g. calcium and magnesium, through the formation of insoluble tungstate mixed oxides[90],[123]. Indeed, Pang et al.[90] showed that the EG yield plummeted for cellulose hydrogenolysis (Y_{EG} = 60 C%) under the addition of divalent chloride salts of calcium (Y_{EG} = 23 C%), magnesium (Y_{EG} = 46 C%) and indeed observed $CaWO_4$ in the spent catalyst. A test with $CaWO_4$ as aldol cleavage catalyst showed that it was not catalytically active as the EG yield (11 C%) was not significantly higher than what was previously reported for cellulose conversion without tungstate species[124].

Based on these observations, it is clear that pretreatment is then a prerequisite, in particular when considering that a low catalyst consumption of <1 $kg_{Catalyst}$ / $tonne_{Product}$ is key for the process viability[105]. Such pretreatment requirements mainly deviate from those of traditional pretreatment processes on three key points:

1. The aim of the pretreatment is to selectively remove potential catalyst poisons present in biomass, in particular lignin and ash, rather than increasing the accessibility or liberating the fibers, which are typical aims for pulp and papermaking[125] and for microbial upgrading[102] of cellulose to fuels and chemicals.

2. Furthermore, the addition of inorganic acids and/or additives, such as HCl and H_2SO_4, to the solvent mixture, which is a popular practice in existing literature, should be averted as these inorganics generally inhibit metal-based catalysts.

3. The by-products (e.g. light alcohols) that are formed during the hydrogenolysis step (e.g. excessive hydrogenation of EG yields ethanol) can be recycled to the pretreatment reactor to serve as a make-up for organic solvent losses.

In this context, the main goal of this study is to develop an integrated process of biomass pretreatment followed by catalytic hydrogenolysis of the saccharide-rich residual solid. We first derived the design criteria for the pretreatment based on heuristics, calculations and past literature knowledge. The pretreatment step was experimentally explored and the solid residue was characterised and subjected to catalytic hydrogenolysis. We also experimentally estimated the net size of the solvent make-up stream by identifying and

quantifying consumption and production pathways of light alcohols and organic acids. These experimental outcomes were input for calculations to determine the required solvent recovery rate. Furthermore, we performed preliminary calculations to estimate the viability of an evaporator operation for the solvent recovery. The purpose of this study is to provide an initial validation of the proposed process concept and to briefly touch upon all its various aspects. The lessons learned from this work may probably be applicable in other biomass valorisation routes that rely on metal-based catalysts.

7.2 Results and discussion

7.2.1 Process concept

The pretreatment goals are to retain the cellulose in the solid residue and maximize lignin and ash removal by dissolution. We envisage an organic solvent-based pretreatment process which utilizes in-situ generated organic acid as catalyst. In fact, the organic acid (e.g. acetic acid) can act as both the catalysts and solvent[126],[127]. For this strategy to be successful, the solvent must be composed of three elements, 1) water as a reactant to cleave lignin-carbohydrate bonds and lignin ether bonds, 2) an acid catalyst for the cleavage reaction, and 3) an organic solvent to facilitate dissolution of (depolymerised) lignin. A wide variety of organic-solvent types has been successfully used to delignify lignocellulosic biomass, among them: alcohols, organic acids, esters, ketones and phenolics[128]. It is worth noting that the organic solvent to be used here is not limited to one organic component, but it will likely be composed of a mixture of light alcohols and light acids that are by-products of the pretreatment and hydrogenolysis steps.

Besides serving as a catalyst in the delignification reaction, the acid is also required to dissolve divalent cations (i.e. tungstate poisons), such as calcium and magnesium, from the biomass. Carbonates and oxalates of calcium and magnesium, which are typically present in lignocellulosic biomass[27], are poorly soluble in water (e.g. K_{sp} $CaCO_3$ (Calcite) = $10^{-8.5}$ mol L^{-2}, from[129]). Dissolution of these species can be achieved by acidifying the solution. Organic acids such as acetic acid and formic acid, which are typical byproducts from biomass conversion, are suitable candidates as the solubility of their corresponding calcium and magnesium salts is sufficiently high. Moreover, these acids are not poisonous to the hydrogenolysis catalysts, unlike for example hydrochloric acid[107] and H_2SO_4. Furthermore, they can be easily separated

from lignin and ashes by evaporation.

Additionally, a match in polarity of the solvent and lignin is required to successfully remove lignin[128],[130]. The polarity of the solvent can be tuned by selecting an appropriate mixture of water and organic solvent. A solvent with a high share of water is desirable from an economic point of view, as organic solvents are more expensive than water.

In our process scheme, see Figure 7.1, biomass is treated at elevated temperature (180-200°C) in the presence of an organic solvent (e.g. ethanol/acetic acid) - water mixture to extract lignin and ashes (PT unit). The organic solvent is composed of organic acids (e.g. acetic acid) that are generated during the pretreatment, and light alcohols, which are byproducts of the hydrogenolysis step. Preferably, the process produces its own solvent, but possibly an additional external solvent make-up is required (not displayed in Figure 7.1). These solvents are all recycled back to the PT step. As such, the separation infrastructure for glycols and byproducts, such as light alcohols, after the hydrogenolysis step is already present.

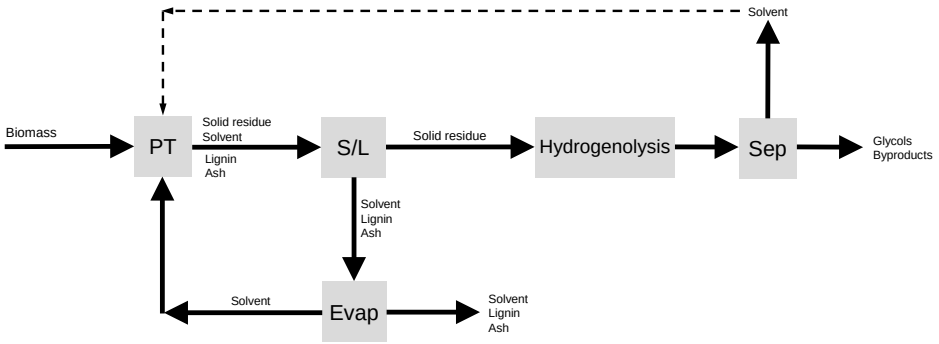

Figure 7.1: Simplified conceptual process scheme. PT = pretreatment, S/L = Solid/liquid separation, Sep = separator

The use of inorganic catalysts, such as Cl^-, in the pretreatment solvent should be avoided, as they are typical poisons to metal catalysts. Moreover, the pretreatment is selected to run under acidic conditions, like the hydrogenolysis, to avoid a pH swing between the two steps. These considerations are important as biomass and its derivatives have the ability to hold vast amounts of liquid and thereby dragging pretreatment solvent and solutes to the hydrogenolysis reactor. After the pretreatment, the spent solvent and solid residue are separated (S/L unit, e.g. by a filter press), and the solvent is recovered by

evaporation (EVAP unit) from the dissolved biomass fraction, i.e. lignin and ashes. Combustion of lignin could provide heat to run the evaporator. The recovered solvent is recycled to the pretreatment reactor and the solid residue enriched in cellulose is fed to the hydrogenolysis section and converted to ethylene glycol. Light alcohol byproducts are separated from glycols (SEP unit) and utilized as a solvent make-up for the pretreatment step.

7.2.2 Experimental validation

In this work, we intend to give an initial experimental validation of this process concept (Figure 7.1). The aim of pretreatment is to selectively remove catalyst poisons such as lignin and ash, i.e. to obtain a solid residue that is enriched in cellulose that can subsequently be fed to the hydrogenolysis section. We display here two examples of organic solvent based pretreatments to support the viability of our process concept, PT-A and PT-B. Pretreatment A was a classical organosolv pretreatment, 50 wt.% H_2O and 50 wt.% EtOH, run at 200°C for 3 h without acid. Pretreatment B was an acetosolv-type pretreatment that uses 70 wt.% HAc and 30 wt.% H_2O, and was run at 180°C for 1 h. The pH of the black liquors after the experiments was 4.2 for PT-A and 1.3 for PT-B.

The solid residue yields were 56 wt.% for PT-A and 50 wt.% for PT-B, which is typical for such pretreatments. As shown in Figure 7.2 (A), both pretreatments succeeded in selectively removing the lignin and ash fractions (>80 wt.%), while preserving the cellulose, as indicated by the hexosan retention of $\sim$100 wt.%. The majority of the hemicellulose was removed as well: only 29 wt.% and 14 wt.% was retained in the solid residue for PT-A and PT-B, respectively.

Besides silica, the majority of the inorganic components in biomass consist of alkali and alkaline earth metals (AAEM). Divalent ions, such as calcium and magnesium, form poorly soluble tungstates[90],[123]. More importantly, Pang et al.[90] previously showed that the EG yield dropped from 60 to 23 and 46 C% under the addition of calcium or magnesium in the cellulose hydrogenolysis experiment. Assuming that deactivation (by precipitation) of tungstates occurs in a 1:1 molar ratio, a maximum allowable concentration of undesirable divalent cations can be calculated to meet the maximum catalyst consumption (<1 $kg_{Catalyst}$ / $tonne_{Product}$[89]), which boils down to < 4 mmol (e.g. <161 mg Ca) per kg of biomass, see Appendix E.1. Precipitation of tungstate species on the surface of the metallic hydrogenation catalyst poses an additional de-

activation risk.

We studied the AAEM composition of the untreated poplar and pretreated substrates A and B, see Figure 7.2 (B). The poplar feedstock was relatively lean in calcium, 173 mg kg^{-1} (4.3 mmol kg^{-1}) and magnesium, 99 mg kg^{-1} (4.1 mmol kg^{-1}), but these levels are still higher than the target value of <4 mmol per kg of biomass. It turns out that an ethanol-water pretreatment, PT-A, successfully removes sodium, potassium and magnesium, but falls short on the calcium removal.

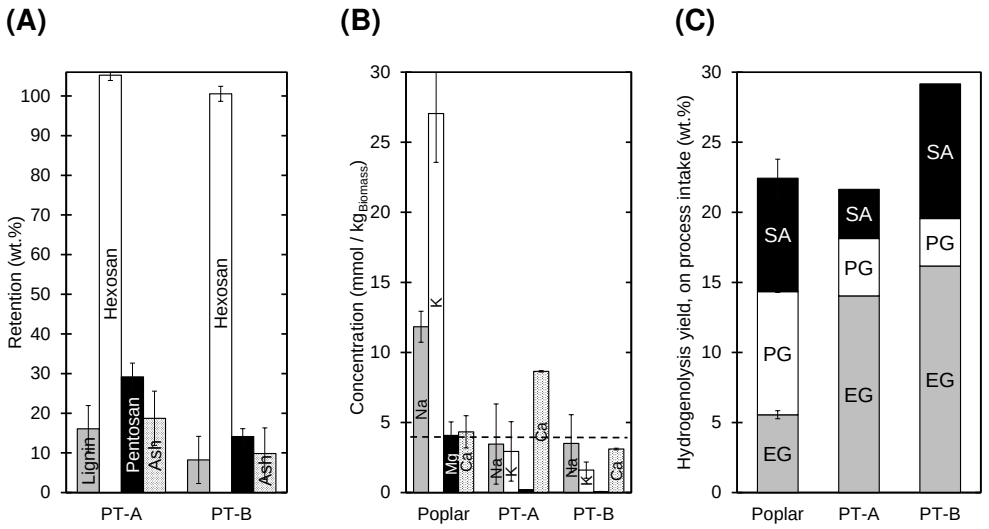

Figure 7.2: (A) Retention of biomass fractions after pretreatment, (B) Alkali and alkaline earth metal composition of untreated poplar and pretreated samples A and B, and (C) Hydrogenolysis yields on biomass intake to the overall process, see Chapter 2 equation 2.2 for untreated poplar and solid residues obtained after pretreatment A & B. Pretreatment conditions: PT-A; 200° C, 3 h, H_2O:EtOH 50:50 w/w , PT-B; 180° C, 1 h, 30 wt.% H_2O, 70 wt.% HAc. Hydrogenolysis conditions: 5 wt.% biomass loading, T = 245° C, t = 1 h, P_{H2} (Initial) = 60 bar, $pH_{Initial}$ ~3.3, Ni-catalyst to biomass mass ratio 0.12, W-catalyst to biomass mass ratio 0.03.

In fact, the solid residue calcium content of PT-A is higher than that of the feed, namely 346 mg kg^{-1} (8.7 mmol kg^{-1}). This is explained by the mass loss during PT (Y_{SR} = 56 wt.%) and hints that an organic solvent (e.g. ethanol) based PT is not an effective tool for calcium removal, which is easily explained by the poor solubility of calcium salts, such as calcium carbonate[131], in water-ethanol mixtures. In addition, the spent liquor was only mildly acidic, pH = 4.2, whereas a pH < 3 is deemed necessary to significantly remove

calcium from biomass[112].

In an attempt to improve calcium removal, we selected a more acidic pretreatment, PT-B, based on a solvent composed of 70 wt.% acetic acid, the remainder being water. Indeed, the calcium level was much lower for the solid residue of PT-B (3 mmol per kg biomass) than of PT-A and meeting the 4 mmol per kg biomass constraint, however, not significantly different than the feed, see Figure 7.2 (B). At the same time, PT-B delivered a solid residue with only $\sim$4 wt.% of lignin. Note that in PT-B the solid residue yield is 50 wt.%, thus also 50% of the calcium must have been removed to end up with the same calcium content as the untreated feed. Nevertheless, also this pretreatment appears to be less effective in calcium removal than a wash with 10 wt.% acetic acid water solution at 90 °C for 2 hours, as was previously demonstrated by Oudenhoven et al.[93], which reduced the pine calcium content from 1771 mg per kg pine to 68 mg per kg pine (1.7 mmol per kg pine) after acid leaching. This is well below the product constraint concentration of 4 mmol of divalent cations per kg of biomass. It thus appears that a high organic solvent share, which is believed necessary for delignification, hampers the removal of calcium.

We then performed hydrogenolysis of untreated poplar and the pretreated samples and chose demanding conditions developed earlier (Chapter 3)[66] to verify whether the chosen pretreatment strategy was indeed successful. The pretreated substrates delivered higher overall glycol yields on process intake, despite the loss of hemicellulose during pretreatment, see Figure 7.2 (C). The EG yield on biomass intake to the overall process was 14 and 16 wt.% for PT-A and PT-B, whereas it was only 6 wt.% for untreated poplar. Note that the hydrogenolysis protocol was not tuned for maximum EG yield, but for maximum sensitivity towards catalyst poisons; it should therefore be possible to significantly raise the glycol yields by optimization of the hydrogenolysis conditions.

Comparison of glycol yields for different studies is cumbersome as 1) different hydrogenolysis protocols[66] are used and 2) the solid residue yield of the pretreatment step is often not reported[75],[91],[104]. It is therefore more useful to compare the glycol yields obtained for treated biomass with a reference experiment with untreated and, importantly, microcrystalline cellulose which has an extremely low content of potential catalyst poisons. Our demanding recipe applied high biomass loading and low catalyst W and Ni loading to exacer-

bate the sensitivity of the system towards catalyst poisoning. The pretreated samples delivered substantially higher glycol yield, expressed on holocellulose basis, than that of untreated poplar (Y_{EG} = 8 wt.%) and very similar to pure cellulose (Y_{EG} = 32 wt.%), namely 27 and 34 wt.% for PT-A and PT-B respectively[66], see Figure E.9 in Appendix E. This is a clear proof that the proposed pretreatment strategy does remove undesirable catalyst poisons and delivers high overall glycol yields.

Despite the limitations, we have calculated the process based glycol yields for the studies by Fabičovicová et al.[122] and Pang et al.[75] on the pretreatment and subsequent hydrogenolysis of barley straw and corn stalk respectively. The process based EG and PG yields for their best-case scenarios were slightly higher namely 17-18 % EG compared to 14-16 wt.% for this work, and PG yields of 8 C% (Pang et al.[75]), 5 C% (Fabičovicová et al.[122]) compared to 3-4 wt.% (this work), see Appendix E.5.2. Although various pretreatments have been tried, we limit the discussion to successful approaches. Pang et al.[75] used pretreatment based on solutions of ammonia, hydrogen peroxide, combinations thereof and sodium hydroxide. Similar pretreatments in combination with ethanol as solvent were performed on Miscanthus in a different study by Pang et al.[91] The alkaline pretreatment approaches require a pH-swap as the hydrogenolysis is operated at acidic conditions and therefore require extensive washing of the solid residue or neutralisation of the alkali, whereas the hydrogen peroxide based approach is costly due to its single-use. Our in-situ produced organic acid based pretreatment avoids these issues. Fabičovicová et al.[122] applied water-ethanol mixtures as pretreatment protocol, similarly as this work, but merely focus their study on the hydrogenolysis outcome and not on the process considerations.

7.2.3 Solvent selection

The organic solvent needs to meet a number of requirements to be attractive in pretreatment. Due to the ability of treated biomass (e.g. cellulose) to retain vast amounts of liquids, a significant share of the pretreatment solvent inevitably ends up in the hydrogenolysis reactor. Therefore, the acidity of the pretreatment solvent should be compatible with the mild acidic (pH = 3-5) conditions required in the hydrogenolysis reactor. Furthermore, additives that are known catalyst poisons, such as hydrochloric acid[107], cannot be part of the pretreatment solvent. Ideally, the solvent should be recovered without degra-

dation to be recycled to the pretreatment. Therefore, the solvent should be resistant to high temperature ($\sim$250 °C) and a reductive environment (i.e. not catalytically converted). For example, a ketone is easily converted to an alcohol during hydrogenolysis and therefore is not a preferred pretreatment solvent. Preferably, the pretreatment solvent consists of a/multiple byproduct(s) of the hydrogenolysis process. This gives two advantages: 1) the byproduct stream can be utilised as make-up for losses in the pretreatment section, and 2) the infrastructure to separate this solvent from the target product (EG) is already present in the process.

We therefore selected light alcohols and organic acids in combination with water as pretreatment solvent, but for the sake of simplicity, we centred our experiments around ethanol-water mixtures. Considering the pretreatment aims (high delignification, high sugars retention), from the results presented in Figure 7.3, it can be concluded that the ideal solvent for delignification is composed of 50-60 wt.% ethanol and the remainder being water. This is also reflected by the low residual lignin content of the solid residues, $\sim$6 wt.%, resulting from these experiments, see Figure E.1 in Appendix E. To the best of our knowledge, the minimum share of organics in the pretreatment solvent to achieve deep delignification does not dramatically change for other light alcohols or light acids[126],[130],[132]–[134]. It is therefore reasonable to expect that a solvent with a minimum of $\sim$50 wt.% organics is needed to achieve deep delignification.

Note that the lignin retention for only water as solvent experiment was 131 wt.%, indicating the formation of humins which are perceived as lignin by our analytical procedure (i.e. it cannot differentiate between lignin and humins). This observation was further confirmed by a total lignin balance greatly exceeding 100% and the presence of 5-HMF and furfural in the black liquor (Figure E.2 in Appendix E), which are known humin precursors[87].

The preservation of hexoses in the solid residue is high over the whole range of water-ethanol mixtures, indicating the recalcitrance of cellulose. The pentose content of the solid residue can be controlled by varying the water content of the solvent. This ultimately affects the EG (C_2) to PG (C_3) ratio in the hydrogenolysis product slate, as pentose (C_5) delivers one mol of EG (C_2) and one mol of PG (C_3), whereas hexose (C_6) can give 3 moles of EG (C_2). However, the majority of the hemicellulose is removed when delignification is maximized, i.e. for a solvent ethanol composition of 50-60 wt.%.

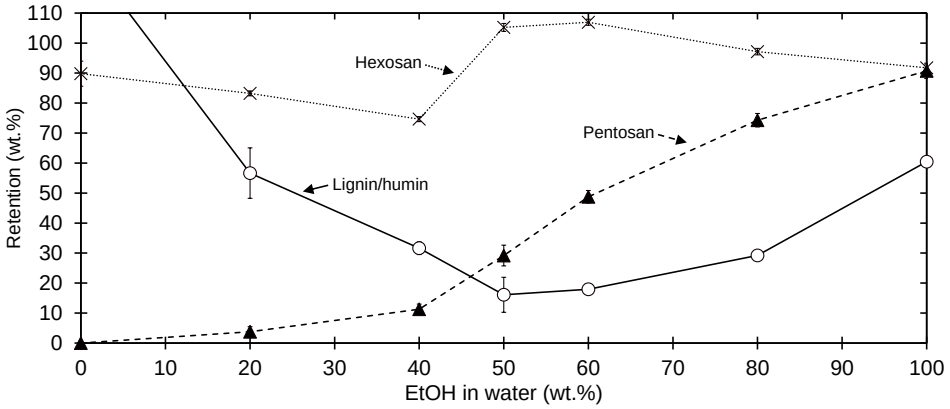

Figure 7.3: Pretreatment of poplar for 3 h at 200° C for varying solvent composition (EtOH - Water mixture), no acid was added. Note: samples were washed prior to yield calculation and compositional characterisation. The composition was determined in duplicate, except for the experiments with 20 and 40 wt.% ethanol, where the sugar fraction was determined by a single measurement. The error in the solid residue yield, which is needed to calculate the retention, is unknown and therefore underestimated.

Various aspects in this process advocate the use of a pretreatment solvent with high water content, namely: 1) low cost, 2) reduces the organic solvent recovery specification, 3) relatively good solvent for ashes, 4) present in the feedstock, and 5) high compatibility with hydrogenolysis step. Consequently, a high-water solvent share results in deep depolymerisation of hemicellulose during the pretreatment. This means that hemicellulose is not utilized for the production of glycols but is present in the lignin downstream and needs to be separated hereof for further valorisation.

7.2.4 In-situ generation of organic solvent

Our process relies on a solvent composed of water, light organic acids and light alcohols. As these cost 300-600 $ per ton, which is similar to the end products, EG & PG (∼800 $ per ton) and vastly more than the feed price (∼80 $ per ton[17],[105]), one intuitively feels that a loss of these organic molecules comes at a high economic penalty. We therefore envision to produce these molecules in-situ to compensate for losses. In this section we estimate the size of this make-up stream. In-situ organic solvent production mainly proceeds via 1) hydrolysis of acetyl groups during pretreatment, 2) acid production via biomass degradation reactions, and/or 3) light alcohol byproduct

formation during hydrogenolysis. The percentage of biomass acetyl groups is typically in the order of 1.2-4.4 wt.%[135], as is also reflected by the measured acetyl groups of three biomass archetypes, see Table 2.1 in Chapter 2 (1.4-4.6 wt.%) and was 3 wt% for poplar used in this study. These acetyl groups are easily liberated from the biomass to yield acetic acid[136]. Indeed, we found an acetic acid yield of 4-5 wt.% on biomass intake for the experiments depicted in Figure 7.3, when the solvent was composed of at least 40 wt.% water see Figure E.3 in Appendix E. Measurement of the residual o-acetyl groups of the solid residue confirmed that over 80 wt.% of the o-acetyl groups were hydrolysed (Figure E.4 in Appendix E). Besides liberation of the o-acetyl groups, degradation of the saccharide fraction can yield organic acids[87],[137]. We found that next to acetic acid, minor fractions of formic, lactic and glycolic acids are produced (3-4 wt.% in total), see Figure E.5 in Appendix E. Lactic and glycolic acid are of less interest as they cannot be recovered by evaporation. However, they could be valuable as chelating agent to trap the alkaline ash, and thereby saving consumption of light acids, such as acetic acid.

During hydrogenolysis roughly 3-5 wt.% of light alcohol byproducts are formed, expressed on biomass intake to pretreatment step, see Appendix E.3.2.

To summarize, a total of 4-5 wt.% of acetic acid, 3-5 wt.% of light alcohols and optionally 3-4 wt.% of other organic acids are generated in the pretreatment and hydrogenolysis steps combined. In total, 10-14 wt.% of organic molecules are produced in-situ.

Besides production, a fraction of the organic solvent is consumed by 1) chemical bonding with a biomass fraction (e.g. cellulose or lignin) or in case of acids, 2) by neutralisation with basic ash.

Cellulose could be acetylated during the pretreatment step. However, we previously discussed that over 80 wt.% of the o-acetylgroups were liberated for the experiments depicted in Figure 7.3. Even for PT-B in which the solvent was composed of 70 wt.% acetic acid (the remainder being water), 40 wt.% of the o-acetylgroups were liberated, see Table E.2 in Appendix E. Thus, overall, the conversion of biomass to solid residue is a source of acetic acid. Furthermore, the solid residue is hydrolysed in the hydrogenolysis step, thereby releasing chemically bound acetic acid and light alcohols, which can then be recycled to the pretreatment step. Note that this is a distinct advantage of this process compared to traditional organosolv aiming for pulp production,

for these processes are truly losing the solvent in the final product.

Acetylation of lignin, however, would result in a loss of acetic acid, as lignin is either sold or combusted. Acid hydrolysis of lignin showed that acetylation of lignin for PT-A (EtOH) was negligible (0.02 wt.% on biomass intake), whereas it was significant for PT-B (HAc), 0.4 wt.% on biomass intake, see Table E.3 in Appendix E. On the other hand, lignin bound some 0.3 wt.% of ethanol (on biomass basis) for the ethanol-water experiment (PT-A), see Table E.4 in Appendix E. Hence, lignin is a minor source of solvent loss.

Neutralisation of poplar wood consumed 0.15 ± 0.01 mol H^+ / $kg_{Biomass}$, which boils down to an acetic acid consumption of 0.9±0.07 wt.% on biomass intake, see Table E.5 in Appendix E. Smit et al.[138] found a very similar value for poplar, namely 0.13 mol H^+ / $kg_{Biomass}$. Typically, acid neutralisation capacity (ANC) is around 0.1 mol H^+ per kg of dry biomass for wood species, but can be up to 1 mol H^+ per kg of dry for herbaceous biomass (i.e. 0.4-6 wt.% of acetic acid on biomass intake)[31],[138]. The measured ANC of poplar was roughly halved after water extraction, see Table E.5 in Appendix E. Optionally a wash step prior to the pretreatment could be considered to reduce the need for acids. In general, the acid consumption by titration of the alkaline material is between 0.5 and 6 wt.% of acetic acid on biomass intake.

Overall, 4-9 wt.% of light organic alcohols and acids are net produced (Table 7.1). This value could be stretched to ∼13 wt.% when considering a biomass prewash to get rid of alkaline material or utilization of heavy acids (e.g. lactic and glycolic acid), that are formed within the process, as titrant of the basic ash.

7.2.5 Solvent recovery target

We previously discussed that biomass is a net producer of light organic molecules that can be utilized as process solvent. The absolute organic solvent loss is preferably lower than the absolute production. An organic solvent deficit could be compensated by additional solvent intake. However, this intake will come at an economic penalty, compared to the in-situ produced molecules. We derived an equation that describes the required organic solvent recovery rate (R) within the process, see equation 7.1 (see Appendix E.4 for derivation). In this equation, Y_{Lights} is the conversion of biomass to light acids and alcohols, B/S is the biomass to solvent mass ratio and $f_{organic}$ is the organic weight fraction of the solvent.

*Table 7.1: Organic solvent production and consumption during pretreatment expressed on dry biomass intake. *6 wt.% Acetic acid (on the worst-case scenario), 2.5 (pessimistic) and 0.5 (optimistic) are used for calculation.*

	Yield (wt.% on biomass intake)
Production	
Acetic-acid (hydrolysis of acetyl groups + biomass degradation)	4-5
Other organic acids (biomass degradation)	3-4
Light alcohols (hydrogenolysis bypdroct)	3-5
Consumption	
Lignin (acetylation or etherification)	-0.4
Neutralisation	-0.5-6*
Total	4-13

A high recovery rate results in a stringent recovery specification, which would ultimately be costly. The upper and lower boundaries for the recovery rate follow from equation 7.1. As discussed in Section 3.4 the conversion of biomass to lights is between 4 and optimistically 13 wt.%. The biomass to liquid ratio in industrial reactors is at max $\sim$0.25, but in academic studies it is typically 0.11[139]. For successful delignification, the process solvent needs to be composed for a large share ($\geq$50 wt.%) of organic molecules, see Section 7.2.3. Filling in equation 7.1 with these numbers results in a recovery rate of 93.5 wt.% (optimistic) to 99.9 wt.% (pessimistic), see Appendix E.4 for details. Even the most optimistic scenario shows that high solvent recovery is pivotal to process viability.

$$\text{R (wt.\%)} = \left(1 - \text{Y}_{\text{Lights}} \times \frac{\text{B}}{\text{S}} \times \frac{1}{\text{f}_{\text{Organic}}}\right) \times 100 \tag{7.1}$$

Although in every scenario a high organic solvent recovery rate is required, missing out on the recovery rate by 1 wt.% (equation 7.1), translates to an additional solvent make up cost, in an optimistic scenario, of 8 $ dollar per ton biomass fed, whereas the margin, defined as *"product price x product yield – biomass price*", is roughly 60 $ dollar per ton biomass fed. Therefore, mitigating or avoiding the need for an external solvent make up presents an important economic advantage. See Appendix E.4 for details.

It is important to realise here that the recovery rate is a linear function of Y_{Lights} and B/S (Note: non-linear with respect to biomass loading) but non-

linear with respect to the organic fraction of the solvent. In a quest to reduce the necessary solvent recovery rate, finding chemistries that allow successful delignification while relying on a low solvent share of organics (e.g. $\leq$50 wt.%) is much more beneficial than increasing the conversion of biomass to lights.

7.2.6 Evaporator

The stringent solvent recovery specification requires the selection of a robust separation technique that can fractionate the solvent and dissolved biomass fraction (e.g. lignin, ash, hemicellulose). We therefore opted to use an evaporator, which is commonly used in the pulp and paper industry. This prohibits the use of strong high boiling acids, such as sulphuric acid. We observed a build-up of polymerised material that was insoluble in acetone and ethanol on the cooking flask wall during solvent recovery by evaporation. The acidity in the solvent increased due to the build-up of sulphuric acid and consequently enhanced unwanted polymerisation reactions.

Furthermore, the process should be operated at an energy efficient manner. As a lower boundary for the available energy, we propose to combust all lignin, that has a higher heating value of $\sim$25 MJ kg^{-1}[140], which translates to $\sim$5.4 MJ per kg of biomass processed. We calculated the required heat duties based on the heat of vaporization for a solvent to biomass ratio S/B of 4 to 1 and 9 to 1, see Table 7.2. It is evident that a low solvent to biomass ratio is imperative. But even for a solvent to biomass ratio of 4/1, the required energy duty largely surpasses the available energy in case of water. Moreover, this is also the case for a 50/50 w/w ethanol/water scenario, which requires 6.6 MJ per kg biomass processed. This shows the need for reclaiming the energy lost by evaporation, for example by multiple-effect evaporation, which is common in the pulp and paper industry.

Table 7.2: Heat of vaporization of pretreatment solvent constituents and required energy duty per kg of biomass processed for a solvent to biomass ratio of 4 to 1 and 9 to 1

	H_{vap} (MJ kg^{-1})	Q (MJ / kg$_{Biomass}$) for S/B of 4	Q (MJ / kg$_{Biomass}$) for S/B of 9
Water	2.4	9.6	21.6
Ethanol	0.9	3.6	8.1
Acetic acid	0.4	1.6	3.6

7.3 Conclusion

In this work, we propose a lignocellulosic biomass pretreatment process that is integrated with a subsequent catalytic hydrogenolysis step, to convert saccharides to ethylene-glycol. The major target of this pretreatment is the selective removal of catalyst poisons, such as lignin and tungstate poisons (i.e. divalent cations), like calcium ($\leq$4 mmol per kg biomass). After careful analysis, we have determined the specific design criteria required for the pretreatment step (Table 7.3).

Table 7.3: Pretreatment design summary.

Consideration	Criteria
Product composition	
Lignin	<5 wt.% in solid residue
Divalent ions (e.g. Ca)	$\leq$4 mmol per kg solid residue
Alkaline ash	Preferably removed
Pretreatment conditions	
Biomass to liquid ratio	as low as possible e.g. 1:4 w/w
Solvent	Compatible with hydrogenolysis: water + light alcohols + light acids
Solvent composition	50/50 w/w organic/H_2O
pH	Acidic
Inorganic additives	Prohibited (Halogens & N & S components)
Others	
In-situ solvent generation	4-13 wt.% on biomass intake
Solvent recovery	>93.5 wt.%
Evaporator	Multi-effect or combined with energy efficient separator

We propose a solvent-based pretreatment utilizing light alcohols, organic acids and water, which are byproducts of the pretreatment and hydrogenolysis reactions, and could therefore compensate for losses in the system. In line with past research, it appeared that the pretreatment solvent should be at least composed of $\sim$50 wt.% of organic solvent to achieve deep delignification. However, such pretreatment did not remove sufficient calcium, a tungstate poison, from the biomass and required the selection of a more acidic pretreatment solvent. Biomass pretreatment with a solvent composed of 70 wt.% acetic acid and the remainder being water produced a solid residue with a calcium and magnesium content of 124 and 2 mg per kg biomass respectively, thereby meeting the performance constraint of $\leq$4 mmol per kg biomass. Hydrogenolysis of this sample resulted in a higher glycol yield compared to untreated biomass, confirming the removal of cata-

lyst poisons during pretreatment. Moreover, the overall process yields were higher, at 16 and 3 wt.% of EG and PG respectively compared to 6 and 9 wt.% for untreated poplar.

We found that 4-13 wt.% of the biomass can be converted to organic solvent, but it turns out that a high solvent recovery is still essential. In an optimistic scenario a minimum solvent recovery of 93.5 wt% is needed while a conservative estimate dictates a 99.9 wt.% requirement recovery. Despite the desired high recovery rate, in-situ generation of solvent appears to present an important economic advantage. We plea to use an evaporator to recover the solvent, which is a robust separation technique, and likely to meet the required high recovery. However, preliminary calculations showed that there is a gap between the heat duty and the available heat obtained from the combustion of lignin.

Countercurrent pretreatment: Experiments and modelling

"All models are wrong, but some are useful"

- George Box -

Abstract

In liquid-phase pretreatment, biomass residue retains substantial amounts of liquid that cannot be removed by a filter press. Consequently, components that are dissolved in this liquid during pretreatment, e.g. lignin, are also retained on the biomass residue. We show here that countercurrent operation is an effective way to overcome this issue and we illustrate this by tracking the lignin removal. Countercurrent operation was mimicked by a series of batch experiments and compared to a mathematical model. A three-stages countercurrent extraction process delivered a solid residue with a lignin content of 4.1 wt.% (experimental) and 4.2 wt.% (model), which was three times lower than the one found for a single stage, namely $\sim$13 wt.% (experimental) and 12 wt.% (model). Insights from the model suggest that optimal lignin removal proceeds best by finalizing the delignification step in spent solvent prior to countercurrent extraction (i.e. washing) of the solid residue.

8.1 Introduction

Routes for the conversion of lignocellulosic biomass to chemicals often proceed via a pretreatment step, which is usually required to ease downstream processing. The aims of such pretreatments vary significantly with the downstream application. For instance, when targeting the microbial conversion of polysaccharides to fuels and chemicals, the main objective of pretreatment is to increase the accessibility of the substrate for the hydrolysis enzymes[102],[141]. Alternatively, the pretreatment for pulp production aims to liberate the fibres from the biomass and to remove the lignin fraction[125]. Another option is to convert the holocellulose fraction to chemicals such as glycols via catalytic hydrogenolysis, which requires removal of lignin[66] and divalent cations[116]. The removal of lignin is also a key target for the production of pulp, which has been extensively studied in the past[126],[127].

Removal of lignin via solvent-based pretreatment, typically comprises two steps: 1) liberation of lignin from the biomass matrix and dissolution in a solvent, and 2) separation of the solid biomass and the liquid solvent, e.g. by a filter press. However, biomass and its solid residue have the ability to trap vast amounts of liquids. As such, the dissolved lignin will still be present in the liquid trapped by the biomass, and thus, it is not removed. This effect worsens when decreasing the biomass to solvent ratio, because the concentration of lignin in the solvent increases when increasing the biomass to solvent ratio. The trapped liquid with dissolved lignin could be displaced by fresh solvent (washing) but the introduction of additional solvent and equipment is costly and is therefore undesirable.

Typical lab experiments are performed batch wise, and the solid residue is extensively washed afterwards, thereby ignoring the implication of the trapped liquid in which unwanted components remain dissolved. Countercurrent operation displaces the dirty solvent that is trapped in the solid by new fresh solvent, thereby delivering a cleaner solid residue and thus more efficient overall removal without the use of additional solvent. There are industrial examples of solid-liquid operations that are based on this principle. This is the case for the Kamyr digesters in the pulp and paper industry and for various types of extractors applied in the food industry[142],[143].

We focus here on a solvent-based pretreatment that aims to selectively remove biomass components that poison a metal-catalyst that would be ap-

plied for valorisation of the solid saccharide fraction. In this work we try to connect laboratory scale experiments with industrial relevant operation. We have mimicked countercurrent pretreatment by a series of lab-scale batch experiments, targeting the removal of lignin. We selected a sensitive case, i.e. a high biomass loading, in order to show that countercurrent operation indeed results in superior lignin removal of the solid residue compared to batch operation. The experimental results were compared with a mathematical model, which was further used to draw lessons for design considerations and to direct further research. Although we focus on lignin removal in this work, the removal of other fractions, e.g. inorganics, is also challenged by the ability of biomass to trap liquid.

8.2 Model description

8.2.1 Liquid flows

Contrary to a regular extraction column, where both liquid flows, solution and solvent, are set, the liquid flows in our biomass extractor are imposed by the solvent retention of the biomass, i.e. its ability to trap liquid ($g_{solvent}$ / g_{solid}). This trapped liquid (L_T) moves with the biomass in the opposite direction, i.e. countercurrent, to the liquid that is not dragged by the biomass, i.e. the free liquid (L_F), as illustrated in Figure 8.1. The biomass feedstock is fed dry and, therefore, no trapped liquid enters at stage 1. In general, the absolute amount of trapped liquid decreases for every succeeding stage as part of the biomass is converted and dissolved, which reduces the amount of biomass to carryover liquid to the next stage (under the assumption that the solvent retention does not change). Importantly, the solvent retention ($g_{Solvent}$ / g_{Solid}), was expected to depend on the characteristics of this sample (e.g. porosity, surface area) and the effectiveness of our filter press, but was typically found to be around 2.

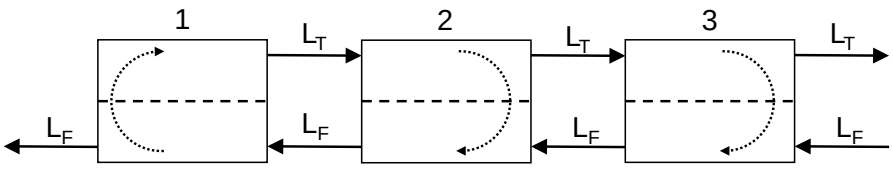

Figure 8.1: Schematic representation of liquid flows in a three-stage countercurrent extractor.

The trapped liquid flow (g) was calculated according to equation 8.1, in which B_{Init} is the initial biomass (g) fed to the process, Y_N the solid residue yield (wt.%) at stage N with respect to the initial fed biomass (B_{Init}) and SR the solvent retention ($g_{Solvent}$ / g_{Solid}).

$$L_T = B_{Init} \cdot \frac{Y_N}{100} \cdot SR \tag{8.1}$$

The free liquid fed to the extractor, stage 3 in Figure 8.1, is set to be lignin-free and fed at the target solvent/biomass (B_{Init}) weight ratio. The free liquid flow on other stages is dictated by the free liquid flow of the succeeding stage and the trapped liquid flow that has been released upon partial biomass digestion in the preceding stage. Thus, the liquid flows at each stage can be calculated when the solid residue yield at every stage, solvent retention and the biomass intake at the first stage and liquid intake at the last stage are known.

The lignin (material) balance over one stage can then be described according to Figure 8.2. Lignin is entering the stage as the trapped liquid ($L_{T,N-1}$ • $C_{T,N-1}$) from the preceding stage (N-1) and as free liquid ($L_{F,N+1}$ • $C_{F,N+1}$) from the succeeding stage (N+1). Lignin is leaving the stage by the liquid that is trapped in the biomass ($L_{T,N}$ • $C_{T,N}$) and the free liquid ($L_{F,N}$ • $C_{F,N}$) that is passed on to the preceding stage (N-1). Delignification of biomass at stage N yields an influx of lignin from the solid biomass matrix defined as P_N to the trapped liquid phase, which concentration equilibrates with the concentration in the free liquid phase when sufficient time is provided.

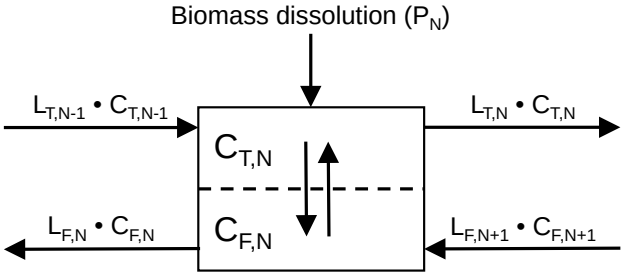

Figure 8.2: Schematic representation of material balance in the liquid over stage N.

The solubility characteristics of the trapped and free liquid are the same as their composition is identical, except the amount of solute (lignin) can be different. We therefore expect that the concentration of solute C_T in the trapped

liquid phase is equal to solute C_F in the free liquid phase, i.e. $C_{T,N}$ / $C_{F,N}$ = D = 1, provided that sufficient time was given to reach equilibrium. Indeed, we experimentally determined the distribution coefficient and found it to be generally around 1, see Figure 8.3.

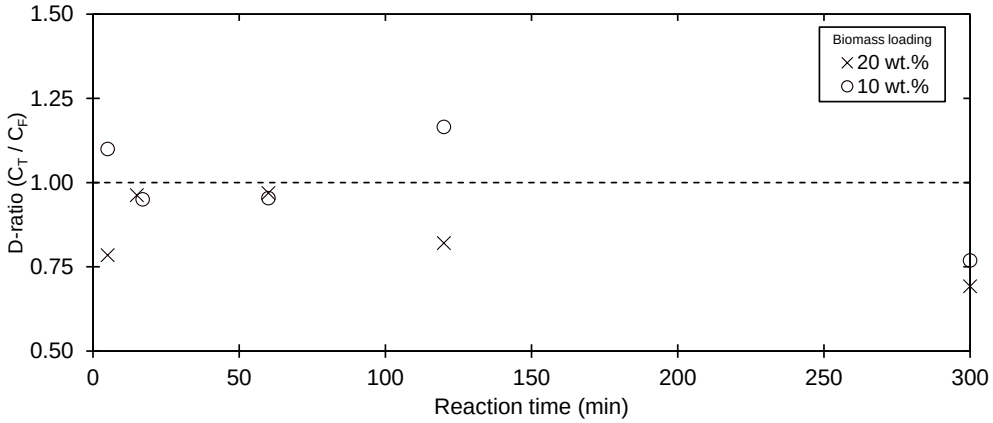

Figure 8.3: Experimentally determined D-ratio: C_T = lignin concentration in trapped liquid (L_T), divided by C_F = lignin concentration in free liquid (L_F), for various experiments performed at 10 and 20 wt.% biomass loading.

As D $\sim$ 1, the material balance for one stage presented in Figure 8.2 can then be simplified, $C_{F,N} = C_{T,N} = C$, which yields equation 8.2, in which P is the production term, i.e. the amount of lignin that is transferred from the solid to the liquid phase.

$$L_{T,N-1} \cdot C_{N-1} - L_{T,N} \cdot C_N + L_{F,N+1} \cdot C_{N+1} - L_{F,N} \cdot C_N + P_N = 0 \qquad (8.2)$$

The system of equations can easily be extended to any desired number of stages. For a system with three stages (N = 1, 2, 3), equation 8.2 results in a set of linear equations that can be described by a tridiagonal sparse matrix, see equation 8.3. Note that liquid flows were previously calculated and therefore constants resulting in set of linear equations.

$$\begin{bmatrix} -L_{T,1} - L_{F,1} & L_{F,2} & 0 \\ L_{T,1} & -L_{T,2} - L_{F,2} & L_{F,3} \\ 0 & L_{T,2} & -L_{T,3} - L_{F,3} \end{bmatrix} \cdot \begin{bmatrix} C_1 \\ C_2 \\ C_3 \end{bmatrix} = \begin{bmatrix} P_1 \\ P_2 \\ P_3 \end{bmatrix} \qquad (8.3)$$

This linear system is solved by linalg.solve routine from the NumPy library in

Python3 which yields the variables vector (C).

8.3 Experimental remarks

The pretreatment experiments were performed according to the procedures described in Chapter 2. Due to the destructive nature of the analytical methods employed, the solid residue of stage N cannot be fed to the next stage N+1. We therefore ran experiments in parallel and offered the resulting solid residue for analysis, as is schematically illustrated in Figure F.1 in Appendix F.

8.4 Results and discussion

The model developed and described in the previous section (Section 8.2), was experimentally validated by a series of batch experiments. A scenario in which there was a great difference for the lignin concentration in the spent solvent at the different stages was simulated. We selected a pretreatment solvent composed of 70 wt.% acetic acid, the remainder being water, which was previously reported in literature[126] as a successful delignification medium. A biomass loading of 20 wt.%, which is considered high in particular for batch wise lab experiments, was selected as this would result in a big differential lignin concentration over the stages. Thus, the justification of such scenario provides high trustworthiness of our model. More importantly, it would show that biomass can be efficiently delignified on such low liquid to biomass ratio. The kinetic data needed for the model, i.e. lignin removal and solid residue yield, was determined by a series of experiments documented in Appendix F.3.

8.4.1 Model validation

To validate the model, we first tested the reliability of our batch experiments. Repetition of every data point is too labour-intensive. We therefore decided to run the single-stage experiment three times, see 1 stage in Table 8.1. It appears that all key figures are reasonably reproducible, and less critical parameters show good reproducibility as well, see Appendix F.2. Moreover, the model predictions are in line with the experimental data. It is striking that the lignin content of the solid residue after washing is low, $\sim$4 wt.%, but a factor 3 higher before washing $\sim$12 wt.%. This illustrates the critical impact that the solvent retention of biomass has on the final solid residue quality.

*Table 8.1: Comparison of the experimental and model outputs for 1 stage versus three countercurrent stages. Assumed SR = 1.9. *Solid residue yield was lower due to spill during the washing step. **Error margin reported as standard deviation*

	one stage		three stages	
	Experimental (n=3)**	Model	Experimental	Model
Free spent solvent				
Lignin concentration (g_{Lignin} / $kg_{Solvent}$)	58±0	49	4.3	3.6
Solid residue (dry)				
Lignin content (wt.%)	13±2	12	4.1	4.2
Yield (wt.%)	62±1	64	48	53
Washed solid residue (dry)				
Lignin content (wt.%)	3.8±0.4	3.6	2	3.6
Yield (wt.%)	51±1	52	38*	52

Following the methods described in the sections 8.2 and 8.3 we have run a three-stage countercurrent biomass delignification. The lignin concentration measured in the spent solvent at the last stage, 4.3 g_{Lignin} / $kg_{Solvent}$, is rather similar as the number found by the model, namely 3.6 g_{Lignin} / $kg_{Solvent}$. More importantly, the lignin concentration is more than ten times lower than for a single stage experiment, namely 58 $\pm$ 0 g_{Lignin} / $kg_{Solvent}$ for the experiment and 49 g_{Lignin} / $kg_{Solvent}$ for the model. Consequently, the lignin content of the solid residue is much lower for 3 stages, namely 4.1 wt.% (experimental) and 4.2 wt.% (model) than for a single stage, $\sim$13 $\pm$ 2 wt.% (experimental) and 12 wt.% (model). Thus, the lignin content of the solid residue was roughly 3 times lower compared to batch processing, which clearly demonstrates the importance of countercurrent processing.

The critical parameter for which the algebraic system of linear equations is solved is the lignin concentration in the solvent. It can be seen in Figure 8.4 that the lignin concentration predicted by the model and the experimental results match well, but the measured concentration is systematically somewhat higher than predicted concentration. The lignin concentration is quantified by a procedure that involves precipitation of lignin by water addition, as such, humins and non-water soluble extractives are also classified as lignin and would lead to an overestimation of the lignin concentration.

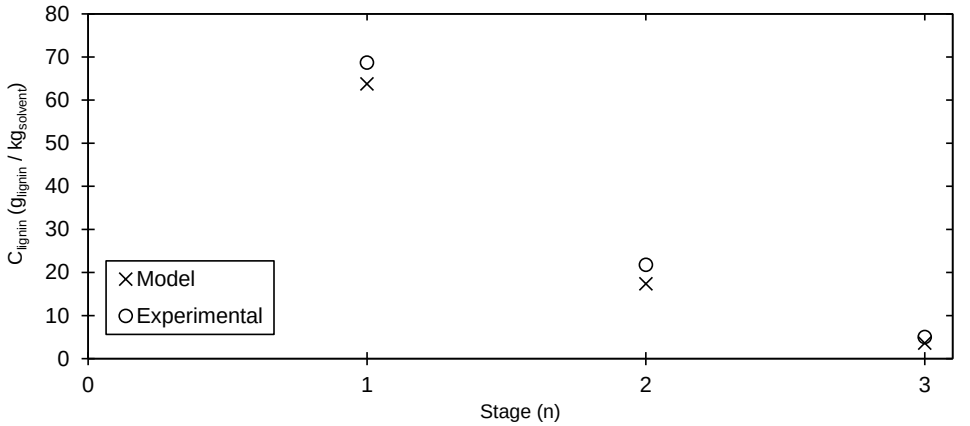

Figure 8.4: Lignin concentration in the solvent per stage, experimental outcome and model output. Simulation parameters: N_{Stages} = 3, Biomass loading = 20 wt.%, Solvent retention = 1.9, total residence time = 60 min.

An important remark here is that the model and experiments are to some extent interwoven. We start the experimental simulation of the countercurrent extractor with untreated biomass which then needs to mix with spent solvent from the succeeding stage, but the concentration of lignin at the succeeding stage is unknown. To overcome this artefact, we took the value determined by the model as input. Consequently, the same had to be done for the next stage, and we schematically indicated this aspect in Figure 8.5. However, the impact is small as the concentration of the next stage (N+1) is rather small compared to the current stage (N), i.e. C_N » C_{N+1}, and the free liquid flows are rather constant (L_F). The lignin concentration at stage 2 is only 27% of the concentration at stage 1 and similarly, the concentration at stage 3 is only 21% of the concentration at stage 2. Note that this issue does not persist for the last stage (3) as this stage is fed with fresh solvent (C_{Lignin} in L_F = 0).

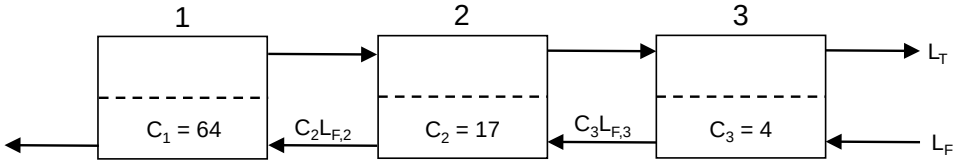

Figure 8.5: Simulated countercurrent experiments; values for C_2 and C_3 were taken from the model.

To further test our model, we have also validated a two-stage model, see Appendix F.4 for details. The difference in lignin concentration in the solvent for the model and experimental result were 7 and 1% for the first and second stage respectively which again shows good agreement between the model and experimental outcome. Moreover, there is good agreement between the experimental and model results for a single stage, see Table 8.1, for which the model and experiments are not intertwined.

8.4.2 Model results

The aim of our pretreatment is to maximize the removal of a contaminant, in this case lignin. The removal efficiency cannot be higher than the theoretical minimum, i.e. the lignin fraction that is liberated from the biomass matrix and subsequently dissolved. We consider here the lignin content of the solid residue as the quality parameter, which ideally is as low as possible. If the biomass would not trap any liquid, all the lignin that was liberated from the matrix would be effectively removed, which is indicated by the dotted line labelled as *"Theoretical minimum"* in Figure 8.6.

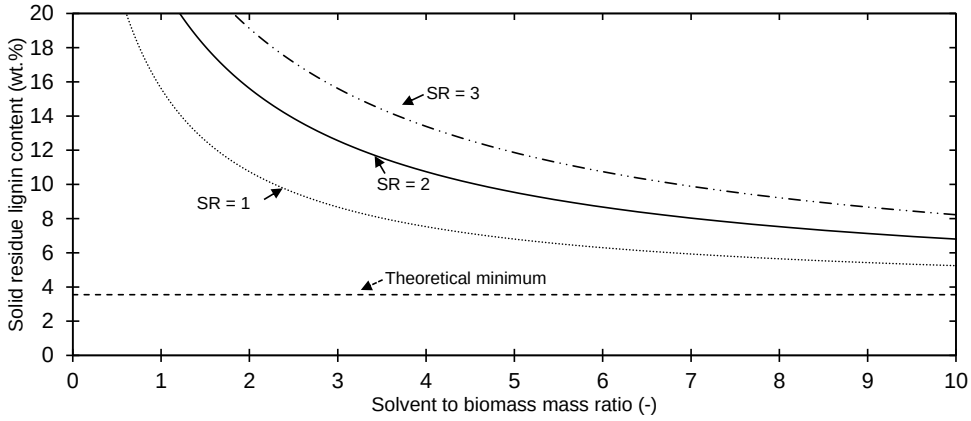

Figure 8.6: Implication of trapped liquid on residual lignin content of solid residue for different values for the solvent retention ($g_{Solvent}$ / $g_{Biomass}$). Simulation parameters: N_{Stages} = 1, total reaction time = 60 min.

As we will discuss shortly after, the removal efficiency and thus lignin content of the solid residue are heavily impacted by the biomass loading (solvent to biomass ratio), solvent retention and number of stages. For a single stage, i.e. batch reactor, the lignin content of the solid residue is roughly two times

as high (7.5 wt.%) than the theoretical minimum (3.6 wt.%), when considering a biomass residue with a solvent retention of 1 ($g_{Solvent}$ / $g_{Biomass}$) and operating at a solvent to biomass ratio of 4 ($g_{Solvent}$ / $g_{Biomass}$), see Figure 8.6.

This demonstrates that solvent retention has a major impact on the quality of the solid residue, i.e. its lignin content. The lignin content of the solid residue further increases to 10.7 and 13.4 for solvent retentions of two and three, respectively. It is therefore evident that the ability of biomass to trap vast amounts of liquids has major implications on the solid residue lignin content. A solution to this problem is to operate at an infinite solvent to biomass ratio, but this is, obviously, not economically attractive. In fact, no dilution is preferred, as this drives up costs as bigger equipment and larger energy duties are requested[105]. Although values for the solvent retention will vary depending on the exact biomass composition, structure as well as applied solid/liquid separation technique, a solvent retention of two is a typical number found for the pressure assisted filter press used in our laboratory.

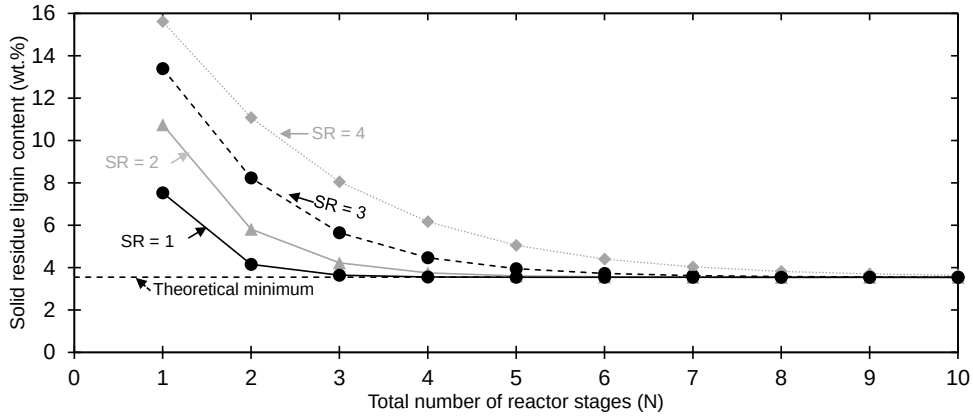

Figure 8.7: Residual lignin content of the solid residue as function of the total number of stages in a reactor for various solvent retentions (SR). Simulation parameters: N_{Stages} = 1, Biomass loading = 20 wt.%, total reaction time = 60 min.

As was experimentally demonstrated, the lignin content of the solid residue can be brought down by applying multiple stages without compromising the solvent to biomass feed ratio (Figure 8.7). Thus, more stages are needed to reduce the lignin content of the solid residue with increased solvent retention; for a solvent retention of 1, only 3 stages are needed to reach a lignin content

of the solid residue less than 4 wt.%, whereas 4, 5 and 8 stages are needed when the solvent retention is 2, 3 and 4 respectively. More importantly, when the reactor-system consists of sufficient stages, e.g. infinite stages, the lignin content of the solid residue will be equal to the theoretical minimum.

8.4.3 Extraction factor

We have observed that an increased solvent retention and a reduced solvent to biomass ratio leads to a poorer delignification of the solid reside. Both phenomena change the ratio of the trapped liquid to free liquid, e.g. an increase in solvent retention results in more trapped liquid and less free liquid.

$$E = D_{Ratio} \times \frac{\text{Free Liquid}}{\text{Trapped Liquid}} \tag{8.4}$$

The same is achieved by reducing the solvent to biomass ratio. We have therefore analysed the extraction factor, which is a well-established concept in liquid-liquid extraction, see equation 8.4. In this equation, D_{Ratio} is 1 as there is no affinity difference for the free and trapped liquids as both are identical in composition, which was experimentally proven, see Figure 8.3.

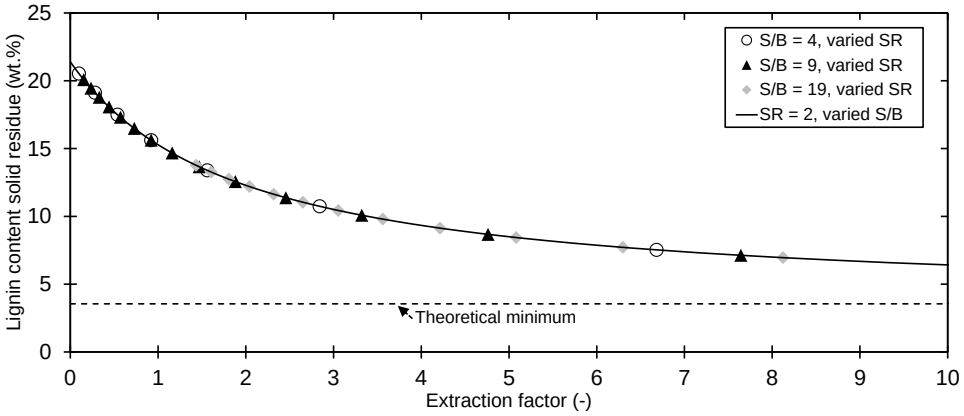

Figure 8.8: Residual lignin content of the solid residue as function of extraction factor for various cases of the solvent retention and solvent to biomass ratio (S/B). Simulation parameters: N_{Stages} = 1, Biomass loading = 20 wt.%, total reaction time = 60 min.

We have simulated various combinations of the solvent to biomass ratio (S/B)

and solvent retention (SR) and found that indeed the extraction factor is the root variable that determines the lignin content of the solid residue in the model, see Figure 8.8.

8.4.4 Extraction and reaction

The proposed countercurrent pretreatment is in fact a combination of simultaneous reaction and extraction. Obviously, when no lignin is liberated from the matrix (no reaction) there is no lignin that can be extracted from the trapped to the free liquid. This suggest that completion of the reaction prior to extraction is more effective than combined reaction and extraction at every stage due to the higher concentration of lignin in the solvent at the first stage in the first scenario. We have simulated both scenarios with 1) an evenly distributed reaction time at every stage and 2) a complete reaction at the first stage, and found that the latter needs less stages to reach a solid residue lignin content below 4 wt.% than the first option (4 instead of 8 stages), see Figure 8.9. This observation can be explained by two effects: 1) the trapped liquid flow becomes smaller with lower solid residue yield, i.e. higher conversion due to longer residence time, which yields a higher extraction factor and 2) the driving force, i.e. the difference in lignin concentration, is reduced when lignin from the solid matrix is introduced to the solvent later than the first stage.

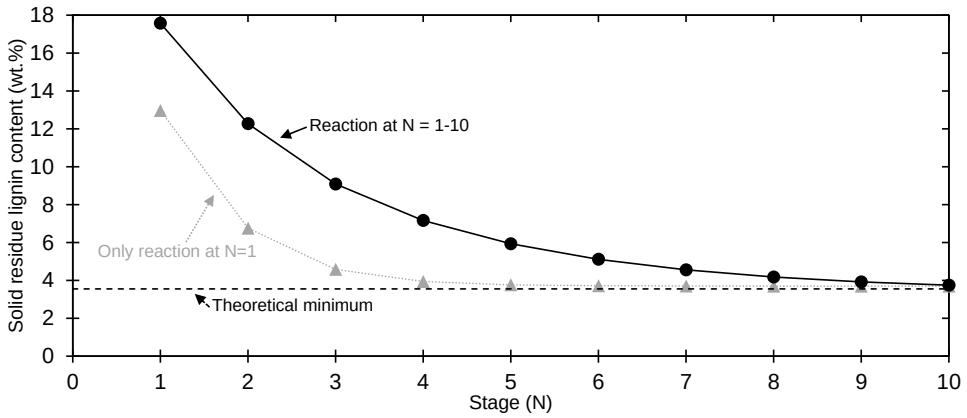

Figure 8.9: Residual lignin content of the solid residue per stage. Simulation parameters: Total stages = 10, Biomass loading = 20 wt.%, total reaction time is 30 min.

8.4.5 Discussion

8.4.5.1 Fundamentals

The extraction factor has a critical impact on the effectiveness of countercurrent pretreatment and can be expressed as function of the solvent to biomass ratio, the solvent retention of the solid residue and the solid residue yield, see equation 8.5. For countercurrent pretreatment to be effective, the extraction factor E, should be greater than 1, which means that for a typical case in which the solid residue yield (Y_{SR}) is 50 wt.% and the solvent retention is 2, the solvent to biomass ratio must be at least 2. In other words, the obtained solid residue yield and solvent retention impose a minimum solvent to biomass ratio. A low solvent to biomass ratio is imperative for economics but operation near an extraction factor of 1 will be impractical and requires an infinite number of stages to approach the theoretical minimum solid residue lignin content.

$$E = D_{Ratio} \times \left(\frac{\text{Solvent to biomass ratio}}{\frac{Y_{SR}}{100} \times SR} \text{-1} \right) \tag{8.5}$$

The solvent retention depends on the solid-liquid separation apparatus. For example, a filter press is more effective than a settling tank, and on the biomass physical and structural properties. Both can be tuned to some extend but we never found a solvent retention smaller than 1 in our experiments and more typically we found a solvent retention of 2. Equation 8.5 suggests that minimizing the solid residue yield is beneficial to increase the extraction factor, however, the solid residue is the product of interest and should therefore be maximized. Therefore, the solvent to biomass ratio and the number of stages are the only true operational parameters. A lower solvent to biomass ratio requires more stages to deliver the same product (lignin content) as a higher solvent to biomass ratio. This is matter of optimizing OPEX (solvent to biomass ratio) and CAPEX (number of stages).

Reaction and extraction can be performed at the same stage, but this is not preferred. It is more effective to achieve deep delignification in the first stage followed by extraction steps.

8.4.5.2 Apparatus

An ideal pretreatment apparatus operates in a countercurrent mode with infinite number of theoretical stages, but such device is envisioned to be highly complex due to the pressurized operation, pressurized feeding of wood chips and opposing solid and liquid flows. Nevertheless, such devices are operated in the pulp & paper industry and induce opposing particle-liquid flows by feeding the high-density material (biomass) at the top and introducing liquid at the bottom[139]. Operation of a continuous digester is, however, an intricate process as a net downwards force of the chip bed must be achieved, which depends on buoyancy, friction and weight of the chip column[139]. Moreover, the structural properties, such as particle size, are altered during digestion of the biomass which affect the forces acting on the particle.

We here found that, in fact, it is more optimal to separate the reaction and extraction functionalities, i.e. one reaction stage followed by multiple extraction stages. In the optimal solution the biomass is contacted in a pressurized vessel (reactor) with spent solvent for a desired reaction time at a desired temperature as such that deep delignification is achieved. The delignified solid residue, which traps a large amount of lignin by holding liquid, is then extracted in a multistage countercurrent device (washer), for example a moving bed reactor. The proposed scheme is shown in Figure 8.10. Note that although the reactor section is depicted as a stirred vessel, reactor design is not limited hereto, we simply want to emphasize that the direction of the fluid compared to biomass is not important. It is also worth noting that the liquid hold-up can be chosen independently from the solvent to biomass ratio. Increased hold up could be beneficial to facilitate sufficient mixing. Thus, reaction and extraction could be carried out in a low solid loading configuration, but systems that can handle a high solid loading are preferred due to higher productivity ($t_{product}$ / ($m^3_{reactor}$ h)).

Splitting the functionalities is more effective, but more importantly leads to a much simpler device as only the extraction step is operated in countercurrent mode but at ambient pressure. In addition, the particles in the extraction step are not subjected to structural changes and therefore do not complicate solid movement. Alternatively, we have observed that only a limited number of stages (e.g. 3) are needed to accomplish a substantial improvement in solid residue quality (Figure 8.9). Such pretreatment could, therefore, be realised by a simulated moving bed reactor (SMBR).

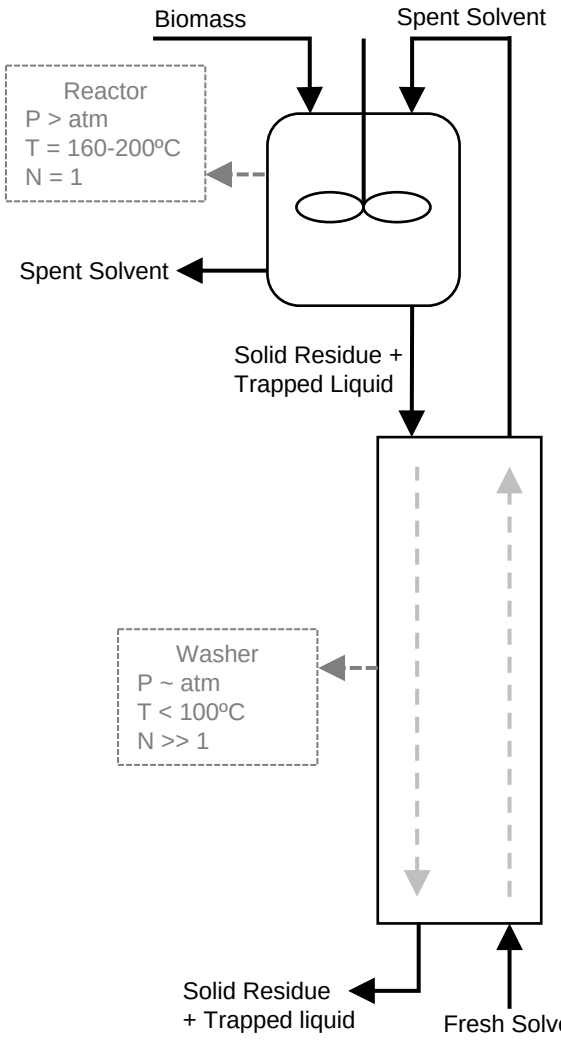

Figure 8.10: Schematic representation of optimal design

The critical note here is that high delignification must be achieved when the pretreatment is run in spent solvent. We have experimentally demonstrated that high delignification was achieved when operating with spent solvent under the chosen reaction conditions in this work. However, when considering alternative acidic pretreatments, spent solvent might be a less efficient delignification medium than fresh solvent as 1) spent solvent is partially neutralised by the alkaline ash present in biomass and 2) spent solvent contains

a higher concentration of lignin and degraded sugars. The first raises the pH which is suboptimal for delignification and the latter results in a higher rate of repolymerisation reactions of lignin and degraded sugars and subsequent deposition of these fractions on the solid residue.

Indeed, we noticed that the delignification kinetics were retarded when running at higher biomass loading (20 wt.% compared to 10 wt.%), which has a similar effect as running in spent solvent, i.e. higher concentration of biomass fragments such as lignin and alkaline ash in the solvent, see Figure F.2 and Figure F.3 in Appendix F. Likely, this can be ascribed to the pH measured after the experiments which was systematically higher for a 20 wt.% biomass loading compared to a 10 wt.% loading, see Figure F.4 in Appendix F. The dependency of pH on the delignification kinetics and maximum delignification has been broadly accepted[126],[127],[144]. The increase in pH due to the alkaline ash present in the biomass can be, at least partly, avoided by (acidic) washing of the biomass prior to pretreatment[111],[115]. The spent solvent leaving the reactor is a suitable candidate herefore. Also lignin repolymerisation and humin formation was more severe for high loading experiments, see datapoints at 120 and 300 minutes in Figure F.2 in Appendix F. For the reasons discussed we encourage others to study the kinetics of their pretreatment system in fresh as well as in spent solvent. Effective delignification in spent solvent is key for successful apparatus development.

8.5 Conclusion

Biomass and its solid residue (after pretreatment) inevitably trap a significant amount of liquid. Ultimately this limits the removal of lignin and other heavy fractions such as ash from the biomass during pretreatment without compromising process economics, i.e. using additional fresh liquid to displace the trapped liquid.

A possible solution is to perform countercurrent pretreatment, which we have described by a mathematical model and validated by series of batch experiments that mimicked countercurrent operation. For a single stage we found that the solid residue had a lignin content of $\sim$13 wt.% for the experiment and 12 wt.% for the model. A 3-stage countercurrent pretreatment delivered a solid residue with only 4.1 wt.% lignin (experimental) and 4.2 wt.% (model) for the same solvent to biomass ratio thereby showing that countercurrent operation is key to remove heavy fractions that are dissolved in the trapped liquid. More importantly, experiments and model results matched well.

We found that the performance of the countercurrent pretreatment is related to the extraction factor, which is described as the distribution coefficient times the free liquid flow divided by the trapped liquid flow. The ratio of these liquid flows is a result of the variable solvent to biomass ratio and invariable solvent retention. Consequently, a minimum solvent to biomass ratio of >2 was found for typical conditions, but operation near this minimum would require an infinite number of stages.

It is more effective to achieve deep delignification at the first stage followed by extraction at succeeding stages compared to simultaneous reaction and extraction due to a higher average driving force. In other words, it is better to split the reaction and extraction sections. This results in a significant simplification of the apparatus as countercurrent and pressurized operation are decoupled. However, critical to such device and any other form of countercurrent pretreatment is the necessity to run in spent solvent. We therefore encourage others that study different delignification chemistries (solvent, temperature, time) to run experiments in fresh but even so important; in spent solvent.

Summary, Conclusion & Outlook

"Things always become obvious after the fact"

- Nassim Nicholas Taleb -

9.1 Summary and conclusion

This thesis has investigated the conversion of lignocellulosic biomass to ethylene glycol (EG) via tungstate catalysed hydrogenolysis.

The specific goals of this work were: 1) identification and preferably quantification of catalyst deactivation phenomena due to the presence of components (other than holocellulose) in lignocellulosic biomass, and in parallel, 2) the development of suitable pretreatment techniques that can effectively remove the identified catalyst poisons (prevention). Although this thesis specifically targeted the production of EG, the lessons learned are likely relevant to other catalytic routes that target the conversion of biomass to fuels or chemicals using hydrogenation catalysts.

9.1.1 Hydrogenolysis protocol

Catalyst deactivation studies were performed by evaluating the glycol and sugar alcohol yield after hydrogenolysis of untreated and treated biomass substrates and mixtures of relevant model components of the biomass. Microcrystalline cellulose, which is free of impurities, was run as a reference. We developed a hydrogenolysis protocol that, in contrast to the literature, allows decoupling of the acid hydrolysis, aldol-cleavage and hydrogenation functionalities (Chapter 3). The protocol offers great flexibility and therefore allows to assign eventual yield deficit to the deactivation of one (or several) of the catalysts. Moreover, we have developed a HPLC method (Chapter 4) to measure the concentration of soluble sodium polytungstate in the reactor effluent, which is presumably the active species. This method thereby provides a standalone indication of the state of the tungstate catalyst, which in combination with the obtained product yields delivers valuable information on the state of the hydrogenation catalyst.

Industrial processes for the manufacturing of base chemicals typically require a catalyst consumption below 1 $tonne_{product}/kg_{catalyst}$[89]. For the present hydrogenolysis process, however, the desired catalytic reactions compete with thermal side reactions. Therefore, a minimum amount of catalyst is required to obtain acceptable product yields. For single batch experiments we found that for the tungstate catalyst a maximum biomass-to-catalyst ratio of about 32 g/g was viable. For the hydrogenation catalyst this ratio was about 8 g/g. Unfortunately, these ratios are far off from the industrial window. Although batch experiments have their limitations, they are useful for initial screening.

We found that a high glycol yield was obtained when running in excess of both catalysts. In fact, it turned out that wood powder, millimetre sized particles and *"single particles"* (Slice size = 22 mm (ø) x 3 mm), gave the same combined glycol yield (∼50 wt.%) as a cellulose reference test when an excess of catalyst was applied (Chapter 6). This means that the biomass structure, e.g. cellulose accessibility, is not limiting the yield. A low glycol yield should therefore be attributed to catalyst deactivation. We then tuned the hydrogenolysis protocol for maximum sensitivity towards catalyst poisons, i.e. by operating at the threshold catalyst to biomass ratio that is needed for high glycol yields. We can thus consider four potential outcomes: 1) no deactivation, 2) only deactivation of the tungstate catalyst, 3) only deactivation of the hydrogenation catalyst, and 4) deactivation of both catalysts, see Table 9.1.

Table 9.1: Hydrogenolysis scenarios when ran under conditions with maximum sensitivity towards catalyst poisons

N	W-catalyst *Active?*	Hydrogenation catalyst *Active*?	Dominant Product
1	✓	✓	Ethylene glycol
2	✗	✓	Sugar alcohols
3	✓	✗	Humins
4	✗	✗	Humins

Poisoning of the hydrogenation catalyst can always be identified from the product slate. However, deactivation of the tungstate catalyst can only be observed from the product slate when the hydrogenation catalyst is active as both scenarios 3 and 4 lead to the formation of humins, see Table 9.1. Moreover, solely relying on the product slate can be misleading as the formation of one of the products could be selectively blocked. For example, we observed that lignin present in the feed hampers the hydrogenation of sugars to sugar alcohols (SA), but not that of glycolaldehyde to EG, see Table 9.2.

As a consequence, scenario 6 from Table 9.2 could be mistakenly interpreted as scenario 3 or 4 from Table 9.1.

*Table 9.2: Hydrogenolysis scenarios when ran under conditions with maximum sensitivity towards catalyst poisons with lignin present in the feed. *Orange symbols: catalyst activity compromised but not fully deactivated.*

N	W-catalyst *Active?*	Hydrogenation catalyst *Active*?	Dominant Product
5			Ethylene glycol
6			Humins

The inability to discriminate between scenarios 3, 4 and 6 can be overcome by running an additional experiment in excess of W-catalyst or hydrogenation catalyst. As an alternative, however, we have developed a method to quantify the amount of soluble tungstate present in the reactor effluent to directly discriminate between scenarios 3 and 4 or 6 by assessing the degree of deactivation of the W-catalyst.

9.1.2 Catalyst deactivation

Our experimental studies have shown that ash components, in particular divalent cations, present in biomass deactivate the homogenous tungstate catalyst by forming insoluble components (Chapter 4). We derived that the concentration of divalent cations in biomass should remain below 4 mmol / $kg_{Biomass}$ to bring the catalyst consumption below the ceiling required for industrial operation. These impurities were selectively removed below the desired level of 4 mmol / $kg_{Biomass}$ by acid leaching of woody biomass. However, acid leaching was unsuccessful in completely removing these impurities from hay, an herbaceous biomass species. These species are notoriously rich in inorganics, extractives and proteins. Unfortunately, we were unable to identify all tungstate poisons, which requires further study.

Sulphur is a known poison for metal catalysts that is rarely addressed in studies related to the catalytic conversion of biomass. Deactivation of Raney nickel by sulphur was not observed for woody species of biomass, such as

pine, poplar and beech, which are lean in sulphur (Chapter 5). However, deactivation was significant when running experiments with hay or a mixture of cellulose and methionine (a sulphur-containing amino acid). From the experimental data we derived a very challenging feedstock specification of < 67-200 µmol (2-6 mg) sulphur per kg of biomass, which is much lower than the sulphur content of lignocellulosic biomass (e.g. $\sim$150 mg S kg^{-1} for pine and poplar).

The glycol yield appeared to reach a plateau upon the addition of nitrogen in the form of an amino-acid and suggests that deactivation of Raney nickel by nitrogen is less worrisome (Chapter 5). We have not observed any effect of amino-acids on the activity of the tungstate catalyst. Washing the biomass at room temperature with water, ethanol or 10 wt.% acetic acid in water were rather ineffective for nitrogen and sulphur removal.

Water-soluble extractives deactivate both tungstate and Raney nickel hydrogenation catalyst, but this is likely related to the removal of (water-soluble) divalent cations and (water-soluble) sulphur, i.e. sulphate.

Lignin, which is one of the major constituents of the biomass, inhibits the hydrogenation function, as was evidenced by a low sugar alcohol yield observed in the absence and presence of tungstate (Chapter 3). However, the hydrogenation catalyst (Raney nickel) seemed sufficiently active to hydrogenate glycolaldehyde to EG. A biomass sample with a lignin content of 44 wt.% did deliver the same EG yield as the cellulose reference test. Nevertheless, feeding large quantities of lignin will likely lead to practical problems as lignin is known to *"glue"* and, therefore, result in accumulation of lignin in the reactor.

9.1.3 Feedstock selection

The feedstock is a key variable for the process. In this work, we have discriminated between three biomass archetypes, softwood, hardwoods and herbaceous. The latter is rich in inorganics, extractives and sulphur/nitrogen, but relatively lean in lignin compared to wood species. This work suggests that sulphur and inorganics are the key inhibitors, and therefore wood species are the preferred feedstock. Note that the feedstock price and availability could impact this proposition.

The hemicellulose of softwood typically consists of hexose (C_6), whereas hardwoods and herbaceous species contain pentose (C_5) rich hemicellu-

lose. Hexoses (only aldoses) are desired when EG is targeted and, therefore, softwood is preferred when hemicellulose or its derivates are fed to the hydrogenolysis step for conversion to EG.

9.1.4 Process development

In parallel to the identification and quantification of catalyst poisons, we have studied pretreatment methods that can remove these poisons. Acid-leaching based on acetic acid successfully removes water-soluble extractives and divalent cations. However, this method does not reduce nitrogen, organic sulphur and the lignin content of the feed. Lignin did not appear problematic in batch tests but could become problematic for continuous operation or in downstream purification of the glycols stream.

We have studied an integrated process concept that allows significant removal of lignin (>80%) while preserving the cellulose fraction ($\sim$100% retention) in the solid residue (Chapter 7). In addition, it also removes the majority of ash >80%). In this process woody biomass is fractionated in a solvent composed of water and at least 50 wt.% of a mixture of light alcohol and organic acid (e.g., ethanol/acetic acid). We chose organic molecules that are by-products from the hydrogenolysis and pretreatment steps and are recycled over the process to minimize the need for solvent make-up. The modest by-product yields and the need for high solvent:biomass ratio in the pretreatment still lead to very high solvent recovery targets (>94 wt.% in a very optimistic scenario).

The removal of the contaminants, i.e. lignin and ashes, is run most efficiently by operating the washing section countercurrently (Chapter 8). The spent solvent (after washing) should be used in the reaction step to minimize solvent use. These guidelines hold for any solid liquid biomass operation which targets the valorisation of the solid residue.

9.2 Outlook

The most promising route to produce EG from a sugar feed proceeds via the aldol cleavage of glucose to glycolaldehyde (GA) followed by hydrogenation of GA to EG, see steps 4 and 5 in Figure 9.1. Major efforts to develop a process with lignocellulosic biomass as feed should be, in the authors view, dictated by the prevention and/or mitigation of catalyst deactivation. Two dis-

tinct pretreatment strategies exists, 1) either all catalyst poisons are removed and a solid cellulose rich residue is obtained (step 1 in Figure 9.1) or 2) the sugars are liberated from the lignocellulose and the poisons are left on the solid residue (step 2 in Figure 9.1). This thesis has targeted option 1 (step 1 in Figure 9.1) and we will therefore focus the discussion on this approach.

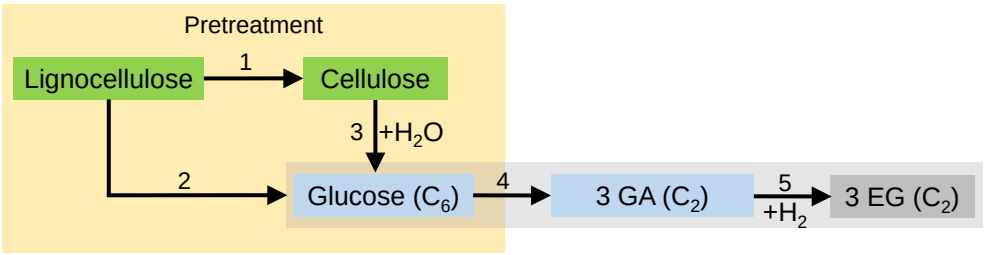

*Figure 9.1: From lignocellulose to EG reaction steps. *steps 1&2 could involve a variety of reactants/products and are therefore not mentioned*

The aldol cleavage of glucose to glycolaldehyde (step 4 in Figure 9.1) can be achieved by A) hydrous thermolysis (∼500°C), or B) W-catalysed in the liquid phase (200-250°C). Option B is challenged by inorganic constituents, mainly divalent ions, present in biomass. However, we have shown that a mild acid wash (10 wt.% acetic acid in water at room temperature) can remove tungstate poisons below the level (< 4 mmol / $kg_{Biomass}$) desired for industrial operation. Thus, both options; A) hydrous thermolysis and B) W-catalysed, show potential. Whereas the tungstate catalyst offers a lower reaction temperature, it requires liquid phase operation and the recovery and recycling of the homogenous tungstate back to the reactor.

Importantly, both options require a hydrogenation catalyst to convert glycolaldehyde to EG (step 5 in Figure 9.1). This step is critical with respect to catalyst poisons and one should avoid contacting the hydrogenation catalyst with high molecular weight species (e.g. lignin, humins, extractives), heteroatoms (e.g. sulphur, nitrogen, except oxygen) and preferably inorganics. In other words, these poisons have to be removed from the feedstock upfront. Or alternatively, mitigation measures during the hydrogenolysis step should be taken. We have not found an effective pretreatment for the removal of sulphur and nitrogen; extraction of biomass at room temperature with water, ethanol or 10 wt.% acetic acid in water was insufficient. The unremoved S and N were released upon hydrogenolysis and led to deactivation of the hy-

drogenation catalyst. We therefore hypothesize that sulphur and nitrogen are released under conditions that facilitate (partial) hydrolysis of the biomass. This hypothesis provides a starting point for further screening of pretreatment options.

Alternatively, or if it turns out that no suitable pretreatment can be found to remove sulphur (and nitrogen), one can engineer a catalyst that is resistant or at least has a higher tolerance to sulphur and nitrogen. The petrochemical industry has a long history in the development of sulphur resistant catalysts, well known are NiMo and CoMo catalysts. The patent literature describes the successful hydrogenation of glycerol by the use of a sulphided CoMo catalyst in the presence of cysteine whereas noble metal catalyst were severely poisoned under similar conditions (aqueous solution, 255°C)[145]. However, such a catalyst is not stable under hydrothermal conditions and displays poor activity in non-sulphided state[145],[146]. It requires the introduction of (reduced) sulphur in the feed at appropriate levels[146]. It was previously shown that cysteine was successfully used for that purpose[146] and, thus potentially, no additional sulphur-source in the feed is required. There are also alternative approaches reported in literature that still rely on a noble metal catalyst that is susceptible to sulphur-poisoning, but devise sulphur resistance/tolerance catalyst by engineering the environment around the active sites[147] or catalyst support[148]. It is also suggested to mitigate the poisoning effect of sulphur by performing the hydrogenation of glycolaldehyde at a low temperature (80-120°C)[83]. However, the production of glycolaldehyde from glucose requires a much higher temperature (∼200°C for W-catalysed or ∼500°C for hydrous thermolysis). GA is thermally unstable at these temperatures and should therefore be quenched or instantaneously converted to EG. Low temperature hydrogenation therefore requires a quench of the GA rich mixture and consequently two process steps instead of one are required, which is undesirable.

In our batch tests, although lignin (and humins) did not emerge as critical poisons, their presence cannot be ignored. In continuous operation lignin can still emerge as a threat for the hydrogenation catalyst. Even after organosolv type treatment the solid residue still contains some ∼5 wt.% of lignin, which is a fairly large amount when targeting a catalyst consumption in the order of 1 $tonne_{Product}$ / $kg_{Catalyst}$. Moreover, lignin is known to *"glue"* reactor equipment and infrastructure at our operating temperature (∼245°C). The lignin content of the solid residue can be brought down by oxidative treatment (bleaching),

but this seems a costly endeavour and often requires the introduction of inorganic species that might harm the catalyst(s). A more favourable option is to perform the hydrogenolysis step in an organic-aqueous solvent which facilitates the dissolution of lignin, humins and extractives and thereby retards their polymerisation and subsequent fouling of reactor equipment and hydrogenation catalyst. The organic-solvent could actually be composed of depolymerised lignin produced in-situ or by reductive catalytic fractionation as a pretreatment step.

Although acid leaching appeared to sufficiently remove tungstate poisons, not all of the inorganic material is removed. The inorganic content of acid leached biomass is particularly rich in silica[93]. Also, our organosolv type approach failed to fully remove the ash fraction. Silica is unstable under hydrothermal conditions[31] and will therefore slowly dissolve in the hydrogenolysis solvent. This could potentially lead to the formation of silicotungstic-acid, which is less effective for the aldol cleavage of sugar to glycolaldehyde[70] and therefore, a less popular choice. Understanding of the potential formation of silicotungstic-acid from biomass ash and the W-catalyst and activity of such catalyst is desired.

Still considerable hurdles exist in the removal of catalyst poisons for a route based on step 1 in Figure 9.1. Despite that, we have not identified a showstopper. A route based on step 1, i.e. the preservation of cellulose during pretreatment, offers the intrinsic advantage that cellulose is relatively stable whereas glucose is prone to coking[149] upon feeding to the hydrogenolysis section and could lead to equipment and catalyst fouling. An approach based on the hydrolysis of cellulose to glucose (step 2 in Figure 9.1) would require the introduction of an additional catalyst. The most practical cases seem: 1) a strong mineral acid (e.g. HCl) as advocated by Avantium[150], or 2) enzymes which is proposed by UPM[59]. Unfortunately, both are known poisons of hydrogenation catalysts and such an approach would require extensive clean-up of the hydrolysis effluent. Therefore, the high potential of the route explored in this thesis (based on step 1 in Figure 9.1) makes it worthwhile for further exploration.

Samenvatting

Samenvatting

In dit proefschrift is de omzetting van lignocellulose biomassa naar ethyleenglycol (EG) via wolframaat-gekatalyseerde hydrogenolyse onderzocht. De specifieke doelen van dit werk waren: 1) identificatie en bij voorkeur kwantificering van katalysatordeactiveringsverschijnselen als gevolg van de aanwezigheid van verschillende componenten (anders dan holocellulose) in lignocellulose biomassa, en parallel, 2) de ontwikkeling van geschikte voorbehandelingstechnieken die de geïdentificeerde katalysatorvergiften effectief kunnen verwijderen (preventie). Hoewel dit proefschrift specifiek gericht is op de productie van ethyleenglycol, zijn de geleerde lessen waarschijnlijk relevant voor andere katalytische routes die gericht zijn op de omzetting van biomassa in brandstoffen of chemicaliën met behulp van hydrogeneringskatalysatoren.

Hydrogenolyse protocol

Studies omtrent de deactivatie van de katalysatoren werden uitgevoerd door het evalueren van de glycol- en suikeralcoholopbrengst na hydrogenolyse van onbehandelde en behandelde biomassamonsters en mengsels van relevante modelcomponenten. Microkristallijne cellulose, die vrij is van onzuiverheden, werd als referentie gebruikt. We ontwikkelden een hydrogenolyseprotocol dat, in tegenstelling tot de literatuur, de ontkoppeling van de zure hydrolyse, aldol-splitsing en hydrogenatie functionaliteiten mogelijk maakte (Hoofdstuk 3). Het protocol biedt een grote flexibiliteit en maakt het daarom mogelijk een eventueel opbrengsttekort toe te wijzen aan de deactivering van een (of meerdere) van de katalysatoren. Bovendien hebben we een HPLC-methode (Hoofdstuk 4) ontwikkeld om de concentratie van oplosbaar natriumpolywolframaat in het reactoreffluent te meten, wat verondersteld wordt als de actieve katalysatorvorm. Deze methode verschaft daarmee een onafhankelijke indicatie van de conditie van de wolframaatkatalysator, die in combinatie met de verkregen productopbrengsten waardevolle informatie geeft over de toestand van de hydrogeneringskatalysator.

De industriële productie van basischemicaliën vereist doorgaans een katalysatorverbruik van minder dan 1 $kg_{katalysator}$ / ton $_{product}$)[89]. De katalytische reacties concurreren echter met thermische nevenreacties en vereisen daarom een minimale hoeveelheid katalysator om deze thermische nevenreacties teniet te doen. We ontdekten dat in enkelvoudige batch experimenten een biomassa-tot-Raneynikkel-verhouding van $\sim$8 g/g en een

biomassa-tot-natriumpolywolframaat-verhouding van ∼32 g/g de hoogst mogelijke biomassa-tot-katalysatorverhouding was die nog steeds voldoende productie van gehydrogeneerde producten mogelijk maakte. Helaas zijn deze verhoudingen ver verwijderd van het industrieel benodigde criteria. Hoewel batchexperimenten hun beperkingen hebben, zijn ze nuttig voor een eerste screening.

We ontdekten dat een hoge glycolopbrengst werd verkregen bij overmaat van de wolframaat- en hydrogenatiekatalysator. Het bleek zelfs dat houtpoeder, deeltjes van millimetergrootte en *"enkele deeltjes"* (schijfgrootte = 22 mm (ø) x 3 mm), bij een overmaat katalysator dezelfde gecombineerde glycolopbrengst (∼ 50 gew.%) gaven als een referentietest met enkel cellulose (Hoofdstuk 6). Dit betekent dat de biomassastructuur, bijvoorbeeld de toegankelijkheid van cellulose, de opbrengst niet beperkt. Een verlaagde glycolopbrengst is dus het resultaat van een gedeactiveerde katalysator(en).

Tabel 1: Hydrogenolysescenario's bij maximale gevoeligheid voor katalysatorvergiften.

N	W-katalysator *Actief?*	Hydrogenatiekatalysator *Actief*?	Dominante Product
1	✓	✓	Ethyleenglycol
2	✗	✓	Suikeralcoholen
3	✓	✗	Humines
4	✗	✗	Humines

Vervolgens hebben we het hydrogenolyseprotocol afgestemd op maximale gevoeligheid voor katalysatorvergiften, met andere woorden door te werken met de drempelwaarde voor de verhouding tussen katalysator en biomassa die leidt tot hoge glycolopbrengsten. We kunnen vier mogelijke uitkomsten beschouwen: 1) geen deactivering, 2) alleen deactivering van de wolframaatkatalysator, 3) alleen deactivering van de hydrogeneringskatalysator, en 4)

deactivering van beide katalysatoren, zie Tabel 1.

Deactivering van de wolframaatkatalysator kan echter alleen worden waargenomen op basis van de gevormde producten wanneer de hydrogeneringskatalysator actief is, aangezien beide scenario's 3 en 4 leiden tot de vorming van humines, zie Tabel 1. Bovendien kan het misleidend zijn om alleen te vertrouwen op de gevormde producten, omdat de vorming van een van de producten selectief kan worden geblokkeerd. Zo zagen we dat de aanwezigheid van lignine in de voeding de hydrogenering van suikers tot suikeralcoholen (SA) belemmert, maar niet die van glycolaldehyde tot ethyleenglycol, zie Tabel 2. Als gevolg hiervan zou scenario 6 uit Tabel 2 ten onrechte kunnen worden geïnterpreteerd als scenario 3 of 4 uit Tabel 1.

*Tabel 2: Hydrogenolysescenario's bij maximale gevoeligheid voor katalysatorvergiften met lignine in de voeding. *Oranje symbolen: katalysatoractiviteit aangetast maar niet volledig gedeactiveerd.*

N	W-katalysator *Actief?*	Hydrogenatiekatalysator *Actief*?	Dominante Product
5	✅	✅	Ethyleenglycol
6	❌	✅	Humines

Het onvermogen om onderscheid te maken tussen scenario's 3, 4 en 6 kan worden overwonnen door een extra experiment uit te voeren met een overmaat wolframaatkatalysator of hydrogeneringskatalysator. Als alternatief hebben we een methode ontwikkeld om de hoeveelheid oplosbaar wolframaat in het reactoreffluent te kwantificeren om zo direct onderscheid te kunnen maken tussen scenario's 3 en 4 of 6.

Katalysatordeactivatie

Onze experimentele studies hebben aangetoond dat ascomponenten, in het bijzonder tweewaardige kationen, aanwezig in biomassa de homogene wolframaatkatalysator deactiveren door onoplosbare componenten te vormen (Hoofdstuk 4). We hebben afgeleid dat de concentratie van tweewaardige kationen in biomassa onder de 4 mmol / $kg_{Biomass}$ moet blijven om het katalysa-

torverbruik onder de grens te brengen dat vereist is voor industrieel gebruik. Deze onzuiverheden werden selectief verwijderd onder het gewenste niveau van 4 mmol / $kg_{Biomass}$ door zure uitloging van houtachtige biomassa. Uitspoeling met zuur was echter niet succesvol in het volledig verwijderen van deze onzuiverheden uit hooi, een kruidachtige biomassasoort die bekend staat om zijn hoge concentratie aan anorganische stoffen, extractiemiddelen en eiwitten. Helaas hebben we vergiftiging van de wolframaatkatalysator door componenten uit hooi niet kunnen identificeren, wat dus verder onderzoek vereist.

Zwavel is een bekend gif voor metaalkatalysatoren terwijl dit zelden aan bod komt in studies met betrekking tot de katalytische omzetting van biomassa. We hebben geen deactivatie van de hydrogenatiekatalysator (Raneynikkel) door zwavel waargenomen na hydrogenolyse van houtachtige soorten die weinig zwavel bevatten zoals dennen-, populieren- en beukenhout (Hoofdstuk 5). Echter, vonden we significante deactivatie van de hydrogenatiekatalysator bij experimenten met hooi en een mengsel van cellulose + methionine, een zwavelhoudend aminozuur. Uit de experimentele gegevens hebben we een zeer uitdagende grondstofspecificatie afgeleid van < 67-200 µmol (2-6 mg) zwavel per kg biomassa, wat veel lager is dan het zwavelgehalte van lignocellulose biomassa (bijv. $\sim$150 mg S kg^{-1} voor dennen en populieren).

De glycolopbrengst bleek een plateau te bereiken bij toevoeging van N in de vorm van een aminozuur en suggereert dat deactivering van Raneynikkel door stikstof minder zorgwekkend is (Hoofdstuk 5). We hebben geen enkel effect van aminozuren op de activiteit van de wolframaatkatalysator waargenomen. Het wassen van de biomassa bij kamertemperatuur met water, ethanol of 10 gew.% azijnzuur in water was tamelijk ondoeltreffend voor de verwijdering van stikstof en zwavel.

In-water-oplosbare extractiemiddelen deactiveren zowel wolframaat als de hydrogeneringskatalysator (Raneynikkel), maar dit houdt waarschijnlijk verband met de verwijdering van (in-water-oplosbare) tweewaardige kationen en (in-water-oplosbaar) zwavel, met andere woorden sulfaat.

Lignine, een van de belangrijkste bestanddelen van de biomassa, remt de hydrogeneringsactiviteit, zoals werd aangetoond door een lage suikeralcoholopbrengst die werd waargenomen in de afwezigheid en aanwezigheid van wolframaat (Hoofdstuk 3). De hydrogeneringskatalysator (Raneynikkel) leek echter voldoende actief om glycolaldehyde tot ethyleenglycol te hydrogeneren. Een biomassamonster met een ligninegehalte van 44 gew.% leverde

namelijk dezelfde ethyleenglycolopbrengst op als de referentietest met cellulose. Desalniettemin zal het toedienen van grote hoeveelheden lignine waarschijnlijk tot praktische problemen leiden, aangezien het bekend is dat lignine een lijmachtige substantie vormt en daardoor leidt tot accumulatie van lignine in de reactor.

Voedingselectie

De grondstof is een belangrijke variabele voor het proces. In dit werk hebben we onderscheid gemaakt tussen drie lignocellulose biomassa-archetypen, namelijk zachthout, hardhout en kruidachtige planten. Deze laatste is rijk aan anorganische stoffen, extractieve stoffen en zwavel/stikstof, maar relatief arm aan lignine in vergelijking met houtsoorten. Dit werk suggereert dat zwavel en anorganische stoffen de belangrijkste katalysatorvergiften zijn, en daarom is de voorkeursgrondstof een houtsoort. Echter, kunnen de grondstofprijs en beschikbaarheid van invloed zijn op deze propositie.

De hemicellulose van zachthout bestaat typisch uit hexose (C_6), terwijl hardhout en kruidachtige soorten hemicellulose bevatten die rijk is aan pentose (C_5). Hexosen (alleen aldosen) zijn gewenst wanneer het doel is om ethyleenglycol te produceren en daarom heeft zachthout de voorkeur wanneer hemicellulose of zijn derivaten worden gevoed aan de hydrogenolysestap.

Procesontwikkeling

Parallel aan de identificatie en kwantificering van katalysatorvergiften, hebben we voorbehandelingsmethoden bestudeerd die deze vergiften kunnen verwijderen. Zuuruitloging op basis van azijnzuur verwijdert met succes de wateroplosbare fractie en tweewaardige kationen. Deze methode vermindert echter niet het stikstof-, organische zwavel- en het ligninegehalte van de voeding. Lignine bleek niet problematisch in batchtests, maar zou problematisch kunnen worden voor continue operatie of bij latere opzuivering van de glycolstroom.

We hebben een geïntegreerd procesconcept bestudeerd dat een significante verwijdering van lignine (>80%) mogelijk maakt met behoud van de cellulosefractie ($\sim$100% retentie) in het vaste residu (Hoofdstuk 7). Bovendien verwijdert deze methode ook het grootste deel van de as (>80%). In dit proces wordt houtachtige biomassa gefractioneerd in een oplosmiddel bestaande uit water en een mengsel ($\geq$50 gew.%) van lichte alcoholen en organische zuren

(bijvoorbeeld ethanol en azijnzuur). We hebben gekozen voor het gebruik van organische moleculen die bijproducten zijn van de hydrogenolyse- en voorbehandelingsstappen en die tijdens het proces worden gerecycled om de noodzaak voor het aanvullen van de oplosmiddelen te beperken. De bescheiden opbrengst aan bijproducten en de noodzaak van een hoge oplosmiddel-tot-biomassa-verhouding in de voorbehandeling leiden nog steeds tot zeer uitdagende criteria voor de terugwinning van oplosmiddelen (>94 gew.% in een zeer optimistisch scenario).

De verwijdering van de verontreinigingen, met andere woorden lignine en as, wordt het meest efficiënt uitgevoerd door het wassen van de biomassa in tegenstroom met de vloeistof uit te voeren (Hoofdstuk 8). Het gebruikte oplosmiddel (na het wassen) moet in de reactiestap worden gebruikt om de consumptie van oplosmiddel te minimaliseren. Deze richtlijnen gelden voor elke processtap met vloeistof-biomassa-operatie die gericht is op de valorisatie van het vaste biomassaresidu.

Appendix A

A.1 Hydrogenolysis protocol

A.1.1 pH control

In our experiments, we employed soluble tungstate species (sodium polytungstate), hereafter referred to as W-catalyst and Raney nickel catalysts. Furthermore, we used a 2 wt.% buffered acetic acid solution to control the pH around ∼3.3. This pH was chosen to ensure substantial cellulose depolymerisation, while avoiding tungstate precipitation (pH∼1-2) and excessive side-product formation. pH control in this process could be important as various elements in the catalytic hydrogenolysis are sensitive to pH; for example, the depolymerisation of cellulose[151], the rate of by-product formation[152], and the solubility and state of tungstate species[153]. Furthermore, untreated biomass can induce pH changes via two ways: 1) increasing pH by liberating basic ash[31] or 2) decreasing pH by the formation of organic acids via hydrolysis of acetyl groups[136] or degradation of saccharides[152]. The pH after all the experiments was typically between 3.0 and 3.6.

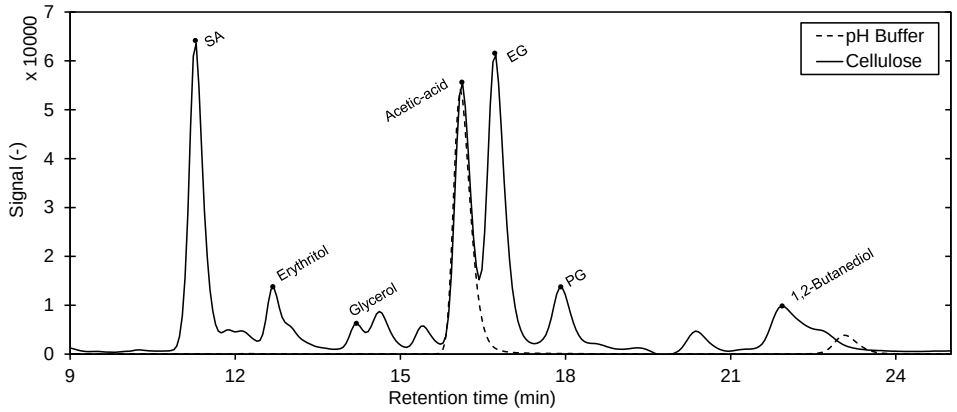

Figure A.1: Hydrogenolysis of cellulose for 60 minutes at 245°C, 5 wt.% biomass loading (black) in presence of buffer, 0.12 Ni-catalyst to biomass ratio and 0.03 W-catalyst to biomass ratio. Note the W-catalyst to biomass ratio for the pH buffer only experiment was 0.06.

Even though acetic acid is not an ideal buffering agent for such a low pH, experiments performed with buffers of formic acid, citric acid and phosphoric acid (acids that exhibit more suitable pK_a values) were unsatisfactory. Both organic acids (formic and citric acid) degraded during catalytic hydrogenolysis, while phosphoric acid/phosphate likely interacted with tungstates to form

phosphopolytungstates. A blank experiment with solely the pH control agent did not yield noteworthy amounts of the targeted products, see Figure A.1.

To further study the impact of the acetic acid buffer on the catalytic hydrogenolysis, we ran two additional experiments; one with no pH control (autocatalyzed), and another using sulphuric acid to set the initial pH at 3.3. The EG yields were similar in all the experiments, namely 46 wt. % (Acetic acid buffer), 48 wt. % (autocatalyzed) and 47 wt.% (sulphuric acid), and the final pH was always 3.2 ± 0.1, see Figure A.2. These results demonstrate that the acetic acid buffer does not impose negative effects on the hydrogenolysis chemistry.

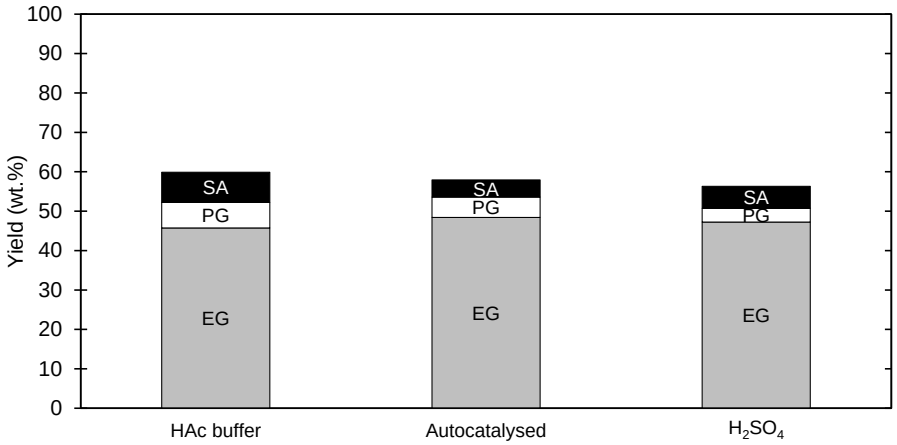

Figure A.2: EG, PG and SA yields for different pH agents after catalytic hydrogenolysis of cellulose. ∼0.04 Ni-catalyst / Biomass ratio and 0.02 W-catalyst / biomass ratio, T = 245°C, 1 wt.% biomass, t = 1 h, P_{H2} (Initial) = 60 bar, $pH_{Initial}$ = ∼3.3, except Autocatalysed.

A.1.2 Tuning the hydrogenation function

Following the described protocol for the hydrogenolysis experiments, we first investigated the sensitivity of hydrogenation power by varying the Ni-catalyst to biomass mass ratio at fixed W-catalyst/biomass ratio. The goal was to find an operating point (biomass to catalyst ratio) at which pure cellulose delivers much higher EG yield than poplar. To do so, the Ni-catalyst to biomass mass ratio was varied from 0.02 to 0.6, while keeping the W-catalyst to biomass mass ratio constant (0.14), with a biomass loading of 1 wt. % and a starting pH of ∼3.3.

According to Figure A.3, the EG yield sharply increases up to 36 wt.% for a Ni/biomass ratio of ∼0.14, where after a plateau is reached while the SA yield keeps increasing roughly linearly with Ni to biomass ratio. The liquid product of experiments with a low Ni to biomass ratio (e.g. $\leq$ 0.1) had a typical brownish colour, indicating the presence of humins. The trends are rather similar for poplar and cellulose. Hay and pine show a substantially lower EG yield (∼25 wt.%), but this is offset by a much higher PG yield for these feedstocks. Overall, increasing the Ni to biomass ratio steered the reaction products from thermal degradation products (e.g. HMF, humins) to glycols and sugar alcohols.

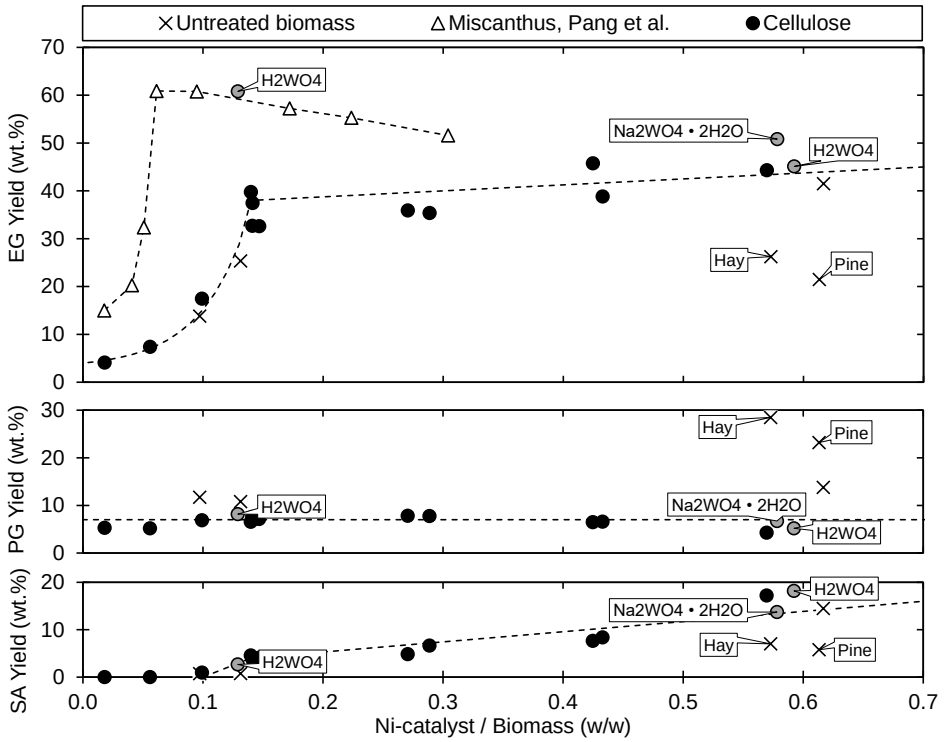

Figure A.3: EG, PG and SA yields on holocellulose basis as function of the Ni-catalyst/biomass ratio after catalytic hydrogenolysis. Untreated biomass, if not labelled, is poplar. Reaction conditions: W-catalyst/biomass mass ratio = 0.14, biomass loading = 1 wt. %, T = 245° C, t = 1 h, P_{H2} (Initial) = 60 bar, $pH_{Initial}$ = ∼3.3. Note, t = 2 h for experiments performed with H_2WO_4 and 3 h for Na_2WO_4. Data by Pang et al.[91] are shown for reference. Lines drawn for clarity.

A similar trend was previously observed by Pang et al.[91] for the hydrogenolysis of Miscanthus over tungstic acid and Raney nickel. The EG yield sharply increased to 61 wt.% for a Ni-catalyst to biomass ratio of 0.06, which is close to the maximum EG yield (Y_{EG} = 65 wt.%) found for cellulose hydrogenolysis over a binary catalyst of tungstic acid and Raney nickel[70]. We are well aware that the EG yield in our work is substantially lower, but the difference can be assigned to the applied W-species. For control, we also ran a cellulose hydrogenolysis experiment with tungstic acid, in absence of buffer, and obtained an EG yield of 61 wt.% for comparable biomass to catalyst ratios, see Figure A.3. However, we chose not to use tungstic acid as it complicates the pH control, which was already discussed in section A.1.1.

A.1.3 Tuning the aldol cleavage function

Similarly, we also investigated the sensitivity of aldol cleavage by varying the W-catalyst to biomass mass ratio, at a fixed Ni-catalyst to biomass mass ratio of $\sim$0.6, using cellulose and poplar as feedstocks, see Figure A.4. The opposite trend was observed for the SA yield, which decreased from 40 wt.% (cellulose) and 37 wt.% (poplar) in the absence of tungstate, to $\sim$15 wt.% at a W-catalyst to biomass ratio of 0.14. This confirms earlier claims that W-species catalyse the aldol cleavage reaction, thereby favouring the formation of glycolaldehyde from glucose, and subsequently, of ethylene glycol, over the formation of sugar alcohols[72]. Only minor differences between the two feedstocks, poplar and cellulose, were observed.

To summarize, the outcome of cellulose and untreated poplar hydrogenolysis was rather similar at 1 wt.% biomass loading. This shows that poplar (<53 µm) can be successfully converted to EG if there is an excess of active catalyst (i.e. changes to particle structure or accessibility are not imperative). The same can be stated for the hydrogenolysis of Miscanthus[91] (Y_{EG} = 61 wt.%) and Jerusalem artichoke[104] (Y_{EG} = 48 wt.%) for 1 wt.% biomass loading, once the yields are calculated on holocellulose basis (see Figures A.7 and A.11).

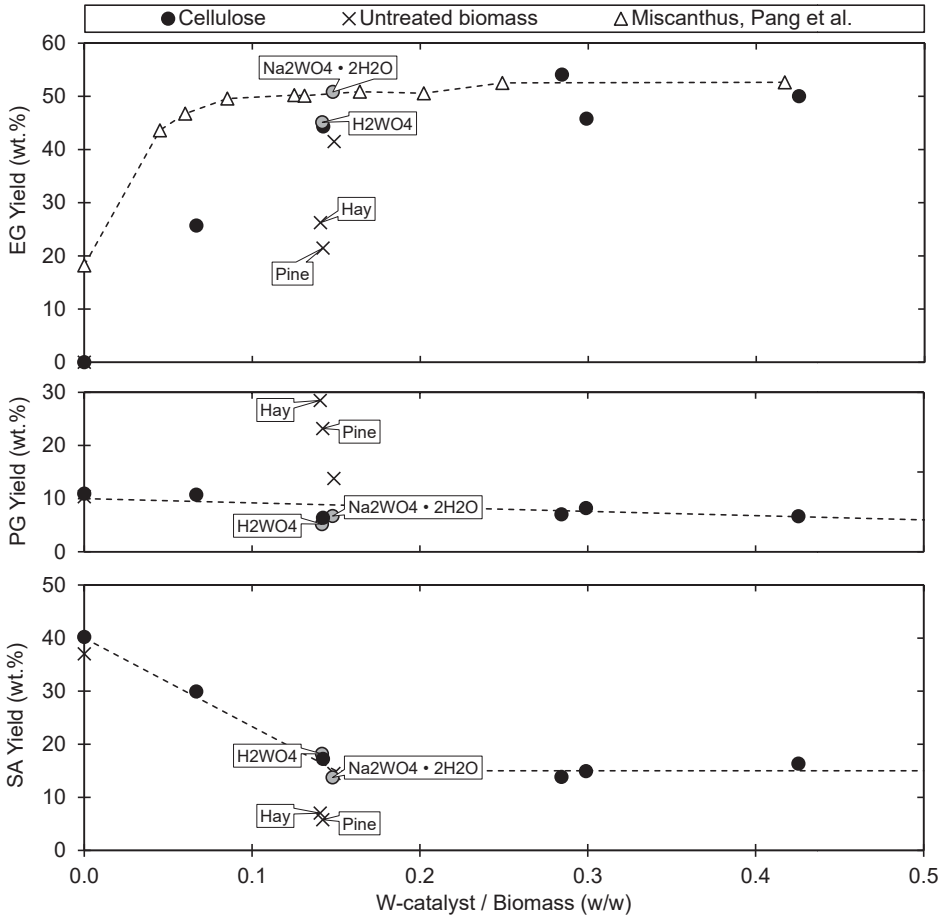

Figure A.4: Product yields expressed on holocellulose basis (EG, PG and SA) as function of the W-catalyst/biomass ratio after catalytic hydrogenolysis. Untreated biomass, if not labelled, is poplar. Reaction conditions, Ni/biomass mass ratio = 0.6, biomass loading = 1 wt. %, T = 245° C, t = 1h, P_{H2} (Initial) = 60 bar, $pH_{Initial}$ = ∼3.3. Note, t = 2 h for experiments performed with H_2WO_4 and 3 h for Na_2WO_4. Data by Pang et al.[91] are shown for reference. Lines drawn for clarity.

A.1.4 Biomass loading

Operation at high biomass loading will be imperative for commercial operation, as discussed elsewhere[105]. To the best of our knowledge, only two studies have reported the hydrogenolysis of lignocellulose at substantially higher loadings ($\geq$4.8 wt.%): the work of Pang et al.[91] on Miscanthus and the study by Fabicovicova et al.[103] on barley straw. The dataset from Pang et al.[91] (see Figure A.7) shows no effect of pretreatment or lignin content for

a biomass loading of 1 wt.%, but significant deterioration of the EG yield at 6 wt.% (max 14 wt.% EG difference) and 10 wt.% (max 24 wt.% EG difference). However, it is worth noting that they raised the catalyst loading together with the biomass loading.

We followed the same strategy as Pang et al.[91] and increased the biomass and catalyst loadings in the hydrogenolysis experiments. As shown in Table A.1 entries 1 and 4, the EG yield indeed dropped from 41 wt.% to 23 wt.%, when increasing the poplar loading from 1 to 5 wt.%, while keeping the biomass to catalyst ratio constant. Note that the cellulose equivalent experiment, Table A.1 entry 3, resulted in a higher EG yield of 32 wt.% (delta of 9 wt.%).

Table A.1: EG yield on holocellulose basis for 1 or 5 wt.% biomass loading, various catalyst loadings, Ni-catalyst to W-catalyst mass ratio was always constant. T = 245 °C, t = 1h, P_{H2} (Initial) = 60 bar, $pH_{Initial}$ = ∼3.3

Entry	Feedstock	Loading (wt.%)	EG (wt.%)	Ni-catalyst (g)	W-catalyst (g)
1	Cellulose	1	44	0.1	0.02
2	Poplar	1	41	0.1	0.02
3	Cellulose	5	32	0.4	0.1
4	Poplar	5	23	0.4	0.1
5	Cellulose (n=2)	5	32.2±0.5	0.1	0.02
6	Poplar (n=2)	5	8.5±0.4	0.1	0.02
7	Pine	5	8	0.1	0.02
8	Hay	5	4	0.1	0.02

In search for detrimental effect of lignin and other feed contaminants on the catalysts performance, we further increased the protocol sensitivity by reducing the catalyst to biomass ratio five-fold. This resulted in an EG yield reduction from 23 wt.% to 8 wt.% for poplar, see Table A.1 entries 3 and 6 respectively. Importantly, however, the EG yield for cellulose (32 wt.%) remained substantially higher than for poplar (8 wt.%) at 5 wt.% biomass loading, see Table A.1 entries 5 and 6. Moreover, hydrogenolysis of other biomasses resulted in poor EG yields as well, namely 8 wt.% for pine and 3 wt.% for hay, see Table A.1 entries 7 and 8. Hence, this hydrogenolysis protocol with high (5 wt.%) biomass loading, low Ni-catalyst and W-catalyst to biomass ratios (∼0.12 and ∼0.03, respectively) shows improved discriminative power and is used for feedstock screening. Note that the Ni-catalyst to biomass ratio of 0.12 corresponds well with the sensitive edge for 1 wt.% biomass loading, see Figure A.3 in section A.1.2. For the W-catalyst to biomass ratio (0.03) this

is even reduced fourfold compared to the sensitive edge for 1 wt.% biomass loading, see Figure A.4 in section A.1.3.

Importantly, Pang et al.[91] applied the same Ni-catalyst to biomass ratio of 0.12 but a four-fold higher W-catalyst (H_2WO_4) to biomass ratio of 0.12. Thus, our protocol is equally sensitive to detect disturbances in hydrogenation activity and more sensitive to homogenous W-catalyst poisons. A comparison with the study by Fabicovicova et al.[103] is troublesome as they applied a lower temperature of 220°C and used a heterogenous Ru-W/AC catalyst Nonetheless, they applied a catalyst to biomass ratio of 0.1.

A.2 Supporting graphs

A.2.1 Total loading versus holocellulose loading

The catalyst to holocellulose ratio is variable for experiments performed at a fixed total biomass loading. It appears that the yield distribution for a total biomass loading (cellulose + lignin) of 5 wt.% and cellulose loading of 5 wt.% are identical, see Figure A.5.

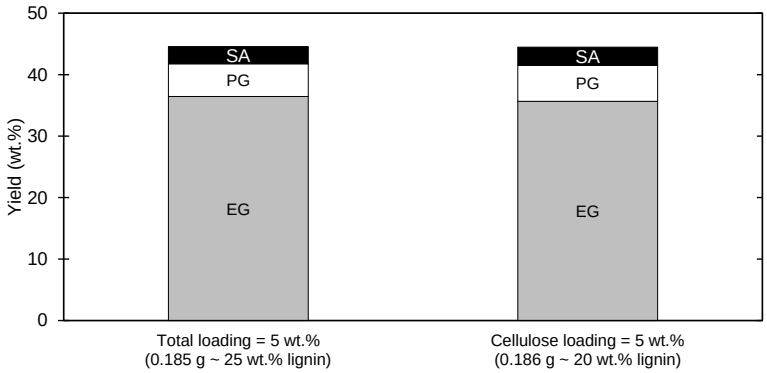

Figure A.5: Hydrogenolysis of cellulose in the presence of lignin at a total loading of 5wt.% (left, 0.185 g, 25 wt.% lignin) and a cellulose loading of 5 wt.% (right, 0.186 g, 20 wt.% lignin). Reaction conditions: T = 245° C, t = 1h, P_{H2} (Initial) = 60 bar, $pH_{Initial}$ ∼3.3, Ni-catalyst to biomass mass ratio 0.12, W-catalyst to biomass mass ratio 0.03.

A.2.2 Catalytic hydrogenolysis of (pretreated) feedstocks

The EG, PG and SA yield after catalytic hydrogenolysis of untreated and pretreated feedstocks as well as physical mixtures in the presence of W-catalyst and Ni-catalyst was presented in Figure 3.3 in Chapter 3. In Figure A.6 the figure is redrawn, but now with a more detailed legend.

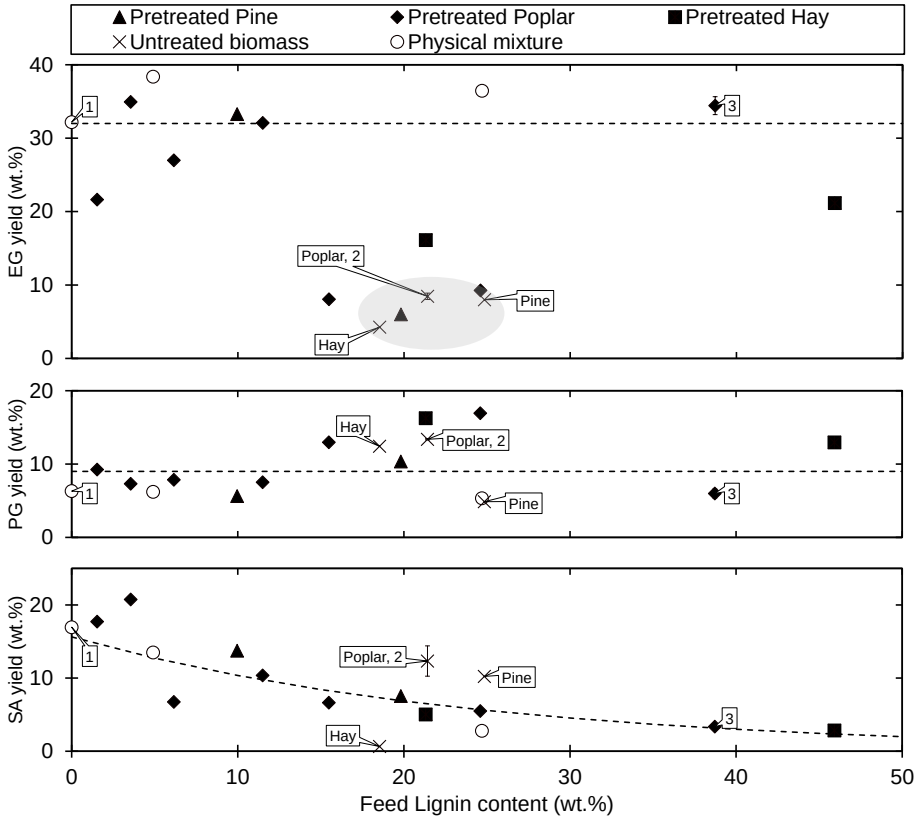

Figure A.6: Product yields (EG, PG and SA) as a function of the feedstock lignin content after catalytic hydrogenolysis. Reaction conditions: 5 wt.% biomass loading, T = 245° C, t = 1h, P_{H2} (Initial) = 60 bar, $pH_{Initial}$= ∼3.3, Ni-catalyst to biomass mass ratio 0.12, W-catalyst to biomass mass ratio 0.03. Experiments 1, 2, 3 were performed in duplicate, the error bars are typically too small to be observed. Drawn lines are for clarity.

A.3 Literature study and statistical analysis

The catalytic hydrogenolysis targeting EG and PG of (preatreated) feedstocks was previously addressed in a number of studies. We analysed these studies, in order to shape a broader picture and direct the development of pretreatment technology suitable for catalytic hydrogenolysis. Sometimes manipulation of the original data was required to reach a fair conclusion. For example, the product yield is occasionally reported on mass intake[75],[91],[104] which is unfair, as only the saccharide fraction of biomass yields EG and PG. The absolute theoretical EG + PG yield drops with increase of feedstock lignin content. In this scenario, biomass samples high in lignin are automatically penalised. Therefore, for these cases, we recalculated the yields and expressed them on holocellulose intake. Furthermore, the carbon content of lignin is greater than that of holocellulose, thus yield expressions on carbon basis (C%) disfavours samples with high lignin content (Note that this only holds for yield expressions on whole biomass basis).

An overview of the literature studies that target EG (and PG) from lignocellulose by catalytic hydrogenolysis is shown in Table A.2. A short description of these literature studies is given in the subsections below. For the sake of clarity and transparency the original data of the discussed literature is repeated. Manipulation methodology of the original data, if applied, is reported here as well.

*Table A.2: Overview of hydrogenolysis studies of (pretreated) biomass targeting EG and PG and applied experimental conditions. *Dim = C% or Wt.%*

Author	Feed	Particle size (mm)	Catalyst	T (°C)	t (h)	P_{H2} (bar)	Biomass Loading (wt.%)	Yield basis	Dim*
Pang et al.[75]	(Pretreated)-Corn stalk	<0.25	2% Ni-W_2C	245	2.5	60, initial	1	Biomass	C%
Pang et al.[91]	(Pretreated)-Miscanthus	<0.25	H_2WO_4 + Raney Ni	245	2	60, initial	1, 6, 10	Biomass	C%
Fabičovicová et al.[103]	(Pretreated)-Barley straw	0.2-0.4	Ru-W/AC	220	3	65, at reaction conditions	4.8	Holocellulose	C%
Li et al.[64]	Various	<0.42	4% Ni-30% W_2C/AC	235	4	60, initial	1	Holocellulose	C%
Zhou et al.[104]	(Pretreated)-Jerusalem artichoke	<0.25	WO_3 + Raney Ni	245	2	60, initial	1	Biomass	Wt.%
This work	(Pretreated)-Poplar		SPT + Raney Ni	245	1	60, initial	1, 5	Holocellulose	Wt.%

A.3.1 Concentrated Miscanthus

Pang et al.[91] studied the impact of pretreatment on the EG yield after catalytic hydrogenolysis. Typical conditions were; H_2WO_4 + Raney nickel catalysts, 1, 6 and 10 wt.% of biomass loading, 245°C, 6 MPa H_2, 2 h of reaction time. The EG yield was increased for pretreated feedstocks compared to the untreated feedstock, in particular at high feed concentration. For the sake of clarity, characteristics of the (pretreated) feedstocks are repeated here, see Table A.3.

*Table A.3: (Pretreated) feedstock properties in the study by Pang et al[91]. Reported as Table 1 in their work. *By difference. EtOH = Ethanol, MeOH = Methanol*

Pretreatment method →	None	EtOH	MeOH	Acetone	EtOH-Ammonia	Ammonia	EtOH-NaOH
Hemicellulose (wt.%)	21.6	29.6	32	29.6	22.2	18.7	23.6
Cellulose (wt.%)	49.9	51.5	50.1	51	65	67.1	65
Lignin (wt.%)	15.9	11.6	11.3	10.7	4.5	3.8	1.4
Soluble (wt.%)	5.3	2.8	2.2	3	3.8	3.4	4.9
Ash (wt.%)	2.4	2.3	2.9	3.1	1.9	1.9	1.5
C (wt.%)	47.3	46.6	46.6	46.8	42.8	43.8	43.1
H (wt.%)	5.7	5.9	5.9	5.9	6.1	6.2	6.1
N (wt.%)	<0.1	<0.1	<0.1	<0.1	<0.1	0.2	<0.1
O (wt.%)*	44.5	45.1	44.5	44.1	49.1	48	49.2

The EG yield data is derived from: Figure 6 (*"The influence of pretreatment methods on EG yield with different concentrations of feedstock."*)[91] and reported here in Table A.4.

Table A.4: EG yield (wt.%) after catalytic hydrogenolysis for different pretreatment methods and varied feedstock loadings in the study by Pang et al[91]. Derived from Figure 6 in their work. EtOH = Ethanol, MeOH = Methanol

Loading (wt.%)	None	EtOH	MeOH	Acetone	EtOH-Ammonia	Ammonia	EtOH-NaOH
1	35	39	38	38	46	46	46
6	23	31	32	32	41	41	42
10	13	27	26	26	39	39	40

However, importantly, the yield is defined on biomass intake, not on holocellulose basis. Pang et al. defined their yield as follow;

"The polyols yields were calculated by the following equation: yield (%) = (mole of carbon in the polyol)/(mole of carbon in feedstock) x 100%."[91]

Which boils down to equation A.1; in which $f_{Carbon}^{Product}$ is the carbon fraction of the product (e.g. EG), f_{Carbon}^{Feed} is the carbon fraction of the feed, $M_{w,carbon}$ the molecular weight of carbon, $m_{Product}$ is the mass of product and m_{Feed} is the mass of the feed.

$$Y_{Product}(C\%) = \frac{m_{Product} \times f_{Carbon}^{Product} \times {}^{1}/M_{w,carbon}}{m_{Feed} \times f_{Carbon}^{Feed} \times {}^{1}/M_{w,carbon}} \times 100 \tag{A.1}$$

Samples with a high lignin content, automatically result in a decreased EG yield as EG cannot be produced from lignin. In addition, lignin is higher in carbon than holocellulose, as a result, samples high in lignin are penalised. We therefore transformed the EG carbon yield expressed on biomass intake, to mass yield expressed on holocellulose intake according to equation A.2, in which $f_{Holocellulose}$ is the holocellulose fraction of the feed.

$$Y_{Product}(wt.\%, \text{holocellulose}) = Y_{Product}(C\%) \times \frac{f_{Carbon}^{Feed}}{f_{Carbon}^{Product}} \times \frac{1}{f_{Holocellulose}} \tag{A.2}$$

The carbon content of EG is 38.7 wt.%. The carbon content of the (pre-treated) feedstocks is deducted from Table A.3. A calculation example, for the non-treated feedstock (1 wt.% feed loading), is shown in equation A.3.

$$Y_{Product}(wt.\%, \text{holocellulose}) = 35 \times \frac{0.473}{0.387} \times \frac{1}{0.715} = 60 \tag{A.3}$$

Applying equation A.2 on the data presented in Table A.4 results in Figure A.7. The claim that the lignin content of the feed is related to the EG yield still holds[91]. However, the yield differences are much less dramatic and do not even exist for a feed loading of 1 wt.%.

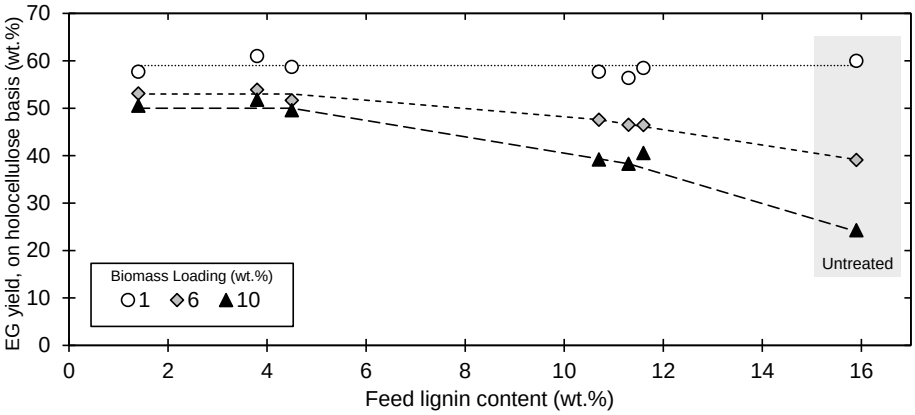

Figure A.7: EG yield on holocellulose basis as function of the feedstock lignin content after catalytic hydrogenolysis of untreated and pretreated miscanthus for different biomass loadings in the study by Pang et al.[91] Lines and grey area drawn for clarity.

A.3.2 Hydrocracking of raw woody biomass

Li et al.[64] performed the hydrocracking of various untreated biomass species over carbon supported Ni-W_2C catalyst. Typical conditions were; 4% Ni- 30% W_2C/AC catalyst, 0.4 catalyst to biomass ratio, 1 wt.% of biomass, 235°C, 6 MPa H_2, 4 h of reaction time. Diol yields were reported based on the feedstock holocellulose content, see Tables A.6 and A.7. No manipulation of the yield data was performed.

*Table A.5: Feedstock composition in the study by Li et al.[64] Reported as Table 2 in their work. *Not reported, assumed.*

Entry	Substrate	Extraction (%)	Hemicellulose (%)	Cellulose (%)	Lignin (%)	Ash (%)
1	Birch	4.5	19.3	56.1	19.8	0.3
2	Corn stalk	33.1	15.1	38	12.9	1
3	Poplar	3.7	20.4	60.3	14.8	0.8
4	Basswood	4.4	28.9	51.2	15.1	0.4
5	Ashtree	10.3	22.7	48.7	17.8	0.5
6	Beech	11.1	20.7	41	25.3	1.9
7	Xylosma	8.6	21.1	45.7	23	1.6
8	Bagasse	10.4	29.2	46.2	13.5	0.7
9	Pine	12.5	10.3	43.2	33.6	0.4
10	Yate	18	18.3	31.5	30.9	1.3
11*	Cellulose			100		

Table A.6: EG and PG yield on holocellulose basis after catalytic hydrogenolysis of various biomass species in the study by Li et al.[64] Reported as Table 3 in their work.

Entry	Substrate	EG (C%)	PG (C%)
1	Poplar	48.6	12.8
2	Basswood	49.2	11.8
3	Ashtree	52.7	11.9
4	Beech	35.2	11.4
5	Xylosma	36.4	13.7
6	Bagasse	32.9	15.3
7	Pine	28.4	8
8	Yate	16.3	11.5

Table A.7: EG and PG yield on holocellulose basis after catalytic hydrogenolysis of various biomass species in the study by Li et al.[64] Reported as Table 1 in their work.

Entry	Substrate	EG (C%)	PG (C%)
1	Corn stalk	7.8	10.8
2	Birch	51.4	14.2
4	Cellulose	61	7.6

The EG and PG yield as function of the feedstock lignin content is shown in Figure A.8. The EG yield does not show a strong dependency on the lignin content of the feedstock. Importantly, corn stalk (13 wt.% lignin) had the lowest lignin content of all untreated feedstocks gave an EG yield of 8 only wt.%. PG formation appears rather independent of the feedstock lignin content.

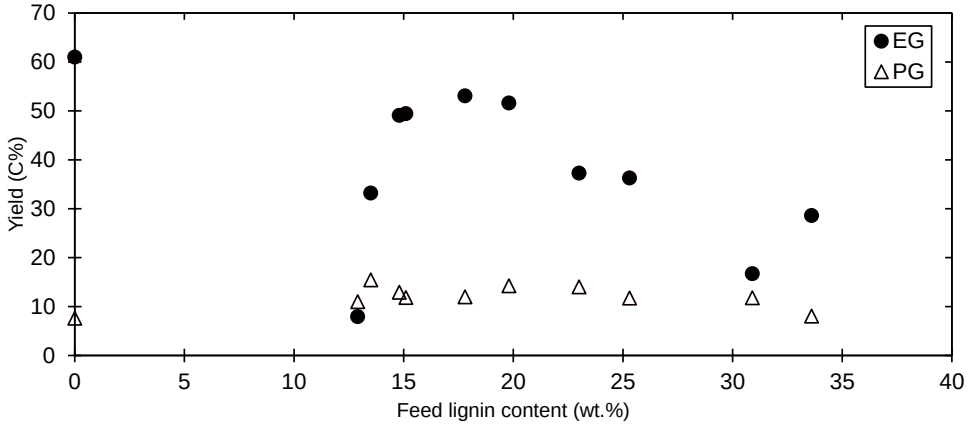

Figure A.8: EG and PG yield on holocellulose basis after catalytic hydrogenolysis of various untreated feedstocks in the study by Li et al.[64] as function of the feedstock lignin content.

A.3.3 Barley straw

Fabičovicová et al.[103] studied the hydrogenolysis of (organosolv pretreated) barley straw over ruthenium tungsten catalyst. Typical hydrogenolysis conditions were; Ru-W/AC catalyst, 4.8 wt.% biomass loading, 220°C, 6.5 MPa H_2 at reaction conditions, 2 h of reaction time. The composition of the (pretreated) barley straw is reported in Table A.8 (*"Table 1 in their work"*). The EG and PG yield were derived from *"figure 3"* in their work and, for clarity, repeated here in Table A.9. The yields were already expressed on holocellulose basis.

*Table A.8: (Pretreated) barley straw properties in wt.% in the study by Fabičovicová et al.[103] Reported as table 1 in their work. *Untreated barley straw, nm = not measured.*

Entry	Lignin	Hemicellulose	Cellulose	Extractives	Ash	Sum
1*	19.6	20.8	40.7	1.8	2.1	85
2	29.1	4.6	55.2	–	nm	88.9
3	19.6	7.7	58.5	–	nm	85.8
4	13.9	19.5	47.7	–	0.8	81.9
5	12.3	22.5	45.4	–	nm	80.2
6	21.6	24.3	36.7	–	nm	82.6
7	18.5	19.5	41.5	–	0.6	80.1
8	16.1	19.6	49.2	–	0.6	85.5
9	13.2	14	57.5	–	0.5	85.2
10	10.4	5.7	65.3	–	nm	81.4
11	6.8	16	52.6	–	nm	75.4

Table A.9: Reported EG and PG yields by Fabičovicová et al.[103], on holocellulose basis (C%), derived from figure 3 in their work.

Entry	EG (C%)	PG (C%)
1	1.5	1.4
2	7.9	1.5
3	13.5	2.8
4	34	11
5	14.6	4.8
6	7.5	2.5
7	24.2	6.2
8	21.5	11
9	36	10
10	26.5	4.7
11	28.1	11.9

The EG and PG yield as function of the feedstock lignin content is shown in Figure A.9. Samples somewhat lower in lignin content than the untreated

feed show higher EG and PG yields. However, also substrates with similar lignin content than the untreated feed show much higher EG and PG yields.

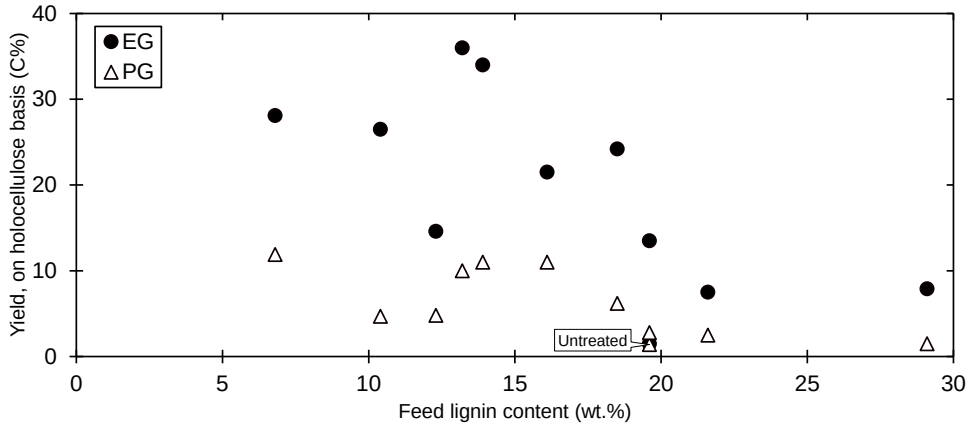

Figure A.9: EG and PG yield on holocellulose basis after catalytic hydrogenolysis of (organosolv pretreated) Barley straw in the study by Fabičovicová et al.[103] as function of the feedstock lignin content.

A.3.4 Corn stalk

Pang et al.[75] performed the hydrogenolysis of (pretreated) corn stalk, microcrystalline cellulose and microcrystalline cellulose lignin mixture over carbon supported Ni-W_2C catalyst. Typical conditions were: 2% Ni-W_2C, 1 wt.% biomass, 245°C, 6 MPa H_2, 2.5 h. The composition of the (pretreated) corn stalk is reported in Table A.10 (Table 2 in their work). The EG and PG yields were derived from *"figure 5"* in their work and, for clarity, repeated here in Table A.11. Furthermore, the EG and PG yields obtained from experiments pure cellulose and cellulose-lignin mixture are shown in Table A.12.

The yield is defined on biomass intake, not on holocellulose basis. Pang et al.[75] defined their yield as follow:

"The polyol yields and gas products were calculated by the equation yield (%) = [(number of moles of carbon in the polyol or gas)/(number of moles of carbon in the feedstock)] x 100%"[75]

Which boils down to equation A.4;

$$Y_{Product}(C\%) = \frac{m_{Product} \times f_{Carbon}^{Product} \times {}^{1}/_{M_{w,carbon}}}{m_{Feed} \times f_{Carbon}^{Feed} \times {}^{1}/_{M_{w,carbon}}} \times 100 \qquad (A.4)$$

*Table A.10: (pretreated) corn stalk composition in wt.% in the study by Pang et al.[75] Reported as Table 2 in their work. *Untreated corn stalk.*

Sample no.	Soluble	Hemicellulose	Cellulose	Lignin	Ash
A	6.1	14.8	72.4	6.2	0.5
B	9.6	7.6	67.7	13.4	1.7
C	4.8	17.2	69.1	8.4	0.5
D	1.5	20.2	63.2	13.4	1.6
E	2.1	18.5	71.3	7.6	0.6
F	1.7	22.1	56.7	18.5	1
G	0.2	20.5	54.5	23.4	1.5
H	0.2	18.6	57.3	22.3	1.7
I	6	10.5	49	32.5	2.1
J*	33.1	15.1	38	12.9	1

Samples with a high lignin content, automatically result in a decreased EG yield as EG cannot be produced from lignin. In addition, lignin is higher in carbon than holocellulose, as a result, samples high in lignin are penalised. We therefore transformed the EG carbon yield expressed on biomass intake, to carbon yield expressed on holocellulose intake according to equation A.5. As the carbon content of the various feedstocks was not reported, the translation of carbon yield to mass yield could not be made.

$$Y_{Product}(C\%, \text{holocellulose}) = Y_{Product}(C\%) \times \frac{1}{f_{Holocellulose}} \tag{A.5}$$

Translation of the reported EG and PG yields by equation A.5 results in Figure A.10. There is a general tendency of high EG and PG yields for feedstocks lean in lignin. However, samples with a similar lignin content as the untreated feed ($\sim$3 wt.% EG and $\sim$3 wt.% PG) show much higher EG ($\sim$25 wt.%) and PG ($\sim$15 wt.%) yields.

*Table A.11: Reported EG and PG yields, on biomass intake (C%), by Pang et al.[75] for (pretreated) corn stalk. Derived from figure 5 in their work. *Untreated corn stalk.*

Sample no.	EG (C%)	PG (C%)
A	31.8	15.8
B	18.1	9
C	22.5	15.8
D	21.3	14.3
E	21.3	14.6
F	8.8	3.8
G	2.9	1.8
H	6.1	6.4
I	6.1	2.3
J*	1.5	1.8

Table A.12: Reported EG and PG yields, on biomass intake (C%), by Pang et al.[75] for cellulose and cellulose lignin mixture. From table 4 in their work.

Sample no	Sample description	EG (C%)	PG (C%)
9	Cellulose	51.2	6.8
12	Cellulose + Lignin (5/1 w/w)	13.1	4.2

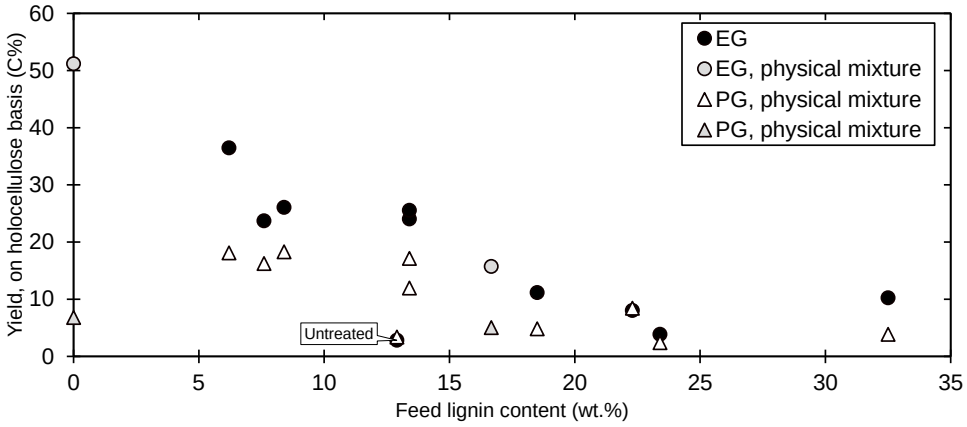

Figure A.10: EG and PG carbon yield on holocellulose basis after catalytic hydrogenolysis of (pretreated) corn stalk and model compounds; microcrystalline cellulose and mixture of microcrystalline cellulose and lignin (5:1 ratio), over carbon supported Ni-W_2C catalysts as function of the feedstock lignin content[75].

A.3.5 Jerusalem artichoke stalk (JAS)

Zhou et al.[104] performed the hydogenolysis of (pretreated) Jerusalem artichoke stalk (JAS) over WO_3 and Raney nickel. Hot water pretreatment was performed at 100°C for 6 or 12 h. Typical conditions were; WO_3 and Raney nickel catalysts, 1 wt.% biomass, 245°C, 6 MPa H_2, 2 h. The composition of the (pretreated) corn stalk is reported in Table A.13 (*Table 1 in their work*). The EG and PG yield in were reported in *Table 2* in their work and, for clarity, repeated here in Table A.14.

*Table A.13: Composition of (pretreated) Jerusalem artichoke in the study by Zhou et al.[104] Reported as Table 1 in their work. *Untreated Jerusalem artichoke.*

Pretreatment time (hr)	Cellulose (wt.%)	Hemicellulose (wt.%)	Lignin (wt.%)	Ash (wt.%)	Water soluble substances (wt.%)
0*	51.6	10.3	17.2	1.7	19.2
6	44.3	18.9	24.9	1.2	10.7
12	42.9	22.8	25	1.2	8.1

The yield is defined on biomass intake, not on holocellulose basis. Zhou et al. defined their yield as follow:

"The yields of products were calculated using the formula: yield = (weight of product) / (weight of JAS placed into the reactor) × 100%."[104]

Which boils down to equation A.6;

$$Y_{Product}(wt.\%) = \frac{m_{Product}}{m_{Feed}} \times 100 \tag{A.6}$$

Samples with a high lignin content, automatically result in a decreased EG yield as EG cannot be produced from lignin. In addition, lignin is higher in carbon than holocellulose, as a result, samples high in lignin are penalised. We therefore transformed the EG carbon yield expressed on biomass intake, to carbon yield expressed on holocellulose intake according to equation A.5. As the carbon content of the various feedstocks was not reported, the translation of carbon yield to mass yield could not be made.

$$Y_{Product}(wt.\%, \text{holocellulose}) = Y_{Product}(wt.\%) \times \frac{1}{f_{Holocellulose}} \tag{A.7}$$

The EG and PG yields are reported in *Table 2 "Catalytic transformation of*

JAS pretreated under different conditions", see Table A.14. Only entries 1-6 are used as the feed composition of entry 7 was not provided and additives were used in entries 8 & 9.

Table A.14: Reported EG and PG yields, on biomass intake (wt.%), by Zhou et al.[104] for (pretreated) Jerusalem artichoke. Reported in table 2 in their work.

Entry	Pretreatment time (hr)	EG (wt.%)	PG (wt.%)
1	0	29.9	5.4
2	6	35.2	5.9
3	12	37.6	6.3
4	12	33.2	5.5
5	12	36.2	6.8
6	12	34.5	7

The entries 1-6 from table 2 (in the original work) are plotted versus their lignin content, see Figure A.11. In contrast with the claim of the authors, no effect of the pretreatment on the hydrogenolysis outcome is observed when expressing the EG and PG yield on holocellulose basis.

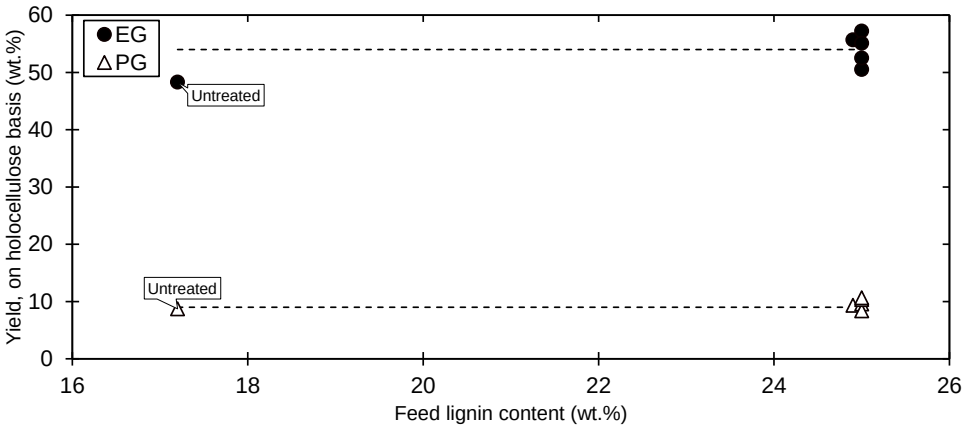

Figure A.11: EG and PG yield on holocellulose basis as after catalytic hydrogenolysis of (pretreated) Jerusalem artichoke as function of feedstock lignin content. Lines drawn for clarity.

A.3.6 Statistical analysis

To further investigate the role of lignin targeting the catalytic hydrogenolysis targeting EG (and PG), we performed statistical analysis of the literature datasets and our work. All parameters were linearly normalised between 0 and 1, wherein the maximum value of the dataset was set to 1 and the minimum to 0. Pretreatment was considered as a binary parameter, 1 for pretreatment, 0 in case of no pretreatment. This imposed stiffness makes it much harder to find a high correlation coefficient for this parameter, pretreatment, compared to a scaled parameter.

The correlation coefficients for the 1 wt.% loading experiments in the study by Pang et al.[91] on concentrated Miscanthus and Zhou et al.[104] on Jerusalem Artichoke were not determined as no significant differences in EG (and PG) yield were observed between the different feedstocks (see Figure A.7 and Figure A.11). The correlation coefficients are documented in Table A.15.

*Table A.15: Correlation coefficients between EG and lignin, EG and pretreatment and pretreatment and lignin. Note pretreatment defined as binary parameter. *Model components such as cellulose and cellulose lignin mixtures not included.*

Study	Feedstock	Loading	EG-Lignin	PG-Lignin	EG-PT	PG-PT	PT-Lignin
Pang et al.[75]	Corn stalk*	1	-0.7	-0.76	0.44	0.38	0.13
Pang et al.[91]	Miscanthus	6	-0.96		0.79		-0.62
		10	-0.95		0.81		-0.62
Fabičovicová et al.[103]	Barley Straw	4.8	-0.68	-0.68	0.53	0.39	-0.17
Li et al.[64]	Various*	1	-0.26				
This work	Hay & poplar & pine*	5	-0.05	0.11	0.62	-0.18	-0.07

A.4 Pretreatment conditions and substrate composition

*Table A.16: Pretreatment operational conditions and composition of resulting substrate. *Biomass loading in this experiment was ∼ 20wt.%*

Pretreatment operational conditions							Substrate composition (wt.%)					
PT	Feed	T (°C)	t (h)	Solvent (wt.%)			Lignin	Glucan	Mannan	Galactan	Xylan	Arabinan
				H_2O	EtOH	HAc						
A	Poplar	180	1	11	0	89	1.5 ± 0.0	75.2 ± 0.2	2.3 ± 0.0	0	6.3 ± 0.1	0.4
B	Poplar	180	1	30	0	70	3.6 ± 0.4	80.6 ± 0.8	2.5 ± 1.3	0	3.2 ± 0.0	0
C	Poplar	200	3	50	50	0	6.2 ± 0.4	74.7 ± 0.6	2.9 ± 0.1	0	5.9 ± 0.2	0
D	Pine	200	0.5	10	0	90	10.0 ± 1.9	70.1 ± 3.7	2.4 ± 0.2	0	2.6 ± 0.0	0
E	Poplar	180	5	50	0	50	11.5 ± 1.3	84	0	0	0.6	0
F	Poplar	200	3	30	0	70	15.5 ± 2.5	67.7 ± 4.9	0.2 ± 0.1	0.8	0	0
G	Pine	200	3	10	0	90	19.8 ± 2.1	63.8 ± 1.3	0.3 ± 0.0	0	0	0
H	Hay	180	1	30	0	70	21.3 ± 1.3	60.1 ± 0.5	0.3 ± 0.0	0	4.0 ± 0.0	0
I*	Poplar	180	5	30	0	70	24.6 ± 0.7	58.7	0	0	0.4	0
J	Poplar	200	3	100	0	0	38.7 ± 2.3	51.1 ± 2.9	0	0	0	0
K	Hay	180	5	80	0	20	45.9 ± 1.9	46.1	0	0	0	0

Appendix B

B.1 Quantification of soluble tungstate

Although we obtained a linear calibration curve for sodium polytungstate in the HPLC, see Figure B.1, we did not obtained a mass balance of ∼100%, see equation B.1, for the majority of experiments performed with cellulose.

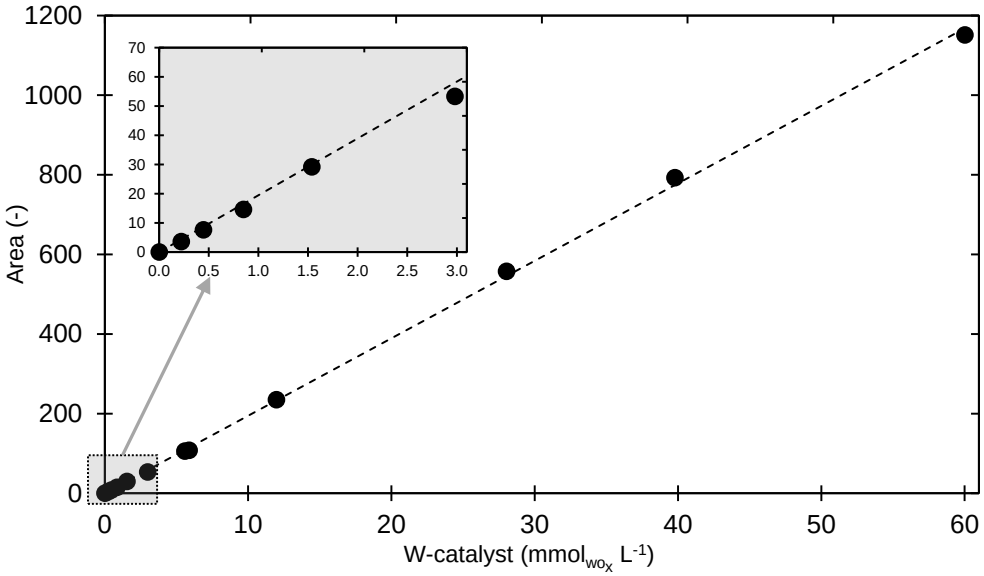

Figure B.1: Calibration curve for sodium polytungstate on HPLC operated with VWD at 285 nm detector, n=12, R^2 = 0.9995. Calibration curve covers whole range found in experiments. Integration was performed in MATLAB®.

B

$$Y_{W_{Catalyst}}(\%) = \frac{W_{Catalyst,\ After\ experiment}}{W_{Catalyst,\ Before\ experiment}} \times 100 \tag{B.1}$$

Cellulose is very lean in catalyst poisons and should not consume a significant amount of tungstate. We found that the mass balance was ∼100% when the amount of W-catalyst fed was high (∼1150 $mmol_{WOx}$ / $kg_{Biomass}$) but decreased when the starting concentration was lowered, see crosses in Figure B.2 on the secondary y-axis. It turns out that there is a consistent loss of tungstate between 20 and 100 $mmol_{WOx}$ / $kg_{Biomass}$ for every experiment, see black dots in Figure B.2 on the primary y-axis. As the cellulose and Raney nickel loading are similar for all these experiments we suspected adsorption and/or consumption of tungstate by cellulose and/or Raney nickel. We mixed sodium polytungstate in the acetic acid buffered solution with cellulose at

room temperature but found a mass balance of ∼100%, even after 1 week of stirring, indicating that the loss cannot explained by adsorption/consumption by cellulose. We repeated the same experiment but now mixed Raney nickel at room temperature instead of cellulose and found that 80 mmol of tugstate per kg of biomass was consumed, which amounted to a mass balance of ∼30%, see labelled (Ni + WO_x) symbols in Figure B.2. This result appears to be systematic deviation and can be explained by 1) precipitation of tungstate with Ni/Al-remnants present in/on the Raney nickel catalyst and/or 2) adsorption of tungstate on the hydrogenation catalyst[84].

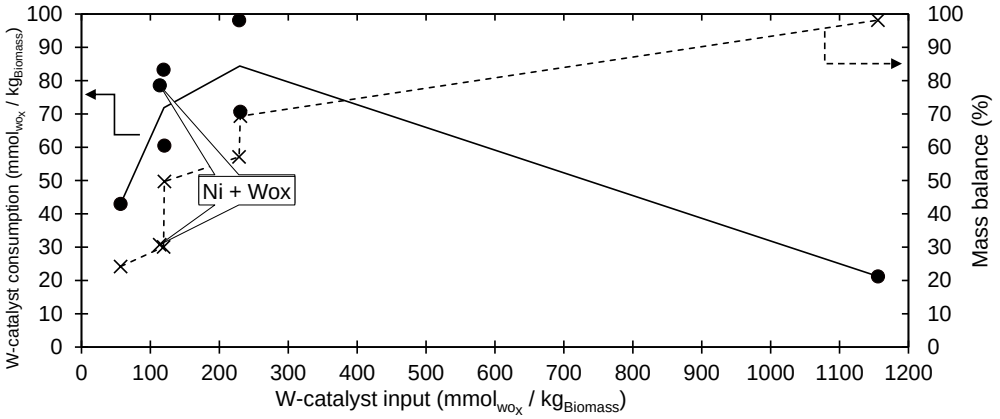

Figure B.2: Tungstate consumption for cellulose as function of W-catalyst input at the start of the experiment per kg of biomass fed. Reaction conditions: 5 wt.% biomass loading, T = 245° C, t = 1 h, P_{H2} (Initial) = 60 bar, $pH_{Initial}$ ∼3.3, Ni-catalyst/Biomass mass ratio = 0.13. Lines drawn for clarity.

B.2 Literature data

B.2.1 Own work

The measured W-catalyst concentration after the experiment relates well with the combined glycol yield found for the experiments performed with cellulose, untreated and treated biomass from our previous work (Chapter 3)[66] displayed in Figure 4.1 in Chapter 4) and this work (Figure 4.2 in Chapter 4), see Figure B.3.

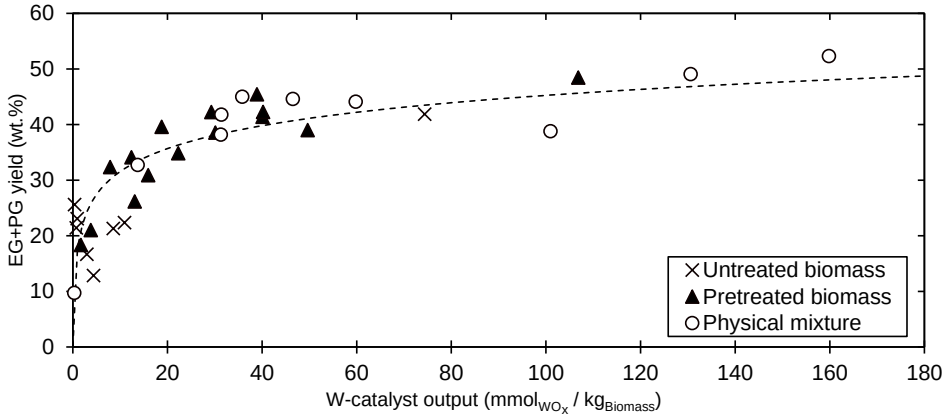

Figure B.3: Combined glycol yield for untreated, pretreated and physical mixtures of cellulose and lignin obtained in Chapter 4 and our previous work (Chapter 3)[66]. Reaction conditions: 5 wt.% biomass loading, T = 245° C, t = 1 h, P_{H2} (Initial) = 60 bar, $pH_{Initial}$ ∼3.3, Ni-catalyst to biomass mass ratio 0.12 (previous work(Chapter 3)[66]) and 0.13 (Chapter 4), W-catalyst to biomass mass ratio 0.03 (previous work(Chapter 3)[66].) and 0.03-0.3 (Chapter 4).

An overlay of all data displayed in the main work (Chapter 4) is shown in Figure B.4. The addition of aluminium chloride appears to deviate from the trend, which could be related to the low pH after the experiment (2.7 compared to 3-3.3 in general), see section B.4.1. Moreover, the addition of minor amounts of $CaCl_2$ resulted in higher glycol yield than expect. No change in selectivity to PG or SA was observed, see Figure B.19 and Figure B.20, and the pH was only somewhat lower (2.9-3.0) compared to the cellulose benchmark (3.3), see Figure B.21.

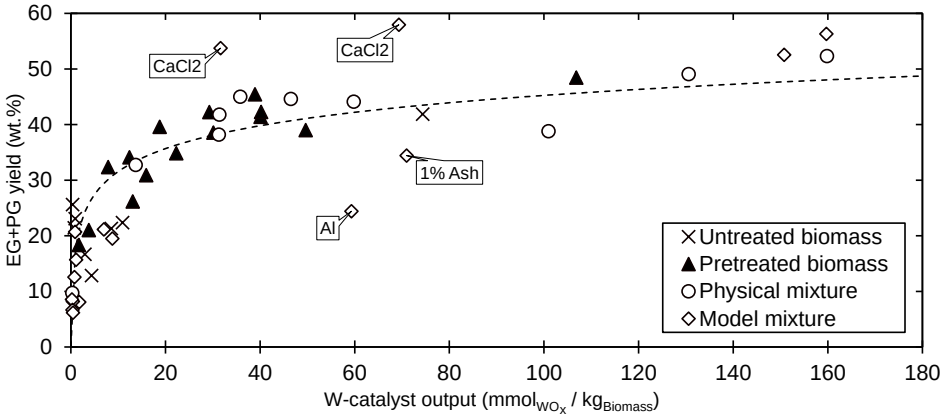

Figure B.4: Combined glycol yield for untreated, pretreated and physical mixtures of cellulose and lignin and model mixtures of cellulose and an additive obtained in this work (Chapter 4) and our previous work (Chapter 3)[66]. Reaction conditions: 5 wt.% biomass loading, T = 245° C, t = 1 h, P_{H2} (Initial) = 60 bar, $pH_{Initial}$ ∼3.3, Ni-catalyst to biomass mass ratio 0.12 (previous work(Chapter 3)[66]) and 0.13 (this work (Chapter 4)), W-catalyst to biomass mass ratio 0.03 (previous work (Chapter 3)[66].) and 0.03-0.3 (this work (Chapter 4)).

B.2.2 Pang et al.[90]

The only other study, to the best of our knowledge, that investigated the impact of inorganics on the tungstate catalysed hydrogenolysis targeting the production of EG was the study by Pang et al.[90] They have evaluated five different (treated) feedstocks, see Table B.1 for their respective composition, besides their evaluation of a series of cellulose + model component mixtures.

B

Table B.1: Feedstock composition of feedstocks used in Pang et al.[90] study.

Feedstock →	Miscanthus	Miscanthus (CaOH treated)	Miscanthus (NaOH treated)	Cellulose	Corn cob cellulose
Lignin (wt.%)	15.9	4.8	3.2	0	2.1
Polysaccharides (wt.%)	71.5	84.3	86.9	100	89.5
Ashes					
Na (mmol / kg$_{Biomass}$)	52	43	109	0	148
Mg (mmol / kg$_{Biomass}$)	457	399	16	0	156
Ca (mmol / kg$_{Biomass}$)	37	180	5	0	157
Fe (mmol / kg$_{Biomass}$)	18	21	2	0	68
Al (mmol / kg$_{Biomass}$)	11	0	4	0	185
Si (mmol / kg$_{Biomass}$)	438	242	46	0	887

Pretreatment of Miscanthus with $Ca(OH)_2$ was not a successful pretreatment as the glycol yield was 34 C% compared to 32 C% for untreated miscanthus. On the contrary, treatment with NaOH delivered a substrate that gave a combined glycol yield of 54 C% in hydrogenolysis. This substrate gave similar glycol yield as micro crystalline cellulose, 60 C%, and corn cob cellulose, 56 C%.

Table B.2: Glycol yields based on holocellulose intake obtained in the study by Pang et al[90]. Reaction conditions: 10 wt.% biomass loading, T = 245°C, t = 3 h, P_{H2} (Initial) = 65 bar, Raney-Ni-catalyst/Biomass mass ratio = 0.12, H_2WO_4-catalyst/Biomass mass ratio = 0.12.

Feedstock →	Miscanthus	Miscanthus (CaOH treated)	Miscanthus (NaOH treated)	Cellulose	Corn cob cellulose
EG (C%)	20.1	25.3	44.1	57.2	51.3
PG (C%)	11.4	9.1	10.2	3.2	4.5
Sum (C%)	31.5	34.4	54.3	60.4	55.8

However, the glycol yields are not easily related to the inorganics content of the substrates, as NaOH treated Miscanthus barely contains any inorganics while corn cob cellulose has comparable inorganics content as the untreated Miscanthus but both gave a combined glycol yield ∼55 C%, see Figure B.5 and Table B.1. Note that sodium and silica are not included in Figure B.5 as they were reported not to affect the glycol yield[90]. The largest discrepancy between corn cob cellulose and $Ca(OH)_2$ treated Miscanthus and untreated Miscanthus is their respective magnesium content, but magnesium only mildly affect the EG yield when added to a cellulose benchmark experiment as was found in this work and in the study by Pang et al.[90]. Unfortunately Pang et al.[90] did not measure the amount of precipitated tungstate after the experiment. Nevertheless, an estimation of the divalent cation input versus the tungstate input could be made, see dotted line in Figure B.5. WO_x to divalent cation ratios of 8.7, 2.4 and 2.1 for untreated Miscanthus, $Ca(OH)_2$ treated Miscanthus and corn cob cellulose are obtained when the magnesium content of the feed is ignored.

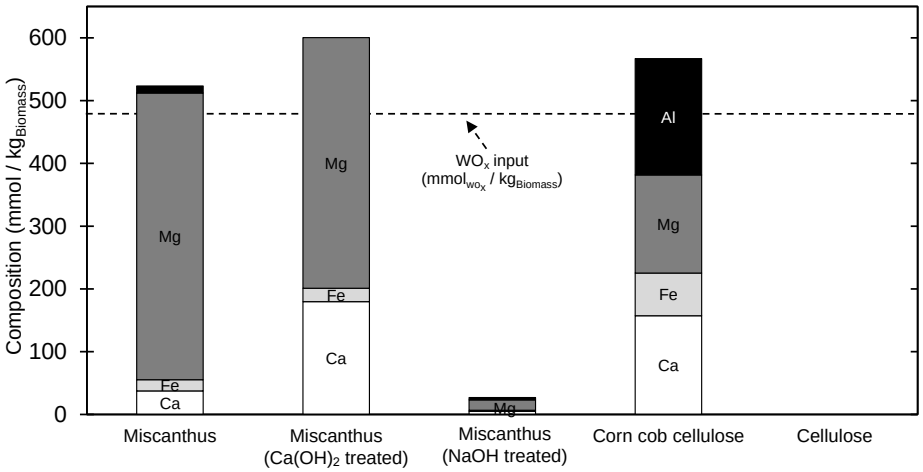

Figure B.5: Calcium, iron, magnesium and alumina content of the feedstocks subjected to hydrogenolysis in the work by Pang et al.[90] In a single experiment 478 $mmol_{WOx}$ / $kg_{Biomass}$ was used.

B.3 Selective ash and extractives removal and reintroduction

B.3.1 Acid leaching

Figure B.6 shows the W-catalyst concentration after the experiment versus the combined glycol yield for the experimental dataset shown in Figure 4.2 in the main work (Chapter 4). The combined glycol yield increases from 10-20 wt.% to ∼50 wt.% with increase in tungstate concentration from 0 to 160 $mmol_{WOx}$ / $kg_{Biomass}$ after which a plateau is observed.

In the main work (Chapter 4) it was shown that the combined glycol yield (EG+PG) for cellulose, acid leached pine and poplar was similar. However, the EG yield, see Figure B.7, was typically lower for the acid leached wood species than for cellulose, whereas the opposite holds for PG, see Figure B.8, which was systematically higher for the woody biomasses. This discrepancy originates from the difference in saccharide composition of the different feedstocks. The wood species contain hemicellulose that is at least partly composed of C_5 monomers such as xylose. These C_5-sugars yield one mole of EG (C_2) and one mole of PG (C_3) whereas hexose (C_6) could theoretically give three mole of EG (C_2).

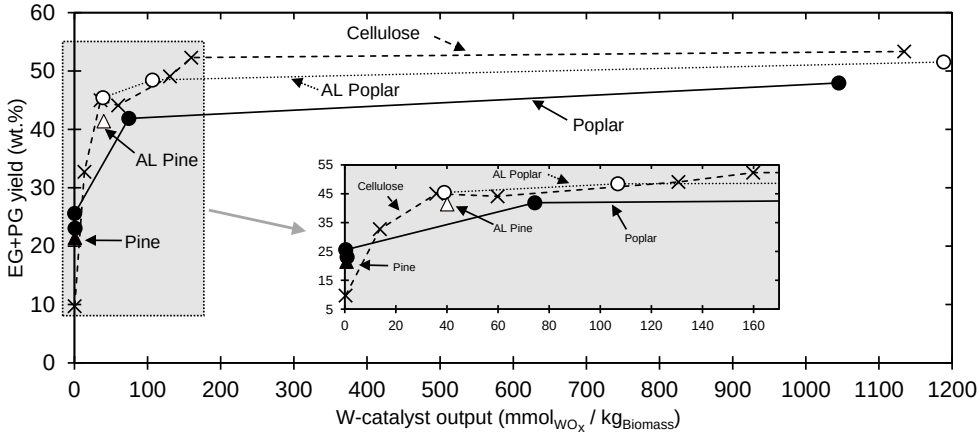

Figure B.6: EG+PG yield expressed on holocellulose content for cellulose, poplar, pine, acid-leached poplar and acid-leached pine as function of W-catalyst output measured after the experiment per kg of biomass fed. Reaction conditions: 5 wt.% biomass loading, T = 245° C, t = 1 h, P_{H2} (Initial) = 60 bar, $pH_{Initial}$ ∼3.3, Ni-catalyst/Biomass mass ratio = 0.13. Lines drawn for clarity.

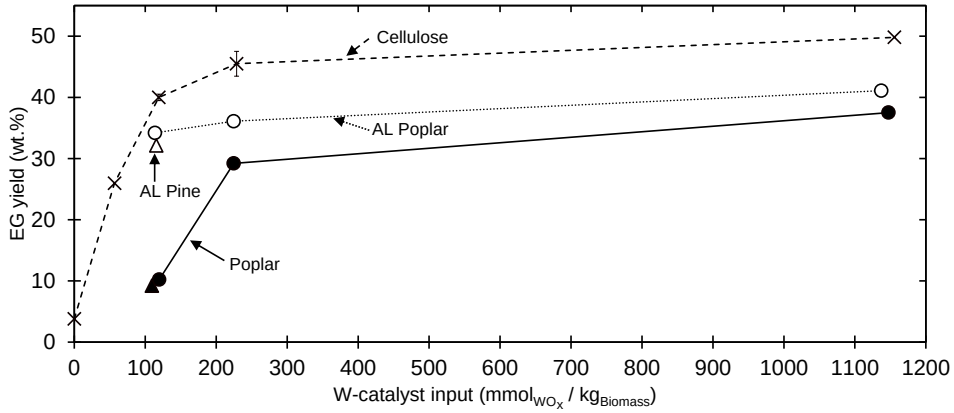

Figure B.7: EG yield expressed on holocellulose content for cellulose, poplar, pine, acid-leached poplar and acid-leached pine as function of W-catalyst input at the start of the experiment per kg of biomass fed. Reaction conditions: 5 wt.% biomass loading, T = 245° C, t = 1 h, P_{H2} (Initial) = 60 bar, $pH_{Initial}$ ∼3.3, Ni-catalyst/Biomass mass ratio = 0.13. Experiments performed in duplicate: Poplar and cellulose at ∼0.03 and cellulose at ∼0.06 W-cat/Biomass mass ratio, error bars plotted but typically too small to be observed. Lines drawn for clarity.

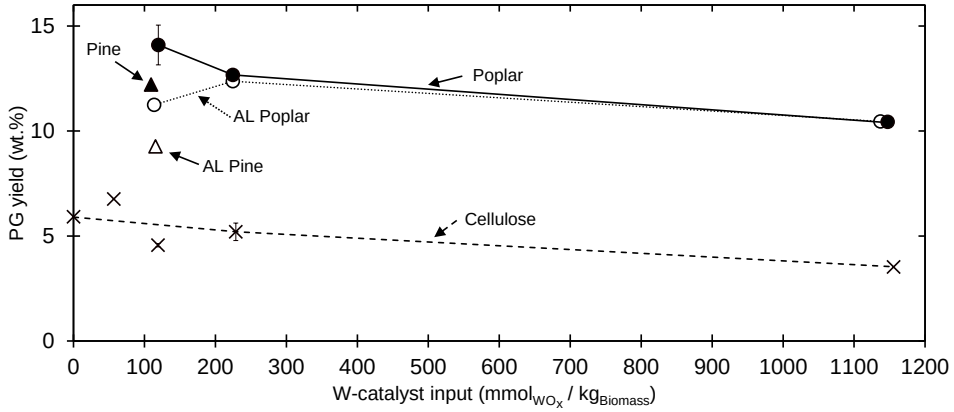

Figure B.8: PG yield expressed on holocellulose content for cellulose, poplar, pine, acid-leached poplar and acid-leached pine as function of W-catalyst input at the start of the experiment per kg of biomass fed. Reaction conditions: 5 wt.% biomass loading, T = 245° C, t = 1 h, P_{H2} (Initial) = 60 bar, $pH_{Initial}$ ∼3.3, Ni-catalyst/Biomass mass ratio = 0.13. Experiments performed in duplicate: Poplar and cellulose at ∼0.03 and cellulose at ∼0.06 W-cat/Biomass mass ratio, error bars plotted but typically too small to be observed. Lines drawn for clarity

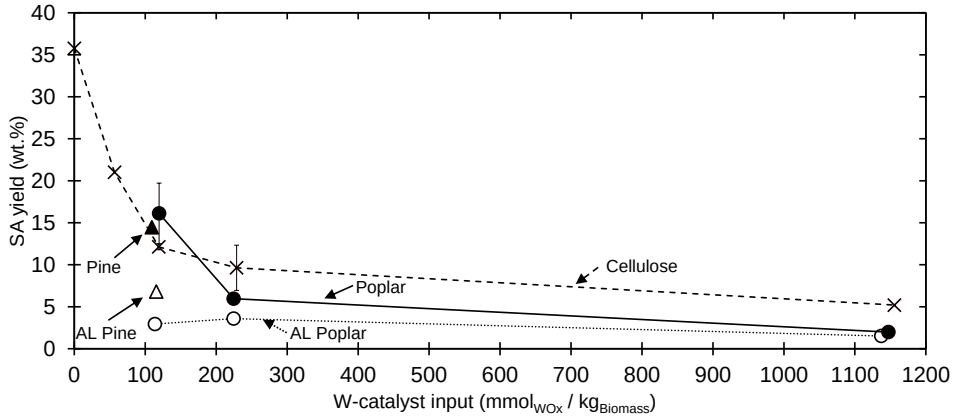

Figure B.9: SA yield expressed on holocellulose content for cellulose, poplar, pine, acid-leached poplar and acid-leached pine as function of W-catalyst input at the start of the experiment per kg of biomass fed. Reaction conditions: 5 wt.% biomass loading, T = 245° C, t = 1 h, P_{H2} (Initial) = 60 bar, $pH_{Initial}$ ∼3.3, Ni-catalyst/Biomass mass ratio = 0.13. Experiments performed in duplicate: Poplar and cellulose at ∼0.03 and cellulose at ∼0.06 W-cat/Biomass mass ratio, error bars plotted but typically too small to be observed. Lines drawn for clarity

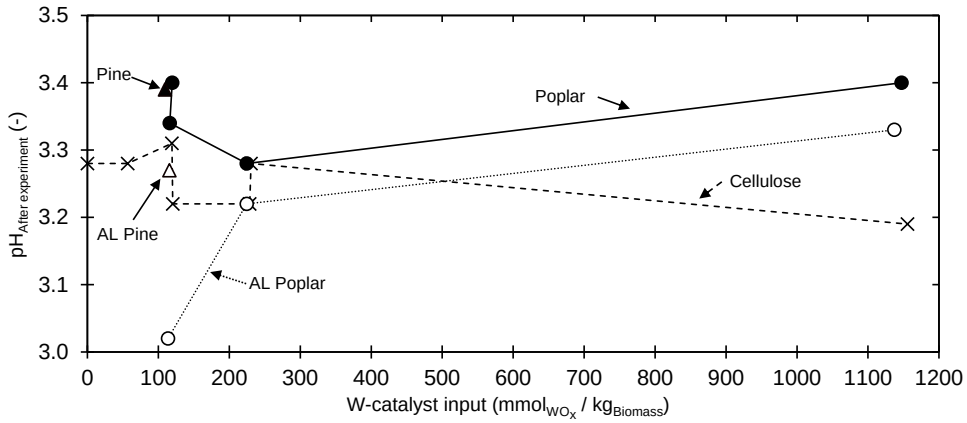

Figure B.10: pH measured after experiments performed for the dataset displayed in Figure 4.2 in the main work (Chapter 4) and Figure B.6, Figure B.7, Figure B.8 and Figure B.9. Reaction conditions: 5 wt.% biomass loading, T = 245° C, t = 1 h, P_{H2} (Initial) = 60 bar, $pH_{Initial}$ ∼3.3, Ni-catalyst/Biomass mass ratio = 0.13. Lines drawn for clarity

B.3.2 Reintroduction of ash

Figure 4.3 in the main work (Chapter 4) showed that the EG yield decreases with increase of ash content in the feed. Concurrently, the PG only mildly increased (Figure B.11) and the sugar alcohol yield slightly increases after the introduction of 1 wt.% ash in the feed, but thereafter decreases indicating that ultimately the hydrogenation catalyst deactivates, see Figure B.12.

The pH measured after the experiments of the dataset displayed in Figure 4.3 in the main work (Chapter 4) appeared to substantially increase with increase in ash addition, see Figure B.13. The measured pH for cellulose, 1 wt.% + cellulose mixture and untreated poplar, importantly, was very similar (3.3-3.4).

Ash appeared to deactivate the tungstate catalyst, as with increase in ash content less tungstate was present in the reactor effluent and concurrently lead to a decrease in EG yield, see Figure B.14.

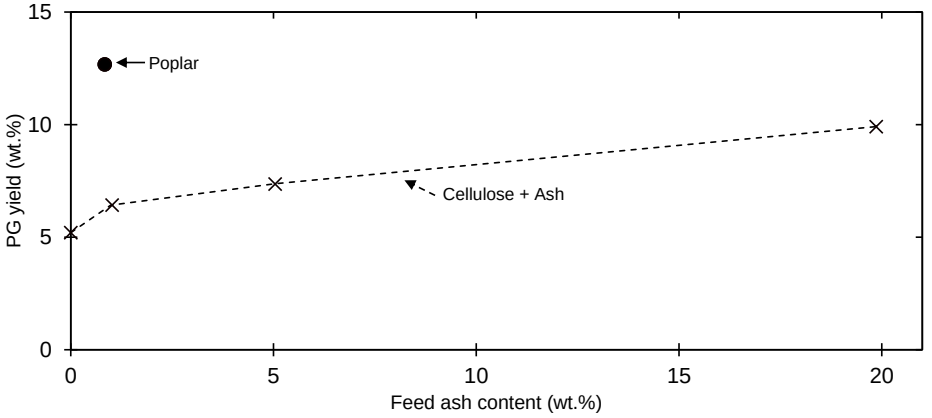

Figure B.11: PG yield expressed on holocellulose content for mixtures of cellulose-ash and untreated poplar as function of the ash content of the feed (mixture). Reaction conditions: 5 wt.% biomass loading, T = 245° C, t = 1 h, P_{H2} (Initial) = 60 bar, $pH_{Initial}$ ∼3.3, Ni-catalyst/Biomass mass ratio = 0.13 and W-catalyst/Biomass mass ratio = 0.06. The ash was obtained after combustion of poplar 575 ℃ for 24 h. Experiment with pure cellulose was performed in duplicate, error bars are plotted, but typically too small to be observed. Line drawn for clarity.

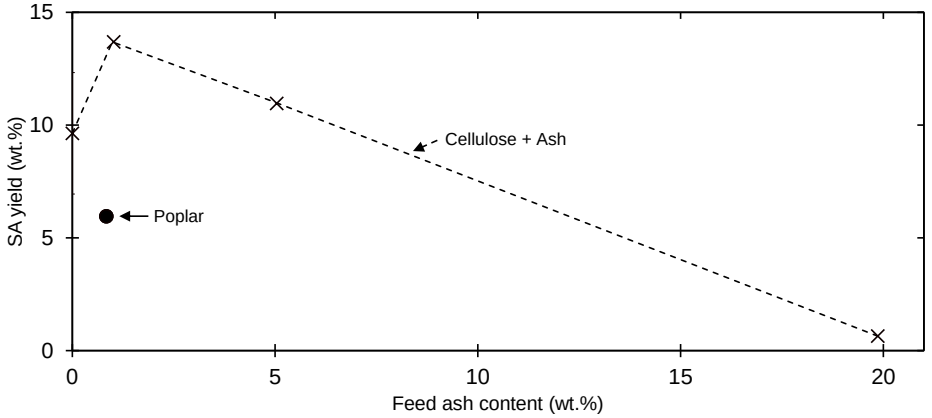

Figure B.12: Sugar alcohol (SA yield expressed on holocellulose content for mixtures of cellulose-ash and untreated poplar as function of the ash content of the feed (mixture). Reaction conditions: 5 wt.% biomass loading, T = 245° C, t = 1 h, P_{H2} (Initial) = 60 bar, $pH_{Initial}$ ∼3.3, Ni-catalyst/Biomass mass ratio = 0.13 and W-catalyst/Biomass mass ratio = 0.06. The ash was obtained after combustion of poplar 575 ℃ for 24 h. Experiment with pure cellulose was performed in duplicate, error bars are plotted, but typically too small to be observed. Line drawn for clarity.

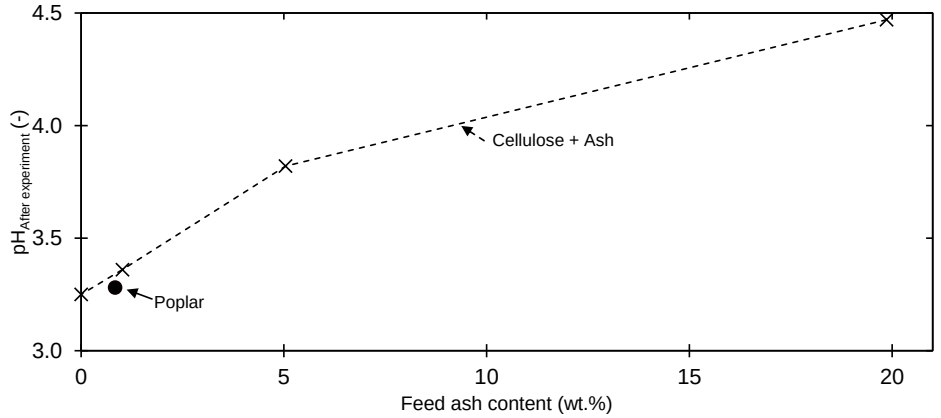

Figure B.13: pH measured after experiments performed for the dataset displayed in Figure 4.3 in the main work (Chapter 4) and Figure B.11, Figure B.12 and Figure B.14. Reaction conditions: 5 wt.% biomass loading, T = 245° C, t = 1 h, P_{H2} (Initial) = 60 bar, $pH_{Initial}$ ∼3.3, Ni-catalyst/Biomass mass ratio = 0.13 and W-catalyst/Biomass mass ratio = 0.06. The ash was obtained after combustion of poplar 575° C for 24 h. Line drawn for clarity.

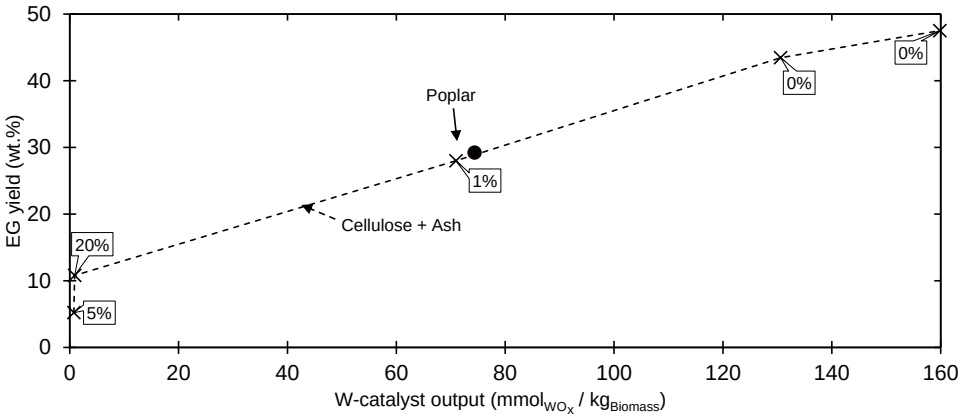

Figure B.14: EG yield expressed on holocellulose content for mixtures of cellulose-ash and untreated poplar as function of W-catalyst output measured after the experiment per kg of biomass fed. Labels indicate ash share (%) of feed mixture. Reaction conditions: 5 wt.% biomass loading, T = 245° C, t = 1 h, P_{H2} (Initial) = 60 bar, $pH_{Initial}$ ∼3.3, Ni-catalyst/Biomass mass ratio = 0.13 and W-catalyst/Biomass mass ratio = 0.06. The ash was obtained after combustion of poplar 575 ℃ for 24 h. Experiment with pure cellulose was performed in duplicate, error bars are plotted, but typically too small to be observed. Line drawn for clarity.

B.4 Model compounds

B.4.1 Cations

The sum of the hydrogenated products (EG+PG+SA) is rather constant independent of tungstate concentration after the experiments, see Figure B.15 with the exception of aluminium chloride (labelled Al in Figure B.15) and various calcium species. The low yield of hydrogenated products for the addition of aluminium chloride can possibly be related to the low pH ($\sim$2.7) measured after the experiment, which was lower than all other experiments, see Figure B.16. At a low pH there is a risk that the hydrogenation catalyst can not keep up with the rate of glucose release from the biomass.

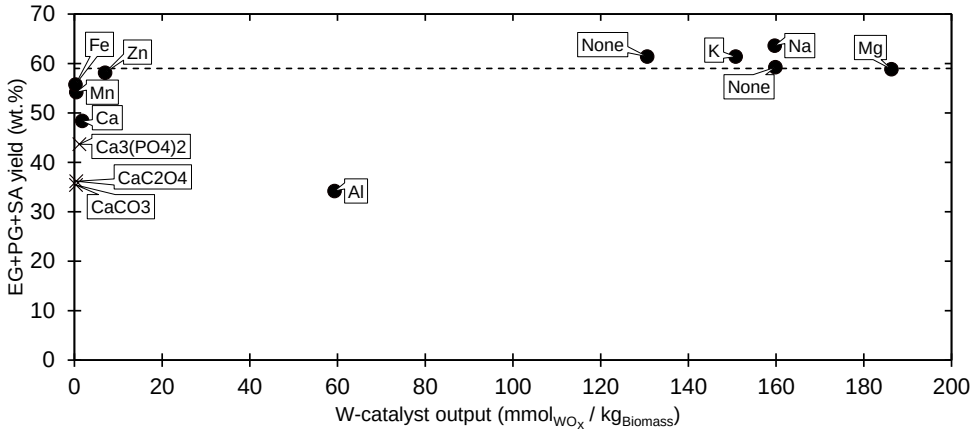

*Figure B.15: EG+PG+SA yield after catalytic hydrogenolysis of cellulose in the presence of chloride salts (black dots) and various calcium salts (crosses) in a 1:1 cation to W molar ratio. *Sodium was added in a 20:1 molar ratio. **$CaSiO_3$ was added in a 1.5:1 cation to W molar ratio. Reaction conditions: 5 wt.% biomass loading, T = 245°C, t = 1 h, P_{H2} (Initial) = 60 bar, $pH_{Initial}$ $\sim$3.3, Ni-catalyst/Biomass mass ratio = 0.13 and W-cat/Bio ratio = 0.06. pH after the experiment is reported in Figure B.16.*

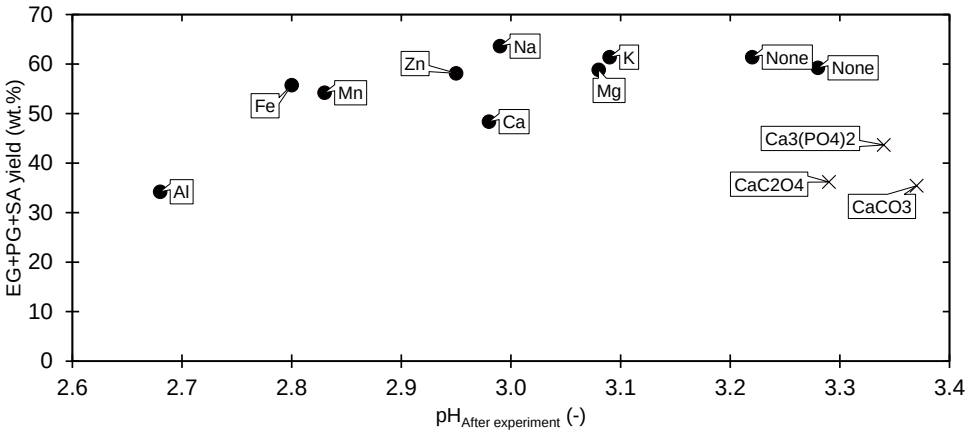

Figure B.16: pH measured after experiments performed for the dataset displayed in Figure 4.5 in the main work (Chapter 4) and Figure B.15. Reaction conditions: 5 wt.% biomass loading, T = 245° C, t = 1 h, P_{H2} (Initial) = 60 bar, $pH_{Initial}$ ∼3.3, Ni-catalyst/Biomass mass ratio = 0.13 and W-cat/Bio ratio = 0.06.

B.4.2 Calcium to tungstate ratio

The cellulose reference experiment was supplemented with various quantities of soluble calcium chloride to test the deactivation sensitivity of tungstate with respect to the calcium loading. The tungstate to calcium ratio was varied from 1 to 3 and it appeared that the measured concentration of W-catalyst in the reactor effluent was directly proportional to the calcium input, see Figure B.17. Furthermore, the EG yield correlated well with the soluble amount of tungstate left after the reaction with and without addition of $CaCl_2$, see Figure B.18. The pH of these experiment after the run was between 2.9 and 3, see Figure B.21, which was similar to the experiments without calcium chloride, for which the pH was between 3.2 and 3.3

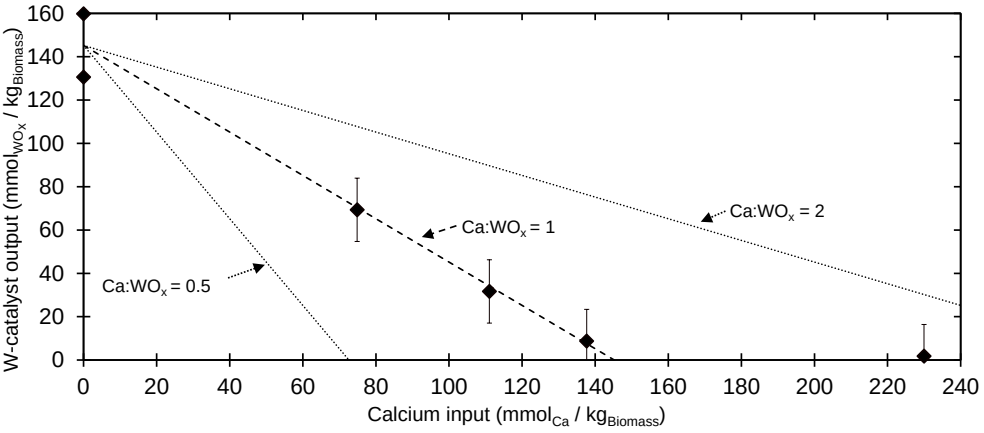

Figure B.17: Measured quantity of W-catalyst in the reactor effluent after the experiment versus the amount of calcium added at the start of the experiment. Reaction conditions: 5 wt.% biomass loading, T = 245° C, t = 1 h, P_{H2} (Initial) = 60 bar, $pH_{Initial}$ ~3.3, Ni-catalyst/Biomass mass ratio = 0.13. pH after the experiment was between 2.9-3.0 for measurements supplemented with $CaCl_2$ and 3.2-3.3 for measurements without additive, see supporting information Figure B.21.

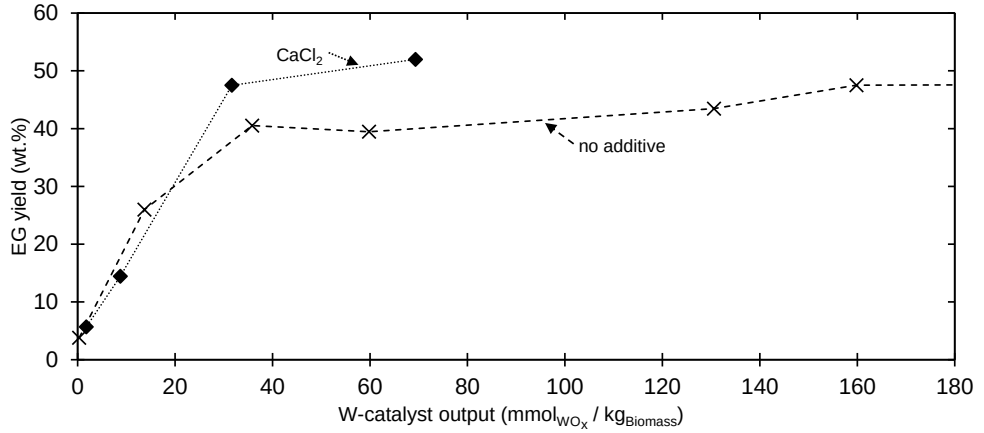

Figure B.18: EG yield after catalytic hydrogenolysis of cellulose in the presence of $CaCl_2$ for a calcium to W molar ratio of 1 to 3. $W_{Active} = W_{Total} - n \times Ca$ in which n = 0.9. Reaction conditions: 5 wt.% biomass loading, T = 245° C, t = 1 h, P_{H2} (Initial) = 60 bar, $pH_{Initial}$ ~3.3, Ni-catalyst/Biomass mass ratio = 0.13. pH after the experiment was always between 2.9 and 3.3 see Figure B.9.

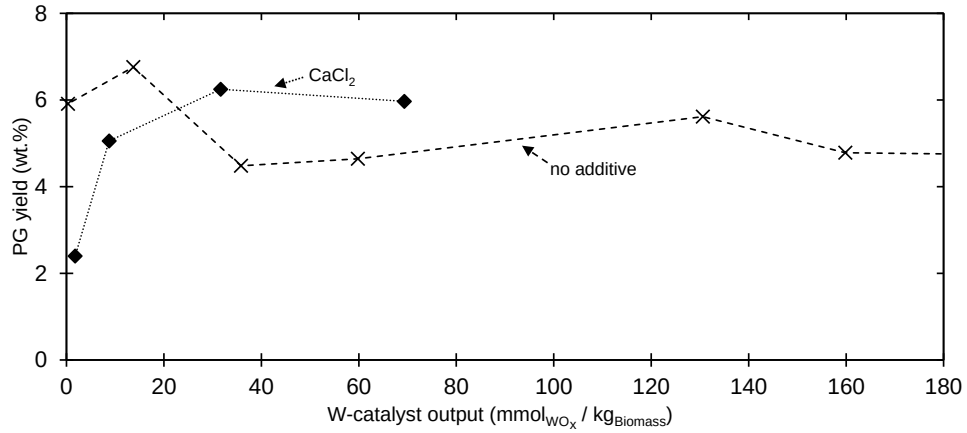

Figure B.19: PG yield after catalytic hydrogenolysis of cellulose in the presence of $CaCl_2$ for a calcium to W molar ratio of 1 to 3. $W_{Active} = W_{Total} - n \times Ca$ in which n = 0.9. Reaction conditions: 5 wt.% biomass loading, T = 245° C, t = 1 h, P_{H2} (Initial) = 60 bar, $pH_{Initial}$ ~3.3, Ni-catalyst/Biomass mass ratio = 0.13. pH after the experiment was always between 2.9 and 3.3 see Figure B.9.

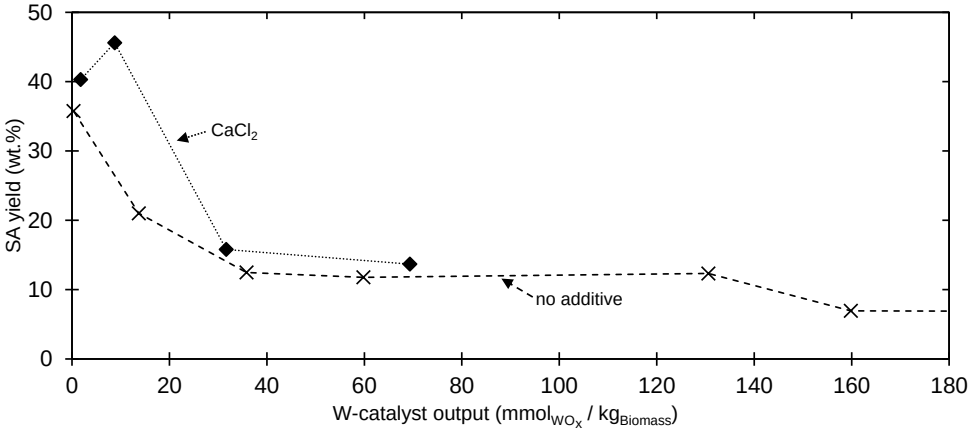

Figure B.20: SA yield after catalytic hydrogenolysis of cellulose in the presence of $CaCl_2$ for a calcium to W molar ratio of 1 to 3. $W_{Active} = W_{Total} - n \times Ca$ in which n = 0.9. Reaction conditions: 5 wt.% biomass loading, T = 245° C, t = 1 h, P_{H2} (Initial) = 60 bar, $pH_{Initial}$ ~3.3, Ni-catalyst/Biomass mass ratio = 0.13. pH after the experiment was always between 2.9 and 3.3 see Figure B.9.

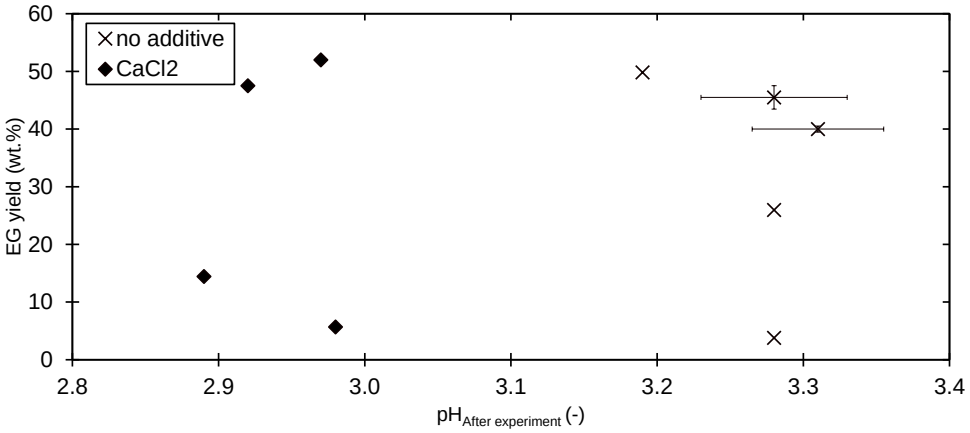

Figure B.21: pH for experiments with and without $CaCl_2$ additive versus EG yield, shown in and Figure B.17, Figure B.18 and Figure 4.5 in the main work (Chapter 4). Reaction conditions: 5 wt.% biomass loading, T = 245°C, t = 1 h, P_{H2} (Initial) = 60 bar, $pH_{Initial}$ ∼3.3, Ni-catalyst/Biomass mass ratio = 0.13.

B.4.3 Calcium versus whole ash

A comparison between calcium chloride and poplar ash used as additive is made in Figure B.22. It can be observed that the addition of *"whole"* ash is much more detrimental than the sum of calcium and magnesium alone. Therefore, it is likely that there are other components present in ash that deactivate the catalyst(s) as well.

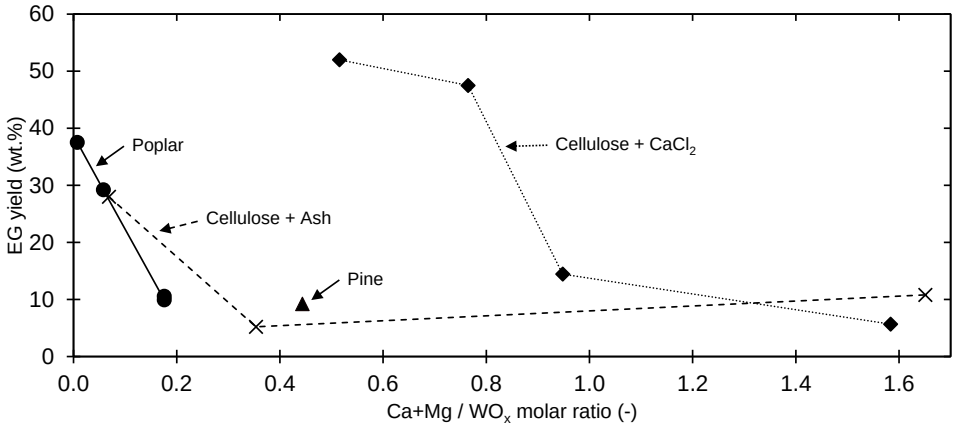

Figure B.22: EG yield for the hydrogenolysis for the addition of calcium + magnesium in the form of chlorides and poplar ash as function of the calcium+magnesium to tungstate input molar ratio. Tungstate input based on cellulose reference experiment. Reaction conditions: 5 wt.% biomass loading, T = 245°C, t = 1 h, P_{H2} (Initial) = 60 bar, $pH_{Initial}$ ∼3.3, Ni-catalyst/Biomass mass ratio = 0.13.

B.5 W-catalyst consumption

B.5.1 Calculation example

We present here a simple calculation to find a typical tungstate to calcium ratio in a single experiment. In a typical experiment the reactor is loaded with 0.021g of sodium polytungstate ($Na_6[H_2W_{12}O_{40}]$), 2986 g mol^{-1} and 0.75g of biomass, which translates to 120 $mmol_{WOx}$ / $kg_{Biomass}$. However, we have noticed that a part of the tungstate is consumed by the Raney nickel catalyst, see section B.1. It was found that on average (n=2) 48 ± 12 $mmol_{WOx}$ / $kg_{Biomass}$ was still present in the reactor effluent in the cellulose reference experiment. The untreated poplar and pine feedstock have a combined calcium and magnesium content of 8 ± 2 and 21 ± 3 Ca + Mg mmol / $kg_{Biomass}$ respectively. The WO_x to divalent cation ratio is between 3.6-10 for poplar and 1.5-3.3 for pine.

Appendix C

C.1 Supporting figures

C.1.1 Addition of water-soluble extractives

We measured a decrease in soluble tungstate in the reactor effluent with increase in water soluble extractives in a physical mixture of cellulose and water-soluble extractives, see Figure C.1. This indicates that these extractives contain tungstate poisons.

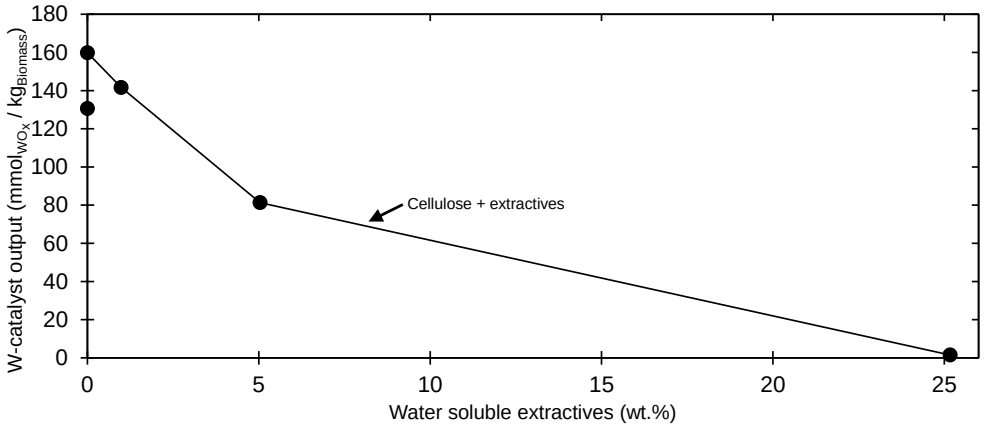

Figure C.1: W-catalyst present in reactor effluent as function of water soluble extractives present in the feed for a physical mixture of cellulose and water soluble extractives. Reaction conditions: 5 wt.% biomass loading, T = 245°C, t = 1 h, P_{H2} (Initial) = 60 bar, $pH_{Initial}$ ∼3.3, Ni-catalyst/Biomass mass ratio = 0.13. W-catalyst input ∼225 $mmol_{WOx}$ per $kg_{Biomass}$. Lines drawn to guide the eye.

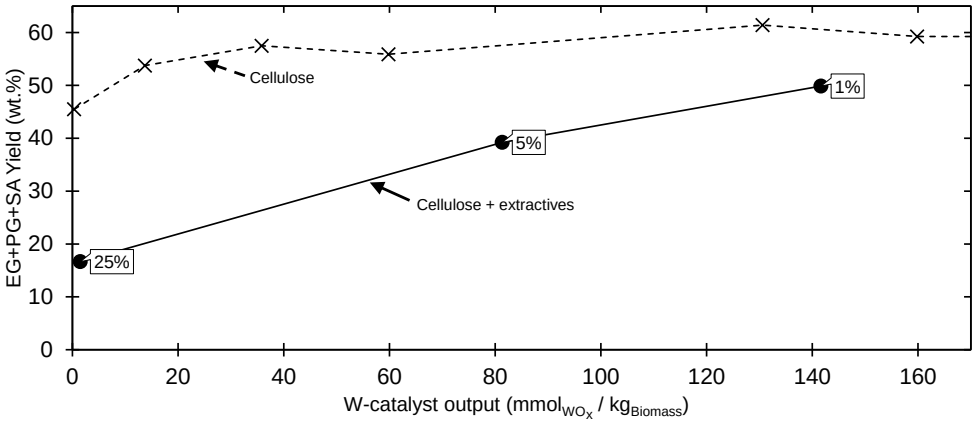

Figure C.2: Sum of key hydrogenated products (EG+PG+SA) as function of W-catalyst measured after the experiment. Labels represent the extractives content in a mixture of cellulose and extractives. Cellulose reference experiments were performed at varying W-catalyst input and consequently W-catalyst output. Reaction conditions: 5 wt.% biomass loading, T = 245°C, t = 1 h, P_{H2} (Initial) = 60 bar, $pH_{Initial}$ ∼3.3, Ni-catalyst/Biomass mass ratio = 0.13. W-catalyst input ∼225 $mmol_{WOx}$ per $kg_{Biomass}$. Lines drawn to guide the eye.

C.1.2 Addition of inorganic model compounds

We have added waterglass (sodium-silicate), colloidal silica and monosodium-phosphate (NaH_2PO_4) to the cellulose reference experiment and found that typically a similar amount of tungstate was found in the reactor effluent as was expected for the cellulose only experiment, see Figure C.3. The exception is the addition of sodium-silicate in a 10:1 ratio which is very extreme ratio and therefore not representative for native biomass, but shows a substantial tungstate consumption (∼170 $mmol_{WOx}$ per kg Biomass). However, we also found that the pH increased to 4.8 (measured after the experiment), whereas the pH in a typical experiment is ∼3.3. Further study is required to attribute this consumption to sodium silicate or to the pH increase.

Note that the data from cellulose reference test does not follow a parity line, which was discussed in our previous work (Chapter 4)[116], and was attributed to precipitation of tungstate by nickel that is leached from the Raney nickel catalyst.

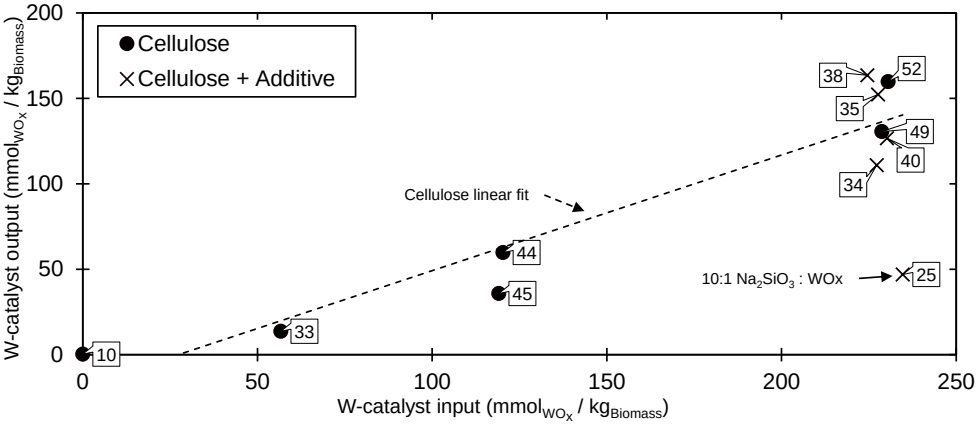

Figure C.3: Soluble tungstate catalyst input and output in the reactor effluent for experiments without and with additives (sodium silicate, colloidal silica and monosodium-phosphate). EG+PG yield denoted by the labels.

C.1.3 Pretreatment

Deactivation of Ni-catalyst by sulphur is typically considered irreversible as it leads to the formation of the relatively stable NiS. Pretreatment to reduce the S/N content of the feed appears, therefore, a more attractive option to overcome this deactivation than regeneration of the poisoned catalyst. We have applied a series of mild extraction pretreatments to evaluate their effectiveness on S and N removal. These extractions were based on water (as reference case), acid (10 wt.% acetic acid in water at RT), which is an inevitable pretreatment step to remove inorganic poisons (Chapter 4)[116], and ethanol, which might facilitate the dissolution of non-water soluble S/N components and is a representative for the organic (by)product stream from hydrogenolysis. The untreated woody biomass species, poplar and pine, contain sulphur levels that are a factor 25-75 and nitrogen levels that are a factor $\sim$8 higher than the target specification, see entries 2 and 5 in Table C.1. In other words, some 96-99% of sulphur and 87-89% of nitrogen must be removed to meet the target specification. The substrates in the previously discussed work by Li et al.[64] exhibit similar S and N levels and none meets the target specification, see Table C.3. Soxhlet extraction with water (E-W) and optionally followed by ethanol (E-EtOH) and acid-leaching did not significantly reduce the nitrogen content of these feedstocks, see entries 3, 4 and 6 in Table C.1. At the same time a small reduction in sulphur content from 5 mmol$_S$ to $\sim$4 mmol$_S$ per kg biomass was observed for the treatments applied to Poplar wood, see entries

2, 3 and 4 in Table C.1. The sulphur content of pine significantly reduced after acid-leaching, namely from 4.7 to <1.6 (detection limit of analytical procedure) $mmol_S$ per kg biomass, see entry 6 in Table C.1.

*Table C.1: S and N content of various (treated) biomasses. *Detection limit of analytical method was reached. E-W = water extracted (soxhlet), E-EtOH = ethanol extracted (soxhlet), WL = water leaching at RT, AL = acetic acid (10 wt.%) leaching at RT.*

Entry	Feedstock	Sulphur (mmol kg^{-1})	Nitrogen (mmol kg^{-1})
Target Specification:		*0.67-0.2*	*4.1*
1	Avicel	<1.6	16
2	Poplar	5	36
3	E-W Poplar	4.1	36
4	E-W + E-EtOH Poplar	3.7	34
5	Pine	4.7	31
6	AL Pine	<1.6	34
7	Hay	34.3	928
8	WL Hay	23.7	714
9	WL+AL Hay	22.8	714
10	E-W + E-EtOH Hay	24.6	857

The removal of sulphur containing components was also noticed for hay, from 34 to ~23 $mmol_S$ / $kg_{Biomass}$, independent of the applied pretreatment method, see entries 7-10 in Table C.1. This suggest that mainly water-soluble species (e.g. sulphate) are removed and that the acidic and ethanol extractions were not beneficial. Nitrogen levels could be brought down from 928 to 714 $mmol_N$ / $kg_{Biomass}$ by water leaching, see entries 7-9 in Table C.1. The soxhlet extracted hay (Water+EtOH) has a higher nitrogen content (857 $mmol_N$ / $kg_{Biomass}$) than water leached hay (714 $mmol_N$ / $kg_{Biomass}$). The development of effective pretreatment techniques that remove S and N are key for the commercialisation of biomass valorisation routes that proceed via a metal catalyst, which are typically very susceptible to N and in particular S poisoning. Overall, the tested mild pretreatment all fail to deliver a feedstock that comes close to the S and N target specifications. These heteroatoms are mostly present in the form of proteins[30],[117]. There is extensive body of research on the pretreatment of biomass for the recovery of proteins for human or animal consumption[154], but these studies typically apply mild conditions to preserve

the proteins and are more concerned with protein quality than with yield. In our previous work (Chapter 4)[66] we applied an acidified (20 wt.% HAc) hot water pretreatement at 180°C for 5 h on hay and found that the resulting substrate gave an EG yield of 20 wt.%, substantially higher than obtained for untreated hay (4 wt.%) but also lower than the cellulose reference test (32 wt.%). The same sensitive biomass to Raney nickel ratio (∼8.5) as in this work was as applied, which suggests that S/N poisoning of the catalyst was reduced. This experimental outcome, therefore, provides an entry point for further study to identify effective pretreatments.

C.1.4 Sugar alcohol yield as function of S and N

The sugar alcohol yield as function of the sulphur and nitrogen to Ni-catalyst loading showed a similar pattern as we reported for the glycol yield in the main work see Figure 5.3 in chapter 5, it declines with increase in S to Ni ratio and initially decreases with N to Ni-ratio after which it appears to reach a plateau value, see Figure C.4.

(A) Sulphur **(B) Nitrogen**

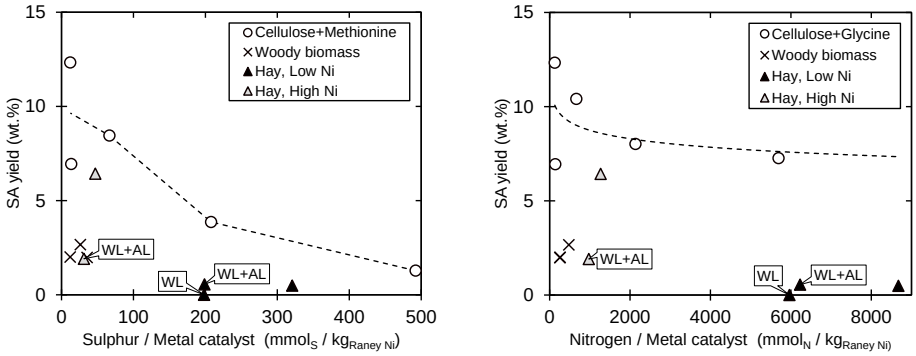

Figure C.4: Combined glycol yield as function of sulphur and nitrogen to metal catalyst ratio for woody biomasses, (treated) hay and physical mixtures of cellulose and glycine (N) or Methionine (S+N). Reaction conditions: 5 wt.% biomass loading, T = 245°C, t = 1 h, P_{H2} (Initial) = 60 bar, $pH_{Initial}$ ∼3.3, Ni-catalyst/Biomass mass ratio; low Ni = 0.13, high Ni = 0.7. Sufficient W-catalyst present in the outlet stream to allow for high glycol yield. Lines to guide the eye.

C.1.5 Addition of organic acids

The yields obtained after hydrogenolysis of cellulose and mixtures of cellulose and 25 wt.% of tannic-acid or glucuronic-acid were very similar, see Figure C.5. Moreover, the concentration of tungstate in the reactor effluent was similar for these experiments. This shows that such components do not deactivate the tungstate and Raney nickel catalyst under the conditions tested.

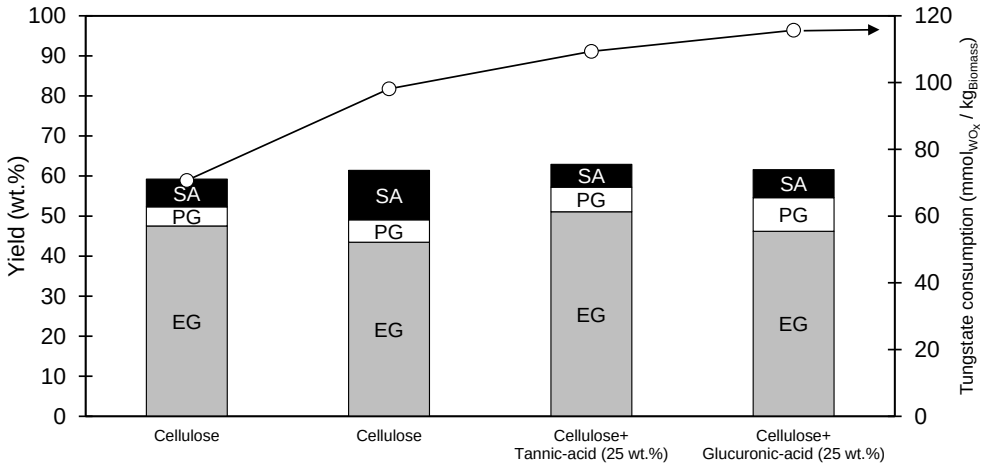

Figure C.5: Experiments performed with cellulose and mixtures of cellulose + 25 wt.% of an additive. Reaction conditions: 5 wt.% biomass loading, T = 245° C, t = 1 h, P_{H2} (Initial) = 60 bar, $pH_{Initial}$ ∼3.3, Ni-catalyst/Biomass mass ratio = 0.13. W-catalyst input ∼225 $mmol_{WOx}$ per $kg_{Biomass}$.

C.1.6 Experiment with sulphate

In addition to the experiments performed with physical mixtures of cellulose and methionine to investigate the impact of S on the glycol yield, we have performed an experiment with sulphate. The glycol yield was much higher than what was expected based on the results for mixtures of cellulose and methionine, namely ∼40 wt.% EG+PG for a S to catalyst ratio of ∼1700 $mmol_S$ per kg of catalyst, whereas the combined glycol yield was ∼10 wt.% for cellulose-methionine mixture at only ∼500 $mmol_S$ per kg of catalyst, see Figure C.6. Measurement of the reactor effluent revealed that 91% of the fed sulphate was still present as sulphate. When comparing the glycol yield on consumed basis we find that the result obtained with sulphate as S-additive matches the trend observed for mixtures of cellulose and methionine, see *"sensitive window"* in Figure C.6.

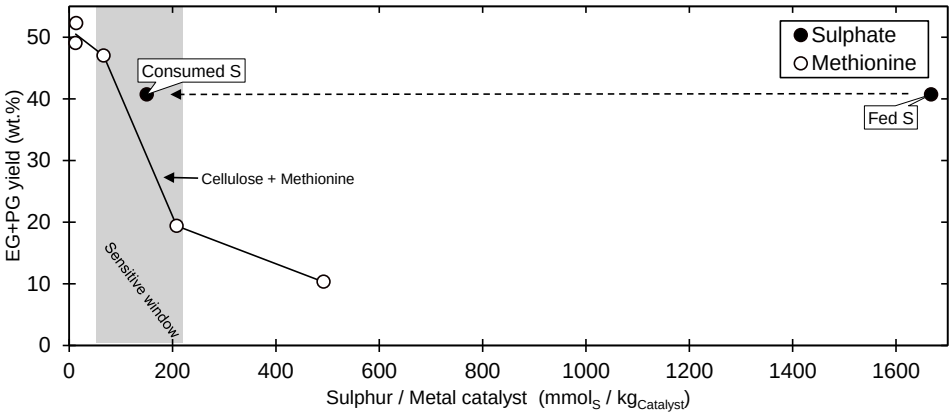

Figure C.6: Combined glycol yield as function of sulphur to metal catalyst ratio for mixtures of cellulose and methionine or sulphate. Reaction conditions: 5 wt.% biomass loading, T = 245° C, t = 1 h, P_{H2} (Initial) = 60 bar, $pH_{Initial}$ ∼3.3, Ni-catalyst/Biomass mass ratio = 0.13. Sufficient W-catalyst present in the outlet stream to ensure high glycol yield. Lines drawn to guide the eye.

C.1.7 S-coverage estimation

We made an attempt to estimate the sulphur coverage of the Raney nickel surface to get an idea of the mode of deactivation. We considered the following model; the Nickel surface is considered as adjacent spherical units on which sulphur atoms can (perpendicular to the Ni-surface) adsorb and subsequently bind to Ni atoms to ultimately form NiS, see Figure C.7. We thus assume that only a monolayer is formed and that the remainder of the S-containing molecule is hydrogenated and subsequently desorbed from the surface. Based on the proposed model we calculated the maximum surface coverage by Sulphur atoms, assuming a Ni-radius of 124 pm and a surface area of 100 m^2 per $g_{Catalyst}$[155]. Full coverage of the Ni surface by S would amount to 2700 $mmol_S$ per kg Raney nickel.

We did, however, observe that the glycol yields plummets from $\geq$46 wt.% to <19 wt.% between 67 and 200 $mmol_S$ fed per kg of Raney nickel. This a factor 40-14 less compared to the estimated maximum coverage. This suggest that only a part of the surface is active for hydrogenation reactions. However, it should be noted that the hydrogenation of the intermediates that ultimately yield EG, PG and SA are in competition with thermal side reactions. The onset for a drop in yield might therefore occur before complete deactivation of the Raney nickel catalyst.

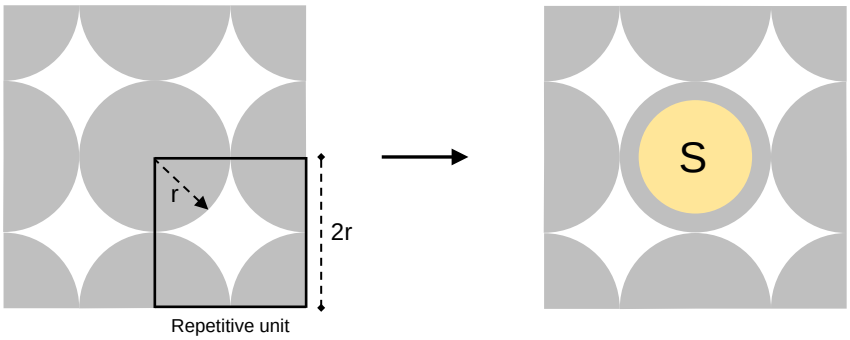

Figure C.7: Unoccupied Raney nickel surface (left) and adsorption of S on that surface (right)

C.2 Comparison with study by Philippov et al.[118]

Philippov et al.[118] studied the transfer hydrogenation of camphor using 2-propanol over Raney nickel at 82°C and thereby investigated the impact of catalyst poisons in particular S-containing components. They ran a series of experiment in which the thiophenol loading was varied, with increase in thiophenol load and thus S to Ni ratio a decrease in camphor conversion was observed, see Figure C.8. There is a particular sharp drop in the camphor conversion from 12 to 0 wt.% from 320 to 420 $mmol_S$ per kg of Ni, indicating that the catalyst is completely deactivated when this S to Ni ratio is exceeded.

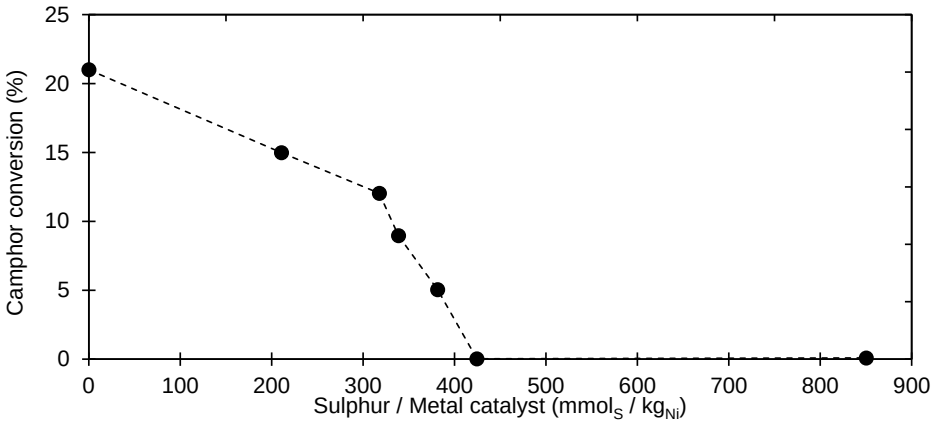

Figure C.8: Camphor conversion as function of thiophenol present in the reaction mixture expressed as sulphur / metal catalyst ratio in the study by Philippov et al.[118]. Reaction conditions: transfer hydrogenation using 2-propanol at 82° C.

C.3 Comparison with study by Li et al.[64]

The study by Li et al.[64] is of particular interest as they evaluated the glycol yield after hydrogenolysis of 10 different untreated biomass species. In their study they employed a 4%-Ni-30%-W_2C/AC catalyst and operated at 235°C, 6 MPa $_{H2}$, 4 h, 1 wt.% of biomass loading and a biomass to catalyst ratio of 2.5 (w/w).

C.3.1 Statistical analysis

We have performed a statistical analysis of their dataset to gain insights in the culprit for catalyst deactivation, see Table C.2. There is a strong correlation between the glycol yield and the phenolics yield (0.85), also see Figure C.9. This indicates that potential deactivation of the catalyst limits the hydrogenation of glycols as well as phenolic, i.e. lignin derivatives, components. Whereas the correlation between EG+PG and lignin is poor (-0.32) there is a very strong correlation with the extractives content (-0.89), see Table C.1. Indeed, the plot for extractives content of the feed and the EG+PG yield is quite striking, see Figure 5.1 in the main work (Chapter 5). Moreover, there is a reasonable correlation with the sulphur content of the feed (-0.71) and to a lesser extent, nitrogen content (-0.60). Importantly, extractives and sulphur content are highly correlated (0.91). The observed effect, possibly finds the same root cause. However, the relation between sulphur and EG heavily leans on the Corn Stalk data point. The dataset also confirms the general thought that a feedstock high in cellulose results in a high EG yield (0.84).

*Table C.2: Correlation coefficient matrix for the study by Li et al.[64], S/N feedstock content were obtained from the supporting information. *Bagasse feed was not included as S and N content of Bagasse were not reported.*

	Y_{EG+PG}	$Y_{Phenolics}$	Lignin	Cellulose	Hemi-cellulose	Extractives	Ash	Sulphur*
Y_{EG+PG}								
$Y_{Phenolics}$	0.85							
Lignin	-0.32	-0.63						
Cellulose	0.84	0.74	-0.49					
Hemicellulose	0.54	0.58	-0.60	0.32				
Extractives	-0.89	-0.55	0.01	-0.74	-0.46			
Ash	-0.35	-0.27	0.26	-0.51	-0.06	0.26		
Sulphur*	-0.71	-0.29	-0.39	-0.41	-0.36	0.91	0.09	
Nitrogen*	-0.60	-0.60	0.40	-0.70	-0.18	0.45	0.27	0.20

C.3.2 Supporting literature figures

There is a good correlation between the combined glycol yield expressed on saccharide basis an the phenolics yield expressed on lignin basis, see Figure C.9.

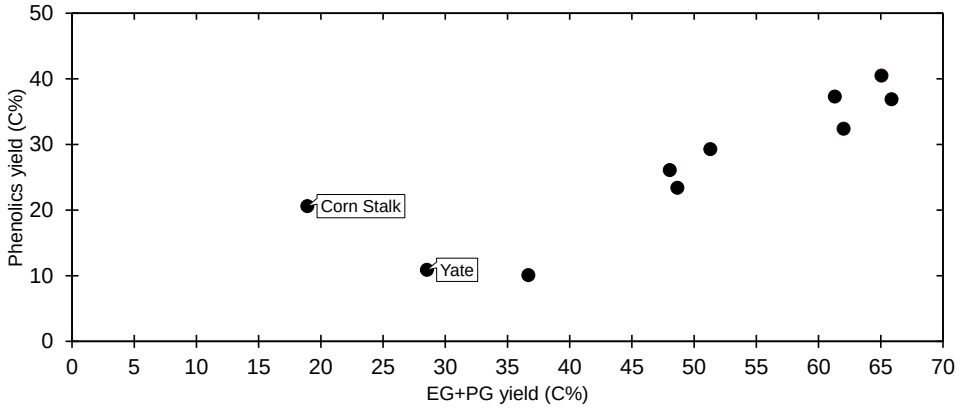

Figure C.9: EG yield versus phenolics yield obtained after hydrogenolysis of various untreated biomasses in the study by Li et al.[64]

The combined glycol yield was between 37 and 66 C% (56 C% on average) for untreated feedstocks (n=7), excluding Corn stalk and Yate, in the study by Li et al.[64], see Figure C.10. It should be noted that within the cluster of 7 feedstocks, pine gives a relatively low combined glycol yield of 37 C%, where the other feedstocks deliver $\geq$48 C%.

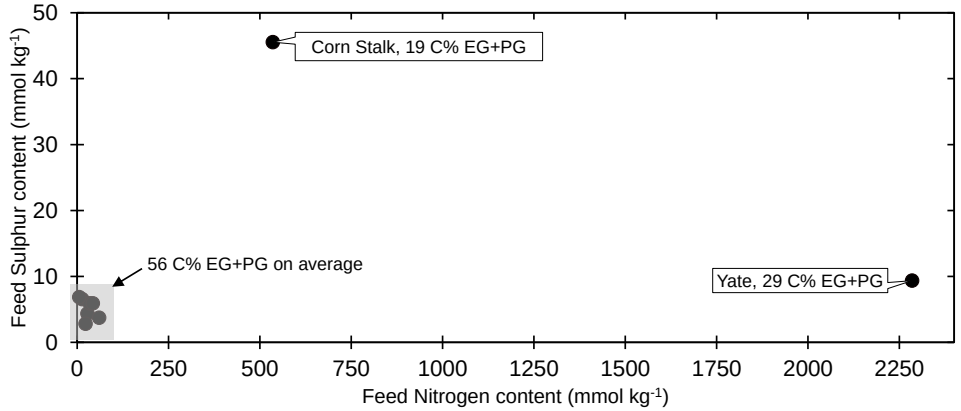

Figure C.10: Feedstock sulphur content versus feedstock nitrogen content, with EG+PG labelled for the study by Li et al.[64]

C.3.3 Sulphur and nitrogen

We have calculated the sulphur and nitrogen to catalyst ratio for the data obtained from the study by Li et al.[64] and added that to Figure 5.3 A and B in the main work (Chapter 5), see Figure C.11 and Figure C.12. Corn stalk falls in the *"sensitive window"* which could suggest that catalyst deactivation by S is the reason for the low glycol yield, see Figure C.11. Similarly, the reduced yield for Yate can be explained by its high N content, see Figure C.12.

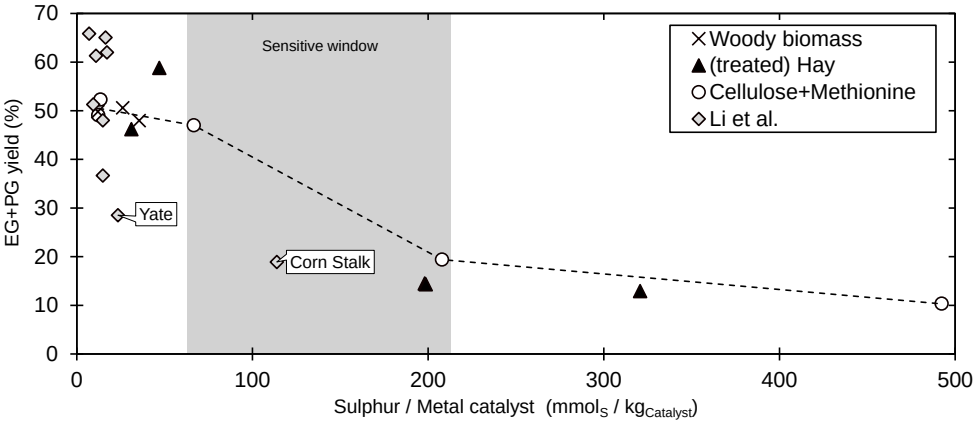

Figure C.11: Glycol yields in wt.% for this work and in C% for the study by Li et al.[64] as function of the sulphur to catalyst ratio.

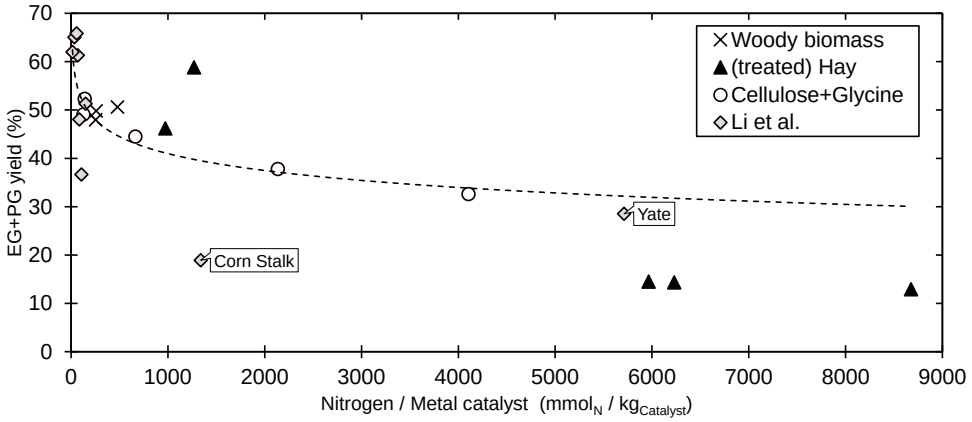

Figure C.12: Glycol yields in wt.% for this work and in C% for the study by Li et al.[64] as function of the nitrogen to catalyst ratio.

The sulphur and nitrogen content of the feedstocks used in the study by Li et al.[64] are reported in Table C.3. None meets the target specification.

Table C.3: Sulphur and nitrogen content of feedstocks tested in the study by Li et al.[64]

	Sulphur (mmol kg^{-1})	Nitrogen (mmol kg^{-1})
Target specification:	*0.067-0.2*	*4.1*
Ashtree	7	14
Bagasse	n.d.	n.d.
Basswood	4	28
Beech	6	34
Birch	3	23
Cellulose	n.d.	n.d.
Corn Stalk	46	535
Pine	6	43
Poplar	7	6
Xylosma	4	60
Yate	9	2285

Appendix D

D.1 Experiments with poplar

Hydrogenolysis of various poplar sieve fractions gave similar glycol yield (∼50 wt.%) as beech wood (reported in the main work (Chapter 6)) and the cellulose reference test, except for the 1-2 mm fraction, see Figure D.1.

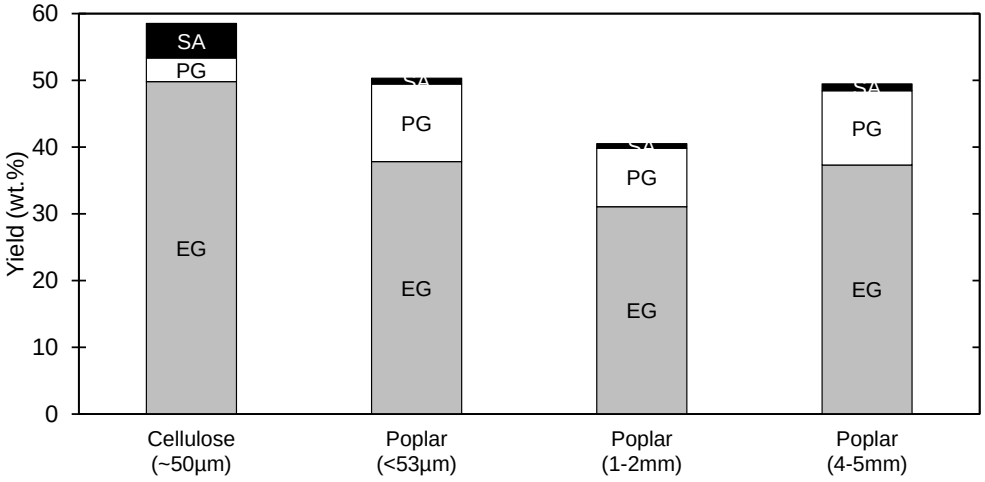

Figure D.1: Hydrogenolysis of cellulose and various sieve fractions of Poplar wood. 5 wt.% biomass loading, T = 245° C, t = 1 h, P_{H2} (Initial) = 60 bar, $pH_{Initial}$ ∼3.3, Ni-catalyst/Biomass mass ratio = 0.13. W-catalyst input ∼1130 $mmol_{WOx}$ per $kg_{Biomass}$.

D.2 In absence of tungstate

Hydrogenolysis of beech powder and slice was performed for 0 and 60 minutes in the absence of tungstate, which would theoretically primarily yield sugar alcohols such as xylitol and sorbitol. Indeed, a substantial amount of pentitol and hexitol were formed, see Figure D.2. The pentitol to hexitol ratio was ∼8 for beech powder for a reaction time of 0 minutes, but reduced to ∼2 for experiments run for 1 hour. This indicates that initially mainly hemicellulose is released after which cellulose is depolymerised.

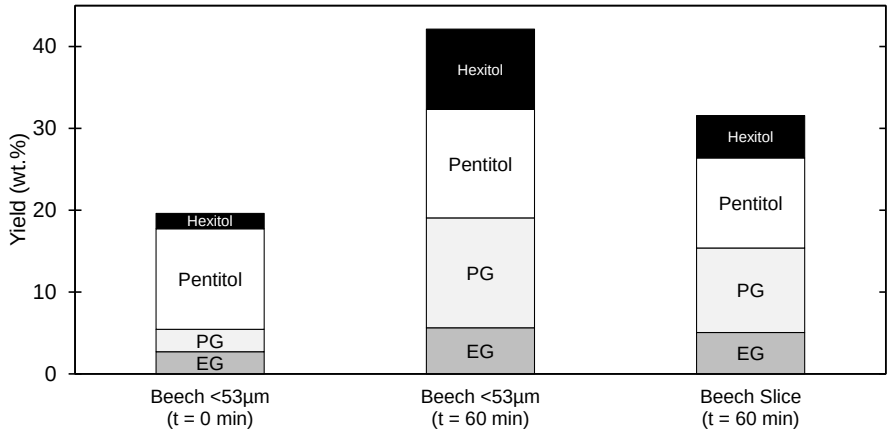

Figure D.2: Hydrogenolysis of Beech powder for 0 and 60 minutes and slice for 60 minutes in the absence of W-catalyst. 5 wt.% biomass loading, T = 245°C, t = 1 h, P_{H2} (Initial) = 60 bar, $pH_{Initial}$ ∼3.3, Ni-catalyst/Biomass mass ratio = 0.13.

D.3 Sensitive amount of W-catalyst

Hydrogenolysis under W-catalyst sensitive conditions was performed for beech wood powder for various run times, see Figure D.3. The EG and PG yields increased with time from 5-10 wt.% for 0 minutes of run time till 15-20 wt.% for an hour of runtime. The hexitol yield gradually increased with time whereas the pentitol yield was rather consistent. This indicates that initially hemicellulose is liberated and that cellulose is released over the course of one hour.

Consequently, the pentitol to hexitol ratio decreased with time, see Figure D.4. We also observed a decrease in pentitol to hexitol ratio for the experiments reported in Figure D.2 that were run in absence of tungstate.

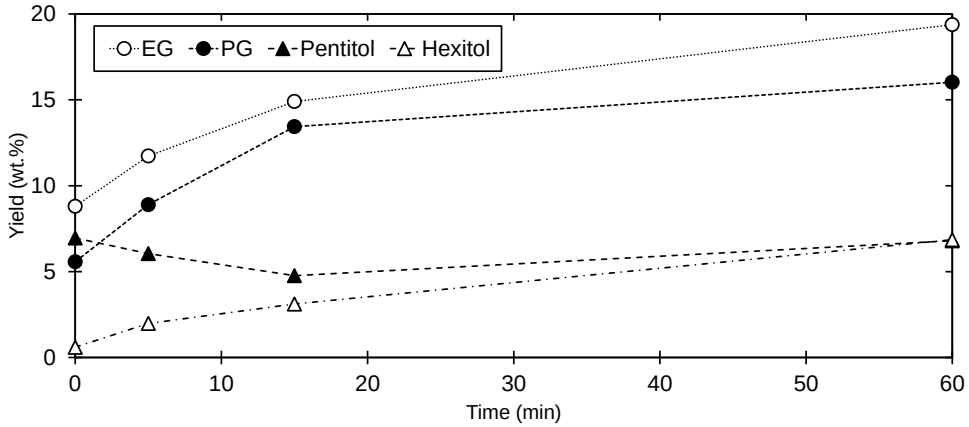

Figure D.3: Hydrogenolysis of beech wood powder. 5 wt.% biomass loading, T = 245° C, t = 1 h, P_{H2} (Initial) = 60 bar, $pH_{Initial}$ ∼3.3, Ni-catalyst/Biomass mass ratio = 0.13. W-catalyst input ∼120 $mmol_{WOx}$ per $kg_{Biomass}$.

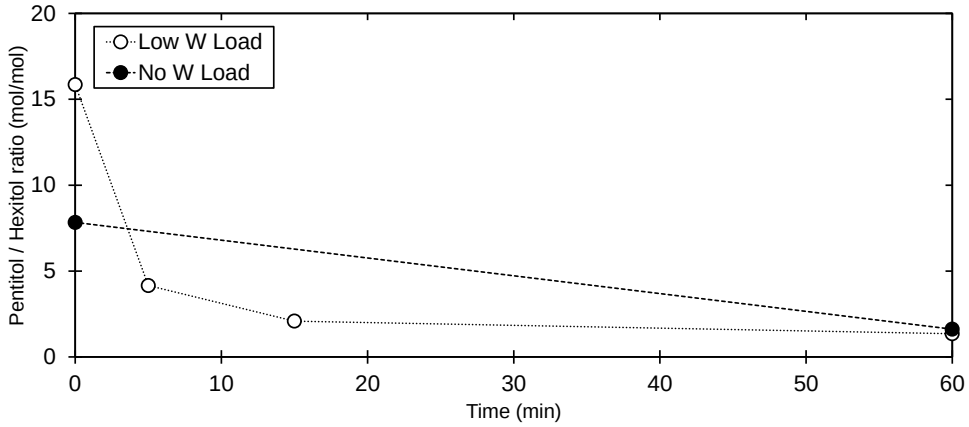

Figure D.4: Hydrogenolysis of cellulose and various sieve fractions of Poplar wood. 5 wt.% biomass loading, T = 245° C, t = 1 h, P_{H2} (Initial) = 60 bar, $pH_{Initial}$ ∼3.3, Ni-catalyst/Biomass mass ratio = 0.13. Low W-load W-catalyst input ∼120 $mmol_{WOx}$ per $kg_{Biomass}$, no W-load W-catalyst input 0 $mmol_{WOx}$ per $kg_{Biomass}$.

D.4 EG to PG ratio

Figure D.5 displays the EG to PG ratio of the product slate for cellulose and beech powder (<53 µm) and slice. EG to PG ratio for beech wood is typically around 3 whereas the product from cellulose results in an EG to PG ratio always greater than 12. The discrepancy originates from the presence of pentose (C_5) in beech wood which delivers more PG than hexose.

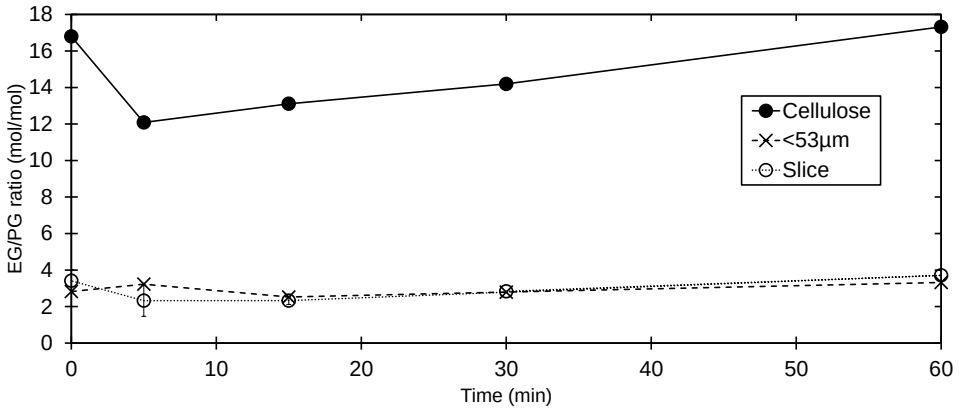

Figure D.5: EG to PG ratio of product obtained after hydrogenolysis of Beech powder (sieve fraction <53µm) and slices (22 mm (ø) x 3 mm (height)). Experiments with slice for 0, 5 and 15 min were performed in duplicate. 5 wt.% biomass loading, T = 245°C, P_{H2} (Initial) = 60 bar, $pH_{Initial}$ ∼3.3, Ni-catalyst/Biomass mass ratio = 0.13. W-catalyst input ∼1130 $mmol_{WOx}$ per $kg_{Biomass}$. Note that all data points are individual experiments.

D.5 Cellulose in time

The hydrogenolysis of cellulose gave a steady increase of EG and PG as function of reaction time, see Figure D.6.

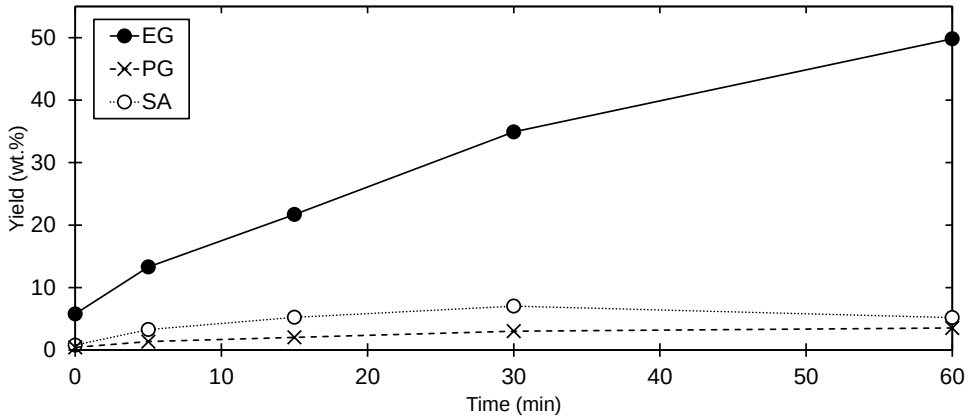

Figure D.6: Catalytic hydrogenolysis of cellulose. Reaction conditions: 5 wt.% biomass loading, T = 245°C, P_{H2} (Initial) = 60 bar, $pH_{Initial}$ ∼3.3, Ni-catalyst/Biomass mass ratio = 0.13. W-catalyst input ∼1130 $mmol_{WOx}$ per $kg_{Biomass}$. Lines drawn to guide the eye.

D.6 Acid-leached beech wood

Acid-leached beech wood of various fractions was subjected to hydrogenolysis under W-catalyst lean conditions which gave a combined glycol yield of 47 wt.%, independent of their size and thereby even surpassing the glycol yield obtained for the cellulose reference test, see Figure D.7.

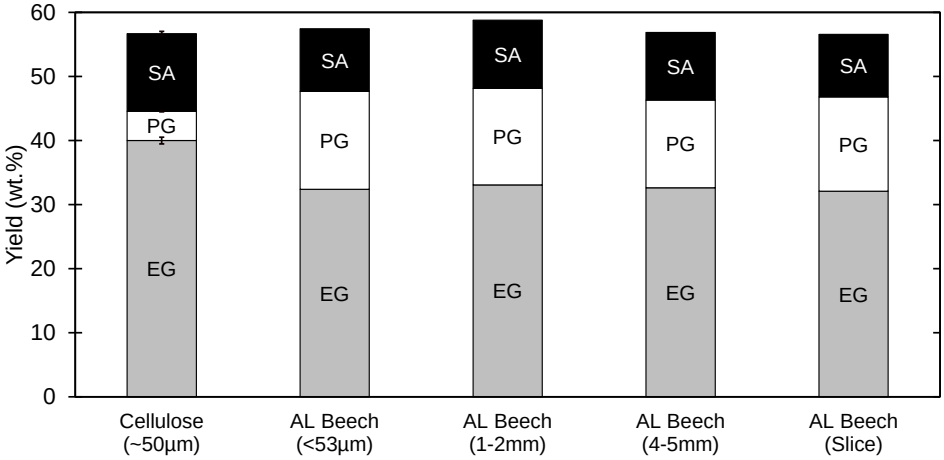

Figure D.7: Hydrogenolysis of acid-leached (AL) Beech wood. Slice size = 22 mm (ø) x 3 mm (height). 5 wt.% biomass loading, T = 245° C, t = 1 h, P_{H2} (Initial) = 60 bar, $pH_{Initial}$ ~3.3, Ni-catalyst/Biomass mass ratio = 0.13. W-catalyst input ~120 $mmol_{WOx}$ per $kg_{Biomass}$

D.7 Yield as function of tungstate concentration

The glycol yield for beech, acid-leached (AL) beech and cellulose appears to correlate with the W-catalyst concentration in the reactor effluent, see Figure D.8.

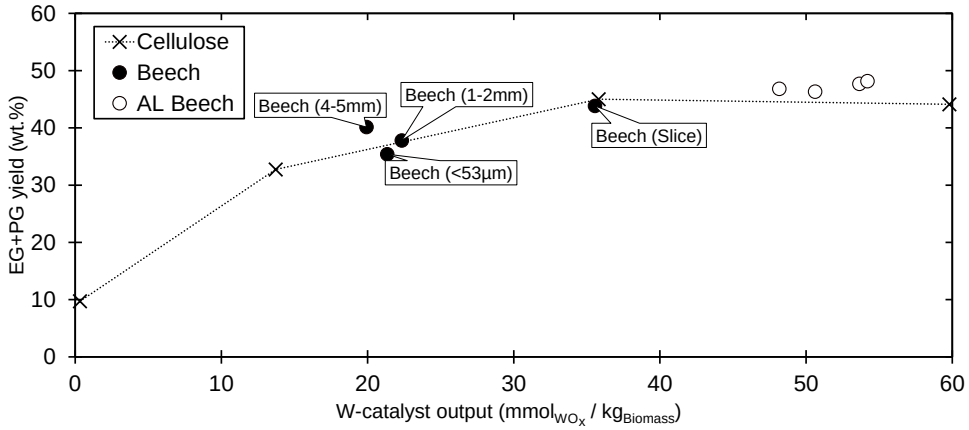

Figure D.8: Hydrogenolysis of acid-leached (AL) Beech wood. Slice size = 22 mm (ø) x 3 mm (height). 5 wt.% biomass loading, T = 245° C, t = 1 h, P_{H2} (Initial) = 60 bar, $pH_{Initial}$ ∼3.3, Ni-catalyst/Biomass mass ratio = 0.13. W-catalyst input ∼120 $mmol_{WOx}$ per $kg_{Biomass}$.

Appendix E

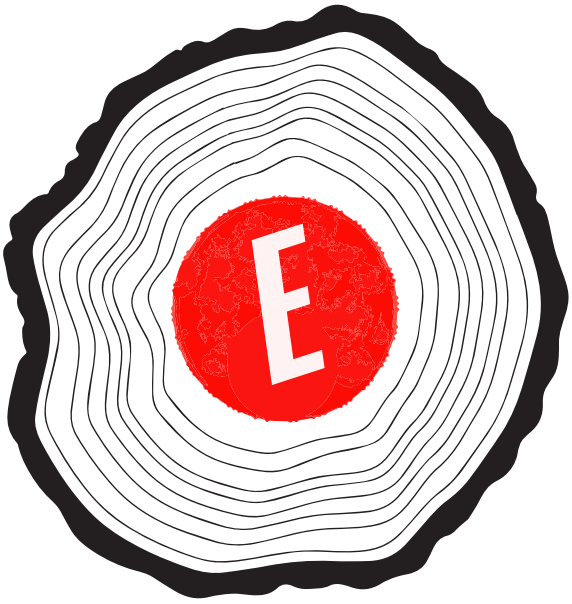

E.1 Tungstate deactivation constraint

The typical performance window for fuel/chemical processes for catalyst stability is (1-100 $tonne_{product}$ / $kg_{Catlalyst}$)[89]. Thus, a catalyst must process at least 1 kg of feedstock per gram of catalyst (assuming 100% selectivity), see equation E.1.

$$1000 \geq \frac{m_{Feed}}{m_{Catalyst}} \tag{E.1}$$

The mass of catalyst can be substituted by the molecular weight of the catalyst times the moles of catalyst, see equation E.2.

$$1000 \geq \frac{m_{Feed}}{M_w \times n_{Catalyst}} \tag{E.2}$$

We consider the chemical reaction X^{2+} + WO_4^{2-} which results in the formation of insoluble XWO_4. The molar ratio of poison to tungstate is assumed to be 1, thus $n_{catalyst} = n_{poison}$. The molecular weight of mono-tungstate (WO_4^{2-}) is 248 g mol^{-1}. With this information a maximum allowable concentration of poisons in the feed can be calculated, see equation E.3.

$$248000 \geq \frac{m_{Feed}}{n_{Poison}} \tag{E.3}$$

This comes down to a limit of 4 mmol of tungstate poisons per kg of biomass which translates to 161 mg Ca^{2+}, 97 mg Mg^{2+} or 225 mg Fe^{2+} per kg biomass.

E.2 Pretreatment solvent composition

The lignin content of the solid residue is displayed in Figure E.1 for pretreatment experiments of poplar for 3 h at 200°C for varying solvent composition (ethanol - water mixture).

The 5-hydroxymethylfurfural (HMF) and furfural yield, expressed on biomass intake, measured by analysis of the spent solvent are shown in Figure E.2. With increase in water content of the solvent, thus decrease of ethanol share of the solvent, HMF and furfural clearly increase.

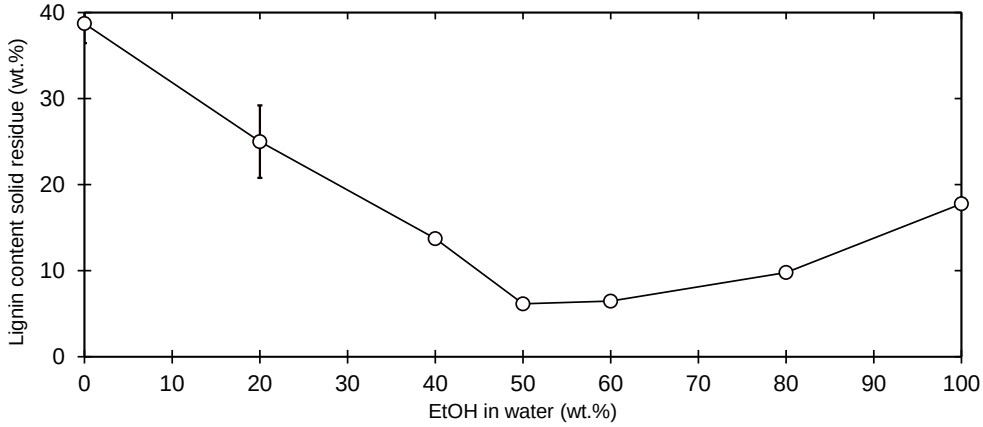

Figure E.1: Lignin content of solid residue as function of pretreatment solvent composition (EtOH-water). Quantification performed in duplo, errorbar typically too small to be seen.

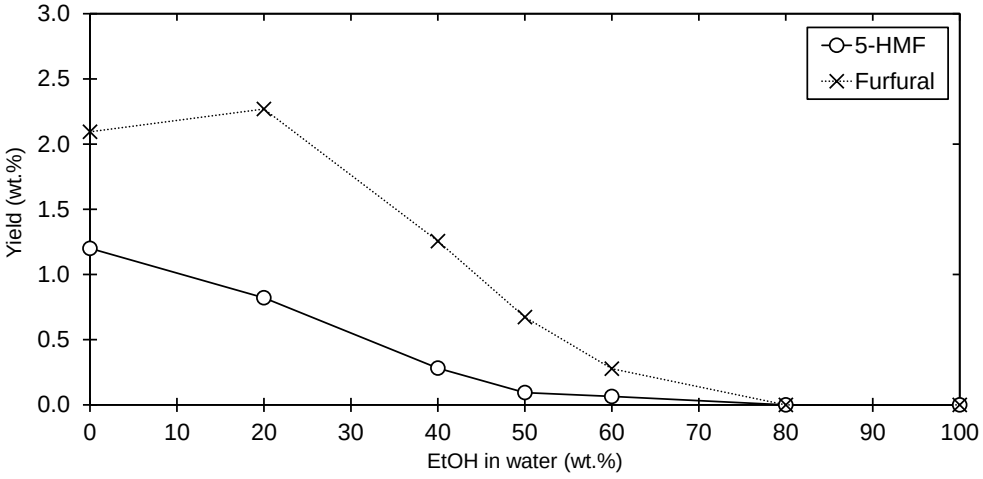

Figure E.2: HMF and furfural yields as function of pretreatment solvent composition (EtOH-water)

E.3 In-situ organic solvent generation

E.3.1 Organic acid formation

The acetic acid yield, on dry biomass intake, was between 4 and 5 wt.% when the water content of the solvent was 40 wt.% or higher, see Figure E.3. A decrease in the pH of the black liquor is associated with a higher yield of acetic acid.

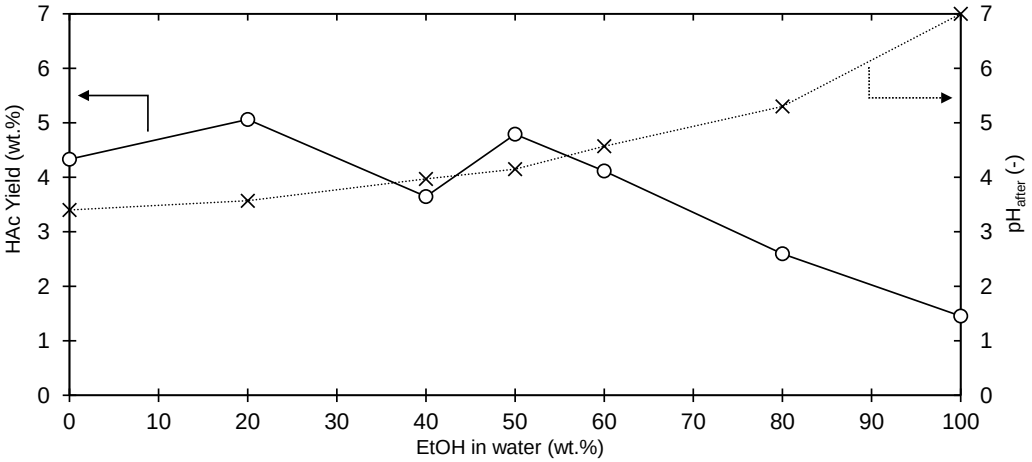

Figure E.3: Acetic acid (HAc) yield expressed on dry biomass intake and pH of the liquor after the experiment as function of the pretreatment solvent ethanol composition.

Less than 0.7 wt.% of the initial acetyl groups were left in the solid residue. Consequently, more than 80 wt.% of the o-acetyl groups were hydrolysed, see Figure E.4. Besides acetic acid, various other organic acids have been detected in the spent pretreatment liquor, see Figure E.5. The trend is similar as the acetic acid yield as function of the pretreatment solvent composition (see Figure E.3), for a pretreatment solvent high in ethanol (80 $\geq$ wt.%) the organic acid yield is limited but increases sharply when the ethanol content of the solvent is reduced to 60 wt.%, after which it becomes rather constant (EtOH content 0-60 wt.%).

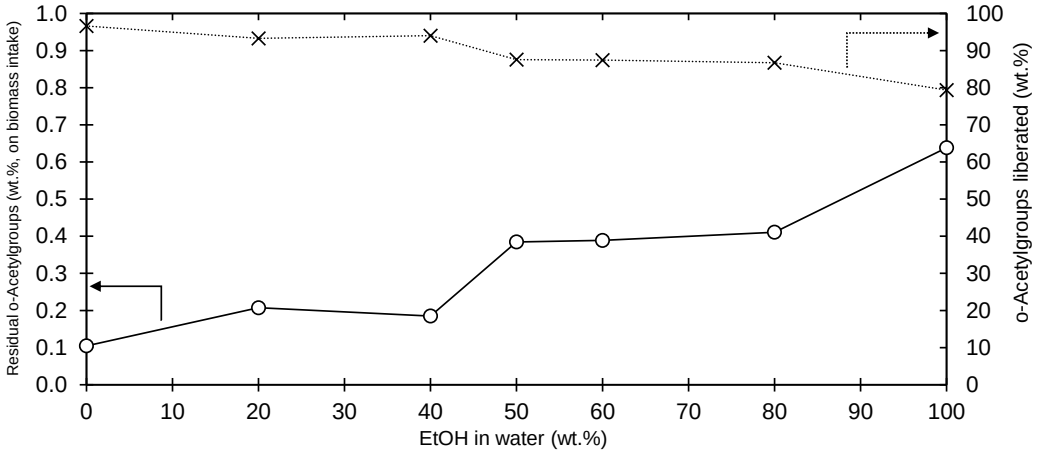

*Figure E.4: Residual acetylgroups and percentage of liberated acetylgroups as function of the pretreatment solvent ethanol composition. *No errobar for experiments with solvent ethanol content of 0 and 60 wt.%.*

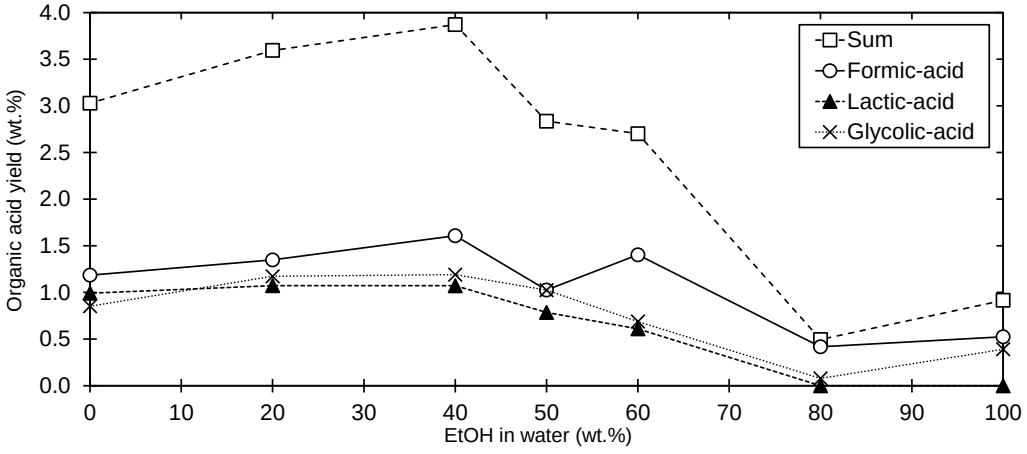

Figure E.5: Formic, lactic and glycolic acid yields as function of the pretreatment solvent ethanol composition.

E.3.2 Light alcohol production

Light alcohols, such as methanol, ethanol, propanol and butanol, are formed during the hydrogenolysis of cellulose during catalytic hydrogenolysis, see Figure E.6.

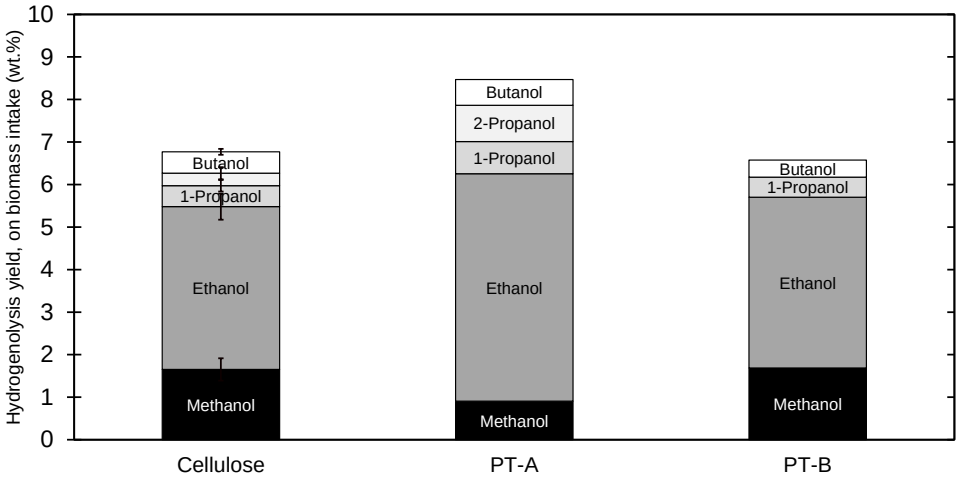

*Figure E.6: Light alcohol byproduct formation during hydrogenolysis. Cellulose is average of two experiments. *Butanol: sum of 1-butanol and 2-butanol. Hydrogenolysis conditions: 5 wt.% biomass loading, T = 245°C, t = 1 h, P_{H2} (Initial) = 60 bar, $pH_{Initial}$ ∼3.3, Ni-catalyst to biomass mass ratio 0.12, W-catalyst to biomass mass ratio 0.03.*

The total yield was between 6 and 9 wt.% on biomass intake to the hydrogenolysis section. However, a substantial amount of mass is lost during the pretreatment step. A typical solid residue yield after pretreatment, that targets deep delignification ($\leq$ 5 wt.% residual lignin), is 50-60 wt.%. The solid residue of pretreatments A and B fall within this range, see Table E.1. After correction for the pretreatment yield, the byproduct yield on biomass intake to the pretreatment steps falls between 3 and 5 wt.%.

Table E.1: Solid residue yield of different pretreatments and the overall light alcohol yield expressed on biomass intake to the pretreatment (PT) step.

PT	Solid residue yield (wt.%)	Overall light alcohol yield (wt.% on biomass intake)
A	56	4.7
B	50	3.2

E.3.3 Organic solvent consumption by reaction

A part of the solvent is consumed by reaction with a biomass fraction or derivative. Acetic acid is lost by acetylation of the solid residue and lignin. Similarly, it has been reported that ethanol participates in various reactions with lignin as well[156].

E.3.3.1 Solid residue

As previously discussed in section E.3.1, acetic acid is produced from biomass predominantly by liberation of the acetyl groups. For a range of ethanol-water pretreatments we found that over 80% of the acetyl groups were released in the form of acetic acid. Even for a pretreatment for which the solvent consisted for 70 wt.% of acetic acid 41 wt.% of the acetyl groups were liberated, thus resulting in a net production of acetic acid, see pretreatment B in Table E.2.

Table E.2: Acetyl groups of the solid residues of pretreatment (PT) A & B

PT	Solid residue o-acetylgroups (wt.%)	Solid residue o-acetylgroups (wt.% on biomass intake)	o-Acetyl groups liberated (%)
A	0.7 ± 0.1	0.4 ± 0.1	87
B	3.7 ± 0.2	1.8 ± 0.1	41

Measurement of the ethanol consumption by the solid residue was complicated by peak interference of an unknown component present in untreated poplar. Moreover, in a different HPLC configuration, i.e. operating on a HiPlex Pb column instead of HiPlex H^+ column, also peak interference of ethanol and arabinose occurred. Nevertheless, we estimated the ethanol consumption by correction for the initially present *"ethanol"* ($\sim$0.3 wt.% ethanol equivalent), see Figure E.7. The data show that at maximum 0.8 wt.% of ethanol is consumed during ethanol-water type of pretreatment, but generally is very minor, <0.3 wt.%. Note that the solid residue is hydrolysed in the hydrogenolysis reactor, thereby releasing organic molecules that previously reacted with the solid residue in the pretreatment step.

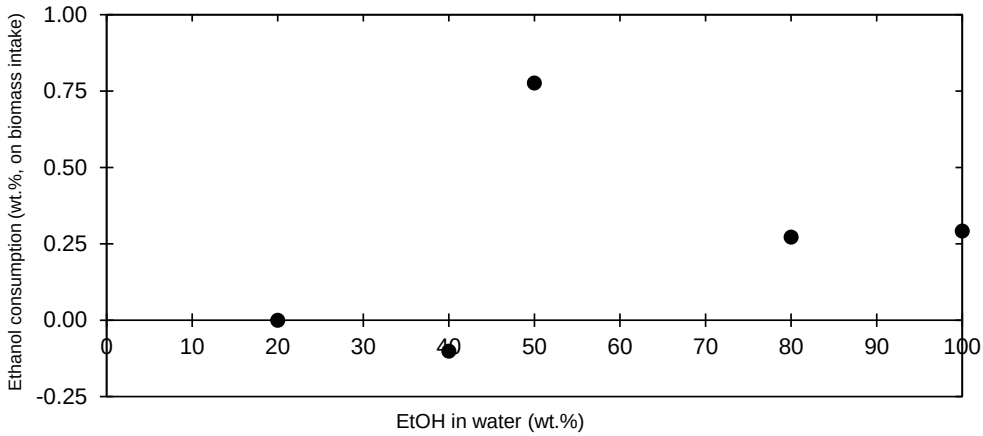

Figure E.7: Ethanol consumption by solid residue on biomass intake for pretreatment of poplar for 3h at 200° C for varying solvent composition (EtOH - Water mixture)

E.3.3.2 Lignin

In our process concept, lignin ends up as a fuel or is directly sold. As a consequence, solvent that reacted with lignin during pretreatment (e.g. acetylation of lignin) is lost, in contrast to the solid residue which is depolymerised in the hydrogenolysis section and thereby releases bound solvent. We quantified the acetyl groups of the lignins from pretreatments A and B, see Table E.3. When ethanol-water is used as solvent (PT-A), an insignificant amount of acetic acid is lost by acetylation of lignin, whereas 2 wt.% of acetic acid is lost on lignin basis for a pretreatment in 70 wt.% acetic acid (PT-B). Still, the acetic acid loss expressed on biomass intake, 0.4 wt.%, is acceptable. A comparable amount of ethanol reacted with lignin in case ethanol-water mixture was used as pretreatment solvent, namely 1.8 wt.% on lignin basis and 0.4 wt.% on biomass intake, see Table E.4.

Table E.3: Acetyl groups of lignins from pretreatment (PT) A and B

PT	Solid residue o-acetylgroups (wt.%)	Solid residue o-acetylgroups (wt.% on biomass intake)
A	0.1 ± 0.00	0.02
B	2.1 ± 0.1	0.4 ± 0.01

Table E.4: o-ethylgroups content of lignin from pretreatment A measured by two techniques

Apparatus	Solid residue o-ethylgroups (wt.%)	Solid residue o-ethylgroups (wt.% on biomass intake)
HPLC HiPlex H^+	1.7 ± 0.6	0.3 ± 0.1
HPLC HiPlex Pb	1.8 ± 0.3	0.3 ± 0.1

E.3.4 Others

Besides reaction of organic solvent with the solid residue (predominantly holocellulose) and lignin, a variety of other reactions with biomass derivatives are possible. Most importantly, the formation of esters by reaction of organic acids and light alcohols. However, these esters are typically volatile and their formation is reversible. For example, esterification of ethanol and acetic acid yields ethylacetate (BP = 77°C) which is easily recovered, together with the rest of the solvent, during the evaporation stage. Nevertheless, we found an ethylacetate yield of 0.3 wt.% on biomass intake for pretreatment A.

E.3.5 Neutralisation by basic ash

The acid neutralisation capacity (ANC) was measured by titration of biomass suspended in demineralised water with nitric acid until the pH was 3 for 24 hours, see Table E.5. We measured a similar number, 0.15 ± 0.01 mole H^+ / $kg_{Biomass}$ as Smit et al.[138] found for poplar, namely 0.13 mole H^+ / $kg_{Biomass}$. Furthermore, the numbers by Smit et al.[138] match well with the numbers reported by Lange[31]. The ANC was halved after soxhlet extraction with first water and then ethanol.

*Table E.5: ANC of poplar and extracted poplar on dry basis. *First extracted with water followed by ethanol according to the procedure described in* **NREL_Extractives_2008**

Feedstock	ANC (mole H^+ / $kg_{Biomass}$)	Required HAc (wt.% on biomass)
Poplar	0.16	0.94
Poplar	0.13	0.81
Extracted Poplar*	0.08	0.44

Table E.6: ANC of various lignocellulosic feedstocks, expressed on dry basis by Smit et al.[138]

Feedstock	ANC (mole H^+ / $kg_{Biomass}$)	Required HAc (wt.% on biomass)
Wheat straw	0.53	3.2
Corn stover	0.45	2.7
Beech	0.15	0.9
Poplar	0.13	0.8
Birch	0.1	0.6
Spruce	0.07	0.4
Pine	0.07	0.4

Table E.7: ANC of three different lignocellulosic archetypes, expressed on dry basis by Lange[31]

Feedstock	ANC (mole H^+ / $kg_{Biomass}$)	Required HAc (wt.% on biomass)
Hardwood	<0.2	1.2
Softwood	<0.1	0.6
Grasses	0.2-1	1.2-6.1

E.4 Solvent recovery target

The in-situ production of organic solvent can be expressed as the conversion to light organics (Y_{Lights}) times the weight of the biomass (B), see equation E.4.

$$\text{Production (wt.\%)} = Y_{Lights} \times B \tag{E.4}$$

Per processing cycle, a certain amount of biomass (B) is suspended in a solvent which is composed of a fraction of organic solvent ($f_{organic}$) and water. The solvent to biomass mass ratio is expressed as S/B. This leads to equation E.5.

$$\text{Cycle (wt.\%)} = B \times \frac{S}{B} \times f_{Organic} \tag{E.5}$$

The percentage of solvent that needs to be recovered is defined by equation E.6.

$$R\ (\text{wt.\%}) = \left(1\text{-}\frac{\text{Production}}{\text{Cycle}}\right) \times 100 \tag{E.6}$$

Substitution of equation E.4 and equation E.5 in equation E.6 yields equation E.7.

$$R\ (\text{wt.\%}) = 100\text{-}Y_{Lights} \times \frac{B}{S} \times \frac{1}{f_{Organic}} \tag{E.7}$$

The minimum and maximum values for the variables in equation E.7 are reported in Table E.8. Note, that minimum and maximum values here refer to their effect on the allowable loss (i.e. 100-recovery rate). The allowable solvent loss is between 0.44 and 6.5 wt.% which translates to recovery rates between 99.6 and 93.5 wt.%.

It can be seen from equation E.7 that the recovery rate scales linearly with the biomass conversion to organic solvent (Y_{Lights}) and linearly with the biomass to solvent ratio (B/S) (i.e. non linearly with the biomass loading), but non-linearly with the organic share of the solvent. Optimizing this parameter, e.g. reducing the organic share of the pretreatment solvent, has the strongest impact on the recovery rate, due to its non-linear relationship, which is illustrated in Figure

E.8.

Table E.8: Minimum and maximum values for parameters in equation E.7 with respect to the allowable solvent loss.

Variable	Minimum	Maximum
Conversion to lights (Y_{Lights} (wt.%))	4	13
Biomass to solvent mass ratio (B/S)	0.11	0.25
Organic fraction of the solvent ($f_{organic}$)	1	0.5
Allowable solvent loss (wt.%)	0.44	6.5

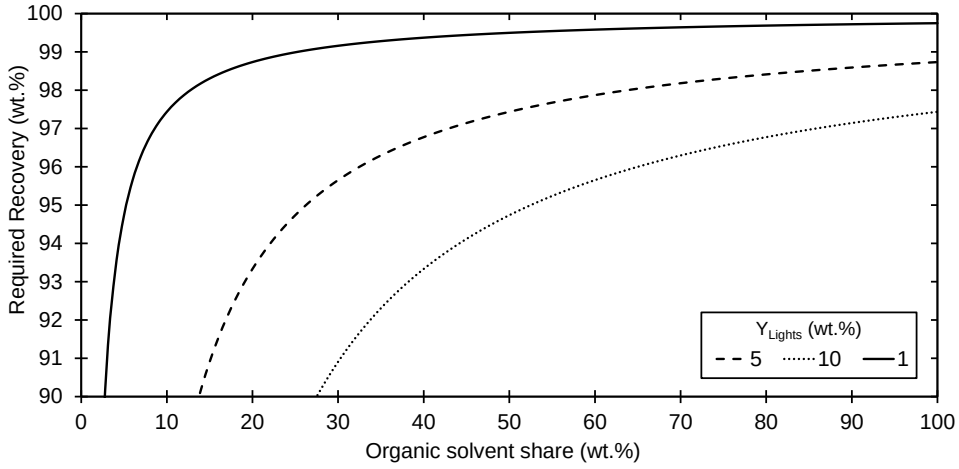

Figure E.8: Required solvent recovery rate for different values of Y_{Lights} as function of the pretreatment solvent composition for a solvent to biomass ratio of 4.

Although, the demanded recovery rate is high for any scenario ($\geq$93.5 wt.%), in-situ solvent generation results in an economic advantage. We here report a quick calculation on the economic impact of solvent recovery. The total feedstock costs is a function of the amount of biomass fed (B) times the price of this biomass ($P_{Biomass}$), see equation E.8. Typically, the at-the-gate cost of dry biomass is at $\sim$80 dollars per tonne[17],[105].

$$\text{Cost (\$)} = B \times P_{Biomass} \tag{E.8}$$

In our example the generated revenue follows from selling the saccharide fraction (i.e. lignin and others are combusted to supply heat to the process), which is generally valued around 300 dollar per tonne[157]. The amount of saccharide produced follows from the amount of biomass (B) times the solid residue yield after pretreatment (Y_{SR}) times the holocellulose (i.e. saccharide) fraction, see equation E.9. $f_{Hydrolysis}$ is the correction factor for the mass increase that follows from hydrolysing a polysaccharide to a monosaccharide (+18 g mol^{-1}).

$$\text{Revenue (\$)} = B \times Y_{SR} \times f_{Holocellulose} \times f_{Hydrolysis} \times P_{Saccharide} \tag{E.9}$$

The margin results from the difference between the revenue and the costs. For example experiment PT-A would provide a revenue of $\sim$140 dollar per tonne of biomass intake (Y_{SR} = 0.56, $f_{Holocellulose}$ = 0.77, $f_{Hydrolysis}$ = 1.11), which would result in a margin of $\sim$60 dollar per tonne dry biomass fed. The organic solvent cost are expressed by equation E.10, which results in a cost of 800 \$ per tonne biomass for an optimistic scenario in which the liquor to biomass ratio (L/B) is 4, the organic fraction of the solvent is 0.5 and the organic solvent price 400 \$.

$$\text{Solvent cost (\$)} = B \times \frac{L}{B} \times f_{Organic} \times P_{Solvent} \tag{E.10}$$

This means that a 1% loss of organic solvent equals 8 \$ dollar per tonne biomass fed.

E.5 Hydrogenolysis yields

E.5.1 This work

The EG yields for pretreated samples A and B are substantially higher than for untreated poplar and comparable to micro crystalline cellulose, see Figure E.9, data was previously reported in Molder et al.[66] (Chapter 3). The hydrogenolysis product yields reported in Figure E.9 were calculated on the basis of the presumed saccharide content of the feed according to equation E.11, in which $m_{Product}$ is the mass of the product (e.g. EG), m_{Feed} is the mass of the biomass fed, and f_{Lignin}, $f_{H2O\text{-}extract}$, $f_{EtOH\text{-}extract}$, f_{Ash}, f_{Acetyl} are the lignin, water extractives, ethanol extractives, ash and acetyl weight fractions of the dry feedstock. This gives a fair comparison as only the saccharide fraction of biomass can yield ethylene and propylene glycol.

$$Y\ (wt.\%) = \frac{m_{Product}}{m_{Feed} \times (1 - f_{Lignin} - f_{H20\text{-}extract} - f_{Ash} - f_{Acetyl})} \times 100 \quad (E.11)$$

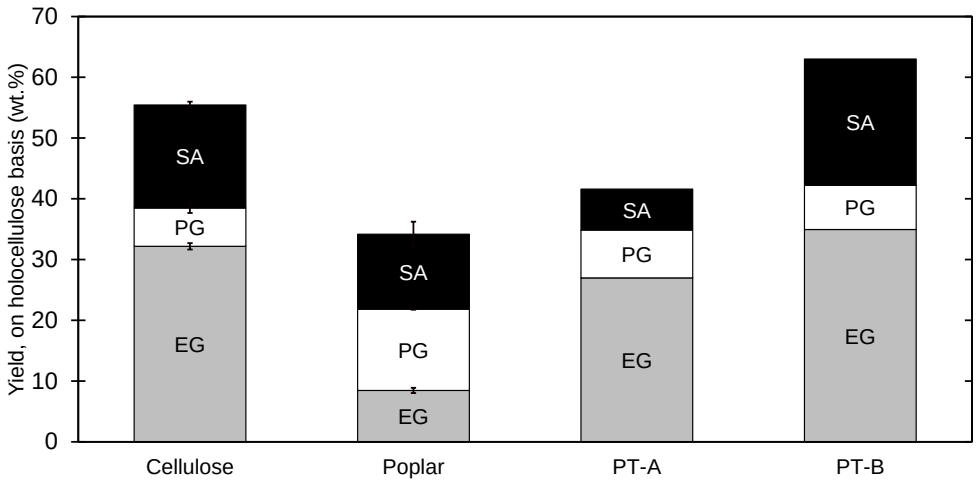

Figure E.9: Hydrogenolysis yields expressed on holocellulose basis for microcrystalline cellulose (n=2), untreated poplar (n=2) and pretreated samples PT-A & PT-B. Also reported in our previous work (Chapter 3)[66]. Hydrogenolysis conditions: 5 wt.% biomass loading, T = 245°C, t = 1 h, P_{H2} (Initial) = 60 bar, $pH_{Initial}$ ~3.3, Ni-catalyst to biomass mass ratio 0.12, W-catalyst to biomass mass ratio 0.03.

E.5.2 Literature

We have previously (Chapter 3) extensively evaluated the glycol yields, on hydrogenolysis intake, of the relevant studies[64],[75],[91],[103],[104] and reported these data in Appendix A. Here we focus on the process based glycol yields, i.e. expressed on biomass intake the (pretreatment) process. Unfortunately, only the studies by Fabičovicová et al.[103] and Pang et al.[75] provide enough data to calculate these yields.

Table E.9: Hydrogenolysis conditions

Study	This work	Pang et al.[75]	Fabičovicová et al.[103]
Feed	(Pretreated)-Poplar	(Pretreated)-Corn Stalk	(Pretreated)-Barley Straw
Particle size (mm)	1-2	<0.25	0.2-0.4
Catalyst	SPT + Raney Ni	2% Ni-W_2C	Ru-W/AC
Catalyst to biomass ratio (w/w)	0.03 (SPT) + 0.12 (Raney Ni)	0.3	0.1
Temperature (°C)	245	245	220
Residence time (h)	1	2.5	3
H_2 Pressure (bar)	60 initial	60 initial	65 at reaction conditions
Biomass Loading (wt.%)	5	1	4.8

E.5.2.1 Barley straw

Fabičovicová et al.[103] studied the hydrogenolysis of (organosolv pretreated) barley straw, see Table E.9 for the hydrogenolysis conditions. The pretreatment conditions and solid residue yield are document in Table E.10.

These pretreatments altered the composition of the barley straw, see Table E.11. Entry 1 is the untreated feedstock.

The reported glycol yields were expressed on holocellulose basis (C%), i.e. *"Yield = carbon in product / carbon in hemicellulose+cellulose at start x 100%"*, which can be expressed as equation E.12, in which $f_{Carbon}^{Product}$ is the carbon fraction of the product, e.g. EG or PG, $f_{Carbon}^{Holocellulose}$ is the carbon fraction of the holocellulose and $f_{Holocellulose}$ the holocellulose fraction of the biomass.

*Table E.10: Pretreatment conditions and solid residue yield in the study by Fabičovicová et al.[103] Reported as table 1 in their work. *Untreated barley straw, nm = not measured*

Entry	EtOH:H_2O (w:w)	t (min)	T (°C)	Solid residue yield (wt.%)
1*	-	-	-	-
2	0:100	150	170	57.6
3	20:80	150	170	55.8
4	50:50	150	170	68.3
5	80:20	150	170	74.8
6	100:0	150	170	78.9
7	50:50	60	170	76
8	50:50	60	185	65.6
9	50:50	60	200	57.6
10	50:50	60	220	43.5
11	50:50	240	170	58.4

$$Y_{Product}\ (C\%) = Y_{Product}\ (wt.\%) \times \frac{f_{Carbon}^{Product}}{f_{Carbon}^{Holocellulose} \times f_{Holocellulose}} \tag{E.12}$$

Which can be rewritten to equation E.13.

$$Y_{Product}\ (wt.\%) = Y_{Product}\ (C\%) \times \frac{f_{Carbon}^{Holocellulose} \times f_{Holocellulose}}{f_{Carbon}^{Product}} \tag{E.13}$$

The fraction of carbon introduced by the feed can be calculated from the hemicellulose + cellulose fractions of the feed ($f_{Carbon}^{Holocellulose} \times f_{Holocellulose}$) and their respective carbon fractions (0.44 for glucan, 0.45 for xylan). The carbon fractions for the products are 0.39 (EG) and 0.47 (PG) respectively. Multiplying the hydrogenolysis yields, equation E.13, with the pretreatment yield, see Table E.10, results in the process based yield on biomass intake, see Figure E.10. The maximum glycol yields on process basis in the study by Fabičovicová et al.[103], 18 wt.% EG and 5 wt.% PG entry 4 in Figure E.10, are similar as the yields obtained in this work, 14-16 wt.% EG and 3-4 wt.% PG.

*Table E.11: (Pretreated) barley straw composition in wt.% in the study by Fabičovicová et al.[103] Reported as table 1 in their work. *Untreated barley straw, nm = not measured*

Entry	Lignin	Hemicellulose	Cellulose	Extractives	Ash	Sum
1*	19.6	20.8	40.7	1.8	2.1	85
2	29.1	4.6	55.2	–	nm	88.9
3	19.6	7.7	58.5	–	nm	85.8
4	13.9	19.5	47.7	–	0.8	81.9
5	12.3	22.5	45.4	–	nm	80.2
6	21.6	24.3	36.7	–	nm	82.6
7	18.5	19.5	41.5	–	0.6	80.1
8	16.1	19.6	49.2	–	0.6	85.5
9	13.2	14	57.5	–	0.5	85.2
10	10.4	5.7	65.3	–	nm	81.4
11	6.8	16	52.6	–	nm	75.4

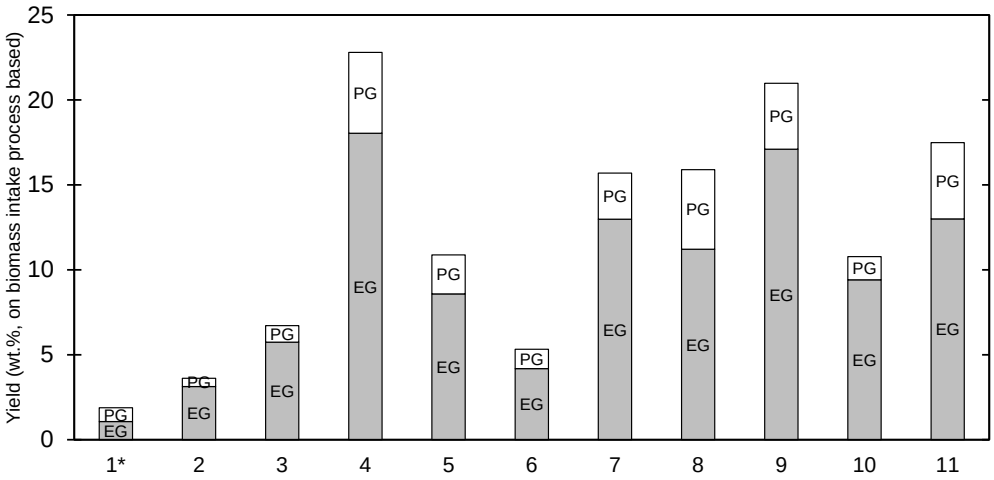

*Figure E.10: EG and PG yield on biomass intake on process basis for the substrates reported in Table S11 and their respective pretreatments, Table E.11, for the study by Fabičovicová et al.[103] The EG and PG yields expressed on holocellulose basis (C%) were originally reported by Fabičovicová et al.[103] in figure 3 in their work and reported in table form in the supporting information of our previous work (Chapter 3)[66].*Untreated feedstock*

E.5.2.2 Corn stalk

Pang et al.[75] performed the hydrogenolysis of (pretreated) corn stalk, see Table E.9 for the hydrogenolysis conditions. A wide variety of pretreatment was applied (A-I), which resulted in corresponding solid residue, see Table E.12.

*Table E.12: (pretreated) corn stalk composition in the study by Pang et al.[75] Reported as Table 2 in their work. *Untreated corn stalk.*

sample no.	soluble (%)	hemicellulose (%)	cellulose (%)	lignin (%)	ash (%)
A	6.1	14.8	72.4	6.2	0.5
B	9.6	7.6	67.7	13.4	1.7
C	4.8	17.2	69.1	8.4	0.5
D	1.5	20.2	63.2	13.4	1.6
E	2.1	18.5	71.3	7.6	0.6
F	1.7	22.1	56.7	18.5	1
G	0.2	20.5	54.5	23.4	1.5
H	0.2	18.6	57.3	22.3	1.7
I	6	10.5	49	32.5	2.1
J*	33.1	15.1	38	12.9	1

Unfortunately the pretreatment solid residue yields were not reported, but the delignification was reported from which the solid residue yield can be calculated. Delignification was defined according to equation E.14, in which $f_{Lignin}^{Raw\ Feed}$ is the lignin fraction of the untreated feed, $f_{Lignin}^{Solid\ residue}$ is the lignin fraction of the pretreated solid residue and Y_{PT} the pretreatment solid residue yield. According to this equation we calculated the pretreatment yield, see Table E.13.

$$\text{Delignification (\%)} = \left(\frac{f_{Raw\ Feed}^{Lignin} - f_{Solid\ Residue}^{Lignin} \times Y_{PT}/100}{f_{Lignin}^{Raw\ Feed}} \times 100 \right) \qquad \text{(E.14)}$$

Unfortunately information on the carbon content of the feed is lacking, thus it is not possible to convert the carbon based glycol yields to mass based yields. Nevertheless, multiplying the pretreatment yield (wt.%) with the glycol yield (C%) gives an indicative process based yield. The glycol yields were derived from *figure 5* in their work[75] and previously reported in table form in the supplementary information of our previous work[66].

*Table E.13: Delignification of pretreatments applied in the study by Pang et al.[75]. *Calculated by us.*

sample no.	Delignification (%)	PT yield (wt.%)*
A	6.1	52.2
B	9.6	45.3
C	4.8	42.4
D	1.5	54.7
E	2.1	56
F	1.7	54.3
G	0.2	55.7
H	0.2	56.2
I	6	39.7
J*	33.1	-

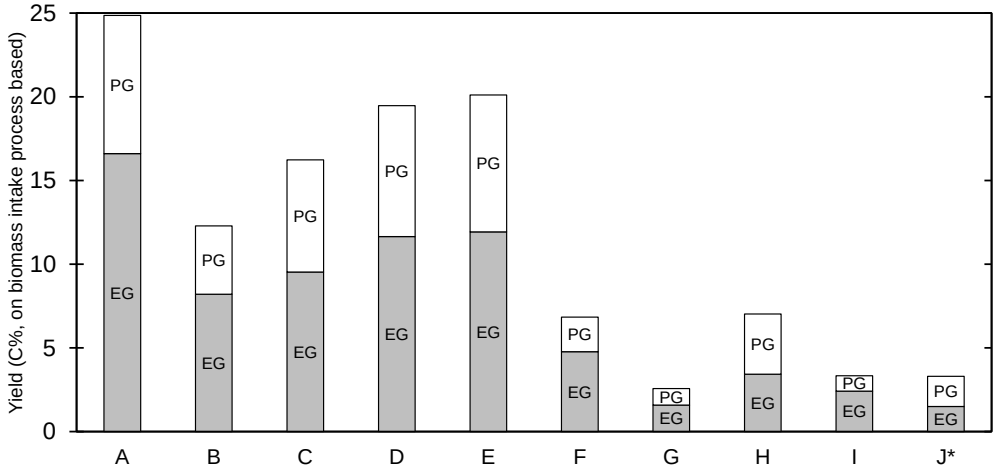

*Figure E.11: EG and PG yield on biomass intake on process basis for the substrates reported in Table E.12 for the study by Pang et al.[75] The EG and PG yields expressed on biomass basis (C%) were originally reported by Pang et al.[75] in figure 5 in their work and reported in table form in Appendix A.*Untreated feedstock*

The calculated glycol yields are shown in Figure E.11 and for the best case, A, a slightly higher than the yield obtained in this work, namely 17 wt.% EG and 8 wt.% PG compared to 14-16 wt.% EG and 3-4 wt.% PG in this work.

Appendix F

F.1 Experimental approach

The compositional characterisation of biomass is performed by a destructive procedure, i.e. the solid residue is consumed by the analytical procedure. We therefore ran an additional series of experiments in parralel, i.e. duplicates, to produce solid residue that can be sacrificied for analysis. Figure F.1 conceptually displays the experimental approach for a 3 stage countercurrent extraction.

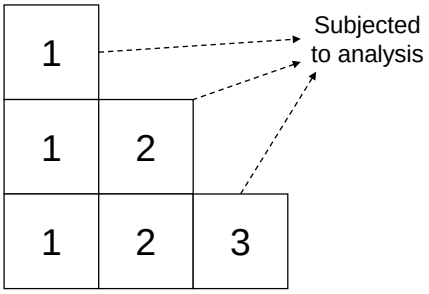

Figure F.1: Experimental approach

F.2 Reproducibility

Biomass pretreatment experiments are labour-intensive. Hence, we checked the experimental reproducibility once by running a single-stage experiment threefold. The experimental result of these three experiments is documented in Table F.1. The reproducibility of all key parameters is satisfactory, for example, the relative standard deviation is <1% for the lignin concentration of the spent solvent (58 $\pm$ 0.5 g_{Lignin} / $kg_{Solvent}$).

*Table F.1: Reproducibility of experiments, experimental conditions: 180° C, 60 minutes, 20 wt.% biomass loading, solvent composition; 70 wt.% acetic acid + 30 wt.% water. *Before washing, **Error reported as standard deviation.*

n	1	2	3	Average**
Operational outcome				
Lignin concentration spent solvent (g_{Lignin} / $kg_{Solvent}$)	57	58	58	58 $\pm$ 0
pH_{After} (-)	1.6	1.6	1.6	1.6$\pm$0.0
Solvent retention (g/g)	1.2	1.9	1.8	1.6$\pm$0.3
D-ratio (-)	1	1	1.1	1.0$\pm$0.0
*Solid residue**				
Yield (wt.%)	61	63	63	62 $\pm$ 1
Lignin content (wt.%)	10	14	15	13 $\pm$ 2
Washed solid residue				
Yield (wt.%)	52	50	51	51 $\pm$ 1
Lignin content (wt.%)	3.7	3.4	4.4	3.8 $\pm$ 0.4
Hexose Retention (wt.%)	100	95	96	97 $\pm$ 2
Pentose Retention (wt.%)	17	16	18	17 $\pm$ 1

F.3 Kinetics

F.3.1 Lignin removal

The removal of lignin compared to the lignin that was initially present in the biomass is defined as the lignin retention, see equation 2.3 in Chapter 2. Lignin retention is independent of the solid residue yield and therefore suitable to describe the delignification kinetics. Kinetics for the delignification in 70 wt.% acetic acid at 180°C were previously reported by Vazquez et al.[126]. Albeit, Eucalyptus globulus instead of poplar was used in their work, this data provide a good starting point. They fitted the lignin retention data by a modified first order reaction rate expression, see equation F.1, in which C_1 (0.684) was the fraction of reactive lignin at the start of the isothermal stage and C_2 (0.05) the fraction of recalcitrant lignin. As a result, the fraction of lignin that was dissolved during the heating trajectory (30 min) was equal to 1-(0.684+0.05) = 0.266.

$$L_R = 100 \times (1\text{-}C_1 \times e^{-kt} + C_2) \tag{F.1}$$

Due to the similarities in operating conditions, we fitted the same equation to our datasets. We have run several experiments with 10 and 20 wt.% biomass loading for varying time and characterised the solid residue to calculate the lignin retention, see Figure F.2.

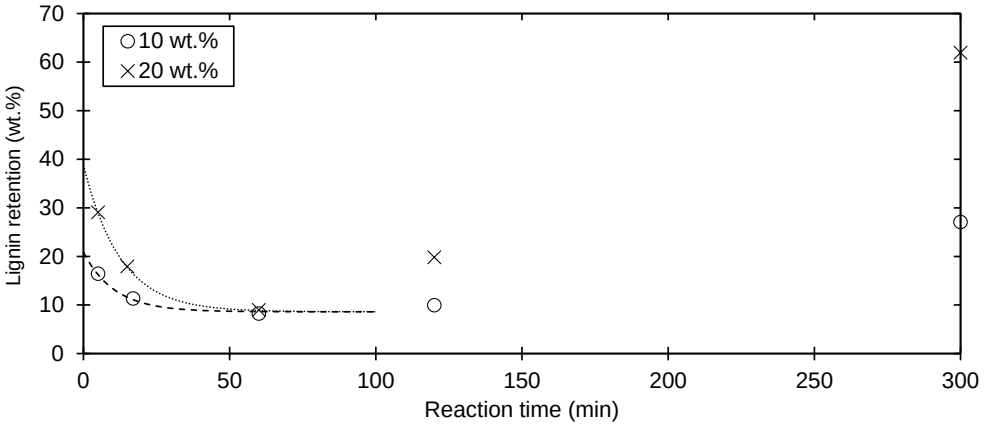

Figure F.2: Lignin retention for experiments performed for different residence times at 10 and 20 wt.% biomass loading

Both datasets appear to plateau around a lignin retention of ∼8.6 wt.%, after which the lignin retention again increases with time, which is likely caused by recondensation and precipitation of lignin and the conversion of saccharides to humins[126],[127]. We therefore set the C_2 coefficient to 0.086. The C_1 coefficients were found much lower than reported by Vazquez et al.[126] at 0.122 and 0.302 for 10 and 20 wt.% biomass loading respectively, see Table F.2. This means that a larger share of the lignin is dissolved during the heat-up trajectory in our work. The parameters that describe the delignification for 20 wt.% biomass loading were used in the model as the experiments reported in the main work (Chapter 8) were always 20 wt.%.)

Table F.2: Fit parameters for delignification in this work and by Vazquez et al.[126] for F.1

	C_1	C_2	k (min^{-1})
10 wt.% loading	0.122	0.086	0.094
20 wt.% loading	0.302	0.086	0.08
Vazquez et al.[126]	0.684	0.05	0.12

F.3.2 Solid residue yield

The solid residue yield is predominantly the result of the degradation of lignin, hemicellulose and the dissolution of extractives and ash. Cellulose is the most recalcitrant fraction present in biomass and does barely degrade under the conditions in this work. The solid residue yield, therefore, converges to a stable value, see Figure F.3.

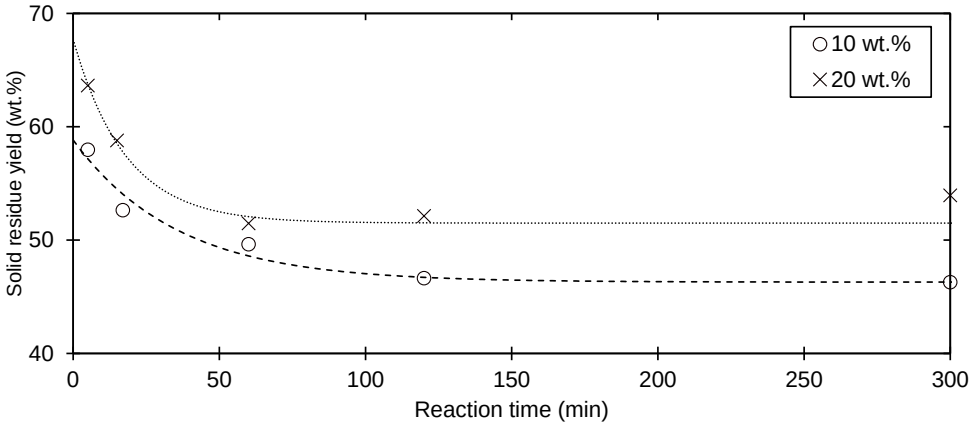

Figure F.3: Solid residue yield as function of reaction time

Biomass degradation is expected to follow a similar trend as the lignin retention as the solid residue yield depends on the lignin and sugar retention. We therefore opted to fit the trend seen in Figure F.3 by the same equation as was used for the lignin retention, see equation F.1. The fit parameters are documented in Table F.3.

Table F.3: Fit parameters for solid residue yield in this work

	C_1	C_2	k (min^{-1})
10 wt.% loading	0.125	0.463	0.0282
20 wt.% loading	0.162	0.515	0.0557

F.3.3 pH after the experiments

Both, delignification and the degradation of sugars was retarded when raising the biomass loading from 10 to 20 wt.%, see Figure F.2 and Figure F.3. These reactions are generally considered acid catalysed. The retarding effect could therefore be related to the concentration of acid in the solvent, which could be affected by the biomass loading as the basic ash present in biomass neutralises a part of the acid. Indeed, the measured pH after the experiment for experiments performed with 20 wt.% biomass loading was systematically higher than for experiments carried out with a biomass loading of 10 wt.%, see Figure F.4. Moreover, the pH at the start (fresh solvent) was 0.72 and thus substantially lower than the pH after the experiment for a biomass loading of 10 wt.%.

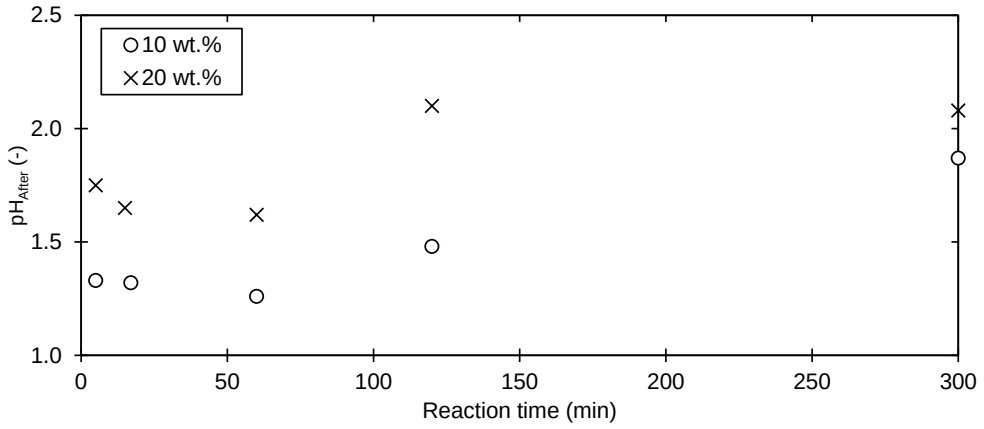

Figure F.4: pH of the spent solvent for experiments performed for different residence times at 10 and 20 wt.% biomass loading

F.4 2-Stage validation

In addition to the three-stage validation shown in the main work (Chapter 8), we performed a two stage validation of the model as well. The experimental and model outcomes generally match well, see Table F.2. For example, the lignin concentration in the spent solvent at the first stage was 61 g_{Lignin} / $kg_{Solvent}$ for the model and 65 g_{Lignin} / $kg_{Solvent}$ in the experiment and 13 g_{Lignin} / $kg_{Solvent}$ for the second stage for both the experiment and the model.

Table F.4: 2 stage, experimental and model output. Biomass loading = 20 wt.%, Solvent retention = 1.9, total residence time = 60 min. Lignin concentration in the solvent per stage, experimental outcome and model output.

	Stage 1		Stage 2	
	Experimental	Model	Experimental	Model
Lignin concentration spent solvent (g_{Lignin} / $kg_{Solvent}$)	65	61	13	13
Solid residue				
Lignin content (wt.%)	13.9	11.9	3.8	5.6
Yield (wt.%)	65	70	63	56
Washed solid residue				
Lignin content (wt.%)	5.1	3.7	1.5	3.5
Yield (wt.%)	55	55	42	52

References

[1] I. E. Agency, “The future of petrochemicals,” Report, 2018. [Online]. Available: https://www.iea.org/reports/the-future-of-petrochemicals.

[2] I. f. G. G. Reductions, “A life cycle quantification of carbon abatement solutions enabled by the chemical industry,” Report, 2009. [Online]. Available: https://cefic.org/app/uploads/2019/01/Greenhouse-gas-emission-reductions-enabled-products-from-Chem_industry_Ecofys_roadmap_Brochure-ICCA.pdf.

[3] R. Stefanini, G. Borghesi, A. Ronzano, *et al.*, “Plastic or glass: A new environmental assessment with a marine litter indicator for the comparison of pasteurized milk bottles,” *The International Journal of Life Cycle Assessment*, vol. 26, no. 4, pp. 767–784, 2020, ISSN: 0948-3349 1614-7502. DOI: 10.1007/s11367-020-01804-x.

[4] J.-P. Lange, “Towards circular carbo-chemicals – the metamorphosis of petrochemicals,” *Energy & Environmental Science*, 2021, ISSN: 1754-5692 1754-5706. DOI: 10.1039/d1ee00532d.

[5] D. A. Walker, “Biofuels, facts, fantasy, and feasibility,” *Journal of Applied Phycology*, vol. 21, no. 5, pp. 509–517, 2009, ISSN: 0921-8971 1573-5176. DOI: 10.1007/s10811-009-9446-5.

[6] R. E. Blankenship, D. M. Tiede, J. Barber, *et al.*, “Comparing photosynthetic and photovoltaic efficiencies and recognizing the potential for improvement,” *Science*, vol. 332, no. 6031, pp. 805–9, 2011, ISSN: 1095-9203 (Electronic) 0036-8075 (Linking). DOI: 10.1126/science.1200165.

[7] E. Williams, A. Sekar, S. Matteson, *et al.*, “Sun-to-wheels exergy efficiencies for bio-ethanol and photovoltaics,” *Environ Sci Technol*, vol. 49, no. 11, pp. 6394–401, 2015, ISSN: 1520-5851 (Electronic) 0013-936X (Linking). DOI: 10.1021/es504377b.

[8] B. H. Pro, R. Hammerschlag, and P. Mazza, “Energy and land use impacts of sustainable transportation scenarios,” *Journal of Cleaner Production*, vol. 13, no. 13-14, pp. 1309–1319, 2005, ISSN: 09596526. DOI: 10.1016/j.jclepro.2005.05.005.

[9] R. Geyer, D. Stoms, and J. Kallaos, “Spatially-explicit life cycle assessment of sun-to-wheels transportation pathways in the u.s,” *Environ Sci Technol*, vol. 47, no. 2, pp. 1170–6, 2013, ISSN: 1520-5851 (Electronic) 0013-936X (Linking). DOI: 10.1021/es302959h.

[10] C. W. Lewis, “Biomass through the ages,” *Biomass*, vol. 1, no. 1, pp. 5–15, 1981, ISSN: 01444565. DOI: 10.1016/0144-4565(81)90011-1.

[11] H. J. Brownlee and C. S. Miner, “Industrial development of furfural,” *Industrial & Engineering Chemistry*, vol. 40, no. 2, pp. 201–204, 1948, ISSN: 0019-7866 1541-5724. DOI: 10.1021/ie50458a005.

[12] W. B. Association, “Global bioenergy statistics 2020,” Report, 2020. [Online]. Available: http://www.worldbioenergy.org/uploads/201210%20WBA%20GBS%202020.pdf.

[13] FAO, “Forest products yearbook,” Report ISSN 2664-7443, 2019. [Online]. Available: https://www.fao.org/3/ca5703m/CA5703M.pdf.

[14] R. Slade, A. Bauen, and R. Gross, “Global bioenergy resources,” *Nature Climate Change*, vol. 4, no. 2, pp. 99–105, 2014, ISSN: 1758-678X 1758-6798. DOI: 10.1038/nclimate2097.

[15] C. O. Tuck, E. Perez, I. T. Horvath, *et al.*, “Valorization of biomass: Deriving more value from waste,” *Science*, vol. 337, no. 6095, pp. 695–9, 2012, ISSN: 1095-9203 (Electronic) 0036-8075 (Linking). DOI: 10.1126/science.1218930.

[16] A. J. J. Straathof and A. Bampouli, “Potential of commodity chemicals to become bio-based according to maximum yields and petrochemical prices,” *Biofuels, Bioproducts and Biorefining*, vol. 11, no. 5, pp. 798–810, 2017, ISSN: 1932-104X 1932-1031. DOI: 10.1002/bbb.1786.

[17] J.-P. Lange, “Lignocellulose conversion: An introduction to chemistry, process and economics,” *Biofuels, Bioproducts and Biorefining*, vol. 1, no. 1, pp. 39–48, 2007, ISSN: 1932104X 19321031. DOI: 10.1002/bbb.7.

[18] J.-P. Lange, “Performance metrics for sustainable catalysis in industry,” *Nature Catalysis*, vol. 4, no. 3, pp. 186–192, 2021, ISSN: 2520-1158. DOI: 10.1038/s41929-021-00585-2.

[19] H. Yue, Y. Zhao, X. Ma, *et al.*, “Ethylene glycol: Properties, synthesis, and applications,” *Chem Soc Rev*, vol. 41, no. 11, pp. 4218–44, 2012, ISSN: 1460-4744 (Electronic) 0306-0012 (Linking). DOI: 10.1039/c2cs15359a.

[20] H. (UPM-Kymmene Corporation, *Upm invests in next generation biochemicals to drive a switch from fossil raw materials to sustainable solutions*, Type, 30-1-2020. [Online]. Available: https://www.upm.com/about-us/for-media/releases/2020/01/upm-invests-in-next-generation-biochemicals-to-drive-a-switch-from-fossil-raw-materials-to-sustainable-solutions/.

[21] K. Loos, R. Zhang, I. Pereira, *et al.*, “A perspective on pef synthesis, properties, and end-life,” *Front Chem*, vol. 8, p. 585, 2020, ISSN: 2296-2646 (Print) 2296-2646 (Linking). DOI: 10.3389/fchem.2020.00585.

[22] A. C. O’Sullivan, “Cellulose: The structure slowly unravels,” *Cellulose*, vol. 4, no. 3, pp. 173–207, 1997, ISSN: 09690239. DOI: 10.1023/a:1018431705579.

[23] B. C. Saha, “Hemicellulose bioconversion,” *J Ind Microbiol Biotechnol*, vol. 30, no. 5, pp. 279–91, 2003, ISSN: 1367-5435 (Print) 1367-5435 (Linking). DOI: 10.1007/s10295-003-0049-x.

[24] A. K. Sangha, B. H. Davison, R. F. Standaert, *et al.*, "Chemical factors that control lignin polymerization," *J Phys Chem B*, vol. 118, no. 1, pp. 164–70, 2014, ISSN: 1520-5207 (Electronic) 1520-5207 (Linking). DOI: 10.1021/jp411998t.

[25] R. Vanholme, B. Demedts, K. Morreel, *et al.*, "Lignin biosynthesis and structure," *Plant Physiol*, vol. 153, no. 3, pp. 895–905, 2010, ISSN: 1532-2548 (Electronic) 0032-0889 (Linking). DOI: 10.1104/pp.110.155119.

[26] M. M. Campbell and R. R. Sederoff, "Variation in lignin content and composition (mechanisms of control and implications for the genetic improvement of plants)," *Plant Physiol*, vol. 110, no. 1, pp. 3–13, 1996, ISSN: 1532-2548 (Electronic) 0032-0889 (Linking). DOI: 10.1104/pp.110.1.3.

[27] H. H. Nimz, U. Schmitt, E. Schwab, *et al.*, "Wood," *Ullmann's Encyclopedia of Industrial Chemistry*, vol. 39, 2000. DOI: 10.1002/14356007.a28_305.

[28] E. Epstein, "The anomaly of silicon in plant biology," *Proc Natl Acad Sci U S A*, vol. 91, no. 1, pp. 11–7, 1994, ISSN: 0027-8424 (Print) 0027-8424 (Linking). DOI: 10.1073/pnas.91.1.11.

[29] H. A. Currie and C. C. Perry, "Silica in plants: Biological, biochemical and chemical studies," *Ann Bot*, vol. 100, no. 7, pp. 1383–9, 2007, ISSN: 1095-8290 (Electronic) 0305-7364 (Linking). DOI: 10.1093/aob/mcm247.

[30] A. V. Barker and D. J. Pilbeam, *Handbook of Plant Nutrition*. 2015, ISBN: 9781439881989. DOI: 10.1201/b18458.

[31] J. P. Lange, "Renewable feedstocks: The problem of catalyst deactivation and its mitigation," *Angew Chem Int Ed Engl*, vol. 54, no. 45, pp. 13 186–97, 2015, ISSN: 1521-3773 (Electronic) 1433-7851 (Linking). DOI: 10.1002/anie.201503595.

[32] S. Rebsdat and D. Mayer, "Ethylene glycol," *Ullman's Encyclopedia of Industrial Chemistry*, 2000. DOI: 10.1002/14356007.a10_101.

[33] J. H. Verkerk and Maarten, *15 Shell OMEGA only monoethylene glycol advanced process* (Process Intensification). 2020, pp. 166–175, ISBN: 9783110657340. DOI: 10.1515/9783110657357-015.

[34] H. Song, R. Jin, M. Kang, *et al.*, "Progress in synthesis of ethylene glycol through c1 chemical industry routes," *Chinese Journal of Catalysis*, vol. 34, no. 6, pp. 1035–1050, 2013, ISSN: 18722067. DOI: 10.1016/s1872-2067(12)60529-4.

[35] C. Qiu, *China meg demand stable; oversupply to worsen on new capacities*, Type, 2020. [Online]. Available: https://www.icis.com/explore/resources/news/2020/06/29/10524157/china-meg-demand-stable-oversupply-to-worsen-on-new-capacities.

[36] K. Göransson, U. Söderlind, J. He, *et al.*, "Review of syngas production via biomass dfbgs," *Renewable and Sustainable Energy Reviews*, vol. 15, no. 1, pp. 482–492, 2011, ISSN: 13640321. DOI: 10.1016/j.rser.2010.09.032.

[37] F. W. Bai, W. A. Anderson, and M. Moo-Young, "Ethanol fermentation technologies from sugar and starch feedstocks," *Biotechnol Adv*, vol. 26, no. 1, pp. 89–105, 2008, ISSN: 0734-9750 (Print) 0734-9750 (Linking). DOI: 10.1016/j.biotechadv.2007.09.002.

[38] M. Zhang and Y. Yu, "Dehydration of ethanol to ethylene," *Industrial & Engineering Chemistry Research*, vol. 52, no. 28, pp. 9505–9514, 2013, ISSN: 0888-5885 1520-5045. DOI: 10.1021/ie401157c.

[39] I. G. Limited, *Product groups: Meg/deg/teg*, Type. [Online]. Available: https://www.indiaglycols.com/product_groups/monoethylene_glycol.htm.

[40] G. Zhao, M. Zheng, R. Sun, *et al.*, "Ethylene glycol production from glucose over w-ru catalysts: Maximizing yield by kinetic modeling and simulation," *AIChE Journal*, vol. 63, no. 6, pp. 2072–2080, 2017, ISSN: 00011541. DOI: 10.1002/aic.15589.

[41] P. Kostetskyy, M. W. Coile, J. M. Terrian, *et al.*, "Selective production of glycolaldehyde via hydrothermal pyrolysis of glucose: Experiments and microkinetic modeling," *Journal of Analytical and Applied Pyrolysis*, vol. 149, p. 104 846, 2020, ISSN: 01652370. DOI: 10.1016/j.jaap.2020.104846.

[42] M. Sasaki, K. Goto, K. Tajima, *et al.*, "Rapid and selective retro-aldol condensation of glucose to glycolaldehyde in supercritical water," *Green Chemistry*, vol. 4, no. 3, pp. 285–287, 2002, ISSN: 14639262 14639270. DOI: 10.1039/b203968k.

[43] P. A. Majerski, J. K. Piskorz, and D. S. A. Radlein, "Production of glycolaldehyde by hydrous thermolysis of sugars," WO2002040436A1, 2006.

[44] M. S. Holm, C. M. OSMUNDSEN, E. Taarning, *et al.*, "Process for the preparation of ethylene glycol from sugars," WO2017118686A1, 2017.

[45] D. Muthusamy, V. Q. Nguyen, and P. Huizenga, "Method for the production of glycols from a carbohydrate feed," WO2017070067A1, 2019.

[46] M. Zheng, J. Pang, A. Wang, *et al.*, "One-pot catalytic conversion of cellulose to ethylene glycol and other chemicals: From fundamental discovery to potential commercialization," *Chinese Journal of Catalysis*, vol. 35, no. 5, pp. 602–613, 2014, ISSN: 1872-2067. DOI: 10.1016/S1872-2067(14)60013-9.

[47] Y. Zhang, A. Wang, and T. Zhang, "A new 3d mesoporous carbon replicated from commercial silica as a catalyst support for direct conversion of cellulose into ethylene glycol," *Chem Commun (Camb)*, vol. 46, no. 6, pp. 862–4, 2010, ISSN: 1364-548X (Electronic) 1359-7345 (Linking). DOI: 10.1039/b919182h.

[48] N. Ji, M. Zheng, A. Wang, *et al.*, "Nickel-promoted tungsten carbide catalysts for cellulose conversion: Effect of preparation methods," *ChemSusChem*, vol. 5, no. 5, pp. 939–44, 2012, ISSN: 1864-564X (Electronic) 1864-5631 (Linking). DOI: 10.1002/cssc.201100575.

[49] J. C. Van Der Waal, P. Dekker, J. Singh, *et al.*, "Continuous or semi-continuous process for the preparation of ethylene glycol and catalyst system for use therein," WO2019175362A1, 2019.

[50] J. Liu; H. Qi; H. Ren; *et al.*, "Methods for preparing diol," WO2016045583A1, 2019.

[51] T. Zhang; A. Wang; M. Zheng; *et al.*, "Continuous catalytic generation of polyols from cellulose," WO2013/015997A2, 2013.

[52] J. Q. Chen; T. N. Kalnes; and J. A. Kocal; "Generation of polyols from saccharides," WO2013015955A2, 2012.

[53] Avantium, *Avantium advances its plant based meg technology with the opening of its demonstration plant final*, Type, 2019. [Online]. Available: https://www.avantium.com/press-releases/avantium-advances-its-plant-based-meg-technology-with-the-opening-of-its-demonstration-plant/.

[54] J. C. V. D. Waal, A. (N.) ; G. Johannes, A. (N.) ; P. Maria Gruter, *et al.*, "Process for preparing ethylene glycol from a carbohydrate source," WO2016114660A1, 2019.

[55] UPM, *The construction of upm's innovative biochemicals facility starts in germany*, Type, 2020. [Online]. Available: https://www.upm.com/about-us/for-media/releases/2020/10/the-construction-of-upms-innovative-biochemicals-facility-starts-in-germany/.

[56] S. Mannonen, "Wood-based biorefineries pave the way to successful bioeconomy," Report, 2018. [Online]. Available: https://www.fao.org/forestry/47194-096cb11406eb00e44a2712a059f89ee49.pdf.

[57] UPMBIOCHEMICALS, *Building a state-of-the-art biorefinery in leuna*, Type, 2021. [Online]. Available: https://www.upmbiochemicals.com/.

[58] UPMBIOCHEMICALS, *Building the future of the biochemicals industry*, Type, 2021. [Online]. Available: https://www.upmbiochemicals.com/biorefinery/?_gl=1*1tbfhjd*_ga*MTM3ODMyNjI1My4xNjI2OTU2OTU4*_ga_HKS85BN03K*MTYyNjk1Njk1OC4xLjEuMTYyNjk1OTU0MC4w.

[59] J. Tamper, S. Turunen, V. Nissinen, *et al.*, "Production of mono-ethylene glycol," WO2021144499A1, 2021.

[60] Y. Yuan; "Method for refining non-petroleum-based ethylene glycol," WO2020048444A1, 2021.

[61] T. C.-C. Company, *Coca-cola, changchun meihe and upm cooperate to commercialize next-generation biomaterials press release*, Type, 2021. [Online]. Available: https://www.coca-colacompany.com/press-releases/coca-cola-changchun-meihe-and-upm-cooperate-to-commercialize-next-generation-biomaterials.

[62] H. Topsoe, *Braskem and haldor topsoe start up demo unit for developing renewable meg*, Type, 2019. [Online]. Available: https://blog.topsoe.com/braskem-and-haldor-topsoe-start-up-demo-unit-for-developing-renewable-meg.

[63] M. B. Larsen, C. M. OSMUNDSEN, and E. Taarning, "Thermolytic fragmentation of sugars," WO2017216311A1, 2017.

[64] C. Li, M. Zheng, A. Wang, *et al.*, "One-pot catalytic hydrocracking of raw woody biomass into chemicals over supported carbide catalysts: Simultaneous conversion of cellulose, hemicellulose and lignin," *Energy Environ. Sci.*, vol. 5, no. 4, pp. 6383–6390, 2012, ISSN: 1754-5692 1754-5706. DOI: 10.1039/c1ee02684d.

[65] M. Zheng, J. Pang, R. Sun, *et al.*, "Selectivity control for cellulose to diols: Dancing on eggs," *ACS Catalysis*, vol. 7, no. 3, pp. 1939–1954, 2017, ISSN: 2155-5435 2155-5435. DOI: 10.1021/acscatal.6b03469.

[66] T. D. J. te Molder, S. R. A. Kersten, J. P. Lange, *et al.*, "Ethylene glycol from lignocellulosic biomass: Impact of lignin on catalytic hydrogenolysis," *Industrial & Engineering Chemistry Research*, vol. 60, no. 19, pp. 7043–7049, 2021, ISSN: 0888-5885 1520-5045. DOI: 10.1021/acs.iecr.1c01063.

[67] G. Zhao, M. Zheng, A. Wang, *et al.*, "Catalytic conversion of cellulose to ethylene glycol over tungsten phosphide catalysts," *Chinese Journal of Catalysis*, vol. 31, no. 8, pp. 928–932, 2010, ISSN: 18722067. DOI: 10.1016/s1872-2067(10)60104-0.

[68] M. S. Hamdy, M. A. Eissa, and S. M. A. S. Keshk, "New catalyst with multiple active sites for selective hydrogenolysis of cellulose to ethylene glycol," *Green Chem.*, vol. 19, no. 21, pp. 5144–5151, 2017, ISSN: 1463-9262 1463-9270. DOI: 10.1039/c7gc02122d.

[69] S. J. You, I. G. Baek, and E. D. Park, "Hydrogenolysis of cellulose into polyols over ni/w/sio2 catalysts," *Applied Catalysis A: General*, vol. 466, pp. 161–168, 2013, ISSN: 0926860X. DOI: 10.1016/j.apcata.2013.06.053.

[70] Z. Tai, J. Zhang, A. Wang, *et al.*, "Catalytic conversion of cellulose to ethylene glycol over a low-cost binary catalyst of raney ni and tungstic acid," *ChemSusChem*, vol. 6, no. 4, pp. 652–8, 2013, ISSN: 1864-564X (Electronic) 1864-5631 (Linking). DOI: 10.1002/cssc.201200842.

[71] Z. Tai, J. Zhang, A. Wang, *et al.*, "Temperature-controlled phase-transfer catalysis for ethylene glycol production from cellulose," *Chem Commun (Camb)*, vol. 48, no. 56, pp. 7052–4, 2012, ISSN: 1364-548X (Electronic) 1359-7345 (Linking). DOI: 10.1039/c2cc32305b.

[72] G. Xu, A. Wang, J. Pang, *et al.*, "Remarkable effect of extremely dilute h2so4 on the cellulose conversion to ethylene glycol," *Applied Catalysis A: General*, vol. 502, pp. 65–70, 2015, ISSN: 0926860X. DOI: 10.1016/j.apcata.2015.05.038.

[73] Y. Liu, C. Luo, and H. Liu, "Tungsten trioxide promoted selective conversion of cellulose into propylene glycol and ethylene glycol on a ruthenium catalyst," *Angew Chem Int Ed Engl*, vol. 51, no. 13, pp. 3249–53, 2012, ISSN: 1521-3773 (Electronic) 1433-7851 (Linking). DOI: 10.1002/anie.201200351.

[74] R. Ooms, M. Dusselier, J. A. Geboers, *et al.*, "Conversion of sugars to ethylene glycol with nickel tungsten carbide in a fed-batch reactor: High productivity and reaction network elucidation," *Green Chem.*, vol. 16, no. 2, pp. 695–707, 2014, ISSN: 1463-9262 1463-9270. DOI: 10.1039/c3gc41431k.

[75] J. Pang, M. Zheng, A. Wang, *et al.*, "Catalytic hydrogenation of corn stalk to ethylene glycol and 1,2-propylene glycol," *Industrial & Engineering Chemistry Research*, vol. 50, no. 11, pp. 6601–6608, 2011, ISSN: 0888-5885 1520-5045. DOI: 10.1021/ie102505y.

[76] A. Wang and T. Zhang, "One-pot conversion of cellulose to ethylene glycol with multifunctional tungsten-based catalysts," *Acc Chem Res*, vol. 46, no. 7, pp. 1377–86, 2013, ISSN: 1520-4898 (Electronic) 0001-4842 (Linking). DOI: 10.1021/ar3002156.

[77] E. Crezee, "Three-phase hydrogenation of ?-glucose over a carbon supported ruthenium catalyst—mass transfer and kinetics," *Applied Catalysis A: General*, vol. 251, no. 1, pp. 1–17, 2003, ISSN: 0926860X. DOI: 10.1016/s0926-860x(03)00587-8.

[78] N. Déchamp, A. Gamez, A. Perrard, *et al.*, "Kinetics of glucose hydrogenation in a trickle-bed reactor," *Catalysis Today*, vol. 24, no. 1-2, pp. 29–34, 1995, ISSN: 09205861. DOI: 10.1016/0920-5861(95)00019-c.

[79] V. A. Sifontes Herrera, O. Oladele, K. Kordás, *et al.*, "Sugar hydrogenation over a ru/c catalyst," *Journal of Chemical Technology & Biotechnology*, vol. 86, no. 5, pp. 658–668, 2011, ISSN: 02682575. DOI: 10.1002/jctb.2565.

[80] S. Tolborg, S. Meier, S. Saravanamurugan, *et al.*, "Shape-selective valorization of biomass-derived glycolaldehyde using tin-containing zeolites," *ChemSusChem*, vol. 9, no. 21, pp. 3054–3061, 2016, ISSN: 1864-564X (Electronic) 1864-5631 (Linking). DOI: 10.1002/cssc.201600757.

[81] L. R. Barsøe, S. Saravanamurugan, E. Taarning, *et al.*, "Heterogeneous base-catalyzed conversion of glycolaldehyde to aldotetroses: Mechanistic and kinetic insight," *ChemCatChem*, vol. 13, no. 24, pp. 5141–5147, 2021, ISSN: 1867-3880 1867-3899. DOI: 10.1002/cctc.202101347.

[82] A. S. Serianni, J. Pierce, S. G. Huang, *et al.*, "Anomerization of furanose sugars: Kinetics of ring-opening reactions by proton and carbon-13 saturation-transfer nmr spectroscopy," *Journal of the American Chemical Society*, vol. 104, no. 15, pp. 4037–4044, 2002, ISSN: 0002-7863 1520-5126. DOI: 10.1021/ja00379a001.

[83] D. J. M. De Vlieger, P. Huizenga, E. Van Der Heide, *et al.*, "Pocess for the hydrogenation of glycolaldehyde," WO2017137355, 2017.

[84] J. Y. Zhang, B. L. Hou, A. Q. Wang, *et al.*, "Kinetic study of the competitive hydrogenation of glycolaldehyde and glucose on ru/c with or without amt," *Aiche Journal*, vol. 61, no. 1, pp. 224–238, 2015, ISSN: 0001-1541. DOI: 10.1002/aic.14639.

[85] P. Dekker; J. Singh; J. C. V. D. Waal; *et al.*, "Process for the conversion of one or more polyols," WO2020182456A1, 2020.

[86] D. Muthusamy and V. Nguyen, "Magnetic separation and recycle of catalyst components in a bio-mass to glycols process," WO2018044971A1, 2018.

[87] I. van Zandvoort, Y. Wang, C. B. Rasrendra, *et al.*, "Formation, molecular structure, and morphology of humins in biomass conversion: Influence of feedstock and processing conditions," *ChemSusChem*, vol. 6, no. 9, pp. 1745–58, 2013, ISSN: 1864-564X (Electronic) 1864-5631 (Linking). DOI: 10.1002/cssc.201300332.

[88] R. Zhang, A. Eronen, X. Du, *et al.*, "A catalytic approach via retro-aldol condensation of glucose to furanic compounds," *Green Chemistry*, vol. 23, no. 15, pp. 5481–5486, 2021, ISSN: 1463-9262 1463-9270. DOI: 10.1039/d1gc01429c.

[89] J.-P. Lange, "Fuels and chemicals manufacturing," *Cattech*, vol. 5, no. 2, pp. 82–95, 2001, ISSN: 13846566. DOI: 10.1023/a:1011944622328.

[90] J. Pang, M. Zheng, R. Sun, *et al.*, "Catalytic conversion of cellulosic biomass to ethylene glycol: Effects of inorganic impurities in biomass," *Bioresour Technol*, vol. 175, pp. 424–9, 2015, ISSN: 1873-2976 (Electronic) 0960-8524 (Linking). DOI: 10.1016/j.biortech.2014.10.076.

[91] J. Pang, M. Zheng, A. Wang, *et al.*, "Catalytic conversion of concentrated miscanthus in water for ethylene glycol production," *AIChE Journal*, vol. 60, no. 6, pp. 2254–2262, 2014, ISSN: 00011541. DOI: 10.1002/aic.14406.

[92] S. Kumar, J.-P. Lange, G. Van Rossum, *et al.*, "Liquefaction of lignocellulose: Process parameter study to minimize heavy ends," *Industrial & Engineering Chemistry Research*, vol. 53, no. 29, pp. 11 668–11 676, 2014, ISSN: 0888-5885 1520-5045. DOI: 10.1021/ie501579v.

[93] S. R. G. Oudenhoven, R. J. M. Westerhof, and S. R. A. Kersten, "Fast pyrolysis of organic acid leached wood, straw, hay and bagasse: Improved oil and sugar yields," *Journal of Analytical and Applied Pyrolysis*, vol. 116, pp. 253–262, 2015, ISSN: 01652370. DOI: 10.1016/j.jaap.2015.09.003.

[94] A. Sluiter, R. Ruiz, C. Scarlata, *et al.*, "Determination of extractives in biomass," National Renewable Energy Laboratory (NREL), Report, 2008. [Online]. Available: https://www.nrel.gov/docs/gen/fy08/42619.pdf.

[95] A. Sluiter, B. Hames, R. Ruiz, *et al.*, "Determination of structural carbohydrates and lignin in biomass," National Renewable Energy Laboratory (NREL), Report, 2012. [Online]. Available: https://www.nrel.gov/docs/gen/fy13/42618.pdf.

[96] A. Sluiter, B. Hames, R. Ruiz, *et al.*, "Determination of ash in biomass," National Renewable Energy Laboratory (NREL), Report, 2008. [Online]. Available: https://www.nrel.gov/docs/gen/fy08/42622.pdf.

[97] A. M. Ruppert, K. Weinberg, and R. Palkovits, "Hydrogenolysis goes bio: From carbohydrates and sugar alcohols to platform chemicals," *Angew Chem Int Ed Engl*, vol. 51, no. 11, pp. 2564–601, 2012, ISSN: 1521-3773 (Electronic) 1433-7851 (Linking). DOI: 10.1002/anie.201105125.

[98] A. N. Marchesan, M. P. Oncken, R. Maciel Filho, *et al.*, "A roadmap for renewable c2–c3 glycols production: A process engineering approach," *Green Chemistry*, vol. 21, no. 19, pp. 5168–5194, 2019, ISSN: 1463-9262 1463-9270. DOI: 10.1039/c9gc02949d.

[99] N. Ji, T. Zhang, M. Zheng, *et al.*, "Direct catalytic conversion of cellulose into ethylene glycol using nickel-promoted tungsten carbide catalysts," *Angew Chem Int Ed Engl*, vol. 47, no. 44, pp. 8510–3, 2008, ISSN: 1521-3773 (Electronic) 1433-7851 (Linking). DOI: 10.1002/anie.200803233.

[100] M. Y. Zheng, A. Q. Wang, N. Ji, *et al.*, "Transition metal-tungsten bimetallic catalysts for the conversion of cellulose into ethylene glycol," *ChemSusChem*, vol. 3, no. 1, pp. 63–6, 2010, ISSN: 1864-564X (Electronic) 1864-5631 (Linking). DOI: 10.1002/cssc.200900197.

[101] N. Li, Z. Ji, L. Wei, *et al.*, "Effect of the surface acid sites of tungsten trioxide for highly selective hydrogenation of cellulose to ethylene glycol," *Bioresour Technol*, vol. 264, pp. 58–65, 2018, ISSN: 1873-2976 (Electronic) 0960-8524 (Linking). DOI: 10.1016/j.biortech.2018.05.026.

[102] Y. Liao, B. O. de Beeck, K. Thielemans, *et al.*, "The role of pretreatment in the catalytic valorization of cellulose," *Molecular Catalysis*, vol. 487, p. 110 883, 2020, ISSN: 24688231. DOI: 10.1016/j.mcat.2020.110883.

[103] K. Fabicovicova, M. Lucas, and P. Claus, "From barley straw to valuable polyols: A sustainable process using ethanol/water mixtures and hydrogenolysis over ruthenium-tungsten catalyst," *ChemSusChem*, vol. 9, no. 19, pp. 2804–2815, 2016, ISSN: 1864-564X (Electronic) 1864-5631 (Linking). DOI: 10.1002/cssc.201600695.

[104] L. Zhou, J. Pang, A. Wang, *et al.*, "Catalytic conversion of jerusalem artichoke stalk to ethylene glycol over a combined catalyst of wo3 and raney ni," *Chinese Journal of Catalysis*, vol. 34, no. 11, pp. 2041–2046, 2013, ISSN: 18722067. DOI: 10.1016/s1872-2067(12)60686-x.

[105] J.-P. Lange, "Catalysis for biorefineries – performance criteria for industrial operation," *Catalysis Science & Technology*, vol. 6, no. 13, pp. 4759–4767, 2016, ISSN: 2044-4753 2044-4761. DOI: 10.1039/c6cy00431h.

[106] S. V. Vassilev, D. Baxter, L. K. Andersen, *et al.*, "An overview of the organic and inorganic phase composition of biomass," *Fuel*, vol. 94, pp. 1–33, 2012, ISSN: 00162361. DOI: 10.1016/j.fuel.2011.09.030.

[107] J. N. Pattison and E. F. Degering, "Some factors influencing the activity of raney nickel catalyst. iii. the poisoning of raney nickel by halogen compounds1," *Journal of the American Chemical Society*, vol. 73, no. 2, pp. 611–613, 1951, ISSN: 0002-7863 1520-5126. DOI: 10.1021/ja01146a034.

[108] P. Ning, W. Xu, H. Cao, *et al.*, "Determination and modeling for the solubility of na2wo4·2h2o and na2moo4·2h2o in the (na++moo42-+wo42-+so42-+h2o) system," *The Journal of Chemical Thermodynamics*, vol. 98, pp. 165–172, 2016, ISSN: 00219614. DOI: 10.1016/j.jct.2016.01.015.

[109] I. L. Khodokovskiy and I. V. Mishin, "Solubility products of calcium molybdate and calcium tungstate; ratio of powellite to scheelite mineralization under hydrothermal conditions," *International Geology Review*, vol. 13, no. 5, pp. 760–768, 2009, ISSN: 0020-6814 1938-2839. DOI: 10.1080/00206817109475495.

[110] M. R. Atademir, J. A. Kitchener, and H. L. Shergold, "The surface chemistry and flotation of scheelite. i. solubility and surface characteristics of precipitated calcium tungstate," *Journal of Colloid and Interface Science*, vol. 71, no. 3, pp. 466–476, 1979, ISSN: 00219797. DOI: 10.1016/0021-9797(79)90321-7.

[111] T. D. J. Molder, S. R. A. Kersten, J.-P. Lange, *et al.*, "Cellulosic glycols: An integrated process concept for lignocellulose pretreatment and hydrogenolysis," *Biofuels, Bioproducts and Biorefining*, 2021, ISSN: 1932-104X 1932-1031. DOI: 10.1002/bbb.2269.

[112] D. Chen, K. Cen, F. Chen, *et al.*, "Are the typical organic components in biomass pyrolyzed bio-oil available for leaching of alkali and alkaline earth metallic species (aaems) from biomass?" *Fuel*, vol. 260, p. 116 347, 2020, ISSN: 00162361. DOI: 10.1016/j.fuel.2019.116347.

[113] A. Saltberg, H. Brelid, and H. Theliander, "Removal of metal ions from wood chips during acidic leaching 1: Comparison between scandinavian softwood, birch and eucalyptus," *Nordic Pulp & Paper Research Journal*, vol. 21, no. 4, pp. 507–512, 2006, ISSN: 2000-0669 0283-2631. DOI: 10.3183/npprj-2006-21-04-p507-512.

[114] X. Liu and X. T. Bi, "Removal of inorganic constituents from pine barks and switchgrass," *Fuel Processing Technology*, vol. 92, no. 7, pp. 1273–1279, 2011, ISSN: 03783820. DOI: 10.1016/j.fuproc.2011.01.016.

[115] S. R. G. Oudenhoven, A. G. J. van der Ham, H. van den Berg, *et al.*, "Using pyrolytic acid leaching as a pretreatment step in a biomass fast pyrolysis plant: Process design and economic evaluation," *Biomass and Bioenergy*, vol. 95, pp. 388–404, 2016, ISSN: 09619534. DOI: 10.1016/j.biombioe.2016.07.003.

[116] T. D. J. te Molder, S. R. A. Kersten, J.-P. Lange, *et al.*, "From woody biomass to ethylene glycol: Inorganics removal boosts the yield," *Industrial & Engineering Chemistry Research*, 2021, ISSN: 0888-5885 1520-5045. DOI: 10.1021/acs.iecr.1c02353.

[117] M. J. Hawkesford, "Plant responses to sulphur deficiency and the genetic manipulation of sulphate transporters to improve s-utilization efficiency," *Journal of Experimental Botany*, vol. 51, no. 342, pp. 131–138, 2000, ISSN: 1460-2431 0022-0957. DOI: 10.1093/jxb/51.342.131.

[118] A. A. Philippov, A. M. Chibiryaev, S. S. Yakushkin, *et al.*, "Poisoning titration of metal nickel-based catalysts – an efficient and convenient tool to quantify active sites in transfer hydrogenation," *Applied Catalysis A: General*, vol. 617, p. 118 115, 2021, ISSN: 0926860X. DOI: 10.1016/j.apcata.2021.118115.

[119] J. Wang, J. Gao, K. L. Brandt, *et al.*, "Energy consumption of two-stage fine grinding of douglas-fir wood," *Journal of Wood Science*, vol. 64, no. 4, pp. 338–346, 2018, ISSN: 1435-0211 1611-4663. DOI: 10.1007/s10086-018-1712-1.

[120] Z. Miao, T. E. Grift, A. C. Hansen, *et al.*, "Energy requirement for comminution of biomass in relation to particle physical properties," *Industrial Crops and Products*, vol. 33, no. 2, pp. 504–513, 2011, ISSN: 09266690. DOI: 10.1016/j.indcrop.2010.12.016.

[121] A. N. Bashkatov, E. A. Genina, Y. P. Sinichkin, *et al.*, "Glucose and mannitol diffusion in human dura mater," *Biophysical Journal*, vol. 85, no. 5, pp. 3310–3318, 2003, ISSN: 00063495. DOI: 10.1016/s0006-3495(03)74750-x.

[122] Z. Zhu, S. S. Toor, L. Rosendahl, *et al.*, "Influence of alkali catalyst on product yield and properties via hydrothermal liquefaction of barley straw," *Energy*, vol. 80, pp. 284–292, 2015, ISSN: 03605442. DOI: 10.1016/j.energy.2014.11.071.

[123] C. Cao, Z. Zhao, and X. Chen, "Selective precipitation of tungstate from molybdate-containing solution using divalent ions," *Hydrometallurgy*, vol. 110, no. 1-4, pp. 115–119, 2011, ISSN: 0304386X. DOI: 10.1016/j.hydromet.2011.09.006.

[124] J. Pang, A. Wang, M. Zheng, *et al.*, "Catalytic conversion of cellulose to hexitols with mesoporous carbon supported ni-based bimetallic catalysts," *Green Chemistry*, vol. 14, no. 3, p. 614, 2012, ISSN: 1463-9262 1463-9270. DOI: 10.1039/c2gc16364k.

[125] C. J. Biermann, *Handbook of Pulping and Papermaking (2nd Edition)*. Elsevier, ISBN: 978-0-12-097362-0. [Online]. Available: https://app.knovel.com/hotlink/toc/id:kpHPPE0001/handbook-pulping-papermaking/handbook-pulping-papermaking.

[126] G. Vazquez, G. Antorrena, and J. Gonzlez, "Kinetics of acid-catalysed delignification of eucalyptus globulus wood by acetic acid," *Wood Science and Technology*, vol. 29, no. 4, 1995, ISSN: 0043-7719 1432-5225. DOI: 10.1007/bf00202086.

[127] G. Vázquez, G. Antorrena, J. González, *et al.*, "Acetosolv pulping of pine wood. kinetic modelling of lignin solubilization and condensation," *Bioresource Technology*, vol. 59, no. 2-3, pp. 121–127, 1997, ISSN: 09608524. DOI: 10.1016/s0960-8524(96)00168-x.

[128] K. AZIZ SALMAN ; SARKANEN, "Organosolv pulping - a review," *TAPPI JOURNAL (VOL 72NRO 3, mar.1989)*, 1989.

[129] M. M. Al Omari, I. S. Rashid, N. A. Qinna, *et al.*, "Calcium carbonate," *Profiles Drug Subst Excip Relat Methodol*, vol. 41, pp. 31–132, 2016, ISSN: 1871-5125 (Print) 1871-5125 (Linking). DOI: 10.1016/bs.podrm.2015.11.003.

[130] W. J. J. Huijgen, J. H. Reith, and H. den Uil, "Pretreatment and fractionation of wheat straw by an acetone-based organosolv process," *Industrial & Engineering Chemistry Research*, vol. 49, no. 20, pp. 10 132–10 140, 2010, ISSN: 0888-5885 1520-5045. DOI: 10.1021/ie101247w.

[131] E. A. Gomaa, "Solubility and solvation parameters of calcium carbonate in mixed ethanol-water mixtures at 301.15 k," *Science and Technology*, vol. 2, no. 1, pp. 51–52, 2012, ISSN: 2163-2669. DOI: 10.5923/j.scit.20120201.10.

[132] J. C. Parajó, J. L. Alonso, and D. Vázquez, "On the behaviour of lignin and hemicelluloses during the acetosolv processing of wood," *Bioresource Technology*, vol. 46, no. 3, pp. 233–240, 1993, ISSN: 09608524. DOI: 10.1016/0960-8524(93)90126-v.

[133] H. L. Chum, D. K. Johnson, and S. K. Black, "Organosolv pretreatment for enzymic hydrolysis of poplars. 2. catalyst effects and the combined severity parameter," *Industrial & Engineering Chemistry Research*, vol. 29, no. 2, pp. 156–162, 1990, ISSN: 0888-5885 1520-5045. DOI: 10.1021/ie00098a003.

[134] J. Wildschut, A. T. Smit, J. H. Reith, *et al.*, "Ethanol-based organosolv fractionation of wheat straw for the production of lignin and enzymatically digestible cellulose," *Bioresour Technol*, vol. 135, pp. 58–66, 2013, ISSN: 1873-2976 (Electronic) 0960-8524 (Linking). DOI: 10.1016/j.biortech.2012.10.050.

[135] P. M. Pawar, S. Koutaniemi, M. Tenkanen, *et al.*, "Acetylation of woody lignocellulose: Significance and regulation," *Front Plant Sci*, vol. 4, p. 118, 2013, ISSN: 1664-462X (Print) 1664-462X (Linking). DOI: 10.3389/fpls.2013.00118.

[136] X. Chen, J. Shekiro, M. A. Franden, *et al.*, "The impacts of deacetylation prior to dilute acid pretreatment on the bioethanol process," *Biotechnol Biofuels*, vol. 5, p. 8, 2012, ISSN: 1754-6834 (Electronic) 1754-6834 (Linking). DOI: 10.1186/1754-6834-5-8.

[137] X. Hu, S. Wang, R. J. M. Westerhof, *et al.*, "Acid-catalyzed conversion of c6 sugar monomer/oligomers to levulinic acid in water, tetrahydrofuran and toluene: Importance of the solvent polarity," *Fuel*, vol. 141, pp. 56–63, 2015, ISSN: 00162361. DOI: 10.1016/j.fuel.2014.10.034.

[138] A. Smit and W. Huijgen, "Effective fractionation of lignocellulose in herbaceous biomass and hardwood using a mild acetone organosolv process," *Green Chemistry*, vol. 19, no. 22, pp. 5505–5514, 2017, ISSN: 1463-9262 1463-9270. DOI: 10.1039/c7gc02379k.

[139] P. Sävelin, "Digester developments," Valmet, Report, 2014. [Online]. Available: https://www.valmet.com/globalassets/media/downloads/white-papers/board-and-paper-making/wppb_dewateringlayout.pdf.

[140] A. Demirbas, "Higher heating values of lignin types from wood and non-wood lignocellulosic biomasses," *Energy Sources, Part A: Recovery, Utilization, and Environmental Effects*, vol. 39, no. 6, pp. 592–598, 2017, ISSN: 1556-7036 1556-7230. DOI: 10.1080/15567036.2016.1248798.

[141] L. J. Jonsson and C. Martin, "Pretreatment of lignocellulose: Formation of inhibitory by-products and strategies for minimizing their effects," *Bioresour Technol*, vol. 199, pp. 103–112, 2016, ISSN: 1873-2976 (Electronic) 0960-8524 (Linking). DOI: 10.1016/j.biortech.2015.10.009.

[142] J. Spaninks, *Design procedures for solid-liquid extractors and the effect of hydrodynamic instabilities on extractor performance*. Wageningen University & Research, 1979, ISBN: 90-220-0693-X.

[143] S. Laakso, *Modeling of chip bed packing in a continuous kraft cooking digester*. Teknillinen korkeakoulu, 2008, ISBN: 9512296780.

[144] M. Oliet, F. Rodríguez, A. Santos, *et al.*, "Organosolv delignification of eucalyptus globulus: kinetic study of autocatalyzed ethanol pulping," *Industrial & Engineering Chemistry Research*, vol. 39, no. 1, pp. 34–39, 2000, ISSN: 0888-5885 1520-5045. DOI: 10.1021/ie9905005.

[145] J. B. POWELL; and J. A. SMEGAL; "Process to produce biofuels from biomass," WO2012174088A1, 2012.

[146] A. Q. M. BOON; and J. B. POWELL, "Method of extending biomass conversion catalyst life," WO2017106228A1, 2017.

[147] T. J. Schwartz, R. L. Johnson, J. Cardenas, *et al.*, "Engineering catalyst microenvironments for metal-catalyzed hydrogenation of biologically derived platform chemicals," *Angew Chem Int Ed Engl*, vol. 53, no. 47, pp. 12 718–22, 2014, ISSN: 1521-3773 (Electronic) 1433-7851 (Linking). DOI: 10.1002/anie.201407615.

[148] J. Ftouni, H. C. Genuino, A. Munoz-Murillo, *et al.*, "Influence of sulfuric acid on the performance of ruthenium-based catalysts in the liquid-phase hydrogenation of levulinic acid to gamma-valerolactone," *ChemSusChem*, vol. 10, no. 14, pp. 2891–2896, 2017, ISSN: 1864-564X (Electronic) 1864-5631 (Linking). DOI: 10.1002/cssc.201700768.

[149] E. V. D. Heide; and P. Huizenga; "Process for the conversion of saccharide-containing feedstock," WO2016038071A1, 2016. DOI: WO2016038071A1.

[150] B. Mckay, G. J. Gruter, and M. Kersbulck, "Process for preparing alkylene glycol from a carbohydrate source comprising hemicellulose, cellulose and lignin," WO2021018560A1, 2021.

[151] Q. Xiang, Y. Y. Lee, P. O. Pettersson, *et al.*, "Heterogeneous aspects of acid hydrolysis of α-cellulose," pp. 505–514, 2003. DOI: 10.1007/978-1-4612-0057-4_42.

[152] M. Watanabe, Y. Aizawa, T. Iida, *et al.*, "Glucose reactions with acid and base catalysts in hot compressed water at 473 k," *Carbohydr Res*, vol. 340, no. 12, pp. 1925–30, 2005, ISSN: 0008-6215 (Print) 0008-6215 (Linking). DOI: 10.1016/j.carres.2005.06.017.

[153] J. W. van Put, "Crystallisation and processing of ammonium paratungstate (apt)," *International Journal of Refractory Metals and Hard Materials*, vol. 13, no. 1-3, pp. 61–76, 1995, ISSN: 02634368. DOI: 10.1016/0263-4368(94)00003-4.

[154] S. Chiesa and E. Gnansounou, "Protein extraction from biomass in a bioethanol refinery–possible dietary applications: Use as animal feed and potential extension to human consumption," *Bioresour Technol*, vol. 102, no. 2, pp. 427–36, 2011, ISSN: 1873-2976 (Electronic) 0960-8524 (Linking). DOI: 10.1016/j.biortech.2010.07.125.

[155] Z. Sun, Z.-H. Zhang, T.-Q. Yuan, *et al.*, “Raney ni as a versatile catalyst for biomass conversion,” *ACS Catalysis*, vol. 11, no. 16, pp. 10 508–10 536, 2021, ISSN: 2155-5435 2155-5435. DOI: 10.1021/acscatal.1c02433.

[156] X. Huang, C. Atay, J. Zhu, *et al.*, “Catalytic depolymerization of lignin and woody biomass in supercritical ethanol: Influence of reaction temperature and feedstock,” *ACS Sustain Chem Eng*, vol. 5, no. 11, pp. 10 864–10 874, 2017, ISSN: 2168-0485 (Print) 2168-0485 (Linking). DOI: 10.1021/acssuschemeng.7b02790.

[157] J. v. Haveren, E. L. Scott, and J. Sanders, “Bulk chemicals from biomass,” *Biofuels, Bioproducts and Biorefining*, vol. 2, no. 1, pp. 41–57, 2008, ISSN: 1932104X 19321031. DOI: 10.1002/bbb.43.

Dankwoord

Voor u ligt het proefschrift waar ik de afgelopen jaren vooral met veel **plezier** aan heb gewerkt. Het belangrijkste dat ik tijdens mijn promotie geleerd heb, maar stiekem eigenlijk al wist is het volgende, en dit wil ik u graag meegeven: *"Time is the most precious commodity out there. It's the one thing you can't buy or ever buy back. Give it your absolute all to whatever task it is your doing, no matter how big or small it is." (bron: ergens gelezen op het internet)*

Uiteraard is dit proefschrift niet enkel door mij tot stand genomen en daarom wil ik de gelegenheid nemen om deze mensen te bedanken. Ik zal hierbij ook ongetwijfeld mensen vergeten. Voor deze onbewust vergeten mensen, ook jullie hartelijk dank voor het tot stand komen van dit boekje.

Zoals velen weten was het privé niet altijd even makkelijk om het dan zo maar even te formuleren. Daarom wil ik in de eerste plaats mijn vader bedanken. *Je bent mijn voorbeeld. Ik heb zoveel van je geleerd. Je hebt me gevormd. Jouw lessen zitten in mijn rugzak. Ik neem ze mee. Je hebt me aanschouwen. Je keurde het goed. We zitten naast elkaar. En we zeggen niet zoveel. Jij hebt jouw ideeën. Ik heb mijn ideeën.*

Dan wil ik Sascha en Jean-Paul bedanken voor de geboden kans om binnen SPT te promoveren. Sascha, jij legt de invulling en verantwoordelijkheid van het project bij de promovendus en komt continu met vragen de gekozen invulling te verdedigen (*"Het is beter om achteraf vergiffenis te vragen, dan toestemming vooraf"*). Ik geloof dat dit cruciaal is om een onafhankelijk onderzoeker te worden. Bedankt voor alle gesprekken en discussies, vakinhoudelijk maar ook met betrekking tot de kijk op de maatschappij en het leven. Jean-Paul, jouw uitermate kritische blik en ongelooflijk oog voor detail hebben mij gepushed mij continue te verbeteren (*"the good is the enemy of the best"*). Ik denk ook dat je een belangrijke bijdrage hebt geleverd in het reduceren van mijn soms langdradige schrijfstijl naar iets dat lijkt op *"to the point"*. Bedankt! Pilar, many thanks! You always had an eye for the timeline of the project and made me focus on the things

that I had to do. Your door was and is always open for discussions and the necessary chit-chat.

I would also like to thank all the members of the graduation committee for accepting the invitation. I look forward to the discussion about this work. In het bijzonder wil ik Evert van der Heide bedanken voor input en discussies binnen dit onderzoek.

Yvonne, zonder jou is het onmogelijk om door het UT-moeras van geniale ICT-applicaties en bureaucratische procedures te manoeuvreren. Hartelijk dank! Zonder jou is de groep ten dode opgeschreven. Hetzelfde geld voor de technici. Benno, Johan, Karst, Ronald en Erna, bedankt voor alle hulp omtrent opstellingen, analyseapparatuur, het meedenken en daarmee het mogelijk maken van dit onderzoek. **Uiteraard ook bedankt voor de mogelijkheid om wekelijks op de woensdag te mogen genieten van jullie culinaire talenten.*

Wim Brilman, ik heb het als uitermate leerzaam ervaren om samen met jou *"Heat and Mass transfer"* te geven. Inmiddels heb ik de illusie dat ik iets van warmte en massatransport begrijp. Ook wil ik de andere leden van de SPT-staff, Henk van den Berg, Louis van der Ham, Boelo Schuur, Wim van Swaaij, Edwin Zondervan and Meik Franke bedanken voor support en discussies.

Of course I also want to thank my (former) colleges, Thomas B, Dion, Rick, Surika (my best labcleaning partner ever), Pushkar (Man, you take efficiency to a new league), Varsha, Martin, Lisette, Ehsan, Natalia, Vincent, Vahideh, Lionel, Michel, Yordi, Mahsa, Tim, Shahab (I decided to be nice and use your official name in this booklet), Jasper, Maryam, An, Eline, Peter and Rick for the good atmosphere and fruitful discussions.

Uiteraard wil ik de studenten die ik begeleid heb bedanken: Ruben, Lotte, Dirk, Eltjo, Shreekanth, Lukas, Koen, Kaan, Douwe, Enrico, Hadi, Siva, Gerco en Romy. Sommige van jullie werken hebben geleid tot hele concrete resultaten, te lezen in deze thesis. Veel van jullie werk, zo nog belangrijker, hebben belangrijke inzichten verschaft in de weg daar naar toe.

Dan mijn paranimfen. Beiden het land ontvlucht. Martijn, Ik heb veel van je geleerd, vooral hoe het niet moet. Martijn, jij hebt een nieuwe standaard neergezet van *"het dankwoord"*; waarheidsgetrouw maar het mag best een beetje *"prikkelend"*. Dat vind ik een goed idee. Herr Kreuger, jij hebt mijn leven verreikt met het concept *"de ontbijtfrituur"* en dat dit een levenselixer-achtige werking kan hebben. Hier dank ik jou hartelijk voor. Juraj, fortunately or unfortunately you also belong to this group. For the better or worse I keep it short. I miss our pre-work coffees, sitting on the ground in your apartment (because you did not have chairs), discussing life and other nonsense. You always appear energized and happy. To me that proofs that money and possesions do not make a person happy. Martijn, Tomas, Juraj, with you guys, the gap between sanity and insanity is non-existent.

Uiteraard wil ik vrienden en familie bedanken voor steun, een goed gesprek, een minder goed gesprek en alle gezelligheid. In het bijzonder wil ik mijn vriendengroep van de middelbare school noemen (Christian, Daan, Jasper, Joren, Martijn, Nico, Rik en Tom). Volgens enkelen *"valt het allemaal uit elkaar"*. Ja, het piept en kraakt wel eens, maar het hangt nog steeds aan elkaar. In goede en minder goede tijden zijn we er voor elkaar.

Ook dank ik de gouden generatie van de RPP, Sam, Daan, Douwe, Dorus, Joost, Joran, Melvin, Rens en Robin voor alle avonturen. Dorus en Joost ik zal jullie spuuglelijke jaarclub vestje nooit vergeten.

Sam, Biem en Maup, bedankt voor een avondje pils en een artistieke kaft.

Bert en Roel, bedankt voor de kans om weer verder aan te modderen binnen de (proces)techniek.

Mam, oneindig respect hoe je het de afgelopen jaren allemaal gemanaged hebt en het leven weer hebt opgepakt. Het heeft mij als kind nooit aan iets ontbroken. Alles kon en mocht. Of mijn opvoeding ook geslaagd is, daar verschillen de meningen over. Tante Tessa, mijn lievelingszus, goed om te zien dat je tegenwoordig ook aan het milieu denkt en in een vrieskist leeft. Ome Stijn, komt wel goed met jou. Helaas zijn ook jullie allemaal een stukje taaier geworden. Bedankt, dat jullie er waren en zijn op de momenten dat het echt telt.

Lieve Tinie, mijn kleine roze kabouter, bedankt voor *"wat eigenlijk niet"*. Ergens had Martijn wel een valide punt, zonder jou ben ik weinig levensvatbaar.

Here we go
On this rollercoaster life we know
With those crazy highs and real deep lows
I really don't know why (Danny Vera)

Ik wil je nog extra bedanken voor het feit dat je langzamerhand ook een soort tolerantie opgebouwd tegen mijn volslagen idiote ideeën & projecten wat vaak gepaard gaat met een briljante timing en hopeloos optimisme.

Max, de kleine grote man. Ik heb mijzelf geen betere vader kunnen wensen, en dat hoop ik ook voor jou te zijn!

ISBN: 978-90-365-5364-3
DOI: 10.3990/1.9789036553643